Kingdom of Morocco
Sultan Moulay Slimane University
Polydisciplinary Faculty of Khouribga

Doctoral School: Science and Technology

PhD. Thesis No: 349 /2021

Doctoral Training Center: Applied Physics

Laboratory: Laboratory of Nanosciences and Modeling

DOCTORAL DISSERTATION

by

Mohamed NFAOUI

for the degree of

Doctor

in

Physics and Engineering Sciences

Option: Material Science and Engineering Modeling

SPATIAL AND TEMPORAL DISTRIBUTION INVESTIGATION OF SOLAR ENERGY POTENTIAL. APPLICATION: NUMERICAL AND MODELING STUDIES OF THE OPTIMAL EXPOSURE, THERMAL BEHAVIOR AND ENERGY PRODUCTION OF A PHOTOVOLTAIC INSTALLATION

12 / 06 /2021

Jury members:

Mr. Lhoucine OUFNI………………………………………………… President

Mr. Moha AROUCH…………………………………………………… Reporter

Mr. Moulay Mustapha CHARAFI ………………………………… Reporter

Mr. Youness ZAHIDI……………………………………………… Reporter

Mr. Moha EL IDRISSI……………………………………………… Examiner

Mr. EL-HAMI Khalil……………………………………………… Director of thesis

Foreword

This thesis has been prepared in fulfilment of the requirements for a Ph.D. at the University of Sultan Moulay Slimane, Beni Mellal, Morocco, under the direction of Professor Dr. Khalil El-Hami.

DEDICATION

I dedicate this thesis report to my two dear parents, who have never stopped supporting me, Thanks to them that I'm here; they will always remain in my heart…. Thank you for always being there for me;

I would like to introduce all the people who are dear to me, my big family especially my brothers and sister for their encouragement and support;

My teachers throughout my study path; for their continued support to complete my studies;

Without forgetting to thank my dear colleagues from FPK-USMS, and from the Laboratory of Nanosciences and Modeling;

To all my friends who gave me moral support during these years of study, I sincerely thank them;

Thank you all.

MOHAMED NFAOUI

Acknowledgements

First and foremost, I would like to thank God Almighty who has given me strength and patience to finish this doctoral thesis.

Apart from the efforts of me, the success of this thesis depends largely on the encouragement and guidelines of many others. I take this opportunity to express my gratitude to the people who have been instrumental in the successful completion of this thesis.

It was a great chance for me to be able to prepare our doctorate within Laboratory of Nanosciences and Modeling "LNM" at the University of Sultan Moulay Slimane, Beni Mellal, Morocco, under the direction of Professor Dr. Khalil EL-HAMI.

The writer hardly knows where to start expressing the gratitude but for sure the gratitude goes to all those who have assisted her in the process of completing this thesis. It would be impossible to list all names but several people deserve her sincere and special thanks.

My deepest gratitude and thanks go to my supervisor and the Laboratory Director, Professor Dr. Khalil EL-HAMI, for welcoming us into his laboratory and also for having watched with his patience, availability in the development of this work and for his careful dedication to my thesis. It should be noted that; for his invaluable excellent guidance, patience, for his ever- ready attitude, and the time which he devoted so generously to render help to carry out our research even when he’s busy with many other very important things, allowed us to work in the best conditions and in a very pleasant environment.

I would like to thank Dr. Sanaa HAYANI-MOUNIR, a qualified Professor in Energy efficiency and Renewable Energy, for her assistance, guidance, advice and encouragement; I do not forget her hard and continuous working with me during the submission phase of our scientific papers to the indexing scientific journals, but also for providing additional guidance in the field of renewable energies towards the successful completion of the thesis.

I would like to pay my special regards to the Jury members for generously offering their time and support throughout the preparation and review of this document.

Lastly, I would like to thank everyone else in the Laboratory of Nanosciences and Modeling for their encouragement and support.

Global abstract

The study or applications of solar energy at a given site are dependent on more complete and detailed data on the solar radiation of this site, the knowledge of this deposit is of major interest to design and size solar energy systems. Thus, good sizing is possible only if the measurements are available continuously in space and time. The aim of this work is presented the method used in the calculation and describes the available data by trying to extract some useful information.

In our study we use programs through MATLAB to estimate the totality of the solar radiation on any inclined surface. Moreover, we will study in the last part the influence of exposure (orientation and inclination) on the amount of solar radiation received on a surface of $1m^2$. Then in order to study the theoretical solar field available in Khouribga, a series of insolation and solar irradiation data calculate. We apply the same strategy of this work to the 20 Moroccan cities in different time scales (every 3min, every day, every month and all year). We also approach from a global perspective, allowing us to reach reliable and real results of the productivity of a PV installation under the shading effect.

And among the objectives of this work is to studying the thermal behavior of a photovoltaic solar panel and the impact of the local ambient temperature, solar radiation and wind speed on the operating cell temperature of the photovoltaic modules in the region of Beni-Mellal Khenifra ". The first of all, we give a general and summary description of the meteorological data of the khouribga city concerning our study; under latitude of 33°41′09″ and Longitude of 7°22′58 ″, then we will approach in the second step a theoretical and experimental study, which explains the thermal behavior of a photovoltaic module from the influence of the cited parameters, as we present the equations adapted to the problem, then we can integrate the results found in two types of applications: the first; is to evaluate the performance of the hybridization of PV system with TEG generator through the electric power produced and to compare it with the PV system operating by itself under the weather conditions of Khouribga city. In the second; we studied this system for two cases, the case with solar tracker and the case with a fixed optimal angle. The last part of this manuscript, we suggest the theoretical calculation and the availability of solar radiation on the large spaces of all Moroccan territory.

This manuscript is organized as follows: The **first chapter** is devoted to reminders on the solar resource and the physical aspects of solar radiation (characteristic, nature ...), the different physical phenomena that will be subject to this radiation, the structure of the atmosphere and its effects on solar radiation. Knowledge of these various parameters makes it possible to establish a radiative balance of the earth-atmosphere system.

The second chapter we will be interested on the geometric aspects of solar radiation intercepted by the earth. The different formulas will therefore make it possible to calculate the position of the sun in the sky, with respect to a face oriented in any way, for a given hour and day at a given latitude. Using a Matlab code that we have developed, we can calculate and plot the variation of the different solar coordinates as a function of the time.

The third chapter we use programs via MATLAB to estimate the total solar radiation on an inclined surface. The implementation developed to allow us to extract the correct angle at which the maximum energy could be absorbed by the solar cells. We could determine the optimum tile angle for monthly, seasonal, and yearly solar radiation relative to the site of Khouribga city (latitude 32◦52′ North and longitude −6◦54′ West), and we used the same method to draw the table of solar gains depending on the optimum tilt angle of the solar panels to the main Moroccan cities.

In **the fourth chapter** we give a presentation of the models used in our study for the estimation of global solar irradiation. The example detailed hereafter relates to a photovoltaic pumping installation installed at Faculty of Science and Technology of Settat-Morocco (latitude 33.029° and longitude −7.619°). The study of our installation, based on estimating the annual production and the losses due to the phenomenon of shading, a simple calculation based on the system performance ratio, allows us to release the electrical productivity of the installation completed by a practical study of the shading effect by the use of ”Shadow Mask Close”.

The fifth chapter is devoted to evaluate the performance of the Thermal behavior of a photovoltaic module and the electric power produced of the hybridization of PV system with TEG generator under the weather conditions of Khouribga city in Morocco. A set of factors have been considered like the radiation, the ambient temperature, the wind velocity and the geographic coordinates.

We'll finish our manuscript with a suggestion of the theoretical calculation of the intensity solar radiation and the availability of large spaces of all Moroccan territory, and we'll present our perspectives on the next research projects concerning our subject and the aim of this thesis. Moreover, we will study the influence of exposure (orientation and inclination) on the amount of solar radiation received on a surface of $1m^2$, then in order to study the theoretical solar field available in Khouribga, a series of insolation and irradiation data calculate, and then we apply the same strategy of this work to the 20 Moroccan cities in different time scales (every 3min, every day, every month and all year).

Keywords: *Solar Energy, PV installation, Optimal Tilt Angle, Operating Cell Temperature, PV-TEGgenerator.*

Résumé de la thèse de doctorat

Les applications de l'énergie solaire sur un site donné dépendent de plusieurs données plus complètes et détaillées sur le rayonnement solaire de ce site, la connaissance de ce gisement est d'un intérêt majeur pour la conception et le dimensionnement des systèmes d'énergie solaire. Ainsi, un bon dimensionnement n'est possible que si les mesures sont disponibles en continu dans l'espace et dans le temps. Le but de ce travail est de présenter la méthode utilisée dans le calcul et de décrire les données disponibles en essayant d'extraire des informations utiles.

Dans notre étude, nous utilisons des programmes sous MATLAB pour estimer la totalité du rayonnement solaire sur toute surface inclinée. De plus, nous étudierons dans la deuxième partie l'influence de l'exposition (orientation et inclinaison) sur la quantité de rayonnement solaire reçue sur une surface de $1m^2$. Afin pour étudier le champ solaire théorique disponible à Khouribga, une série de données d'ensoleillement et d'irradiation solaire sont calculées. Nous appliquons la même stratégie de ce travail aux 20 villes marocaines à des échelles de temps différentes (toutes les 3min, tous les jours, tous les mois et toute l'année). Nous abordons également dans une perspective globale, nous permettant d'atteindre des résultats fiables et réels de la productivité d'une installation PV sous l'effet d'ombrage.

Ce travail de thèse a pour objectif principal d’établir une cartographie spatio-temporelle couvrant tout le territoire national et prenant en comptes les principales composantes du rayonnement solaire, dans ce contexte les études suivantes ont été menées à évaluer le potentiel solaire et de caractériser sa variabilité spatiotemporelle à long terme sur tout le territoire marocain, dans le but d’identifier les régions favorables à l’implantation des systèmes énergétiques solaires (Appliqué aux systèmes solaires photovoltaïques), une cartographie de ce potentiel en termes de rayonnement globale reçu sur une surface incliné de façon optimal a été réalisée.

Et parmi les objectifs de ce travail consiste à étudier le comportement thermique d'un panneau solaire photovoltaïque, et l'impact de la température ambiante locale, du rayonnement solaire et de la vitesse du vent sur la température de fonctionnement d'une cellule solaire photovoltaïque dans la région de Beni-Mellal Khenifra ". Tout d'abord, nous donnons une description générale et synthétique des données météorologiques de la ville de

khouribga concernant notre étude; sous une latitude de 33°41′09″ et une longitude de 7°22′58″, puis nous aborderons dans la second part une étude théorique et expérimentale qui expliquent le comportement thermique d'un module photovoltaïque à partir de l'influence des paramètres cités, et nous présentons des équations mathématiques adaptées au problème, par la suite on peut intégrer les résultats trouvés dans deux types d'applications: la première; est d'évaluer la performance de l'hybridation du système PV avec le générateur TEG à travers l'énergie électrique produite et le comparer avec le système PV fonctionnant seul dans les conditions météorologiques de la ville de Khouribga. Dans la seconde ; nous avons étudié ce système pour deux modes de positions, le cas avec tracker solaire et le cas avec un angle optimal fixe.

Le présent manuscrit est organisé de la façon suivante :

Le premier chapitre est consacré à des rappels sur la ressource solaire et les aspects physiques du rayonnement solaire (caractéristique, nature…), aux différents phénomènes physiques qui seront sujettes à ce rayonnement, la structure de l’atmosphère et ses effets sur le rayonnement solaire. La connaissance de ces divers paramètres permet d’établir un bilan radiatif du système terre- atmosphère.

Dans **le deuxième chapitre**, nous allons nous intéresser à l’aspect géométrique du rayonnement solaire intercepté par la terre. Les différentes formules vont donc permettre de calculer la position du soleil, par rapport à une face orientée de manière quelconque, pour une heure et un jour donné à une latitude donnée.

Dans **le troisième chapitre,** nous utilisons des programmes via MATLAB pour estimer la totalité du rayonnement solaire sur une surface inclinée. Le programme développé nous permet d'extraire l'angle sous lequel l'énergie maximale pourrait être absorbée par les cellules solaires. De plus, nous étudierons l'influence de l'exposition (orientation et inclinaison) sur la quantité de rayonnement solaire reçue sur une surface de $1m^2$,

Dans **le quatrième chapitre**, nous donnons une présentation des modèles utilisés dans notre étude pour l'estimation de l'irradiation solaire globale. Nous mettons en évidence les différentes procédures de calcul de la radiation solaire globale sur une surface horizontale hors atmosphère et au sol. Dans notre étude on utilise des programmes sous MATLAB qui nous permet d’extraire le bon angle pour la ville de Settat sous lequel le maximum d’énergie pourrait être absorbée par une installation photovoltaïque. Un calcul basé sur le ratio de performance du système nous permet de dégager la production d'électricité de notre installation complétée par une étude pratique de l'effet d'ombrage, cette méthode a été appliquée à une installation PV de 1,5KWc se trouvant à la FST de Settat-Maroc (latitude 33,029 ° et longitude −7,619 °), et à calculer l'énergie des panneaux photovoltaïques de sortie. Avant de calculer l'effet d'ombrage influence sur les cellules photovoltaïques. L'un des objectifs de ce chapitre est de proposer des cycles d'optimisation, afin de minimiser les effets néfastes de l'ombrage partiel sur les systèmes de panneaux solaires photovoltaïques par l'utilisation de différents modes de position. Nous abordons également dans une perspective globale, nous permettant d'atteindre des résultats fiables et réels de la productivité d'une installation PV sous l'effet d'ombrage.

Le cinquième chapitre est consacré à l'évaluation la performance du comportement thermique d'un module photovoltaïque à partir de l'influence des paramètres météorologiques (radiation solaire, la température ambiante et la vitesse du vent) sur la température de fonctionnement d'une cellule solaire photovoltaïque. Enfin, nous aborderons dans une ultime étape la production électrique du système hybride PV-TEG sous conditions climatiques local. Ces conditions climatiques varient annuellement, mensuellement et quotidiennement, dépendent également des coordonnées géographiques. Le but de ce chapitre est d'évaluer les performances du comportement thermique d'un module photovoltaïque et la puissance électrique produite par l'hybridation d'un système PV avec un générateur TEG dans les conditions météorologiques de la ville de Khouribga au Maroc.

Nous terminerons notre manuscrit par une suggestion du calcul théorique de l'intensité du rayonnement solaire et de la disponibilité sur les grands espaces de tout le territoire marocain, et nous présenterons nos perspectives sur les prochains projets de recherche concernant notre sujet et l'objectif de cette thèse. De plus, nous appliquons la même stratégie de ce travail aux 20 villes marocaines à différentes échelles de temps.

Mots clés: *Énergie Solaire, Installation-PV, Angle d'Inclinaison Optimal, Température de Fonctionnement d'une Cellule Photovoltaïque, Générateur PV-TEG.*

Table of contents

DEDICATION 3
Acknowledgements 4
Global abstract 5
Résumé de la thèse de doctorat 8
List of figures 15
List of tables 18
Nomenclature Table 19
General Introduction 21
Introduction Générale 22

Chapter I: OVERVIEW ON SOLAR ENERGY POTENTIAL
I.1. Introduction 24
I. 2. The sun's vital statistics 24
I. 3. Interior structure of the Sun 28
I. 3. 1. Anatomy of the Sun 28
I. 3. 2. Inner layers and the core 30
I. 3. 3. Radiative and convective zones 30
I. 3. 4. Photosphere, Chromosphere and Corona 30
I. 4. Solar radiation 31
I. 4. 1. Electromagnetic solar radiation 33
I. 4. 2. Three laws of Radiation 35
- Stefan–Boltzmann Law 1879 36
- Wein's Law 1895 37
- Planck's Law 1900 38
I. 4. 3. Extraterrestrial solar insolation (I_0) 39
I. 5. D*epletion of solar radiation* 41
I. 5. 1. Absorption 43
I. 5. 2. Dispersion 44
I. 5. 3. Reflective Earth 46
Conclusion I 46
References I 47
Chapter II: INVESTIGATION ON SOLAR RADIATION
II. 1. Introduction 50
II. 2. Solar Geometry: Tracking the Sun 50
II. 2. 1. Latitude and Longitude 51
II. 2. 2. Apparent Path of the Sun 52
II. 2. 2. 1. The Equatorial Coordinates 52
II. 2. 2. 2. The Horizontal Coordinates 55

II. 3. Solar Time vs. Clock Time 61
II. 3. 1. Sunshine duration 62
II. 3. 2. Sunrise and Sunset Time 63
II. 3. 3. Solar Time (ST) 63
II. 3. 3. 1. Universal Time (UT) 64
II. 3. 3. 2. Local Clock Time (LCT) 65
II. 3. 3. 3. Mean Solar Time (MST) 65
II. 3. 3. 4. True Solar Time (TST) 66
II. 3. 3. 5. Equation of Time (Et) 67
II. 4. Study of solar radiation received on ground surface "Clear day" 67
II. 4. 1. Direct radiation 68
II. 4. 2. Diffused radiation 69
II. 4. 3. Reflected radiation 69
II. 5. Results and discussion of solar radiation received on horizontal plane "clear day" 70
II. 5. 1. The typical day of the month 71
II. 5. 2. Calculation of daily irradiation 71
II. 5. 3. Calculation of monthly irradiation 73
II. 5. 4. Cumulative energy for each month of the year 73
Conclusion II 76
References II 76
Chapter III: OPTIMAL TILT ANGLE AND ORIENTATION FOR SOLAR MODULES
III. 1. Introduction 78
III. 2. Influence of location on the solar field 78
III. 2. 1. Annual distribution of sunshine in the world 79
III. 2. 2. Annual solar energy in Morocco 81
III. 3. Exposure effect on the reception of solar radiation 83
III. 3. 1. Orientation of solar panel 84
III. 3. 2. Tilt angle of solar panel 84
III. 4. Calculation of optimal tilt angle and orientation for solar photovoltaic arrays 85
III. 4. 1. Optimal orientation 86
III. 4. 2. Optimum Tilt Angle 88
III. 5. Optimal Tilt angle and orientation in Khouribga city: 88
III. 5. 1. Monthly Tilt Angle 89
III. 5. 2. Seasonal Tilt Angle 90
III. 5. 3. Annual Tilt Angle 91
III. 6. Results and discussion 92
III. 6. 1. Optimal Tilt angle in Khouribga city: 92
III. 6. 2. Calculation of solar radiation received on the optimum tilt angle surface 93
III. 6. 2. 1. Daily irradiation 93
III-6-2-2 The energy that accumulates for each month 94
III. 6. 3. Effect of Tilt and Orientation angles of solar panels on their production 96

Conclusion III **98**
References III **99**

Chapter IV: MODELING OF SOLAR RADIATION ON THE GROUND
IV. 1. Introduction...**101**
IV. 2. Statistical models for calculating solar radiation **102**
IV. 2. 1. Extra-terrestrial solar radiation I_0 (W/m^2)...102
IV. 2. 2. Air mass effect 104
IV. 2. 3. The incidence angle 106
IV. 2. 4. Theoretical solar irradiation on the earth 108
IV. 2. 4. 1. Hottel's method..108
IV. 2. 4. 2. Davies & Hay model...112
IV. 2. 4. 3. Complete model for tilted plane global radiation 115
IV. 3. Study of global solar radiation and optimal tilt angle and orientation for solar photovoltaic arrays: case of Settat city, Morocco **116**
IV. 3. 1. Study of solar radiation received on the surface of our installation in Settat city 117
IV. 3. 1. 1. Daily distribution of solar radiation throughout the year..............................117
IV. 3. 1. 2. The cumulative energy for each month of the year 118
IV. 3. 1. 3. Sunshine Tables 119
IV. 3. 2. Influence of the tilt angle on the acceptance of the solar irradiation 121
IV. 3. 2. 1. Calculation of daily irradiation...122
IV. 3. 2. 2. Cumulative energy for each month of the year..124
IV. 4. Study of the influence of shading on the productivity of our photovoltaic installation..**127**
IV-4-1 Identify the characteristic points of the obstacle geometry..................................129
IV. 4. 2. Calculation of both electricity production and electrical productivity 132
Conclusion IV...**136**
References IV **137**

Chapter V: EVALUATION OF THE THERMAL BEHAVIOR OF A PHOTOVOLTAIC CELL AND ANNUAL PRODUCTION OF THE PV-TEG HYBRID SYSTEM
V. 1. Introduction **140**
V. 2. Meteorological data of khouribga city. **141**
V. 2. 1. Rainfall 141
V. 2. 2. Temperatures..142
V. 2. 3. Wind regime...143

V. 2. 4. Solar energy 143
V. 2. 5. Summary table of the meteorological data 145
V. 3. Heat exchanges between the Photovoltaic module and its environment 145
V. 3. 1. Description of the thermal behaviour of a Photovoltaic silicon module 146
V. 3. 2. Theoretical approaches "mathematical models" 147
V. 3. 2. 1. Operating cells Temperature T_c. 147
V. 3. 2. 2. Modelisation of the PV-TEG Hybrid System 149
V. 4. Results and Discussion 156
V. 4. 1. Modeling of the Thermal Behavior of a Photovoltaic Cell under Arid and Semi-arid Sites Conditions: Case of Khouribga City in Morocco 156
V. 4. 1. 1. Properties of the photovoltaic module used: (BP 585 (BP Solar)). 157
V. 4. 1. 2. Influence of the ambient temperature on the operating cell temperature 158
V. 4. 1. 3. Influence of the solar radiation on the operating cell temperature 159
V. 4. 1. 4. Influence of the wind speed on the operating cell temperature 160
V. 4. 1. 5. Effect of the operating cell temperature on the efficiency of the photovoltaic module 161
V. 4. 2. Evaluation of the Annual Production of the PV-TEG Hybrid System at Khouribga City in Morocco 162
V. 4. 2. 1. Daily power evolution of the PV and PV-TEG hybrid system 163
V. 4. 2. 2. Monthly energy production of the PV and PV-TEG hybrid system 164
V. 4. 2. 3. Annual evolution of energy production of the PV and PV-TEG hybrid system 166
Conclusion V 168
References V 169

GENERAL CONCLUSION AND PERSPECTIVES 171

List of figures

Figure I.1 : The potential of solar energy captured by the earth for a year, compared to other types of energy. 25
Figure I.2 : Illustrations of the planets of our solar system. 26
Figure I.3 : Position of the solar system in the Milky Way. 26
Figure I.4: A slice of the Sun. The nuclear fusion reactions occur in its center. 29
Figure I.5 : Electromagnetic wave spectrum 32
Figure I.6 : The spectral distribution of solar electromagnetic radiation 34
Figure I.7 : The solar spectrum as a function of temperature. 35
Figure I.8 : Josef STEFAN (1838 - 1893). 37
Figure I.9 : Wilhelm WIEN (1864 - 1928). 38
Figure I.10 : Max Planck (1858-1947) 39
Figure I.11: Extraterrestrial solar radiation outside of the earth's atmosphere. 40
Figure I.12: The fraction of the sunbeam that strikes the ground. 41
Figure I.13: Components of the energy balance of the earth. 42

Figure II.14 : Latitude and longitude representation on a terrestrial globe. 51
Figure II.15 : Geographical coordinates of the place. 52
Figure II.16 : Equatorial coordinate frame. 53
Figure II.17 : Trajectory of the earth around the Sun. 53
Figure II.18 : Yearly Variation in Declination. 54
Figure II.19 : The solar horizontal coordinates and the angle of incidence. 56
Figure II.20 : Temporal variations of (zenith and elevation) angles for the two days of year, 57
Figure II.21 : Daily variations of Solar Azimuth Angle in the two days of year,. 58
Figure II.22 : Diagrams of the azimuth ϕ VS elevation h. 58
Figure II.23 : Diagrams of the azimuth ϕ and elevation h with the notion of time. 59
Figure II.24 : Representation of the azimuth ϕ and elevation h. 60
Figure II.25 : Variation of the angle of incidence in the two solstice's days of the year. 61
Figure II.26 : Variation in the sunshine duration during the year in Khouribga city. 62
Figure II.27 : Graphic representation of the sun evolution and the concept of the solar time. 64
Figure II.28 : Greenwich Civil Time: Time along zero longitude line passing through Greenwich. 65
Figure II.29 : Plot of the Equation of time. 67
Figure II.30 : The solar flux on a collecting surface. 68
Figure II.31 : Both direct and diffuse powers received in function of time. 72
Figure II.32 : Annual powers radiations in Khouribga. 73
Figure II.33 : Distribution of monthly energy in Khouribga. 74

Figure III.34 : Worldwide distribution of solar radiation into belts indicating feasibility of solar applications. 80
Figure III.35 : Distribution of Solar Energy among the world. 81
Figure III.36: Potential of solar energy in Morocco. 82
Figure III.37 : Different orientation and inclinations, and quantity of solar radiation received on each surface compared to the optimum of 30° and orientation due south. 83
Figure III.38 : Percentage of solar gains depending on the orientation of the solar panel. 84

Figure III.39 : Tilt angle for the solar module. 85
Figure II.40: Diagrams of the azimuth ϕ and elevation h with the notion of time. 87
Figure III.41 : The annual solar energy for the different tilt angle. 88
Figure III.42: Optimal tilt angle, orientation and the solar energy received for each season of the year. 90
Figure III.43 : Annual solar energy yield (kWh/m2) for various tilt angles and orientations. 91
Figure III.44 : Evolution of direct, diffuse and global solar radiation in the year, on optimum exposure. 94
Figure III.45: The monthly direct, diffuse and global solar radiation, of optimum exposure. 95
Figure III.46 : Annual solar energy yield (kWh/m2) for various tilt angles and orientations. 97

Figure IV.47 : Solar constant according to the two expressions of the equations. 103
Figure IV.48 : Variation of the extra-terrestrial solar irradiance. 104
Figure IV.49 : Representation of Air mass. 105
Figure IV.50 : The geometric relations between the solar horizontal coordinates and the incidence angle ω. 107
Figure IV.51 : Conversion between extra-terrestrial radiation with normal incidence and extraterrestrial radiation on the horizontal plane. 116
Figure IV.52 : Image of the photovoltaic pumping installation at FST of Settat. 117
Figure IV.53 : 3D drawing of the PV installation in real exposure. 122
Figure IV.54 : 3D drawing if the PV installation is well exposed. 122
Figure IV.55 : The daily power evolution of direct, diffuse and global solar radiation, of optimum exposure (June21). 123
Figure IV.56 : Daily power evolution of direct, diffuse and global solar radiation, of actual exposure (december21). 123
Figure IV.57 : Evolution of direct, diffuse and global solar radiation in the year, for optimum exposure and actual or real exposure. 124
Figure IV.58 : The monthly direct, diffuse and global solar radiation, of optimum and actual exposure. 125
Figure IV.59 : Solar radiation (in percentage) with respect to the ideal situation as a function of inclination and orientation. 127
Figure IV.60 : The shading on the our installation at FST Settat. 128
Figure IV.61 : Presence of obstacles (five trees and a pole) for the case of our PV installation. 128
Figure IV.62 : The instrument for measuring elevation and azimuth. 129
Figure IV.63 : Measure the height of each characteristic point. 129
Figure IV.64 : Measure the azimuth of each of the characteristic points. 130
Figure IV.65 : The characteristic points on the graph of the course of the sun. 130
Figure IV.66 : Mask of shadow of the obstacles reported on the 1st line of the installation. 131
Figure IV.67 : Surface of the drop shadow on the entire installation. 131

Figure V.68 : Climate summary of Khouribga. 141
Figure V.69 : Average Monthly Rainfall. 142
Figure V.70 : Average High and Low Temperature. 142
Figure V.71 : Compass wind rose. 143

Figure V.72 : Average Daily Incident Shortwave Solar Energy. 144
Figure V.73 : Modeling of the thermal behavior of a photovoltaic module. 146
Figure V.74 : Description of the layers constituting the PV-TEG hybrid system. 151
Figure V.75 : Electrical Characteristics of BP 585 (BP Solar) module. 157
Figure V.76 : Relationship between the operating cell temperatures and the ambient temperature, under an illumination of 800 W/m² and a wind of 1 m/s. 159
Figure V.77 : Relation between the illumination and the difference of temperature between the module and the ambient temperature ($T - T_a$), for a wind speed of 1 m/s. 160
Figure V.78 : The relationship between (T - Ta) and the wind speed, for an illumination of 800 W/m². 161
Figure V.79 : Effect of the operating cell temperature on the efficiency of the photovoltaic module. 162
Figure V.80 : Daily variation of the power generated by the TEG and PV-TEG with optimal tilt angle. 163
Figure V.81 : Daily variation of the power generated by the TEG and PV-TEG set up on a solar tracker system. 164
Figure V.82 : The monthly energy produced by the TEG and PV-TEG with optimal tilt angle. 165
Figure V.83 : Monthly energy produced by the TEG and PV-TEG set up on a solar tracker system. 165
Figure V.84 : Daily energy produced in the year by the TEG and PV-TEG with optimal tilt angle. 166
Figure V.85 : Daily energy produced in the year by the TEG and PV-TEG set up on a solar tracker system. 167

Figure VI.86 : The 20 Moroccan cities concerned by the study. 172
Figure VI.87 : The Annual solar energy of direct and global radiation to 20 Moroccan cities. 174
Figure VI.88 : Need monograph in Irrigation Water, province of Khouribga. 175
Figure VI.89 : Global Horizontal Irradiation in Morocco ($kWh/m^2/year$) 176

List of tables

Table I.1: Temperature, density and size of every layer of the Sun 32
Table I.2 : Distribution of electromagnetic waves according to their wavelength. 33
Table II.3 : The geographic data of Khouribga City. 70

Table II.4 : List of typical days per month proposed by Klein... 71
Table II.5 : The energy received per days (wh/m^2).. 72
Table II.6 : The monthly and yearly energy received. 74
Table II.7 : Daily, monthly and yearly energy received 75

Table III.8 : The optimum inclination for each month of the year. 89
Table III.9 : Seasonal and annual solar energy at Seasonal tilt angle.. 91
Table III.10 : Annual solar radiation at different tilt angle. 92
Table III.11 : Values of the daily irradiation of the typical days of each month................................... 93
Table III.12 : The monthly cumulative energy of optimum exposure. 95
Table III.13 : Relative distribution in percent (%), of the solar radiation received as a function of the orientation and tilt angle in Khouribga city.. 98

Table IV.14: The solar constant (I_0) and solar height (h) as a function of the number of Air Mass. ... 105
Table IV.15: The values of b1 and b2 obtained by linear regression for the regions of Casablanca. . 110
Table IV.16: The annual average according to this table is : 110
Table IV.17: Values of H_h according to Angstrom Black's relationship for the city of Casablanca..... 110
Table IV.18: Values of Factor Fc Depending On the Zenith Distance from Robinson 114
Table IV.19: Energy received for each typical day in (Wh/m^2).. 118
Table IV.20: The monthly and annual irradiation received on our installation (kwh/m^2). 119
Table IV.21: The diffuse solar irradiation received on the surface of our installation....................... 120
Table IV.22 : The global solar irradiation received on the surface of our installation. 121
Tableau IV.23: The daily solar radiation of the typical days of each month in (Wh/m^2) for the two modes of positions 125
Table IV.24: The monthly cumulative energy for the two modes of positions................................. 126
Table IV.25: Representative table of the solar energy received on our PV installation with shading in Wh/m^2. 132
Table IV.26: The monthly electricity production of our installation for the two modes positions..... 134
Table IV.27: monthly productivity of our installation kW_h /kW_p.. 135

Table V.28 : Daily, monthly and yearly energy received. 144
Table V.29 : The July average variation of temperature, wind speed and solar radiation. 145
Table V.30 : Empirically determined coefficients used to predict module back surface temperature as a function of irradiance, ambient temperature, and wind speed... 148
Table V.31 : Thermal and physical properties of the materials of a PV module................................ 158

Table VI.32: The daily average energy of twenty Moroccan cities in (kWh/m^2.day).. 173
Table VI.33: Optimum tilt angle and Annual energy Received. 176

Nomenclature Table

Equatorial & Horizontal coordinates

δ : Declination.
AH : Hour angle.
Z : Zenith angle.
φ : Azimuth angle.
ω : Angle of incidence.
Z' : is the angle between the vector normal to the panel and the vertical of the place
φ': is the angle between the projection of the vector to the normal panel on the horizontal plane and the north
j: Sequence number of days in the year.

Elements of time

TSV : Local solar time.
TSM : Mean solar time.
TU : Universal time.
Et: Equation of time.
Sd : Sunshine duration.
$t_{Sunrise}$: Sunrise Time.
t_{sunset}: Sunset Time.
ST : Solar Time.
UT : Universal Time.
LCT : Local Clock Time.
MST : Mean Solar Time.
TST : True Solar Time.

Thermal change elements

WS = Wind speed.
α_g : Glass absorption coefficient.
G : The solar radiation reached the surface of the photovoltaic panel;
Ga : Absorbed.
Gr : Reflected.
Gt : Transmitted.
Q: Conduction Heat Transfer;
Q_N: Natural convection.
Q_F: Forced convection.
Q_R : Radiation to the sky.
R : The thermal resistances;
T_{PV}, T_{gro} & T_{sky}: are the temperature of the PV panel,
L & k : are length and conductivity of each layer.
F_{gro} & F_{sky} are configuration factor of the

Coordinate systems

θ : Latitude.
λ : Longitude.

Elements of the photovoltaic properties

E : monthly or annual electricity production of PV installation.
E_0 : Reference solar irradiance.
S : available module surface [m²] of the PV installation.
η_{global} : Overall efficiency of the PV installation.
Pr : Electrical productivity of the PV installation.
P : The power available at the terminals of the photovoltaic panel.
P_{stc} : Power of a cell, a module, a system measured in the Standard Test Conditions.
η_{pv} : The Efficiency of the PV Cell.
Tc : Cell temperature °C.
Ta : Ambient temperature °C.
S : solar irradiance.
T_m : Measured back-surface module temperature, (°C).

Solar Energy concept elements

I_{Dir} : Direct radiation.
I_{Dif} : Diffused radiation.
I_{ref} : Reflected radiation.
A: Apparent extraterrestrial flux.
k: Optical depth.
R_{dif} : Form factor between collector and sky.
R_{ref}: Geometric factor of the ground.
C : Factor of the sky diffuses.
ρ : Ground reflectance.
α_{opt} : Optimum Tilt Angle.
I_0: Extra-terrestrial solar radiation.
I_h : Global values received on a horizontal plane on the ground.
AM : Air mass.
H_h : Global energy received by a sky whose veiling is defined by unit of horizontal surface.
H_{hc} : Energy received under the same conditions of measurements but by clear sky.
H_0 : Energy received by a surface arranged horizontally, outside the atmosphere.
I_h and H_h : Global power values received on a

ground and the sky. h_w : Heat Transfer Coefficient for the Forced Convection. h_N : Heat Transfer Coefficient for the Naturel Convection. Gr_{cr} : The Critical number; Gr : Grashof number; Pr : Prandtl number; R_a : Rayleigh number; n_{TE} : The TEG Efficiency. I_{TE} : The electrical current passes through the TEG element. η_T : The Overall Efficiency.	horizontal plane on the ground. K_t : Indices of clarity. α_0 : Coefficient corresponding to the absorption of direct solar radiation. PV-TEG Hybrid System U_0 : Thickness of the ozone layer corrected by the optical path of the solar radiation through the layer. T_r : Transmission coefficient of molecular diffusion. X_w : Thickness of condensable water corrected by the optical path of the radiation through the layer. D_r : Diffuse radiation after Rayleigh scattering. T_0 : Transmittance after absorption by ozone. ρ : The ground albedo. ρ' : The clear sky albedo for the site in question. A_i : Anisotropy index. R_b : Geometric factor of the converting beam radiation between planes.

General Introduction

Overview

Morocco has a significant solar deposit considering the values of the duration of insolation recorded on almost the whole national territory exceeding the 2000 hours annually and reaching even 3900 hours in the highlands and the Moroccan Sahara. As a result, the amount of energy received on the ground exceeds 5 kWh / m^2 on average in several regions of Morocco, ie nearly 700 kWh / m^2 per year in the north and 2263 kWh/m^2 in the south, which favors the use of electricity. solar energy in different fields such as electricity generation, agro-food drying, etc. the knowledge of this deposit is of major interest to design and size solar energy systems. Thus, good sizing is possible only if the measurements are available continuously in space and time. The aims of this work are presented the method used in the calculation and describe the available data by trying to extract some useful information.

The needs and the possibility of using the solar energy are directly linked to climatic conditions. This source is intermittent in time and space, which poses problems in the sizing of solar energy systems. These aspects require a perfect knowledge of the solar deposit before undertaking any action or recovery program. This goal can only be achieved if horizontal and tilted global radiation data are continuously available in space and time. In this context, the following studies have been carried out to assess the solar potential and to characterize its long-term spatiotemporal variability over the entire territory, for the purpose of identifying regions favorable to the installation of solar energy systems, a mapping of this potential in terms of overall radiation received on an optimally inclined surface was carried out.

Introduction Générale

Le Maroc dispose d'un gisement solaire important compte tenu des valeurs de la durée d'insolation enregistrées sur la quasi-totalité du territoire national dépassant les 2000 heures annuellement et pouvant atteindre même les 3900 heures sur les hauts plateaux et le Sahara Marocain. Par conséquent, la quantité d'énergie reçue au sol dépasse en moyenne 5kWh/m^2 dans plusieurs régions du Maroc soit près de 700 kWh/m^2 par an au nord et de 2263 kWh/m^2 au sud, ce qui favorise l'utilisation de l'énergie solaire dans différents domaines tel que la production de l'électricité, le séchage agroalimentaire, etc. la connaissance de ce gisement est d'un intérêt majeur pour concevoir et dimensionner les systèmes énergétiques solaires. Ainsi, un bon dimensionnement n'est possible que si les mesures sont disponibles d'une manière continue dans l'espace et dans le temps. La meilleure manière pour ce faire est de se disposer d'une série de mesures météorologiques et physiques issues d'un système d'exploitation Androïde, et un microcontrôleur qui est relié à des capteurs pour chaque mesure, les données recueillies sont envoyés à un serveur centralisé qui traite l'information.

Sans nourriture pas de vie, sans énergie pas d'activité. Bien que la nourriture soit aussi une forme d'énergie, il est d'usage de ne pas l'inclure quand on parle d'énergie. Tout le monde a besoin d'énergie et l'on ne peut s'en passer pour vivre et se développer. On a besoin aujourd'hui d'électricité pour faire fonctionner la multitude d'appareils que l'on trouve dans une maison moderne, pour l'éclairage et, éventuellement, pour le chauffage ou la climatisation.

Chapter I

OVERVIEW ON SOLAR ENERGY POTENTIAL

I.1. Introduction

The majority of the energy sources used by humanity originate from solar energy. Fossil fuels were created hundreds of millions of years ago from marine or terrestrial biomass. Humanity has exploited them intensively for about two centuries and they have greatly increased the standard of living of the inhabitants of the earth.

Most of the renewable energy comes from the sun. It is obvious for solar energy that we collect directly (solar thermal or photovoltaic). This is also the case for hydraulics which is based on the water cycle. Indeed, solar energy evaporate water from oceans, rivers ... Energy is recovered from water by using gravitation, which causes an object to fall when dropped.

The wind also comes from solar energy since our planet is not heated in the same way at all points, this results in temperature differences which create air currents, therefore wind. Finally, plant biomass grows by solar energy, carbon dioxide in the atmosphere and water in the soil. The waste that we use to produce energy also comes indirectly from solar energy since it is either organic matter rejected by living beings, or compounds formed for example from petroleum.

I. 2. The sun's vital statistics

(Solar energy could fully meet the needs of humanity)

Each year, the sun provides fifteen thousand more energy than the commercial consumption of the world's population. He is so generous that he could satisfy our most energy needs, even if the human, animal and plant again multiplied considerably. It is therefore perfectly grotesque to continue to assert that the sun alone cannot cover the energy needs of humanity [1].

As public opinion begins to realize the potential of solar energy for electricity generation, the photovoltaic sector continues to rise. The powers installed all over the world are increasing.

Even if theoretical calculations show that the energy brought to the earth by the sun is very much greater than the needs of humanity, electricity of solar origin cannot be efficiently and massively stored and its transport over a long distance causes losses.

The diagram below allows to better visualize the potential of solar energy received on the terrestrial globe, compared to other types of energy sources.

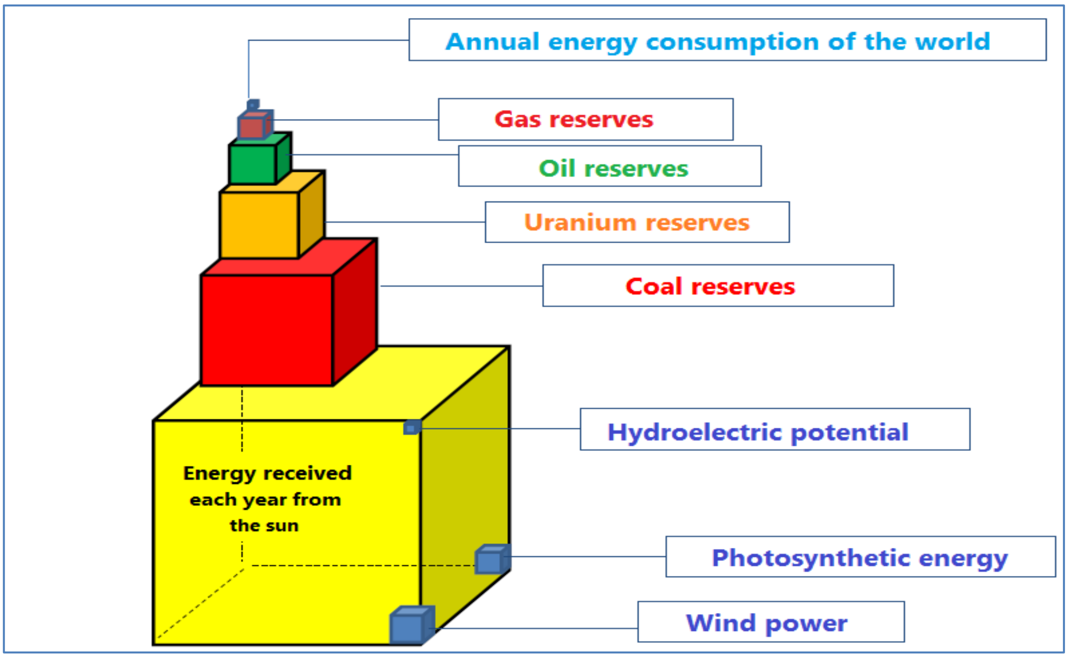

Figure I.1 : The potential of solar energy captured by the earth for a year, compared to other types of energy [2].

Electricity produced from solar energy therefore has certain environmental advantages. Indeed, the production of photovoltaic electricity is free from pollution locally and globally: it does not emit greenhouse gases, does not tap into large quantities of mineral resources, and can easily be integrated into the urban environment, close to the most important consumption needs.

So the photovoltaic solar energy is excellence renewable energy: its source the sunlight is inexhaustible and is not affected by human activities.

(The sun our star and the center of our solar system)

More than 4.6 billion years ago, the sun brings us light and heat, today man's ambition is to control this source of energy.

The sun is an ordinary star among the 200 billion in our Galaxy, so a huge ball of hot gas that produces energy and radiates. While the word "star" represents any bright spot at night in the sky. It was at the beginning of the 20th century that its star status in the sense of "being a producer and emitter of energy" was established; astrophysicists are revealing the secrets of his molten heart today.

The Sun is the center of our Solar System and contains most of the mass in the Solar System. All of the planets in our Solar System, including Earth, orbit around the Sun [2].

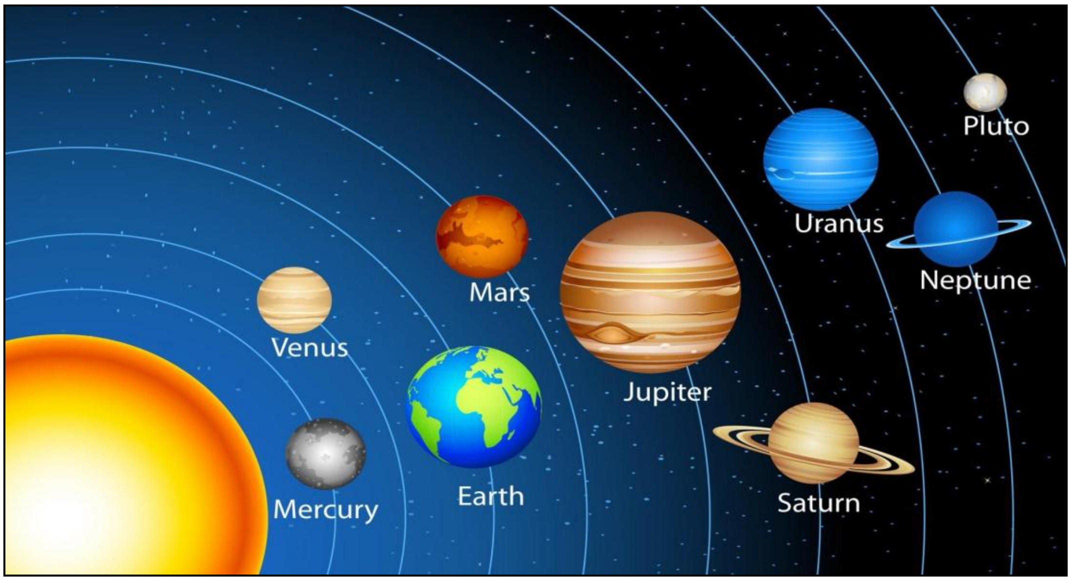

Figure I.2 : Illustrations of the planets of our solar system [3].

The solar system, assemblage consisting of the Sun and those bodies orbiting around it: 8 (formerly 9) planets with about 170 known planetary satellites (moons); countless asteroids, some with their own satellites; comets and other icy bodies; and vast reaches of highly tenuous gas and dust known as the interplanetary medium.

Like many others among the 200 billion stars that populate our galaxy. Located at the center of the solar system and influencing the motion of all the other bodies through its gravitational force is the Sun, which in itself contains more than 99 percent of the mass of the system. The planets, in order of their distance outward from the Sun, are Mercury, Venus, Earth, Mars, Jupiter, Saturn, Uranus, and Neptune.

Figure I.3 : Position of the solar system in the Milky Way [3].

For thousands of years, astronomers and astrologers believed that the Earth was at the center of our Universe. This perception was due in part to the fact that Earth-based observations were complicated by the fact that the Earth is embedded in the Solar System. It was only after many centuries of continued observation and calculations that we discovered that the Earth (and all other bodies in the Solar System) actually orbits the Sun.

Much the same is true about our Solar System's position within the Milky Way. In truth, we've only been aware of the fact that we are part of a much larger disk of stars that orbits a common center for about a century. And given that we are embedded within it, it has been historically difficult to ascertain our exact position. But thanks to ongoing efforts, astronomers now know where our Sun resides in the galaxy.

The Milky Way is really, really big! Not only does it measure some 100,000–120,000 light-years in diameter and about 1,000 light-years thick, but up to 400 billion stars are located within it (though some estimates think there are even more). Since one light year is about 9.5 x 10^{12} km (9.5 trillion km) long, the diameter of the Milky Way galaxy is about 9.5 x 10^{17} to 11.4 x 10^{17} km, or 9,500 to 11,400 quadrillion km [3].

The Sun is a huge, glowing sphere of hot gas. Most of this gas is hydrogen (about 70%) and helium (about 28%). Carbon, nitrogen and oxygen make up 1.5% and the other 0.5% is made up of small amounts of many other elements such as neon, iron, silicon, magnesium and sulfur. The Sun shines because it is turning hydrogen into helium via the process of nuclear fusion in its extremely hot core. This means that as time goes on, the Sun has less hydrogen and more helium.

The temperature at the surface of the Sun is about 10,000 Fahrenheit (5,600 Celsius). The temperature rises from the surface of the Sun inward towards the very hot center of the Sun where it reaches about 27,000,000 Fahrenheit (15,000,000 Celsius). The temperature of the Sun also rises from the surface outward into the solar atmosphere. The uppermost layer of the solar atmosphere, called the corona, reaches temperatures of millions of degrees. The corona is the bright halo of light that can be seen during a total solar eclipse.

The Sun has been shining for about 4.6 billion years and it will continue to shine for about 5 billion more years.

The Sun shines by turning hydrogen into helium in its core. This process is called nuclear fusion. Fusion happens when lighter elements are forced together to become heavier elements. When this happens, a tremendous amount of energy is created. The famous scientist Albert Einstein discovered a formula which shows how much energy can be created from a small amount of mass. You may have heard of the famous formula $E=mc^2$. E is energy, m is mass, and c is the speed of light. The speed of light is 186,000 miles or 300,000 km per second. So you can see that a tiny amount of matter can be changed into an enormous amount of energy. This can only happen in places which have extremely high pressures and temperatures. At the center of the Sun, the temperature reaches 16 million degrees K, and the pressure is more than a billion times the atmospheric pressure on Earth! The Sun converts about 5 million tons of mass into energy every second. This energy heats the Sun, and in turn, the Sun heats Earth and all the other planets [3].

- The sun transforms 700 million tonnes of hydrogen into 695 million tonnes of helium every second.

$$\mathbf{4\,{}_1^1H \rightarrow {}_2^4He + 2e^+ + 2\upsilon e + 2,5.10^{12}\ J/mole}$$

- The sun: Are approximately 26,000 light-years from the galactic center.
- The sun diameter: 1. 39 million km (10^9 x D_{Earth}).
- The sun mass: (1.989±0.004) x 10^{30} kg, equivalent 2.0 × 10^{30} kg = 300 Jupiter = 90,000 Earths).
- Power radiated by the Sun: The luminosity of the Sun is about 3.86 x 10^{26} watts.
- The Earth receives 1353 $J.m^{-2}.s^{-1}$ of incoming solar radiation at the upper atmosphere. Approximately 30% is reflected back to space while the rest is absorbed by clouds, oceans and land masses.
- Temperature at the Center of the Sun: The temperature at the center (core) of the Sun is about 15,000,000 K.
- Surface temperature of the sun: The temperature at the surface of the Sun is about 10,000 Fahrenheit (5,600 Celsius).
- The age of the Sun: The sun was born about 4.6 billion years ago.
- Surface area of the Sun : 6.09×10^{12} km^2; 12,000 × Earth.
- Density: not meaningful to give average because varies by orders of magnitude from surface to center.

I. 3. Interior structure of the Sun

(The solar ray)

I. 3. 1. Anatomy of the Sun

The Sun, like other stars, is a huge spherical object made of hydrogen and helium. Its diameter reaches 1.400.000 km, or 10^9 times the Earth's diameter; but is 4 times less dense than the Earth due to its composition. The Sun is not only made of the glowing gas that we see with a telescope. It has, exactly like the Earth, different layers at different temperatures. Every layer has its own features which makes them interesting. Below is a figure of the structure of the Sun with all the different layers and components named [4 & 5].

The core is where nuclear fusion takes place. The energy emitted by the surface represents energy transported from the core through the radiative zone, the convection zone, and finally the photosphere, which by definition is the thin atmospheric layer that is thin enough for the radiation to escape.

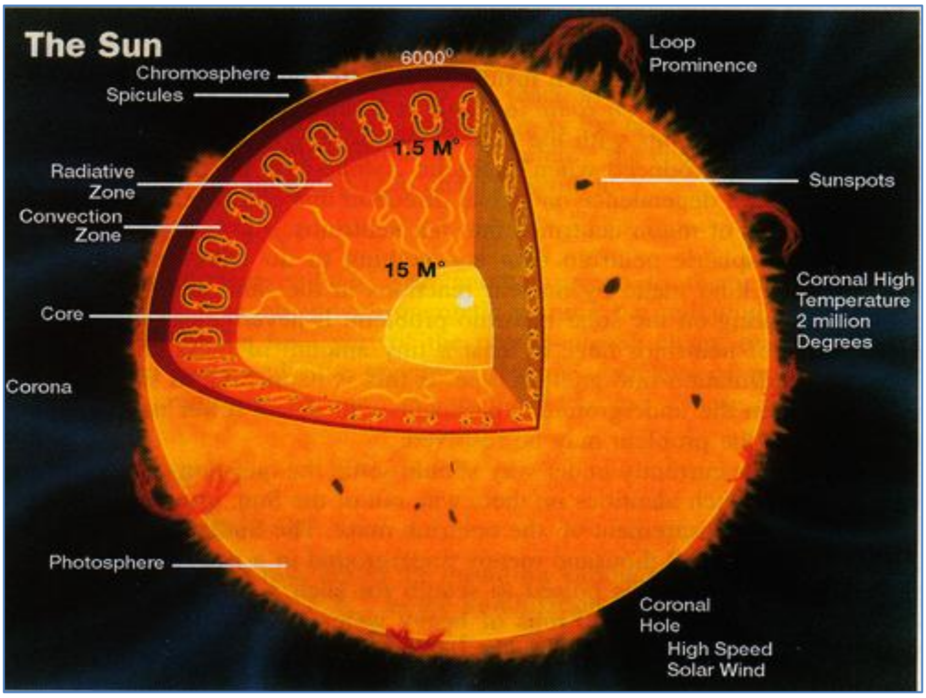

Figure I.4: A slice of the Sun. The nuclear fusion reactions occur in its center [5].

It is in the center of the sun that thermonuclear fusion reactions transmute Hydrogen into Helium, producing the energy and radiation of our star. These reactions are confined in an environment where the density is extreme and the temperature reaches 15 million Kelvins. The energy produced passes slowly through the sun to reach the surface layers and is then emitted in the form of radiation that we receive.

The relationship between mass and energy comes from Einstein's famous equation:

$$E = mc^2$$

In this equation, c is the speed of light, which is a very large number. What this equation is telling us is that a small amount of mass is the equivalent of a large amount of energy-tapping into that energy is how the Sun keeps shining so long.

I. 3. 2. Inner layers and the core

The core of the Sun is the source of all its energy. The amount of energy produced is nearly continuous, so we do not see a considerable variation in its brightness or the heat that is given off. The core has a very high temperature and the material it is composed of is very dense due to the extremely high pressure. It is the combination of these two properties that creates an environment where nuclear reactions can take place. These nuclear reactions always produce heavier elements on the periodic table.

I. 3. 3. Radiative and convective zones

The radiative zone

The transport of energy from the Sun's core (where it is produced) to the regions that surround it can be done by transferring it by radiation. This is how it travels from the center of the Sun to the outer regions, hence the name "radiative zone". Through this area of the solar interior, the energy (in the form of radiation) is transmitted by its interaction with the particles in the surrounding. Some atoms are able to remain intact in the radiation zone, since the temperature is slightly cooler than what it is in the core. These particles are capable to absorb energy, stock it for a short time, and then later release that energy as new radiation. In this way the generated energy in the core is passed from one atom to another, wandering on an upwards path, through the radiation zone.

The convective zone

The energy that is initially created in the core needs a new transport mechanism to carry on its passage to the Sun's surface once it is out of the radiation zone. This is necessary since the temperature is relatively cool outside of the radiation zone (2 million degrees Kelvin compared to 5 million in the radiation zone). Atoms will absorb energy much more easily at this temperature, but they do not release it so readily since their surrounding is cool and dense. Therefore, the energy transfer by radiation slows down considerably. The atoms are heated up by absorbing the and rise through the convection zone, bringing this energy (heat) towards the surface.

I. 3. 4. Photosphere, Chromosphere and Corona

The Photosphere

The photosphere is also named the apparent surface of the Sun. Since the Sun is wholly made of gas, there is no solid surface (like there is on Earth). However, when we observe the Sun, there is a depth past which the density of the gas becomes so high that we cannot see through it. This region is called the photosphere, or as mentioned the apparent surface. This is the disk that one sees in the sky when one looks at the Sun through a telescope that has a filter, or as a projection on, for example, a sheet of paper.

The Chromosphere

The chromosphere is the layer above the photosphere and is thicker than it. With a very low density, it´s impossible to observe it without narrowband filters or during a total solar eclipse due to the brightness of the photosphere behind it. Furthermore it's less dense than the photosphere.

The Corona

It is the biggest and least dense structure of the Sun and it surrounds it. Composed of plasma escaping from the Sun that reaches 1.000.000 kelvin, but with a density even lower than the chromosphere. Furthermore, the solar wind transports the material of the corona out to the interplanetary medium. From Earth, the corona is only visible during a total solar eclipse.

Table I.1: Temperature, density and size of every layer of the Sun [6].

Type of radiation	Temperature	Thickness of the layer	Density
Photosphere	8000 – 4500 K	500 km	~10^{-4} kg/ m^3
Chromosphere	4500 - 20000 K	1600 km	~10^{-8} kg/ m^3
Transition Zone	20000 – 10^6 K	100 km	~10^{-10} kg/ m^3
Corona	10^6 - 3x10^6 K	> 10^7 km	~10^{-13} kg/ m^3

I. 4. Solar radiation

(The light and energy aspects of the sun)

The sun sends energy to Earth in a few different ways: visible light that you can see, infrared radiation that you feel as heat, and rays of UV radiation that you can't see or feel. Fortunately, the Earth's atmosphere protects us from most UV radiation. While we need some exposure to sunlight to help our bodies make vitamin D, too much UV is dangerous.

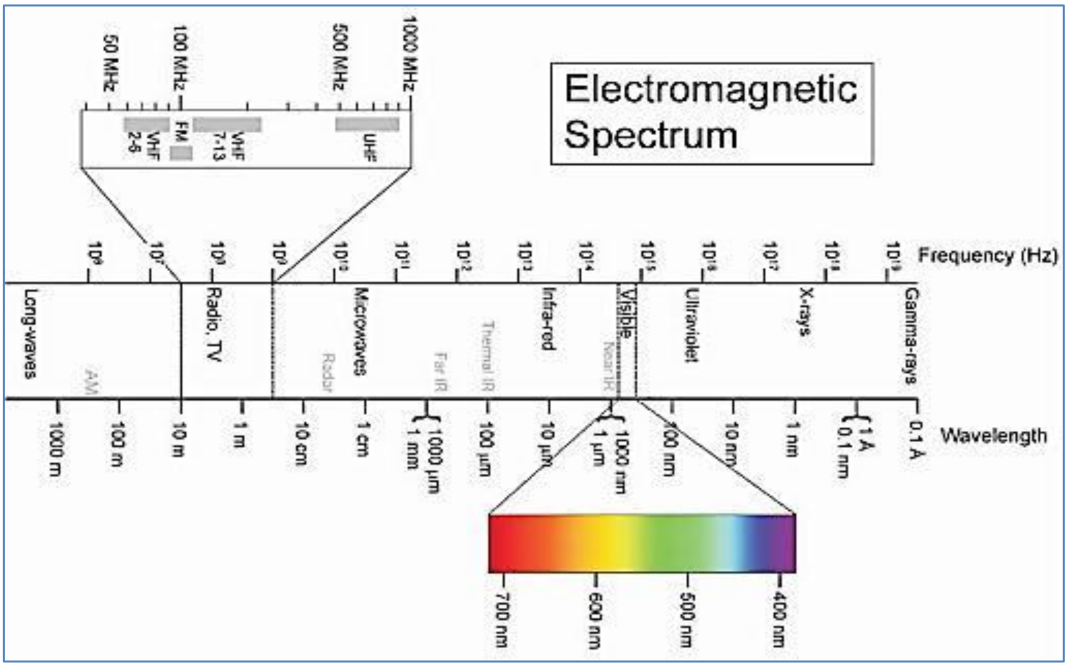

Figure I.5 : Electromagnetic wave spectrum [6].

There are three types of UV rays:

Ultraviolet A rays (UVA)

- The atmosphere does little to shield these rays—most UVA radiation reaches Earth's surface.
- UVA rays cause skin aging and eye damage, and can lower your body's ability to fight off illness. UVA rays also contribute to the risk of skin cancer.
- Ultraviolet B rays (UVB)
- The Earth's atmosphere shields us from most UVB rays—the amount of UVB rays that reach the Earth's surface depends on latitude, altitude, time of year and other factors.
- UVB rays cause sunburns, skin cancer, skin aging, and snow blindness (a sunburn to your cornea that causes a temporary loss of vision) and can lower your body's ability to fight illness.
- Ultraviolet C rays (UVC)
- UVC rays do not reach the Earth's surface because they are completely absorbed by the atmosphere.
- Harmful effects from UVC rays are minimal.

The UV radiation that reaches the Earth's surface is mostly UVA and some UVB. Almost half the daytime total of the more harmful UVB radiation is received between the hours of 10 a.m. and 4 p.m. Even on a cloudy day, you can be sunburned by UVB radiation.

The most energetic waves that exist are gamma rays. These rays are extremely dangerous but the atmosphere stops almost all of the gamma rays emitted by the sun. These rays are also produced during nuclear reactions.

Table I.1 : Distribution of electromagnetic waves according to their wavelength [6].

Electromagnetic wave		Wavelength in meters
Cosmic rays, Gamma rays, X-rays		10^{-10}à 10^{-9} m
UV C,B,A		0,2 à $0,3.10^{-6}$m
Visible (blue, yellow, red)		0,38 à $0,76.10^{-6}$m
Infrared	short	2.10^{-6}m
	Way	4.10^{-6}m
	long	10.10^{-6}m
Hertzian waves	UHF	About 1m
	HF	Of the order of 10 to 100 m
	LF	Of the order of 1000 to 10000 m

I. 4. 1. Electromagnetic solar radiation

The Sun also emits heat radiation with a lower energy than visible light. We call it infrared light or infrared radiation. We feel it as heat on our skin, similar to the invisible heat radiation of a hot plate. The radiation of the Sun rushes with the unbelievable speed of 300,000 km/s (speed of light) through space and covers a distance of 150 million kilometers from the Sun to the Earth in about 8 minutes.

Solar radiation is electromagnetic radiation in the 280...3000 nm wavelength range. The solar spectrum includes a small share of ultraviolet radiation (280...380 nm) which is invisible to our eyes and comprises about 5% of the solar spectrum, the visible light which range from 380 to 780 nm and accounts for around 43% of the spectrum and finally of infrared radiation with long wavelength (780...3000 nm), which makes up most of the remaining 52% of the solar spectrum.

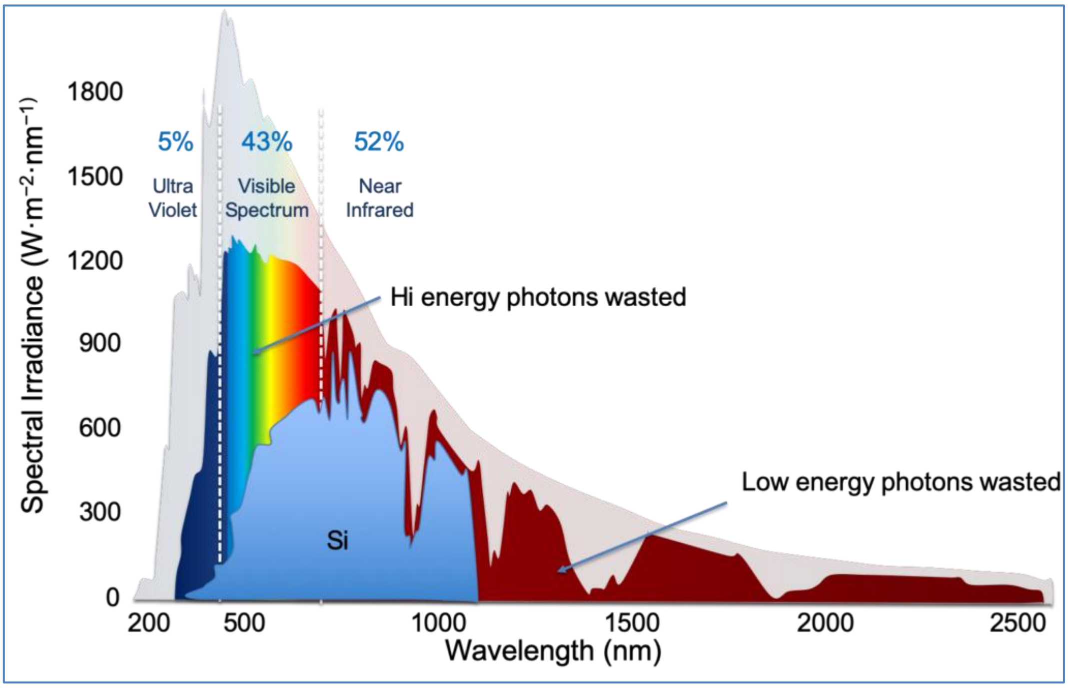

Figure I.6 : The spectral distribution of solar electromagnetic radiation [7].

We notice that the solar spectrum is different depending on whether we observe it from space or from Earth: the Earth's atmosphere therefore interacts with electromagnetic radiation.

The surface temperature of stars being very variable (between 3000 and 50,000 K depending on the star mass), there will also be a great diversity of stellar energy spectra.

Wien’s law, also called Wien’s displacement law, relationship between the temperature of a blackbody (an ideal substance that emits and absorbs all frequencies of light) and the wavelength at which it emits the most light. It is named after German physicist Wilhelm Wien, who received the Nobel Prize for Physics in 1911 for discovering the law.

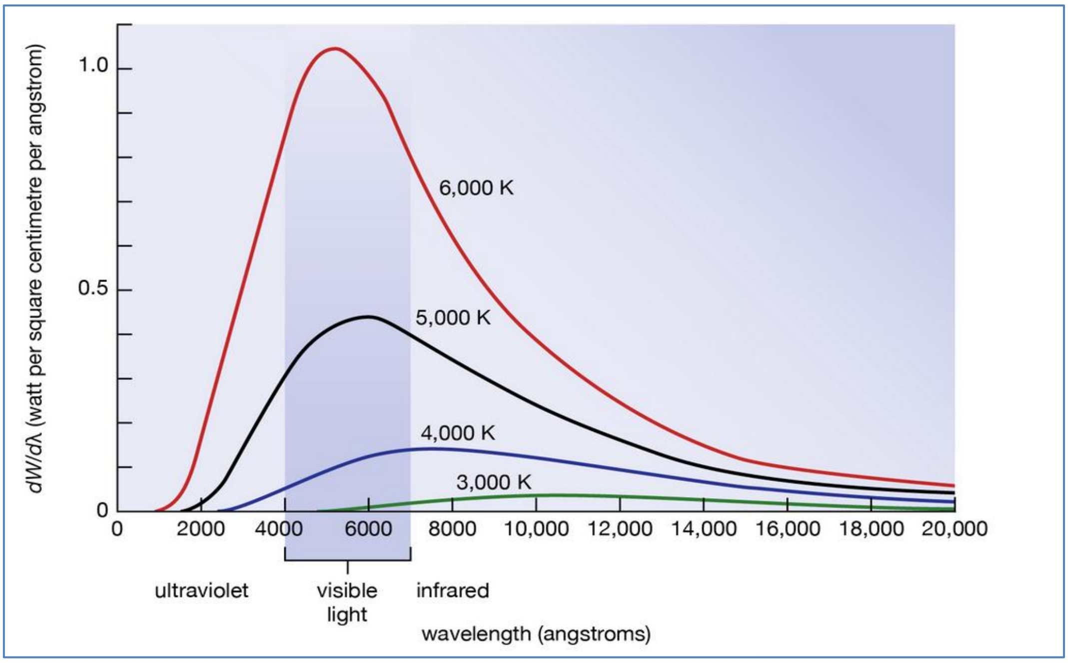

Figure I.7 : The solar spectrum as a function of temperature.

Wien studied the wavelength or frequency distribution of blackbody radiation in the 1890s. It was his idea to use as a good approximation for the ideal blackbody an oven with a small hole. Any radiation that enters the small hole is scattered and reflected from the inner walls of the oven so often that nearly all incoming radiation is absorbed and the chance of some of it finding its way out of the hole again can be made exceedingly small. The radiation coming out of this hole is then very close to the equilibrium blackbody electromagnetic radiation corresponding to the oven temperature. Wien found that the radiative energy dW per wavelength interval dλ has a maximum at a certain wavelength λm and that the maximum shifts to shorter wavelengths as the temperature T is increased. He found that the product λm_T is an absolute constant: λ_{mT} = 0.2898 centimetre-degree Kelvin.

I. 4. 2. Three laws of Radiation

Thermal radiation is a phenomenon characterized by an exchange of electromagnetic energy, without the intermediate medium necessarily participating in this exchange. For example, solar radiation is capable of heating the earth although the medium traversed is at a lower temperature than the earth.

Thermal energy is disordered energy. The temperature is a measure of this internal, disordered energy. The absolute temperature of any substance is proportional to the average kinetic energy associated with the random motion of the substance.

Despite the great diversity of experimental facts highlighting the energy properties of electromagnetic radiation, the scientific laws of thermal radiation only date from the end of the XIXth century [7].

- **1879 Stefan-Boltzmann:** gives the total energy being emitted at all wavelengths by the body.
- **1895 Rayleigh and Wien:** gives the wavelength of the peak of the radiation distribution.
- **1900 Planck:** gives the intensity of radiation emitted by a blackbody as a function of wavelength for a fixed temperature. The Planck law gives a distribution, which peaks at some wavelength.

- **Stefan–Boltzmann Law 1879**

(Total energy emittance)

According to Stefan Boltzmann law, the amount of radiation emitted per unit time from an area A of a black body at absolute temperature T is directly proportional to the fourth power of the temperature.

$$\mathbf{P = S.\sigma.T^4}$$

- where σ is Stefan’s constant σ = 5.67 × 10-8 W/m2 k4
- P is Power radiated.
- S is the surface area of a blackbody.
- T is temperature.

Stefan Boltzmann Law relates the temperature of the blackbody to the amount of the power it emits per unit area. The law states that: ***“The total energy emitted/radiated per unit surface area of a blackbody across all wavelengths per unit time is directly proportional to the fourth power of the black body’s thermodynamic temperature [8].”***

$$\boldsymbol{\varepsilon = \sigma.T^4}$$

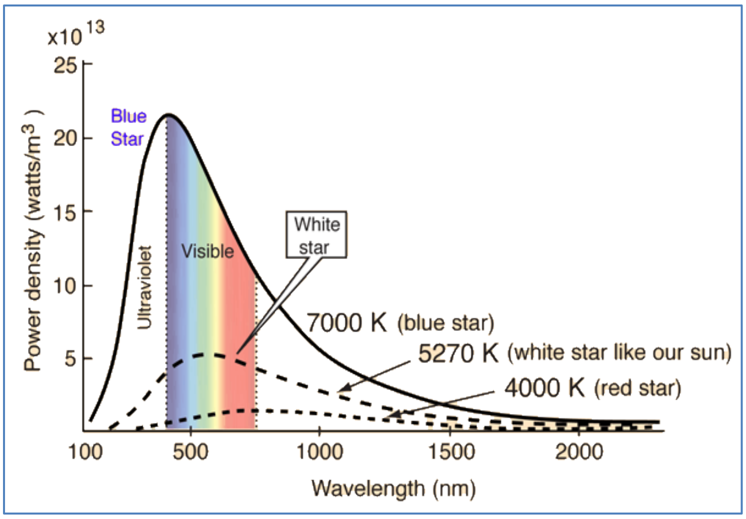

Figure I.8 : Josef STEFAN (1838 - 1893) Total power as a function of the temperature of a black body [8].

Stefan-Boltzmann's law applied to the Sun:

- The ray of the Sun $r = 6{,}960.10^{8}\,\mathrm{m}$
  The surface of the Sun is $S = 4.\pi.r^{2}$
  $= 4.\pi.(\,6{,}960.10^{8})^{2}$

The total energy radiated by the sun is:

$$P_{Sun} = S.\,\sigma.\,T_{sun}^{\;4}$$
$$= 4.\pi.(\,6{,}960.10^{8})^{2} \times 5.67 \times 10^{8} \times (5800)^{4}$$
$$= 3.94.10^{26}\ \mathrm{W}$$

- **Wein's Law 1895**

(Value of λ_{max} as a function of T)

The wavelength λmax (µm) which corresponds to the maximum radiation emitted by a black body, is inversely proportional to its absolute temperature T (K).

$$\lambda_{max} = \frac{\sigma_w}{T} = \frac{2898}{T}$$

σ_w : Wien constant (σ_w = 2898m.K)

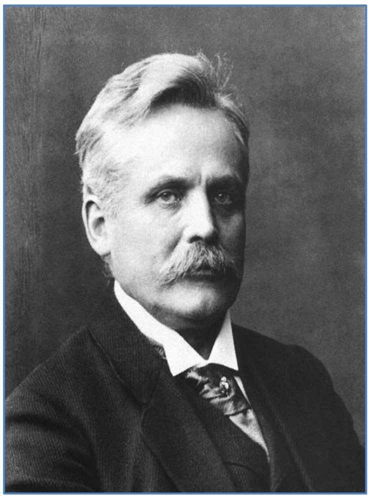

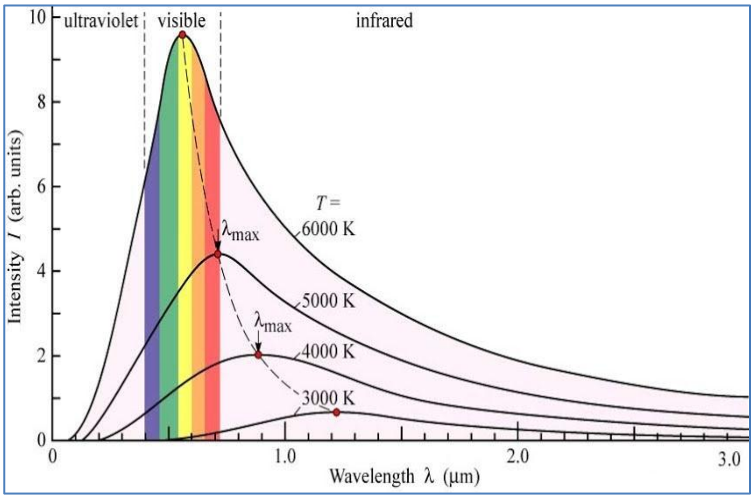

Figure I.9 : Wilhelm WIEN (1864 - 1928) black body spectral density [8].

This law shows that λ_{max} moves towards short wavelengths when the temperature rises.

λ_{max} = 0.5 μm for the sun at T = 5800 K

This maximum intensity for a given wavelength gives the body its dominant color.

Wien's law applied to the Sun:

$$\lambda_{max} = \frac{\sigma_W}{T_S} = \frac{2898}{T_S}$$

$$= \frac{2898}{5800}$$

$$= 0{,}499\ \mu m$$

The maximum solar emission is observed at λ_{max} = 0.499 μm. Form Wien's Law it follows that the Sun's temperature is about 5800 K.

- **Planck's Law 1900**

(The emittance of the black body as a function of the wavelength λ and at its absolute temperature T)

The spectral distribution of the light emitted by a black body only depends on its temperature. For each wavelength λ of a black body of temperature T gives a radiation of intensity Iλ.

Classical physics assumed that radiation is emitted continuously by the matter with smooth continuous spectrum of all possible energy levels.

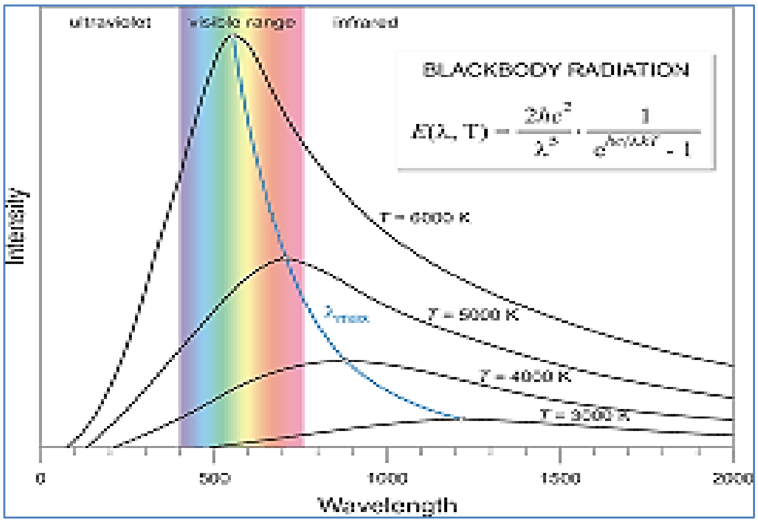

Figure I.10 : Max Planck (1858-1947) Energy distribution of black bodies as a function of temperature [8].

In 1900, Max Planck postulated that the electromagnetic energy is emitted not continuously (like by vibrating oscillators), but by discrete portions or quants. Quantum mechanics was born! Planck's Law states that:

$$\mathbf{I_\lambda = \frac{2.h.c^2}{\lambda^5} \frac{1}{e^{\left(\frac{h.c}{\lambda.K.T}\right)} - 1}}$$

Where :

h : Is the Planck's constant (h= 6,626. 10^{-34}J. S)

k : Boltzmann constant (k= 1,380. 10^{-23}J.K^{-1})

c : Speed of light in vacuum (c = 2,998. 10^{8}m.s^{-1})

Light is emitted in quants and can be considered not only as a wave-like entity but also as a particle, or photon, with the energy given by the Planck Einstein relation:

$$\mathbf{E = h.\upsilon = \frac{h.c}{\lambda}}$$

I. 4. 3. Extraterrestrial solar insolation (I_0)

For many radiation calculations it is useful to know the extraterrestrial radiation on the horizontal plane. The extraterrestrial solar insolation or solar constant is the power received by the earth outside the atmosphere, is the total energy received in one minute upon a unit of surface perpendicular to the sun's rays, in free space at the earth's mean distance from the sun.

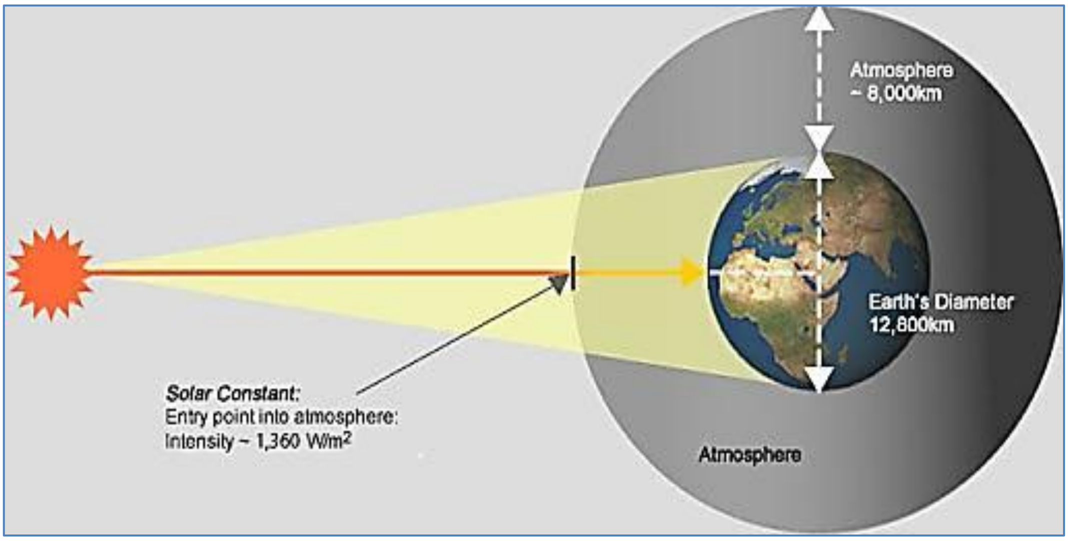

Figure I.11: Extraterrestrial solar radiation outside of the earth's atmosphere [9].

Before reaching the ground, the solar radiation was partly absorbed by the atmosphere. This absorption depends on the thickness of the atmosphere crossed and the purity of the sky, and the thickness of the atmosphere crossed depends on the inclination of the solar rays which is given by the zenith distance Z [9].

When the Sun is overhead, 100% of a beam of Cosine Law of sunshine intensity Copyrighted Material, from internet width, I0 strikes a piece of ground of width, I0.

As the Sun goes down and Zenith Angle, Z increases, progressively less of the sunbeam of width I0, strikes the piece of ground. More of the sunbeam misses that piece of ground and is lost [9].

Z = 90° - h (with h: height of the sun on the horizon in (°)).

$$\textit{COSINE LAW} \quad \boldsymbol{I_z = I_0 \cos(Z)}$$

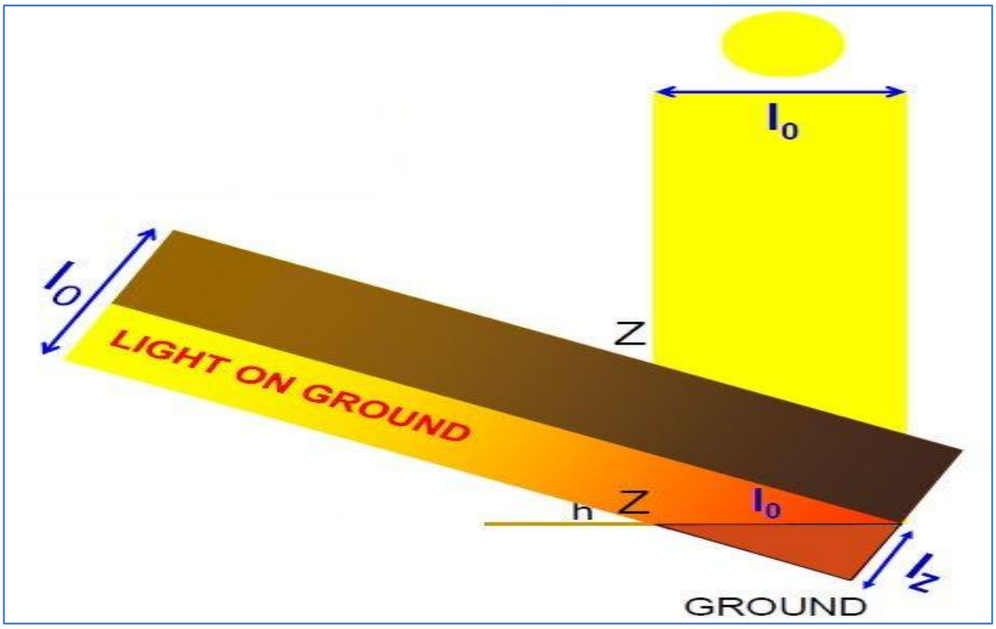

Figure I.12: The fraction of the sunbeam that strikes the ground [10].

The surface found at the limit of the atmosphere and at an average distance of 150x10^6km (average distance from Earth to Sun) [9].

$$\mathbf{I_0} = \frac{\epsilon.\sigma.T_s{}^4.4\pi.R_s{}^2}{4\pi.(d_{s-t})^2}$$

$$\mathbf{I_0} = \frac{\epsilon.\sigma.T_s{}^4.R_s{}^2}{(d_{s-t})^2}$$

$$\mathbf{I_0} = \frac{1.(5{,}67 \times 10^{-8}).(5800)^4.(696.10^6)^2}{(1{,}5 \times 10^{11})^2}$$

$$\mathbf{I_0} = 1367\ w/m^2.$$

$\mathbf{I_0}$: Intensity of solar energy falling on a surface which is perpendicular to the sun's rays.

ϵ : Sun surface emissivity (≊1,0).
σ : Stefan-Boltzmann constant.
$\mathbf{T_s}$: Sun surface temperature.
$\mathbf{R_s}$: Sun Ray.
$\mathbf{d_{S-E}}$: Average distance between the earth and the sun.

I. 5. D*epletion of solar radiation*

(Energy Balance of the Earth)

While the solar radiation incident on the Earth's atmosphere is relatively constant, the radiation at the Earth's surface varies widely due to:

- Atmospheric effects, including absorption and scattering;
- Local variations in the atmosphere, such as water vapor, clouds, and pollution;

- Latitude of the location;
- The season of the year and the time of day.

The above effects have several impacts on the solar radiation received at the Earth's surface. These changes include variations in the overall power received, the spectral content of the light and the angle from which light is incident on a surface. In addition, a key change is that the variability of the solar radiation at a particular location increases dramatically. The variability is due to both local effects such as clouds and seasonal variations, as well as other effects such as the length of the day at particular latitude. Desert regions tend to have lower variations due to local atmospheric phenomena such as clouds. Equatorial regions have low variability between seasons.

The maximum value of solar radiation is approximately 1415 W/m² at the summer solstice in June and the minimum value of 1326 W/m² at the winter solstice in December to which an uncertainty of 10 W/m² must be added. Of the 342 W/m^2 that the earth receives from the sun alone 160 W/m^2 reaches the ground while 102 W/m^2 are reflected (82 W/m^2 by the atmosphere and 20 W/m^2 by the earth's surface) and 80 W/m^2 are absorbed by ozone in the stratosphere, water vapor and carbon dioxide from the troposphere. For the earth to reach a temperature of 15 °C, it would take 490 W/m^2. The missing 330 W/m^2 are supplied by the atmosphere and constitutes what is called the greenhouse effect [4 & 11].

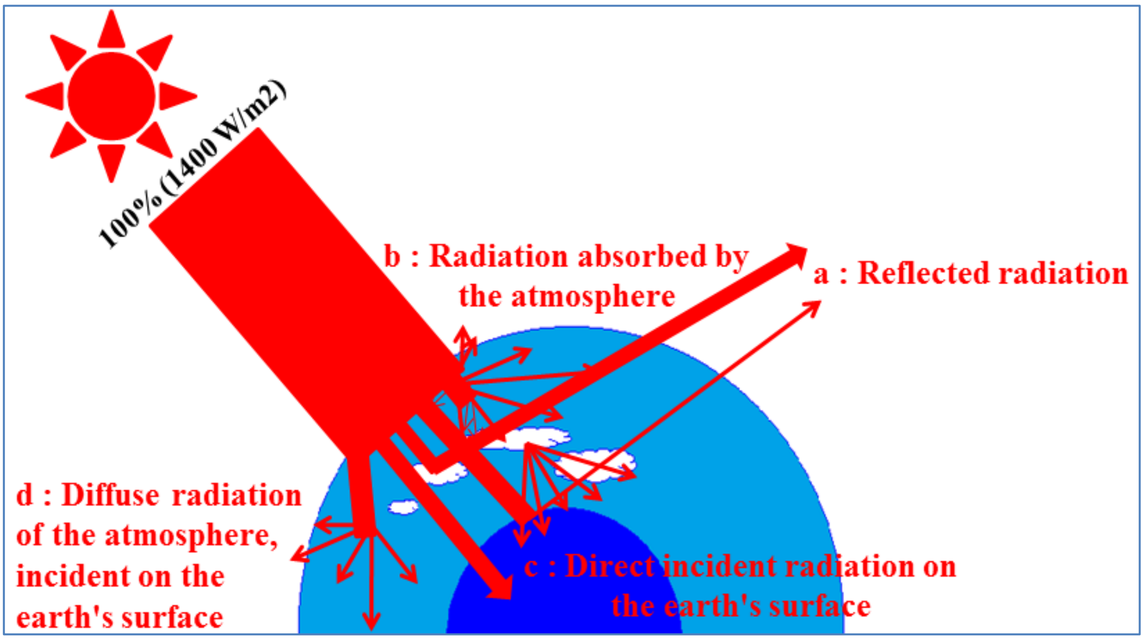

Figure I.13: Components of the energy balance of the earth.

- ***Direct-beam radia***tion: that passes in a straight line through the atmosphere to the receiver.

- ***Diffuse radiation:*** that has been scattered by molecules and aerosols in the atmosphere.
- ***Reflected radiation:*** that has bounced off the ground or other surface in front of the collector.

The atmosphere can be seen as a selective filter with different wavelengths. There are physical processes that affect the atmospheric transmittance, and they do not allow a transmittance of 100% [12].

I. 5. 1. Absorption

(By gaseous components and solid and liquid particles)

Solar Radiation transfers energy to the particles of the atmosphere, increasing the kinetic energy (translational, vibrational and rotational). It has entered the atoms excitation by electromagnetic radiation. These particles can be molecules of dust, gases, and water droplets. Absorption causes the attenuation of solar radiation. Every time a gas absorbs radiation originates internal molecular movement which macroscopically causes an increase in temperature.

Specific gasses, notably ozone (O3), carbon dioxide (CO2), and water vapor (H2O), have very high absorption of photons that have energies close to the bond energies of these atmospheric gases. This absorption yields deep troughs in the spectral radiation curve. For example, much of the far infrared light above 2 µm is absorbed by water vapor and carbon dioxide. Similarly, most of the ultraviolet light below 0.3 µm is absorbed by ozone (but not enough to completely prevent sunburn!) [13].

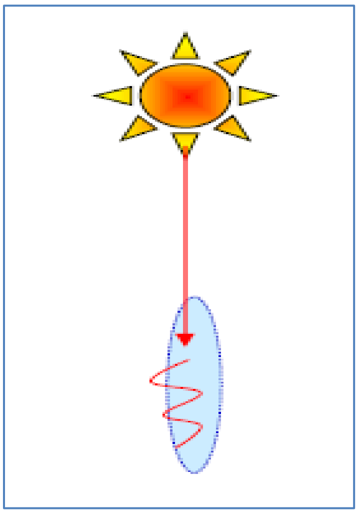

Thus, we can distinguish 4 types of absorption according to the energy of the incident photon:

- **Ultraviolet:** the molecules are dissociated, the absorption is not quantified.
- **Visible:** molecules change their electronic configuration, the absorption is quantified.
- **Infrared:** the molecules vibrate. The absorption is quantified.
- **Microwave:** the molecules rotate. The absorption is quantified.

While the absorption by specific gasses in the atmosphere change the spectral content of the terrestrial solar radiation, they have a relatively minor impact on the overall power.

Instead, the major factor reducing the power from solar radiation is the absorption and scattering of light due to air molecules and dust. This absorption process does not produce the deep troughs in the spectral irradiance, but rather causes a power reduction dependent on the path length through the atmosphere. When the sun is overhead, the absorption due to these atmospheric elements causes a relatively uniform reduction across the visible spectrum, so the incident light appears white. However, for longer path lengths, higher energy (lower wavelength) light is more effectively absorbed and scattered. Hence in the morning and evening the sun appears much redder and has a lower intensity than in the middle of the day.

I. 5. 2. Dispersion

Occurs when particles of the atmosphere reflect back the solar radiation. The dispersion shows no absorption but it causes an attenuation of solar radiation because radiation is redirected. Hence, a photon meets an obstacle without being absorbed, changing only the direction of travel. This action is known as dispersion. The degree of dispersion is dependent on the transmissivity of a wavelength. The dispersion of large wavelengths is smaller. Very small gas molecules, compared to the wavelength. It causes that solar radiation is dispersed in all directions (back and forth). This phenomenon is known as Rayleigh scattering. The Rayleigh scattering is significant only for short waves (=0.6nm) having little effect on atmospheric transmittance.

During its atmospheric crossing, the radiation can interact with particles and molecules in the atmosphere that act as barriers to the propagation of energy [13].

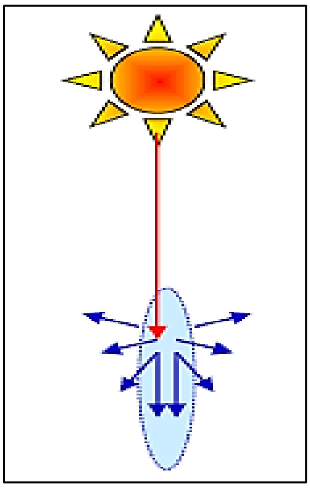

When radiation is not absorbed, it can be partially deflected in all directions. It is the phenomenon of atmospheric diffusion, the nature of which depends on several parameters:

- The wavelength of the radiation.
- The density and size of atmospheric particles and molecules.
- The thickness of the atmospheric layer to be crossed.

Scattering is the redirection of electromagnetic energy by suspended particles in the atmosphere. The type and amount of scattering that occurs depends on the size of the particles and the wavelength of the energy. There are three main types of scattering that impact incoming solar radiation:

Rayleigh scattering:

Rayleigh scattering refers to the scattering of light off of the molecules of the air, and can be extended to scattering from particles up to about a tenth of the wavelength of the light. It is Rayleigh scattering off the molecules of the air which gives us the blue sky.

Rayleigh scattering can be considered to be elastic scattering since the photon energies of the scattered photons is not changed. Scattering in which the scattered photons have either a higher or lower photon energy is called Raman scattering. Usually this kind of scattering involves exciting some vibrational mode of the molecules, giving lower scattered photon energy, or scattering off an excited vibrational state of a molecule which adds its vibrational energy to the incident photon.

The scattered intensity is then inversely proportional to the power of 4 of the wavelength of the incident radiation ($D \approx \lambda^{-4}$).

Mie Scattering:

The scattering from molecules and very tiny particles (<1/10 wavelengths) is predominantly Rayleigh scattering. For particle sizes larger than a wavelength, Mie scattering predominates. This scattering produces a pattern like an antenna lobe, with a sharper and more intense forward lobe for larger particles.

Mie scattering is not strongly wavelength dependent and produces the almost white glare around the sun when a lot of particulate material is present in the air. It also gives us the white light from mist and fog.

Non-Selective Scattering:

Non-selective scattering occurs when the diameter of the particles in the atmosphere are much larger than the wavelength of radiation. Non-selective scatter is primarily caused by water droplets in the atmosphere. Non-selective scattering scatters all radiation evenly through out the visible and infrared portions of the spectrum - hence the term non-selective. In the visible wavelengths light is scattered evenly, hence fog and clouds appear white. Since clouds scatter all wavelengths of light, this means that clouds block most energy from reaching the Earth's surface.

This can make interpreting and analyzing remote sensed imagery difficult in areas prone to cloud and fog cover. Clouds also cast shadows that change the illumination and relative reflectance of surface features. This can be a major limitation in remote sensing imagery.

I. 5. 3. Reflective Earth

Any object that can absorb radiation will also reflect some of that radiation. This is the reason why, from space, Earth appears bright and glowing, reflecting away some of the Sun's light. Earth's albedo, the amount of radiation reflected, is about 30% of the total incoming radiation from the Sun. The other 70% of the radiation is absorbed. The reflected radiation simply bounces off of Earth's atmosphere and is re-emitted into space [13].

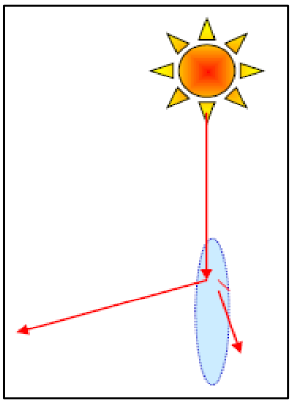

Example of the rainbow, Refraction and reflection of solar rays through a spherical raindrop.

When we look at a rainbow, we see the spectrum of visible colors: red, orange, yellow, green, blue and violet. Every ray of color we see came from the Sun (he was contained in his light) and it was refracted by the water from the rain at an angle all its own.

All objects have some degree of albedo, except for theoretical blackbody objects, which absorb 100% of the radiation it receives and reflect none, hence appearing to be black. A black hole would be one such object, since its gravitation is so strong that no radiation can escape it, much less be reflected.

Conclusion I

The sun provides us with light energy and heat, both necessary to sustain life on Earth. This energy arrives in the form of electromagnetic radiation, and the solar energy is readily harnessed for low temperature heat, and in many places domestic hot water units (with storage) routinely used it. It is also used simply by sensible design of buildings and in many ways that are taken for granted. Industrially, probably the main use is in solar salt production – some 1000 PJ per year in Australia alone (equivalent to two-thirds of the nation's oil use). It is increasingly used in utility-scale plants, mostly photovoltaic (PV). Domestic-scale PV is widespread. However, economic and political reasons are a brake on its exploitation and development. Indeed the countries likely to exploit solar energy on a large scale (the rich countries) would be forced to install their exploitation in the countries having the best solar radiation that is to say in countries close to the Sahara.

However, a solution will have to be taken soon since, according to forecasts, in 2030 world energy demand will be a third higher than today, it is not yet possible for us to say whether solar energy will be able to meet these needs, seen that to date the yields of this energy remains low.

References I

[1] Extrait du livre «le solaire et l'économie mondiale » d'Hermonn Scheer, édition Actes Sud, 2012,

[2] Etude du CEMAGREF- France, réalisée en 2007 Panorama des ordres de grandeurdes réserves et potentiels énergétiques, Ressources documentaires, http://www.pactes-energie.org,

[3] Pierre Chastenay, 'un tour d'horizon du système solaire 'Centre de développement pédagogique, université du Québec- Canada, 2006

[4] J.-M. Malherbe « Service d'Observation du Soleil » Laboratoire d'Etudes Spatiales et d'Instrumentation en Astrophysique l'observatoire de Paris – 2016

[5] M. Aggour, "Energies Renouvelables "Master ER, Faculté des sciences Université Ibn Tofail –Kénitra, 2013.

[6] Hoijeon et Didier Walliang, "Le spectre électromagnétique de la lumière" http://astro.vision.free.fr/spectre.php ,2000

[7] Olivier PERROT, LE RAYONNEMENT, I.U.T de Saint-Omer Dunkerque Département Génie Thermique et énergie2010-2011

[8] J.P. BARDON, Températures de surface, Notions fondamentales (R2730) Edition Techniques de l'ingénieur2010-2011

[9] N.SELAMI et N.BENABADJI, 'Etude des structures nuageuses ', JAS09 de l4AUF, Alger, Novembre 2009.

[10] http://www.photovoltaique.info/Fiscalite.html#Impositiondurevenuphotovoltaque 2008.

[11] Abraham, E. et J. Semonsous, J. -L'Auvergne : Sa géographie, son histoire - Paris : Charles-Lavauzelle et Cie, 1949. - fig. et cartes, carte color. ; 8º. Cote : A 37087. https://www.bibliotheques-clermontmetropole.eu;

[12] Ahmed Ennaoui, "Photovoltaic Solar Energy Conversion (PVSEC)" Helmholtz-Zentrum Berlin für Materialien und Energie- Free University of Berlin- Allemand, 2014,

[13] A. Oudrane, B. Zeghmati, X. Chesneou, B. Aour "Modeling the radiate and energy balance of a building located in the adrar region" collection of mechanics, El Wancharissi University Center of Tissemsilt vol .1 n° 002 (2017),

[14] A. Djafour, Thesis "Study of a solar hydrogen system" University of Kasdi Merbah-Ouergla, 2013, pp. 10-12,

[15] Alain Ricaud Jan, "Gisement solaire et transferts énergétiques," Master Renewable Energies University of Cergy-Pontoise, 2011,

[16] EL-ASSEFRY Karim & M'HAMDI Kamilia, "Etude, conception et dimensionnement de la deuxième tranche du projet solaire d'OUARZAZATE : La centrale photovoltaïque 100 MW," Phd, Ecole Nationale de l'Industrie Minérale (E.N.I.M.), 2011, pp.18,

[17] Bendjellouli Zakaria, "Contribution à la modélisation d'une cellule solaire" Mémoire deMagister, Université de BECHAR – Algérie - Faculté des Sciences et Technologie, 2009, pp. 8-10,

[18] Schonhauser Allee 10-11"ReGrid : grid integration of renewables", Renewables Academy (RENAC) AG, 2014.

[19] S. Yohann, T. Alistair, R. Giovan “Projet 1004 : Conception d’un dispositif optique pour l’amélioration de la performance énergétique d’un site de production d’électricité photovoltaïque”, Département Génie Thermique Energétique, 2009/2010.

[20] INFOS FICHES-ENERGIER"le Photovoltaique facteurs influençant la production", Bruxelles Environnement, 2014.

http://maroc.energie-ren.com/salon/politique-energetique-du-maroc/la politique-energetique-du-maroc

http://www.pactes-energie.org,

http://astro.vision.free.fr/spectre.php

http://www.goodprepa.tech 2017

http://www.photovoltaique.info/Fiscalite.html#Impositiondurevenuphotovoltaque 2008.

http://www.ef4.be/fr/pv/composants-dun-systeme/orientation-structure.html.

http://www.ef4.be/fr/pv/composants-dun-systeme/orientation-structure.html

http://www.photovoltaique.guidenr.fr/cours-photovoltaique.

Chapter II

INVESTIGATION ON SOLAR RADIATION

II. 1. Introduction

Solar energy is the most abundant energy resource on the earth. It is origin of the majority of other renewable energies. The solar radiation can be used to produce the electricity directly by using photovoltaic semiconductors, or thermal solar heat for heating or electricity production. However, this radiation is subject to several disturbances.

The study or applications of solar energy at a given site are dependent on more comprehensive and detailed sunshine data from this site. Each of us constitutes the center of a sphere on which we see the celestial bodies: we call it the local celestial sphere and we will measure the all angles on this sphere, then from these angles and a universe model, deduce the distance of these bright points that we observe.

The local celestial sphere defined by a horizontal plane (the horizon of the place) and a pole: the zenith (Z). The observer is the center of the sphere and a fixed direction is that of the South, defined by the direction in which the stars which rise in the east and set in the west.

In this chapter, we will focus on the geometric aspects of solar radiation intercepted by the earth. The different formulas will therefore make it possible to calculate the position of the sun in the sky, with respect to a face oriented in any way, for a given hour and day at a given latitude.

Using a Matlab code that we have developed, we can calculate and plot the variation of the different solar coordinates as a function of the time.

II. 2. Solar Geometry: Tracking the Sun

The Earth's daily rotation about the axis through its two celestial poles (North and South) is perpendicular to the equator, but it is not perpendicular to the plane of the Earth's orbit. In fact, the measure of tilt or obliquity of the Earth's axis to a line perpendicular to the plane of its orbit is currently about 23.5°.

We call the plane parallel to the Earth's celestial equator and through the center of the sun the **plane of the Sun**.

The Earth passes alternately above and below this plane making one complete elliptic cycle every year.

(Locating Points on the Surface of the Earth)

When describing location, it is common to mention the city, state, or country as a location descriptor. It is also common to talk about landmarks that may be nearby. Another way to describe location is to use reference lines to describe coordinates, or absolute position, on the globe.

Two types of imaginary reference lines are used to locate positions or points and to make accurate globes and maps. These lines are called parallels of latitude and meridians of longitude. Two of these imaginary reference lines, the equator and the prime meridian, are called primary reference lines because they are where we start the numbering system.

II. 2. 1. Latitude and Longitude

A given place on the terrestrial globe will be perfectly defined by the data of its latitude (L) and its longitude (λ):

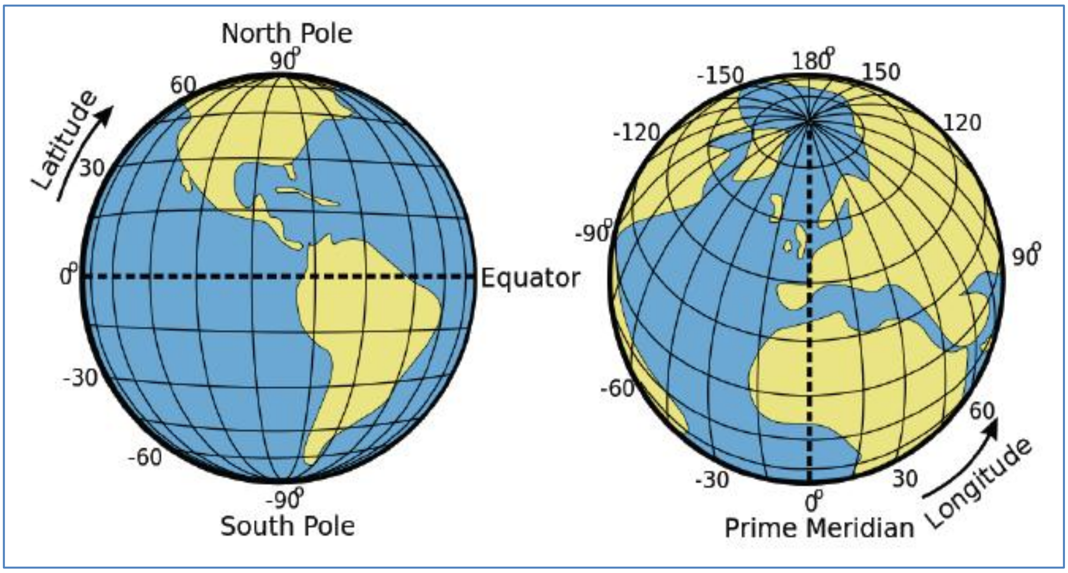

Figure II.14 : Latitude and longitude representation on a terrestrial globe [1].

Latitude (θ): is a point's angular distance from the Equator, where the Equator is an imaginary line that is exactly halfway between the North Pole and the South Pole and runs around the circumference of the Earth. Latitudinal lines are the horizontal lines of the Earth's grid that are parallel to the equator. They are measured in degrees from 0 to 90 degrees north or south of the equator. Points that lie above the Equator are given in degrees north, and points that lie below the Equator are given in degrees south.

Longitude (λ): is the angular distance of a point from the Prime Meridian, where the Prime Meridian is an imaginary line that runs perpendicular to the Equator from the North Pole to the South Pole and passes through Greenwich England. Longitudinal lines, also called meridians, differ from latitudinal lines in that they do not run parallel to the Prime Meridian. They are measured in degrees from 0 to 180 degrees east or west of the Prime Meridian. Points to the east of the Prime Meridian are given in degrees east, and points to the west of the Prime Meridian are given in degrees west [2].

The altitude: This is the vertical distance expressed in meters, separating the point considered in the land relief from the sea level, taken as a reference surface.

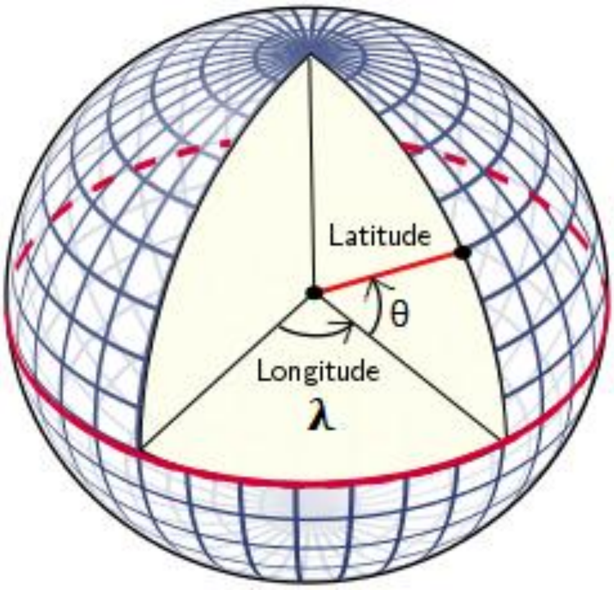

Figure II.15 : Geographical coordinates of the place.

Using latitude and longitude, we can locate points on the Earth's surface using the following format: Latitude Degrees N or S, Longitude Degrees E or W.

II. 2. 2. Apparent Path of the Sun

The sun's position in the celestial sphere is identified at any time of the day by two coordinate systems:

- Equatorial coordinates.
- The horizontal coordinates.
- Latitude (θ) and longitude (λ).

We have developed a code By using Matlab, we can calculate it and plot the different coordinate systems, according to time in our city (Khouribga) of latitude 32°52.8648 'North and Longitude -6°54.378' West.

II. 2. 2. 1. The Equatorial Coordinates

The equatorial coordinates are independent of the position of the observer on the earth, but they are related to the time of observation.

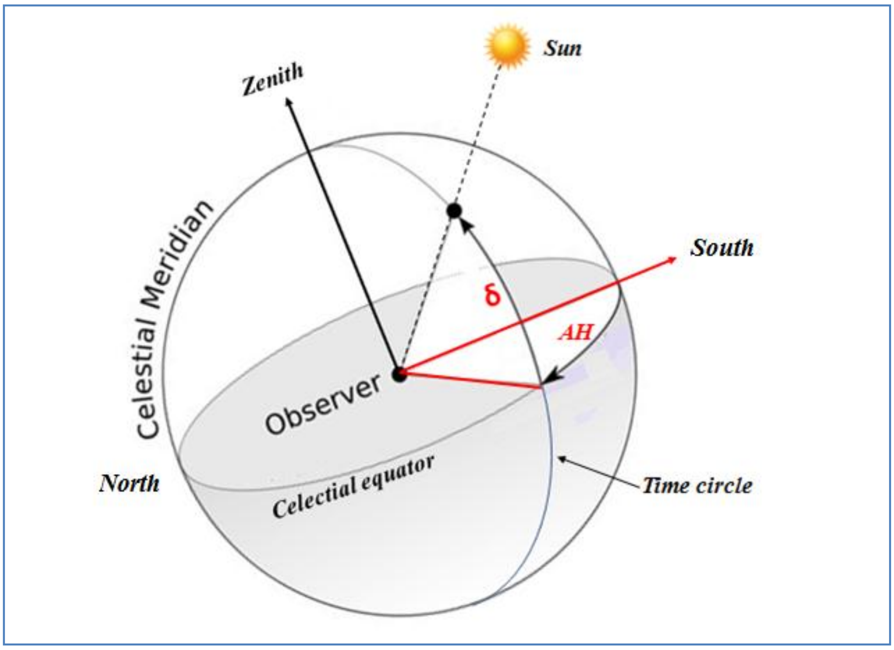

Figure II.16 : Equatorial coordinate frame.

The sun's position is expressed by two angles that are:

A- The Declination δ

Declination (δ) is the angle between the vector "center of the earth-sun" and the equatorial surface of the earth, varies seasonally due to the tilt of the Earth on its axis of rotation and the rotation of the Earth around the sun. If the Earth were not tilted on its axis of rotation, the declination would always be 0°. However, the Earth is tilted by 23.45° and the declination angle varies plus or minus this amount. Only at the spring and fall equinoxes is the declination angle equal to 0° [3].

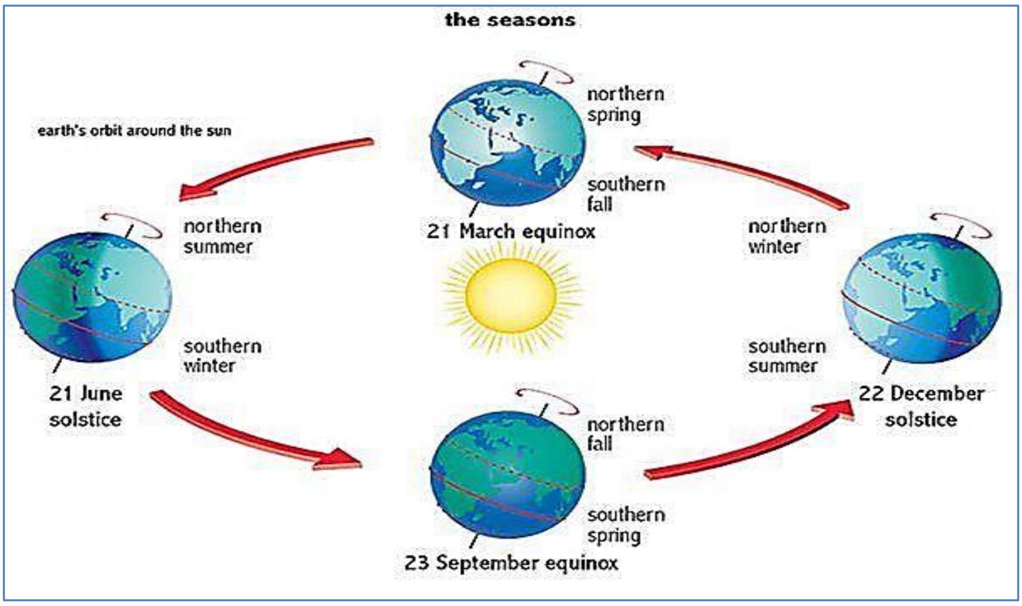

Figure II.17 : Trajectory of the earth around the Sun.

Declination varies from 23°27 'at the summer solstice (June 21-22) to -23°27' at the winter solstice (December 21-22) through the value 0 at the equinoxes (March 21 and September 23):

Spring equinox:	**21 March**	**$\delta = 0$**
Summer solstice:	**22 June**	**$\delta = +23°27'$**
Autumn equinox:	**21 September**	**$\delta = 0$**
Winter solstice:	**22 December**	**$\delta = -23°27'$**

Between these 4 remarkable points, δ takes all the intermediate values which can be calculated by the following relation [3]:

$$\delta = 23.45\sin\left[\frac{360}{365}(j+284)\right] \quad (1)$$

j: is the sequence number of days in the year.

The Sun declination angle, δ, has the range: $-23.5° < \delta < +23.5°$ during its yearly cycle. By using a Matlab code that we have developed, we can plot the value of the solar declination as a function of the number day of the year.

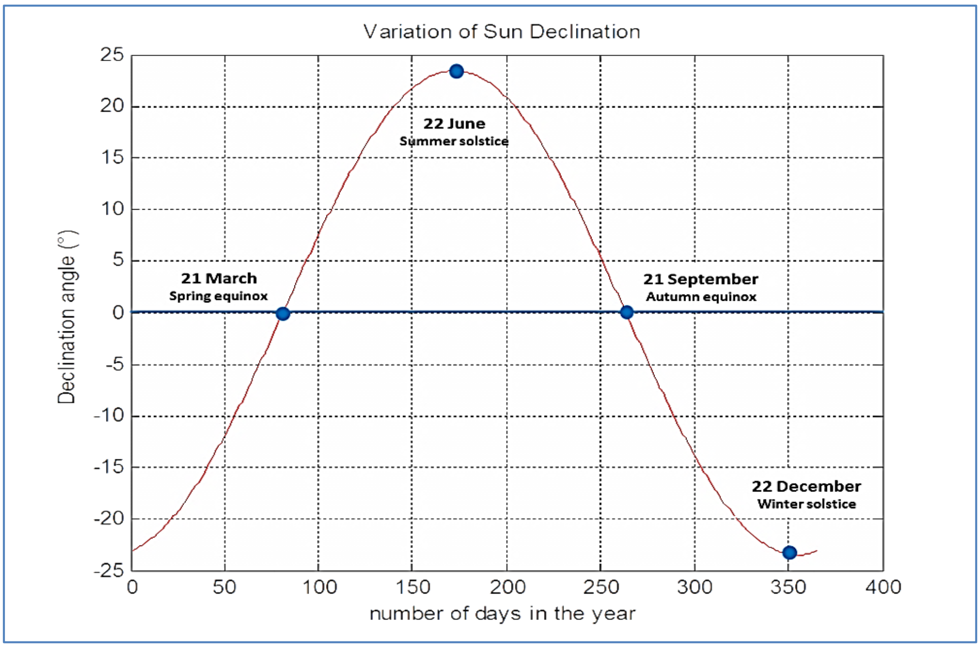

Figure II.18 : Yearly Variation in Declination.

Accurate knowledge of the declination angle is important in navigation and astronomy. For most solar design purposes, however, an approximation accurate to within about 1 degree is adequate.

B- The hour angle AH

The hour angle AH is calculated by the daily rotation of the earth around its axis. It is the measure of the arc of the solar trajectory between the sun and the meridian surface of the place defined by [3]:

$$\mathbf{AH} = 15.(TSV-12) \tag{2}$$

TSV is the local solar time corrected for the time equation, a universal astronomical datum related to the eccentricity of the earth's orbit around the sun.

$$\mathbf{TSV} = TSM+E \tag{3}$$

TSM is the mean solar time,

$$\mathbf{TSM} = TU+\frac{\lambda}{15} \tag{4}$$

TU is the universal time and λ the longitude.

E is the equation of time, which is the value of the difference between true solar time and the mean solar time given by [4]:

$$\mathbf{E} = -9.9\sin 2.(0.986j+100)+7.7*\sin(0.986*j-2)) \tag{5}$$

The hour angle is measured from solar noon, it is positive if it is before noon and negative if it is afternoon (AH is 0° at noon, -90° at 6 p.m. and 90° at 6 a.m., in TSV, each hour shifts it by 15 °, positive in the morning and negative in the afternoon).

II. 2. 2. 2. The Horizontal Coordinates

The horizontal reference is formed by the plan of the astronomical horizon and the vertical of the place.

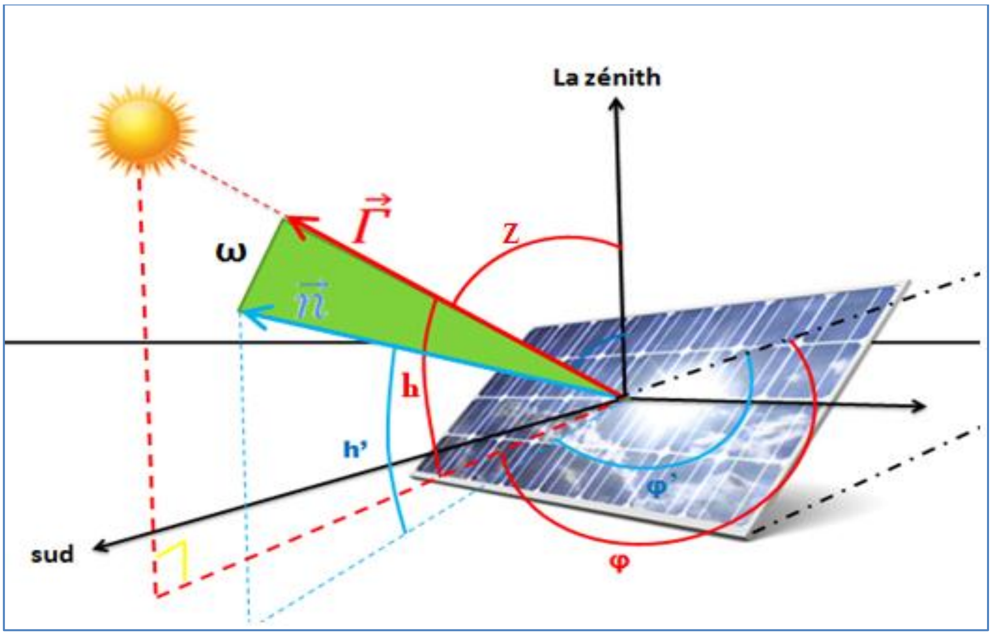

Figure II.19 : The solar horizontal coordinates and the angle of incidence.

In this frame, The Sun spotted by the following sizes:

A- The angle of the solar height – Elevation (h)

The angle of the sun's height (h), or the altitude is the angle between the direction of the sun and the horizontal surface; the elevation h from 0 ° to 90 ° towards the zenith [5].

$$\mathbf{sin(h)} = \sin(\theta)\sin(\delta) + \cos(\theta)\cos(\delta)\cos(Ah) \quad (6)$$

θ is the latitude

B- The zenith angle (Z)

It is the angle between the direction of the sun and the vertical of the place (zenith). The angle Z is complementary to h [5].

$$\mathbf{cos(Z)} = \sin(\delta).\sin(\theta) + \cos(\delta).\cos(\theta).\cos(Ah) \quad (7)$$

We develop a Matlab code that calculates and plots the expression of the height of the sun and the zenith angle for the khouribga city of latitude 32°52.8648 'North and Longitude -6°54.378' West, for the winter solstice (December 21) and the summer solstice (June 21).

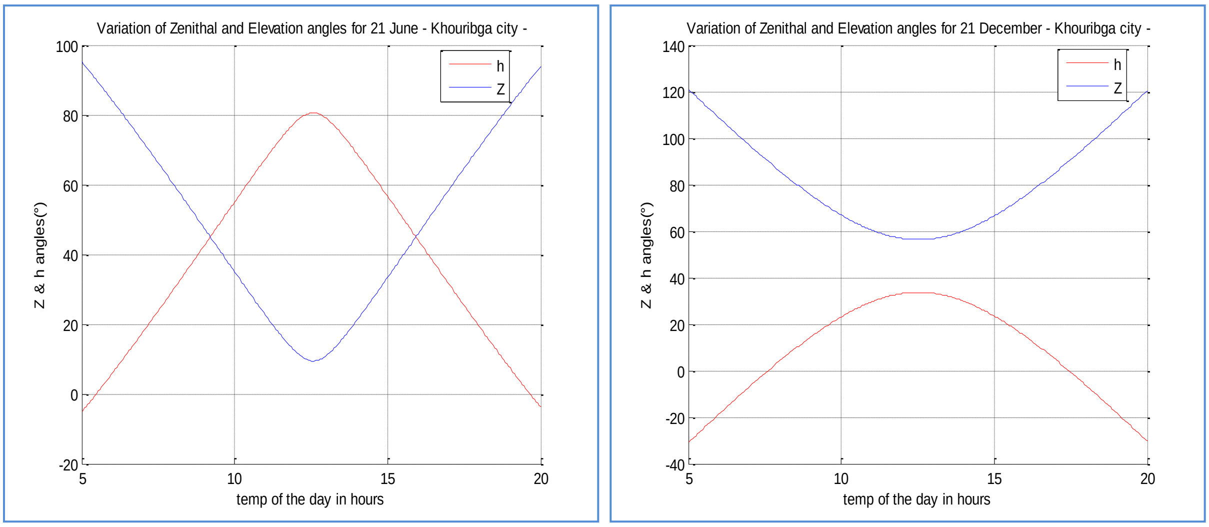

Figure II.20 : Temporal variations of (zenith and elevation) angles for the two days of year, a; for 21 June and b; for 21 December at Khouribga city.

C- The Azimuth angle (φ)

This is the angle between meridian and the location of the vertical surface passing through the sun.

The knowledge of azimuth is required for the calculation of the angle of incidence of solar radiation on a non-horizontal surface. The origin azimuth corresponds to the direction of the south in the northern hemisphere. The azimuth angle is counted positively towards the west [5].

$$\sin(\varphi) = \frac{\cos(\delta) * \sin(Ah)}{\cos(h)} \qquad (8)$$

By using a Matlab code, we can calculate the Azimuth of the sun for the two days of solstice of the year;

- Summer solstice (21 June the longest day of the year).
- Winter solstice (21 December, the shortest day of the year).

The calculation result is shown in the following figures.

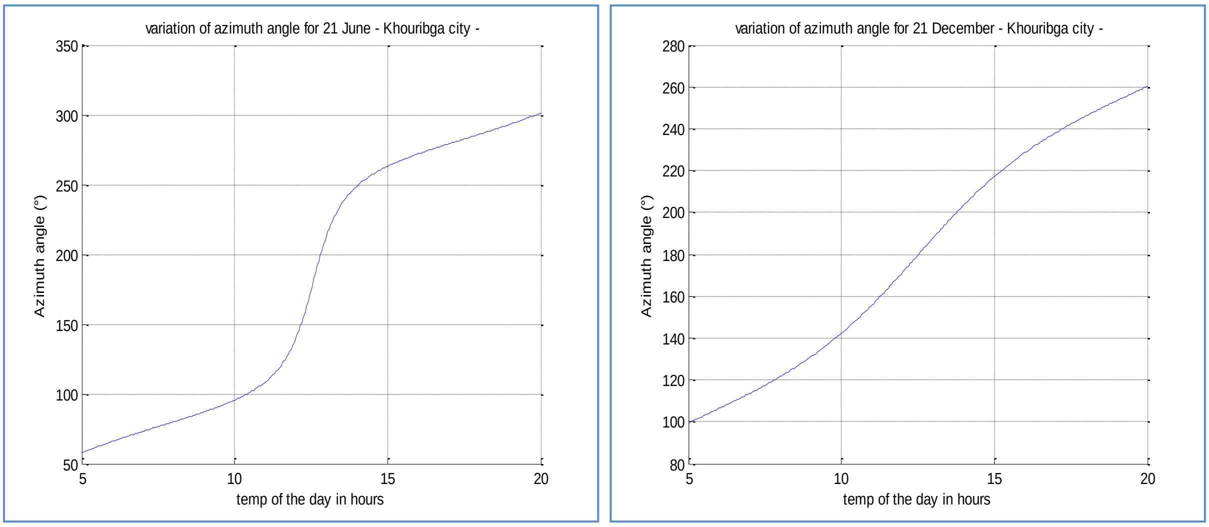

Figure II.21 : Daily variations of Solar Azimuth Angle in the two days of year, a; for 21 June and b; for 21 December at Khouribga city.

D- The relationship between the two angles (Azimuthφ and solar height h)

Every day, the sun describes a trajectory whose two main coordinates, φ and h, are represented on a graph. The latter also makes it possible to indicate the azimuth and the height of the possible obstacles which stand in front of a determined solar installation.

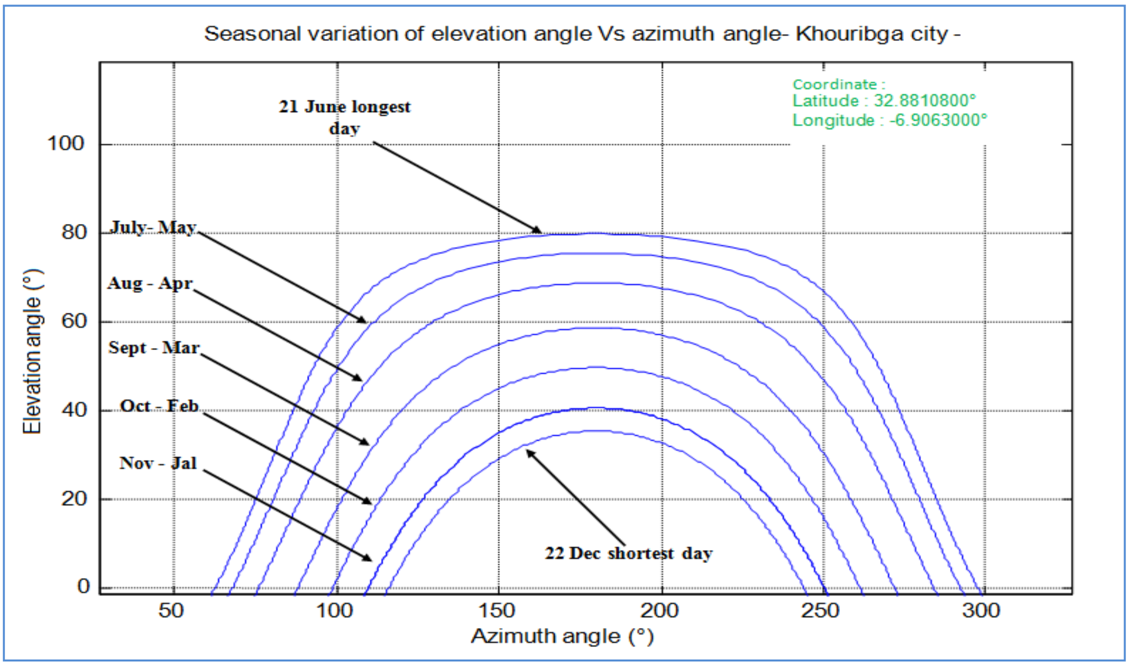

Figure II.22 : Diagrams of the azimuth ϕ VS elevation h.

This graph, consequently allows determining the periods of time and days during which the installation will not directly receive the direct solar radiation.

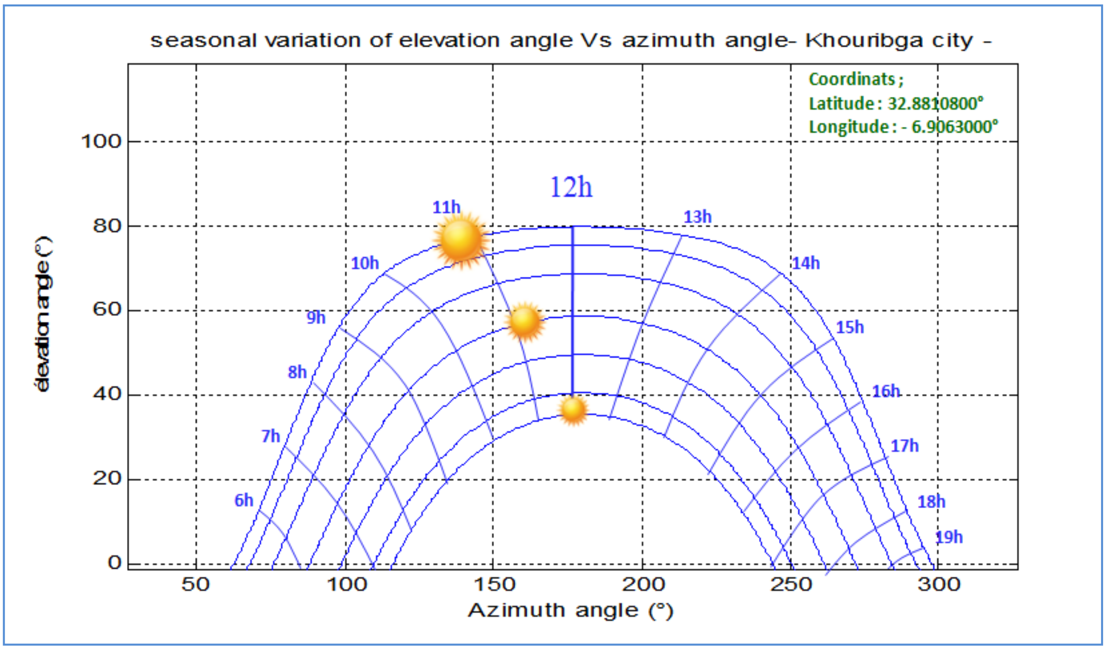

Figure II.23 : Diagrams of the azimuth ϕ and elevation h with the notion of time.

Each geographical point potentially has its own graph of the race of the sun, whose graphs depend on the longitude, latitude and altitude of the place, the graph above presented the race of the sun at Khouribga, with the hours of the day.

The azimuth is the local angle φ between the direction of due North and that of the perpendicular projection of the Sun down onto the horizon line measured clockwise.

0° = due North, 90° = due East, 180° = due South, and 270° = due West.

It follows that if an observer is directly facing the sun, then they are pointed in the direction of the azimuth, φ. Recall that the angle of solar elevation, h, is the angular measure of the Sun's rays above the horizon. I.e., h is the angle between the direction of the geometric center of the Sun and the horizon.

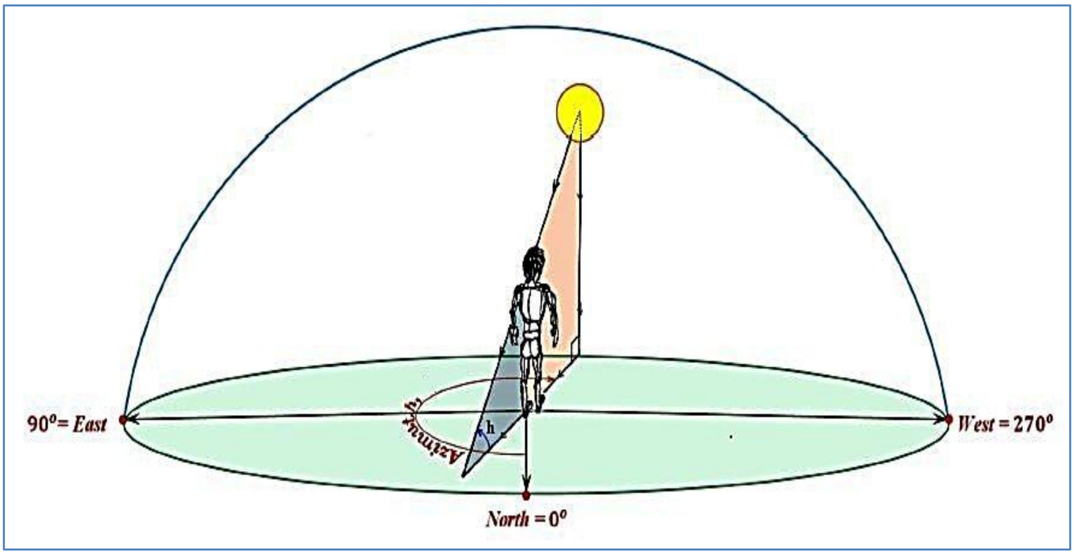

Figure II.24 : Representation of the azimuth ϕ and elevation h.

E- Calculate the angle of incidence (ω)

The angle of incidence of the solar beam with any surface of inclination and orientation is the angle formed by the direction vector of the solar beam and the normal leaving the surface [6].

- $\vec{\Gamma}$: The unit vector carried by the direction of the solar rays.
- $\vec{n}$: The unit vector carried by the normal to the surface.
- ω: The angle of incidence between ($\vec{\Gamma}$, $\vec{n}$).

$$\vec{\Gamma}=\begin{cases}\sin(\theta).\cos(\varphi)\\ \sin(\theta).\sin(\varphi)\\ \cos(\theta)\end{cases} \quad \text{and} \quad \vec{n}=\begin{cases}\cos(\theta').\cos(\varphi')\\ \cos(\theta').\sin(\varphi')\\ \cos(\theta')\end{cases}$$

We make the scalar product of two vectors, $\vec{\Gamma}$ and $\vec{n}$ for determining the angle ω ;

$$\vec{\Gamma}.\vec{n} = \overline{\|\Gamma\|}.\|\vec{n}\|.\cos(\omega) = \cos(\omega) \tag{9}$$

$$\vec{\Gamma}.\vec{n}=\sin(\theta)\sin(\theta')\cos(\varphi)\cos(\varphi')+\sin(\theta).\sin(\varphi).\sin(\theta').\sin(\varphi')+\sin(\theta).\sin(\theta')$$

And we have:

$$\sin(\varphi)\sin(\varphi') + \cos(\varphi)\cos(\varphi') = \cos(\varphi - \varphi') \tag{10}$$

We thus find:

$$\cos(\omega) = \cos(h)\cos(\varphi - \varphi')\sin(\theta')+\sin(h)\sin(\theta') \tag{11}$$

We develop a Matlab code that plots the variation of the angle of incidence in the two solstice's days of the year in Khouribga city, the calculation results are presented on the following curves:

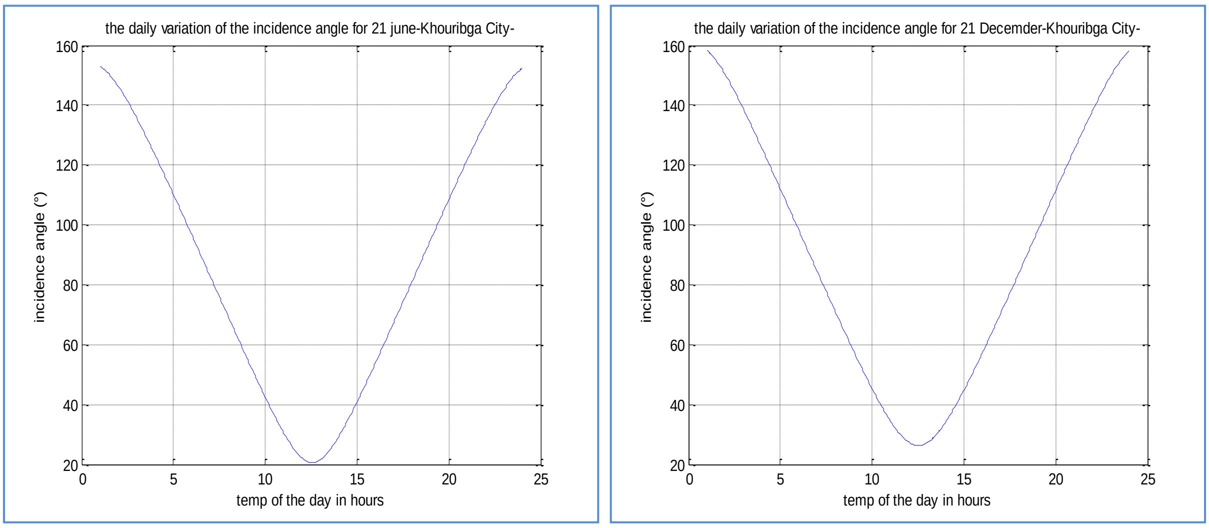

a) Angle of incidence for summer solstice

b) Angle of incidence for winter solstice

Figure II.25 : Variation of the angle of incidence in the two solstice's days of the year.

II. 3. Solar Time vs. Clock Time

The earth undergoes two types of displacement; the rotation of the earth around the axis of the poles and its revolution around the sun. The movement of the earth on itself defines the concept of solar day; a complete rotation takes place in 24 hours. It thus brings the definition of time, since each hour corresponds to an angular deviation of 15°. The rotation of the earth around the sun defines the seasons and makes it possible to distinguish true solar time.

Using this notation, at the vernal equinox on March 21, and the autumnal equinox on Sept. 21, the 12-hour day starts at 06:00 hours (6 a.m.), moves through 12:00 hours (noon), and ends at 18:00 hours (6 p.m.).

It is also very important to note that there is another time correction that must be considered. In the interest of convenience, the agreed upon "local time" of a given site is influenced by time zone, daylight savings time and other man-made decisions and demarcations. It is the time on your watch.

The sun however does not recognize any of these man-made adjustments. According to the sun or "solar time", at any given point on the earth "solar noon" occurs at the instant that the sun is positioned due south of that specific geographic location [7].

II. 3. 1. Sunshine duration

Depending on atmospheric conditions, the sky can be more or less cloudy during the day. These obscuring the Sun totally or partially, thus preventing the radiation from reaching the ground directly.

The effective duration of sunshine or insolation is the time during which, over the course of a day, the direct solar radiation reached the ground of the place considered. Direct radiation is the radiation which reaches the earth's surface without having undergone any deviation from its emission by the Sun.

Other definition of sunshine duration; is the length of time that the ground surface is irradiated by direct solar radiation (i.e., sunlight reaching the earth's surface directly from the sun) or the period during which direct solar irradiance exceeds a threshold value of 120 watts per square meter (W/m2). This value is equivalent to the level of solar irradiance shortly after sunrise or shortly before sunset in cloud-free conditions.

The sunshine duration represents the maximum duration of the day [7 & 8]:

$$\mathbf{Sd} = \frac{2}{\frac{15.\mathrm{arcCos}(-\tan(\theta).\tan(\delta))}{15}} \qquad (12)$$

We have developed a Matlab code that calculates and plots the daily sunshine duration over the year for the city of Khouribga.

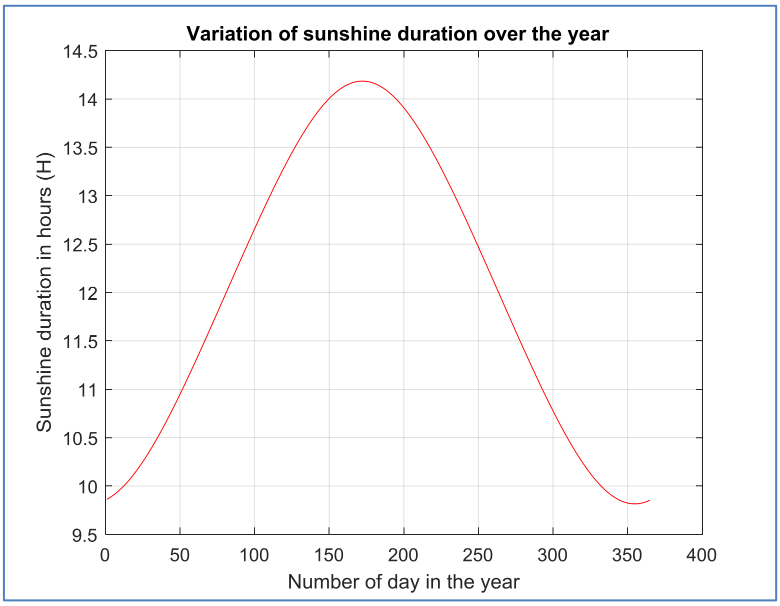

Figure II.26 : Variation in the sunshine duration during the year in Khouribga city.

The astronomical day length is maximum on June 21 (the longest day of the year) and minimum on December 21 (the shortest day of the year).

II. 3. 2. Sunrise and Sunset Time

For the planning of observations, it is useful to know the times during which a certain body is above the horizon as well as the times of sunrise, sunset, and twilight.

A body can be always above the horizon, always below the horizon, or above the horizon during a part of the day, depending on the observer's latitude and the declination of the body.

From the latitude and the declination, it is possible to know the true solar time of sunrise and sunset [9]:

$$\mathbf{t}_{\mathbf{Sunrise}} = 12 - \left(\frac{\text{arcCos}(-\tan(\theta).\tan(\delta))}{15}\right) \tag{13}$$

$$\mathbf{t}_{\mathbf{sunset}} = 12 + \left(\frac{\text{arcCos}(-\tan(\theta).\tan(\delta))}{15}\right) \tag{14}$$

II. 3. 3. Solar Time (ST)

Since a man regulates his time with the recurrence of light and darkness due to rising and setting of the sun, the sidereal division of time is not suited to the needs of everyday life, for the purposes of which the sun is the most convenient time measurer. A solar day is the interval of time that elapes between two successive lower transits of the sun’s centers over the meridian of the place. The lower transit is chosen in order that the date may change at mid-night.

The solar time at any instant is the hour angle of the sun’s centre reckoned westward from 0 h to 24 h. This is called the apparent solar time, and is the time indicated by a sun-dial. Unfortunately, the apparent solar day is not of constant length throughout the year but changes. Hence our modern clocks and chronometers cannot be used to give us the apparent solar time.

The sun changes its right ascension from 0 h to 24 h in one year, advancing eastward among the stars at the rate of about 1° a day. Due to this, the earth will have to turn nearly 361° about its axis to complete one solar day, which will consequently be about minutes longer than a sidereal day. Both the obliquity of the ecliptic and the sun’s unequal motion cause a variable rate of increase of the sun’s right ascension. If the rate of change of the sun’s right ascension were uniform, the solar day would be of constant length throughout the year.

From the above information’s, the solar time is the time of day determined by the apparent movement of the Sun, equal to 12:00 at true noon. To obtain the legal time, you have to add the equation of time, the longitude correction and possibly summer time. With True noon or solar noon is the local time at which the sun crosses the meridian of the observation point.

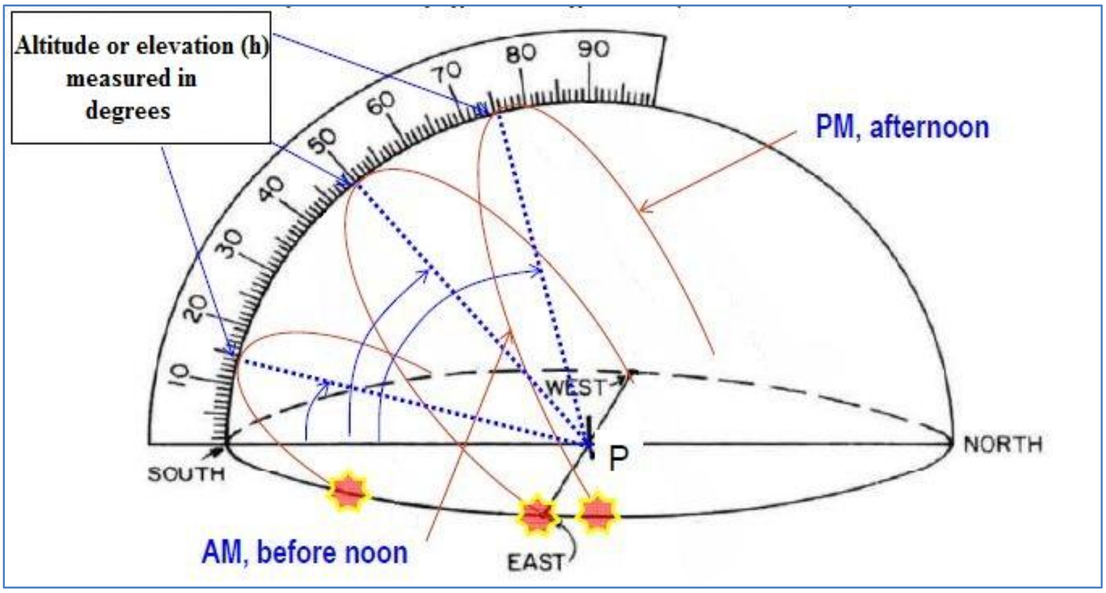

Figure II.27 : Graphic representation of the sun evolution and the concept of the solar time.

We are measuring relative to solar noon (sun is on our line of longitude).

ST is depending on the exact longitude where solar time is calculated.

II. 3. 3. 1. Universal Time (UT)

Coordinated Universal Time (UTC) or unofficial English: "Universal Time Coordinated", unofficial French: "Universel Temps Coordonné" is the primary time standard by which the world regulates clocks and time. It is one of several closely related successors to Greenwich Mean Time (GMT). For most purposes, UTC is synonymous with GMT, but GMT is no longer precisely defined by the scientific community.

To deduce the legal time or local clock time (LCT) it is necessary to add to the universal time the time zone offset [8]:

$$\boldsymbol{LCT} = UT + shift \tag{15}$$

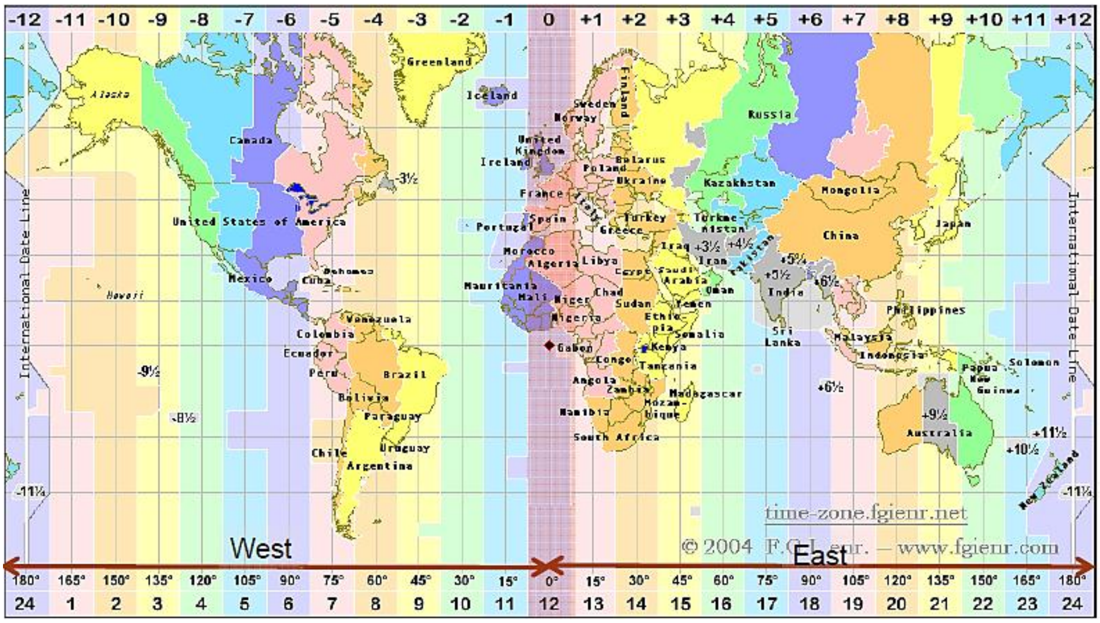

Figure II.28 : Greenwich Civil Time: Time along zero longitude line passing through Greenwich.

II. 3. 3. 2. Local Clock Time (LCT)

Legal time or local clock time is the time in common use in a country; it is defined by a law or a decree. It generally takes into account the time zone in which most of the country is located and is therefore offset by a whole number of hours from the original time zone (meridian 0).

Local Standard Time: is the clock time for the time zone in which the observing site is situated, but which does not include any shift in time due to the implementation.

There is a fixed relationship between local standard time and Coordinated Universal Time based on the longitude that represents the local time zone [8].

II. 3. 3. 3. Mean Solar Time (MST)

Mean solar time (also known as local mean solar time or mean local time) is the solar time which would apply if there was no day to day variation in the Coordinated Universal Time of solar noon at a location. It is determined by the local standard time and the difference between the GHA of the location and the GHA equivalent to the local time zone. The difference between true solar time and mean solar time can range between + 16 and – 16 minutes throughout a year.

With:

(GHA) Greenwich Hour Angle is the angular distance west of the prime meridian, and is measured from 0° to 360°. For example, a location which has a longitude of 45° W (or -45°) has a GHA of 45°, while the GHA of a location at a longitude of 45° E is 315°. While longitude is the most commonly used approach to specify positions east or west of the prime meridian on the earth's surface, GHA is similarly used in celestial navigation for objects in the sky.

The mean Sun is a Sun that returns to the meridian exactly after 24 hours. Average solar time therefore corresponds to 24 h. The equation of time (noted Et) is the value of the difference between the true solar time and the mean solar time. This deviation is due to the fact that the Earth moves in an elliptical orbit, while having its axis of rotation inclined on the ecliptic [8].

$$\boldsymbol{SMT} = UTC + \frac{\lambda}{15} \tag{16}$$

λ: The longitude of the location.

II. 3. 3. 4. True Solar Time (TST)

True solar time (TST, also known as local apparent time or apparent solar time) is determined by the difference between the Greenwich Hour Angle of a location (which is fixed) and that of the sun, which changes by approximately15° an hour as it traverses the sky. The reference time for true solar time is solar noon (12:00:00 TST), which is defined as the time at which the sun's GHA is equal to the location's GHA. Solar noon is commonly referred to as being when the sun's direction is true north and its position is highest in the sky.

True solar time is indicated by a sundial and a Heliograph. It is the time defined by the true angular coordinates of the sun [8 & 9].

$$\boldsymbol{TST} = SMT + Et \tag{17}$$

Et: the equation of time,

To know the position of the sun, it is therefore necessary to determine the true solar time from the Legal time or local clock time, Then to go from (LCT) to (TST) three corrections must be made:

- ***First correction C_1 :*** bringing the LCT back to Greenwich Mean Time. In Morocco the addition of an hour in all the year that we are ahead of C_1 = 1, In Ramadane C_1 = 0.
- ***Second correction C_2 :*** correction in longitude. It is 4 min per degree of longitude, (+) for East longitudes and (-) for West.
- ***Third correction C_3 :*** equation of time which takes into account the irregularities of the movement of the earth.

$$\boldsymbol{TST} = LCL - C_1 + C_2 + C_3 \tag{18}$$

II. 3. 3. 5. Equation of Time (Et)

The difference between mean solar time and apparent solar time, equal to the difference between the right ascensions of the true sun and the mean sun. The equation of time is often defined as the difference between apparent time and mean time; in this case, the equation has the opposite sign, a fact that must be borne in mind when reference books are used.

The equation of time varies continuously. The variation is due to the fact that the passage of apparent solar time, as measured by the hour angle of the true sun, is no uniform because of the no uniformity of the earth's orbital motion and the inclination of the ecliptic to the equator.

This equation allows the correction due to the irregularities of the movement of the earth which varies according to the date from -15 min to +17 min.

A good approximation of the time Et is given by the following equation:

$$Et = 9.9\sin 2.(0.986j + 100) - 7.7*\sin(0.986*j-2)) \qquad (19)$$

J is the order of the day number in the year.

The evolution of the equation of time is given by the following figure:

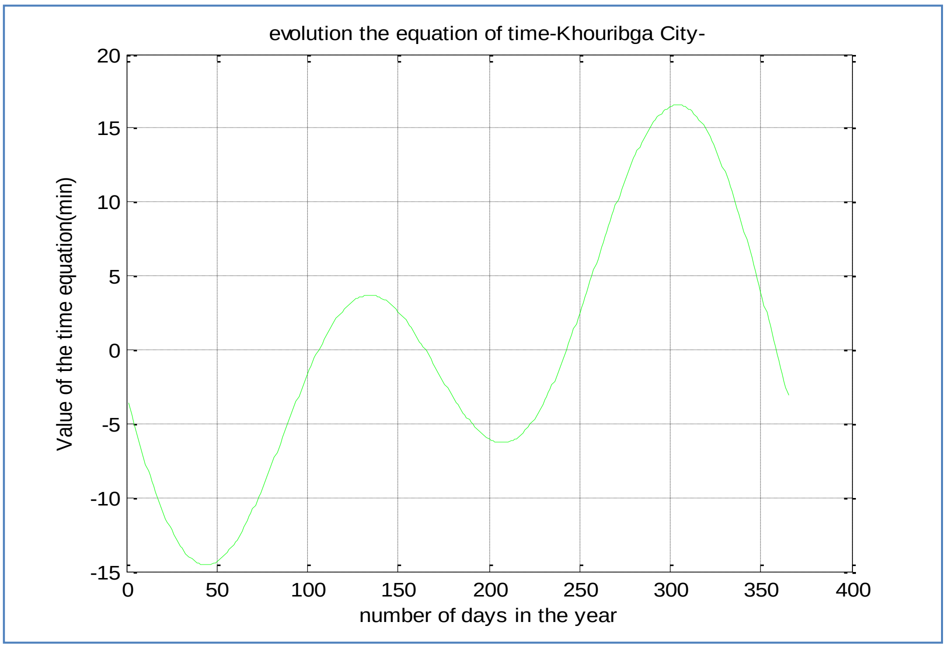

Figure II.29 : Plot of the Equation of time.

II. 4. Study of solar radiation received on ground surface "Clear day"

In the previous section, we posed a number of definitions allowing us to formulate the concept of solar radiation outside the atmosphere. This quantity is readily measurable because it is considered that it depends only on the distance between the measuring points of the Sun.

We will see in this paragraph, the passage through the atmosphere will tend to complicate the understanding of the phenomenon, the multiple interactions that may occur [8 & 10].

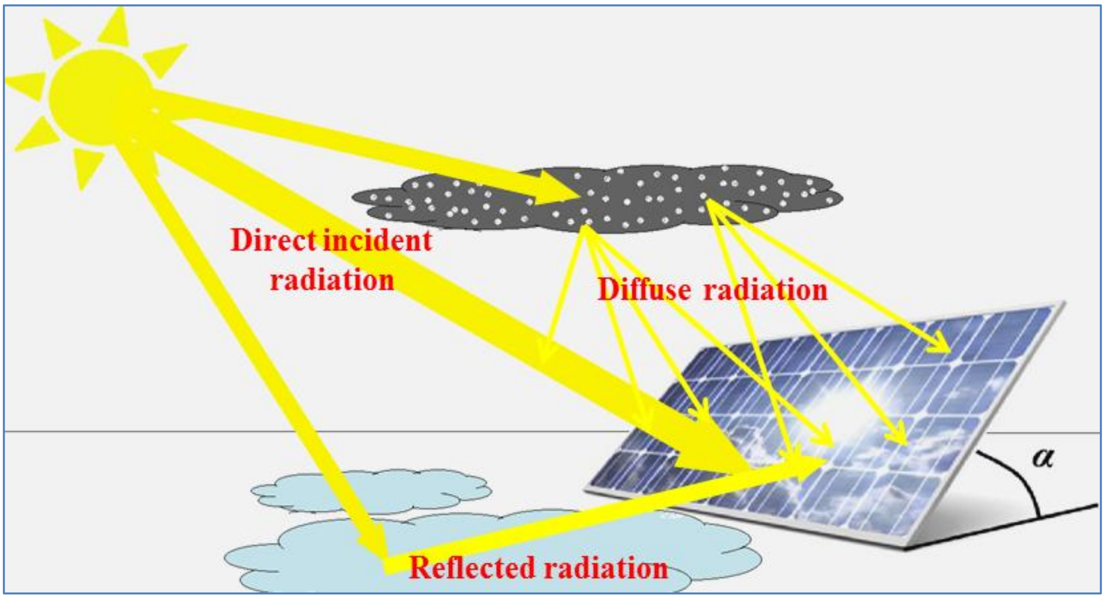

Figure II.30 : The solar flux on a collecting surface.

In what follows, we consider the model of inclination of global radiation in the case of a clear sky.

Direct-beam radiation: that passes in a straight line through the atmosphere to the receiver.

Diffuse radiation: that has been scattered by molecules and aerosols in the atmosphere.

Reflected radiation: that has bounced off the ground or other surface in front of the collector.

II. 4. 1. Direct radiation

This irradiation is received directly from the sun traveling through the atmosphere without modification. The capture area is placed in the following conditions:

- The sun's position is defined by its elevation (h) and azimuth (φ), they will be measured relative to the south.
- The collector plan is oriented with respect to the south and inclined at an angle α as tilt angle.

The received power on the capture area is given by [7] :

$$I_{Dir} = A.\exp(-K.m) \quad (20)$$

This is an amount that includes the geographic parameters of the system and the astronomical data of the sun in its movement.

$$A = 1160+75.\sin\left(\frac{360}{365}(j\text{-}275)\right) \quad (21)$$

$$K = 0.175+0.035\sin\left(\frac{360}{365}(j\text{-}100)\right) \quad (22)$$

$$m = \frac{1}{\sin(h)} \quad (23)$$

A: apparent extraterrestrial flux.

k: optical depth.

j is the order of the day number in the year, and h is the elevation of the sun.

m is the relative length of the path traveled by the sun's rays through the atmosphere.

The evaluation of the direct energy received in one day on an incline south facing is done by integrating the instantaneous power received.

II. 4. 2. Diffused radiation

Clouds, aerosols partly diffuse radiation, as we have previously quantified. It is assumed that the diffuse flux is uniform in its distribution in the sky which is treated as an infinite surface. This assumption allows us to calculate the correction factor R_{dif} on the diffuse radiation; once the chosen inclination [8 & 11].

$$R_{dif} = \frac{1+\cos(\alpha)}{2} \quad (24)$$

The power received on a capture area is :

$$I_{Dif} = C.I_{Dir}.R_{dif} \quad (25)$$

$$C=0.095+0.04\sin\left(\frac{360}{365}(j\text{-}100)\right) \quad (26)$$

C is the diffuse sky factor,

R_{dif} is the form factor between collector and sky. The diffused energy received is also calculated in the same way by integrating the power received.

II. 4. 3. Reflected radiation

The third and last component of the total radiation on the tilted plane is the radiation reflected from the ground. In reality, numerous objects such as buildings, different ground materials, trees, etc., reflect incident radiation onto the tilted surface.

A simplified but standard approach is to assume reflected radiation from one composite source, a horizontal, diffusely reflecting ground. The ground-reflected radiation on the tilted plane is then dependent only on the reflectance of the ground and the view factor to the ground of the tilted surface [8 & 11]:

$$I_{ref} = \rho . I_{dir}(\sin(h) + c). R_{ref} \qquad (27)$$

With:

$R_{ref} = (\frac{1-\cos(\alpha)}{2})$: Geometric factor of the ground

$C = 0.095 + 0.04\sin(\frac{360}{365}(j-100))$: factor of the sky diffuse

ρ : is the ground reflectance.

Where ρ is the ground reflectance and $I = I_{Dir} + I_{Dif}$ is the global radiation on the horizontal plane. The ground reflectance ρ depends on the surroundings. At high latitudes, a seasonal variation in ground reflectance is likely because of snow coverage in the winter.

II. 5. Results and discussion of solar radiation received on horizontal plane “clear day”

The programming of these mathematical formulas, allows to have a quantified idea on the different values of the energy; daily, for each month and for the whole year. The calculations of direct diffuse and global radiation component was carried via Matlab view. The different formulae discussed above were used to get to the final equations for I_{dir}, I_{dif} and global radiation given by equations 20 to 28. The one day simulation results shown in Figure 18 represent the radiation case of Khouribga city. The geographic site data used in the simulation for site are given in table II.3.

Table II.2 : The geographic data of Khouribga City.

Site	Lat	Log	Altitude	Ground Albedo	Optimum Exposure	
					Tilt angle	Orientation
Khouribga	**33° 35'N**	**−6◦54′W**	**820 m**	**0,2%**	**29 °**	**To the South**

To take into account this dynamic aspect of solar radiation, it was necessary to qualify the temporal distribution of the latter during the day, The implementation of the theoretical mathematical formulas gives a clear idea about the different values of solar energy and a graphic representation of the evolution due to direct, diffuse and global radiation for typical days of the year.

II. 5. 1. The typical day of the month

For a given magnitude, the typical day is the day of the month approximating the monthly average of that magnitude.

The list of the typical days proposed by Klein is shown in the following table:

Table II.3 : List of typical days per month proposed by Klein.

Month	Jan	Feb	Mar	Apr	May	Jun	Jul	Aug	Sept	Oct	Nov	Dec
typical days	**17**	**16**	**16**	**15**	**15**	**11**	**17**	**16**	**15**	**15**	**14**	**10**
N° of Day	**17**	**47**	**75**	**105**	**135**	**162**	**198**	**228**	**258**	**288**	**318**	**344**

The results that will be presented in the following part represent:

- The variation of intensity of solar radiation calculated at Khouribga City.
- Daily, monthly and annual averages of direct, diffuse and global irradiation on a horizontal plane in the tables and histograms form.

By using a MATLAB code, we can calculate the daily, annual and the distribution of monthly energies of the solar radiation received on a horizontal surface in Khouribga city.

II. 5. 2. Calculation of daily irradiation

The monthly average daily global horizontal solar radiation can be obtained by calculating the average for the entire month or by using for each month, the day when the extraterrestrial solar radiation is equal with the average for the entire month.

There are differences between the daily global horizontal solar radiation for a selected day and the monthly average. These differences can appear because the selected days can be clear days in winter or cloudy days in summer, so that they significantly differ from the average.

The selected days for every month are used to reduce the calculation time. Taking into consideration these differences, it is better to use the average for the entire month in this study as the software allows the quick calculation of the monthly daily global horizontal solar radiation.

By using a Matlab code, we can calculate the daily distribution of solar radiation received on a horizontal surface in Khouribga city (the corresponding value of 21 June).

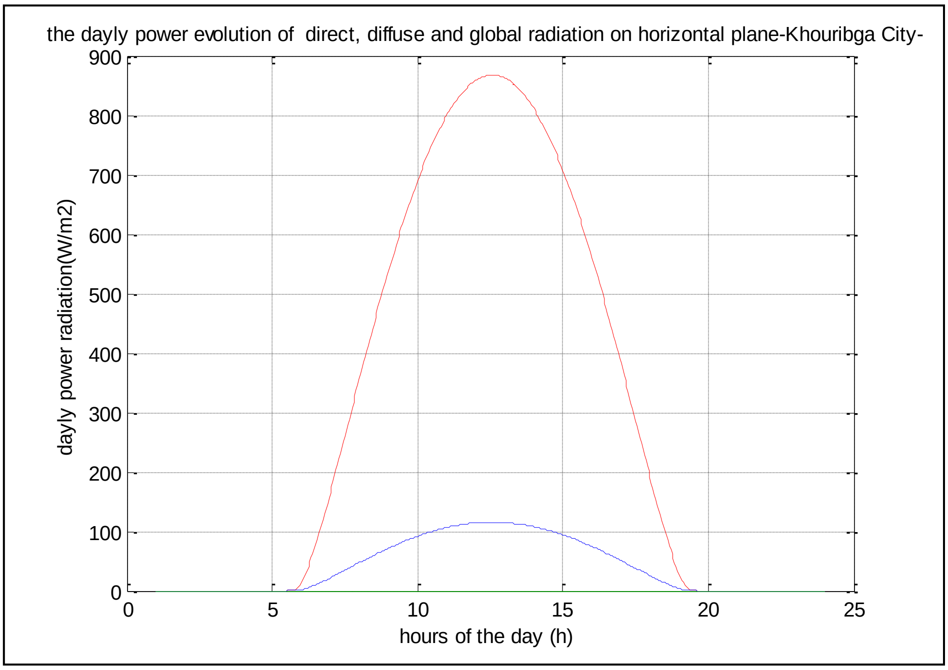

Figure II.31 : Both direct and diffuse powers received in function of time.

The Matlab code that we have developed, also allows calculating and plotting the daily irradiation of typical days of each month for Khouribga city on a horizontal surface.

The results of daily variations of solar irradiation arriving on a horizontal surface are given in the table below;

Table II.4 : The energy received per days (wh/m^2)

Month	Days typical	N° of days	Direct energy	Diffuse energy	Total energy
January	**17**	**17**	3441.45	397.09	3838.55
February	**16**	**47**	4346.29	525.71	4871.99
March	**16**	**75**	5489.93	713.13	6203.06
April	**15**	**105**	6438.23	947.28	7385.51
may	**15**	**135**	6906.00	1153.06	8059.06
June	**11**	**162**	6982.33	1272.53	8254.87
July	**17**	**198**	6804.58	1247.90	8052.48
August	**16**	**228**	6350.32	1162.97	7513.29
September	**15**	**258**	5545.77	970.14	6515.91
October	**15**	**288**	4480.87	742.29	5223.16
November	**14**	**318**	3534.57	544.21	4078.78
December	**10**	**344**	3122.29	431.10	3553.39

II. 5. 3. Calculation of monthly irradiation

Using the same methodology as for the monthly average daily global horizontal radiation the following models are developed in order to determine the monthly average daily diffuse horizontal radiation.

The graph below shows the evolution of the monthly irradiation on a horizontal surface;

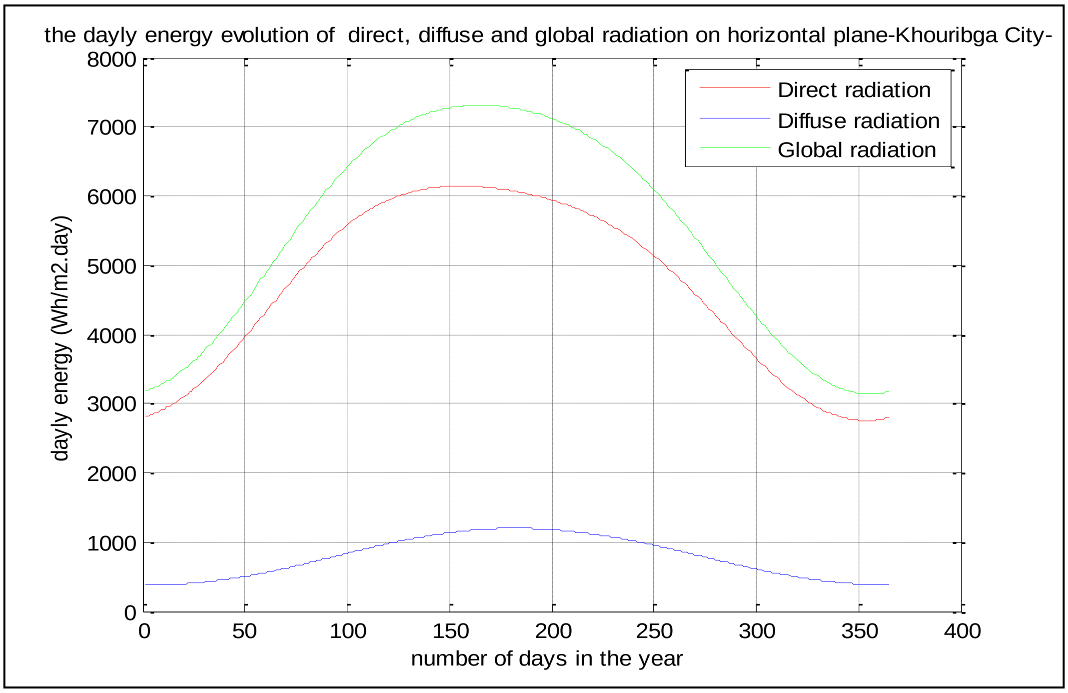

Figure II.32 : Annual powers radiations in Khouribga.

The figure shows the values of the daily energies of the solar radiation received on a surface relative of the Khouribga city, according to the days of the year in [kWh/(m^2.day)].

The curve analysis obtained above indicates that the values of direct, diffuse and global solar radiation are maximum in summer and minimum in winter. The global solar energy has exceeded 7000 Wh/m^2 for summer days, on the other hand, for winter days to extend between (3000 and 6000 Wh/m^2).

II. 5. 4. Cumulative energy for each month of the year

The cumulative energy calculation is done by integrating the power formulas between sunrise and sunset. This method makes it possible to estimate the energy received by a horizontal surface.

Use the same Matlab code that calculates and tracks the evolution of cumulative solar energy in each month of the year.

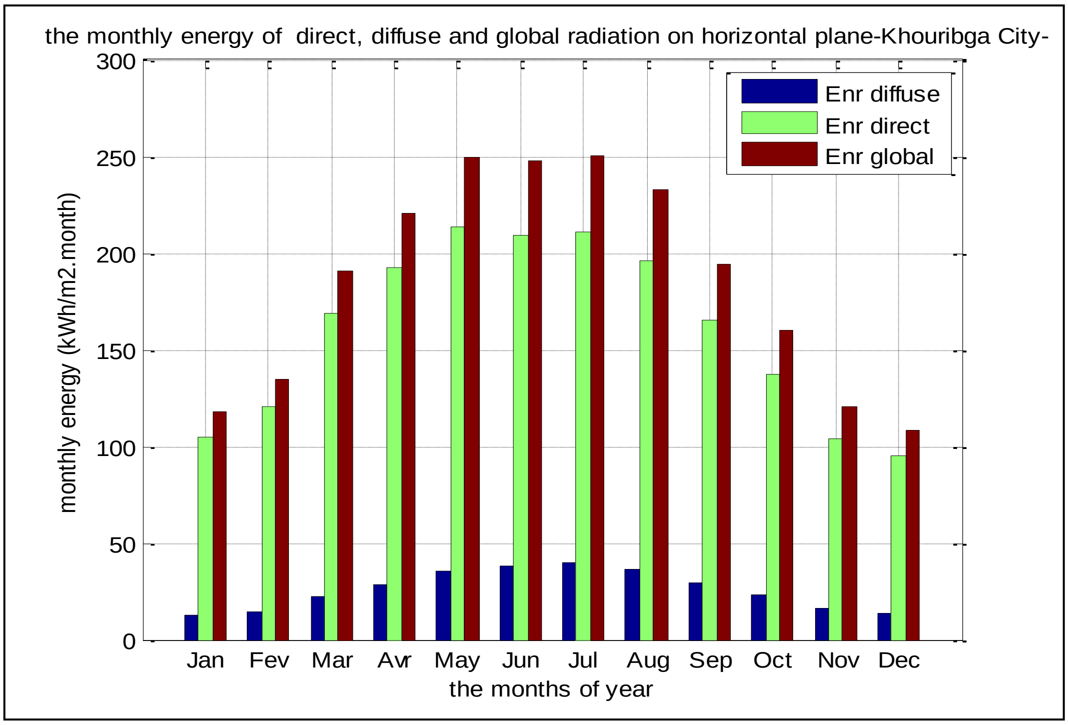

Figure II.33 : Distribution of monthly energy in Khouribga.

In the figure representing the energy of solar radiation calculated for the Khouribga site, the summary of the results is given in the table below;

Table II.5 : The monthly and yearly energy received.

Months	The Energy Received per Month (kwh/m^2)		
	Direct Energy	Diffuse Energy	Total Energy
January	106,68	13,21	119.89
February	121,69	14,71	136.41
March	170,18	22,1	192.29
April	193,12	28,41	221.56
may	214,08	35,74	249.83
June	209,47	38,17	247.65
July	210,94	39,52	250.46
August	196,86	36,05	232.91
September	166,37	29,12	195.47
October	138,9	23,04	161.91
November	106,06	16,32	122.36
December	96,79	13,36	110.15
Annual radiation [kWh/m2.year]	1931,14	309,75	2240,9

The table and the histogram representing the monthly distribution of solar irradiation and for the whole year, informs us about the cumulative energy distribution of the months, we note that the maximum solar radiation greater than 200 kWh/m^2 corresponding the summer months (days with high sunstroke), and below 120 kWh/m^2 for the winter months, a very remarkable seasonal effect appears on the form of grouping the bars of the histogram.

Through this representation, the annual energy received on a horizontal plane of the Khouribga city is 2241 kWh/m^2.

Summary of average distribution of solar irradiation in Khouribga city

The aim of this chapter is calculate the annual solar energy received on a horizontal surface by using MATLAB, in the case of Khouribga city is located under 32°52 'North as latitude and under -6°54 'West as longitude.

The results of daily, Monthly and annual variations of solar radiation arriving on a horizontal surface are summarized in the following table;

Table II.6 : Daily, monthly and yearly energy received

			The energy received per days (wh/m2)			The energy Received per Month (kwh/m2)		
Month	Days typical	N° of days	Direct energy	Diffuse energy	Total energy	Direct Energy	Diffuse Energy	Total Energy
January	17	17	3442	397	3839	106,7	13,2	119.9
February	16	47	4346	526	4872	121,7	14,7	136.4
March	16	75	5490	713	6203	170,2	22,1	192.3
April	15	105	6439	947	7386	193,2	28,4	221.6
may	15	135	6906	1153	8059	214,1	35,7	249.8
June	11	162	6982	1273	8255	209,4	38,2	247.6
July	17	198	6804	1248	8052	210,9	39,6	250.5
August	16	228	6350	1163	7513	196,9	36	232.9
September	15	258	5546	970	6516	166,4	29,1	195.5
October	15	288	4481	742	5223	138,9	23	161.9
November	14	318	3535	544	4079	106,1	16,3	122.4
December	10	344	3122	431	3553	96,8	13,4	110.2
Annual radiation [kWh/m^2.year]						**1931,1**	**309,8**	**2240,9**

Conclusion II

This chapter allowed us to introduce the basic notions necessary for the study of the solar radiation. We discussed the various astronomical and geographic parameters as well as the characteristics of solar radiation at the edge of the atmosphere.

The energy or power received on the ground is strongly influenced by geographic parameters, astronomical, and meteorological. The latter have a random character which conferred multiple dispersions in the results obtained by the different models of investigations.

The precise assessment of the radiation received at a given site requires human resources (competence and diligence) and high-performance measuring equipment (Pyranometer, Sensors, automated computer readings, analysis of measurements by software, etc...). The meteorological stations are the most suitable for this purpose.

References II

[1] P.I. Cooper, 'the absorption of solar radiation in solar stills' Sol. Energy 12(3), 333-346, 1969

[2]Abraham, E. et J. Semonsous, J. -L'Auvergne : Sa géographie, son histoire - Paris : Charles-Lavauzelle et Cie, 1949. - fig. et cartes, carte color. ; 8º. Cote : A 37087. https://www.bibliotheques-clermontmetropole.eu;

[3] Z. Bendjellouli, Memory of Magister "Contribution to the modeling of a solar cell," University of BECHAR, Algerie, Faculty of Science and Technology, 2009, pp. 8-10,

[4] M. Aggour, course of Mster "Renewable Energy," Faculty of Sciences, University of Ibn Tofail –Kenitra, 2013.

[5] A.ZEROUAL, 'contribution à l'étude statistique et stochastique des données solaires au site de marrakech' Diplôme d'étude supérieur de 3ème Cycle sciences physique, spécialité traitement du signal, Université CADI AYYAD, 1988.

[6] A. Oudrane, B. Zeghmati, X. Chesneou, B. Aour "Modeling the radiate and energy balance of a building located in the adrar region" collection of mechanics, El Wancharissi University Center of Tissemsilt vol .1 n° 002 (2017),

[7] http://herve.silve.pagesperso-orange.fr/solaire mercredi 23 juillet 2017

[8] Ahmed Ennaoui, "Photovoltaic Solar Energy Conversion (PVSEC)" Helmholtz-Zentrum Berlin für Materialien und Energie- Free University of Berlin- Allemand, 2016,

[9] Hoijeon and Didier Walliang, "Le spectre électromagnétique de la lumière" http://astro.vision.free.fr/spectre.php ,2000

[10] Alain Ricaud Jan, "Gisement solaire et transferts énergétiques," Master Renewable Energies University of Cergy-Pontoise , 2011

[11] N.SELAMI et N.BENABADJI, 'Etude des structures nuageuses ', JAS09 de l4AUF, Alger, Novembre 2009.

Chapter III

OPTIMAL TILT ANGLE AND ORIENTATION FOR SOLAR MODULES

III. 1. Introduction

Fossil fuels are generally used to meet the electricity needs. However, energy policies of the countries are directed at encouraging the use of renewable energy sources since fossil fuels will be exhausted in the near future, they give harm on the environment and they have rising prices. Among the renewable energy sources, the solar energy has gained popularity for energy demand recently and has been prompted. Therefore, the costs have reduced and studies in this field have increased. Solar energy is among the most plentiful renewable energy sources in Morocco. The Morocco is located between 35º-23º North latitude and Morocco's yearly average total sunshine exceeding 2,000 hours annually and even reaching 3,900 hours in the highlands and the Moroccan Sahara. The average solar radiation is 5 kWh/m^2 of energy received on the ground. Therefore, Morocco is well situated in terms of solar energy potential.

The performance of solar systems to convert solar radiation depends on its inclination angle to the horizontal plane, independently from meteorological conditions, and the design of solar systems requires knowledge of the useful solar radiation received on the surface of the installation, it is one of the essential parameters of the preliminary study. For a given energy need, more energy received means fewer panels to install and vice versa, so in order to study the solar field available on an inclined surface at Khouribga city, a series of insolation and irradiation data compute according to the inclination and orientation of the solar panel, and then we apply the same strategy of this work in 20 Moroccan cities.

Sunlight should fall with steep angle to extract maximum power from solar panels. Therefore, optimum fixed tilt angles of solar panels should be changed monthly and seasonally. In our study, MATLAB program is used to estimate the total solar radiation on a tilted panel surface with any inclination. The implementation developed to allow us to extract the correct angle at which the maximum energy could be absorbed by the solar cells. We could determine the optimum tile angle for monthly, seasonal, and yearly solar radiation relative to the site of Khouribga city (latitude 32◦52′ North and longitude −6◦54′ West), and we used the same method to draw the table of solar gains depending on the optimum tilt angle of the solar panels to the main Moroccan cities.

III. 2. Influence of location on the solar field

It is common knowledge that solar radiation is unevenly distributed, and that it varies in intensity from one geographic location to another depending upon the latitude, season, and time of day. Until recently, valid records for solar radiation have been very scanty in the vast majority of the developing countries. In the absence of such useful information as a guide for the proper exploitation of solar energy, only general hints can be offered regarding the geographic areas with favourable conditions for solar energy applications [1].

III. 2. 1. Annual distribution of sunshine in the world

The solar resource is present everywhere but unequally distributed. There is a variation in a factor of 1 to 3.5 in areas populated by humans. The 1st parameter is the latitude, that is to say the distance from the equator. Solar irradiation decreases as we approach the poles (or that we move away from the equator).

For convenience and simplicity, the geographic distribution of total solar radiation on a global scale is divided in terms of intensity into four broad belts around the earth. These are illustrated in the Figure, and also described briefly hereunder with respect to the northern hemisphere, with the understanding that the same conditions apply to the corresponding belts in the southern hemisphere [2]:

- ***The most favourable belt:*** This belt, lying between latitudes 15°N, and 35°N, embraces the regions that are naturally endowed with the most favourable conditions for solar energy applications. These semi-arid regions are characterized by having the greatest amount of solar radiation, more than 90% of which comes as direct radiation because of the limited cloud coverage and rainfall (less than 250 mm per year). Moreover, there is usually over 3,000 hours of sunshine per year.
- ***Moderately favourable belt:*** This belt lies between the equator and latitude 15°N, and is the next most favourable region for the purpose previously mentioned. Because the humidity is high, and cloud cover is frequent, the proportion of scattered radiation is quite high. There is a total of about 2,500 hours of sunshine per year. The solar intensity is almost uniform throughout the year as the seasonal variations are only slight.
- ***Less favourable belt:*** This belt lies between latitude 35°N and 45°N. Although the average solar intensity is roughly about the same as for the other two belts, there are marked seasonal variations in both radiation intensity and daylight hours. During the winter months solar radiation is relatively lower than in the rest of the year.
- ***Least favourable belt:*** The regions in this belt lie beyond latitude 45°N. They include the USSR, and the greater parts of northern Europe and North America. Here, about half of the total radiation is diffuse radiation, with a higher proportion in winter than in summer primarily because of the rather frequent and extensive cloud coverage.

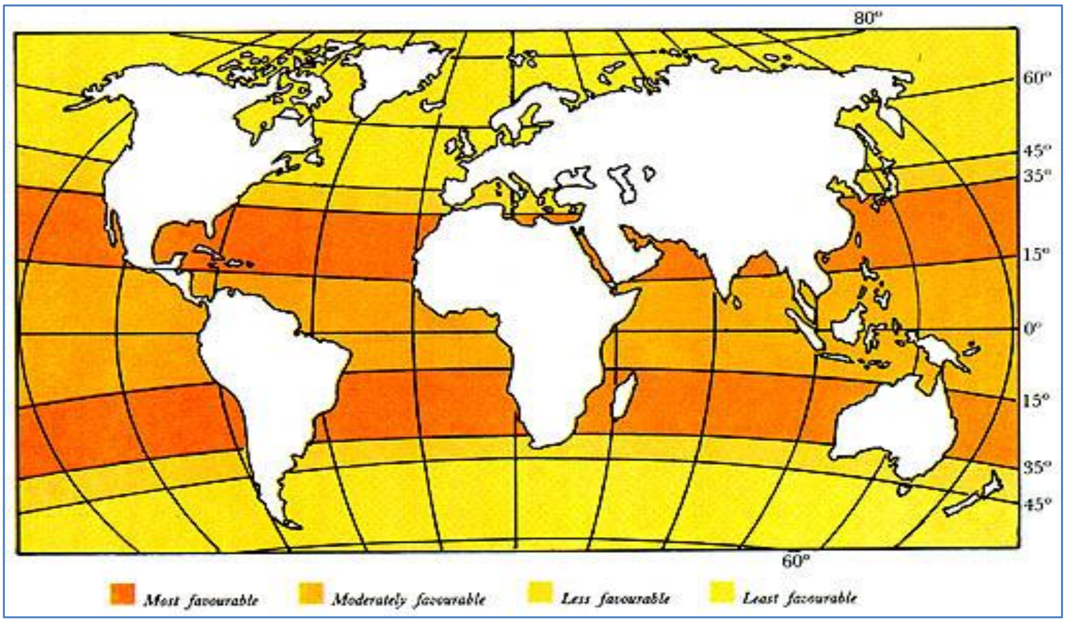

Figure III.34 : Worldwide distribution of solar radiation into belts indicating feasibility of solar applications [2].

It is important to note that the majority of developing countries fall within the more favorable regions between latitudes 35° N and 35° S. For this reason they can count on solar radiation as a steadfast source of energy that can be readily exploited cheaply by both rural and urban households for a multitude of purposes, including solar disinfection of drinking water and oral rehydration solutions.

Knowing that the Earth receives every year 1,070,000 Petawatt-hours (PWh = 10 power 15 Wh) or more than 8000 times the annual world energy consumption and that if we could manage to exploit only 0.01% of this energy, we could ensure the energy needs of the planet, this resource therefore has immense potential.

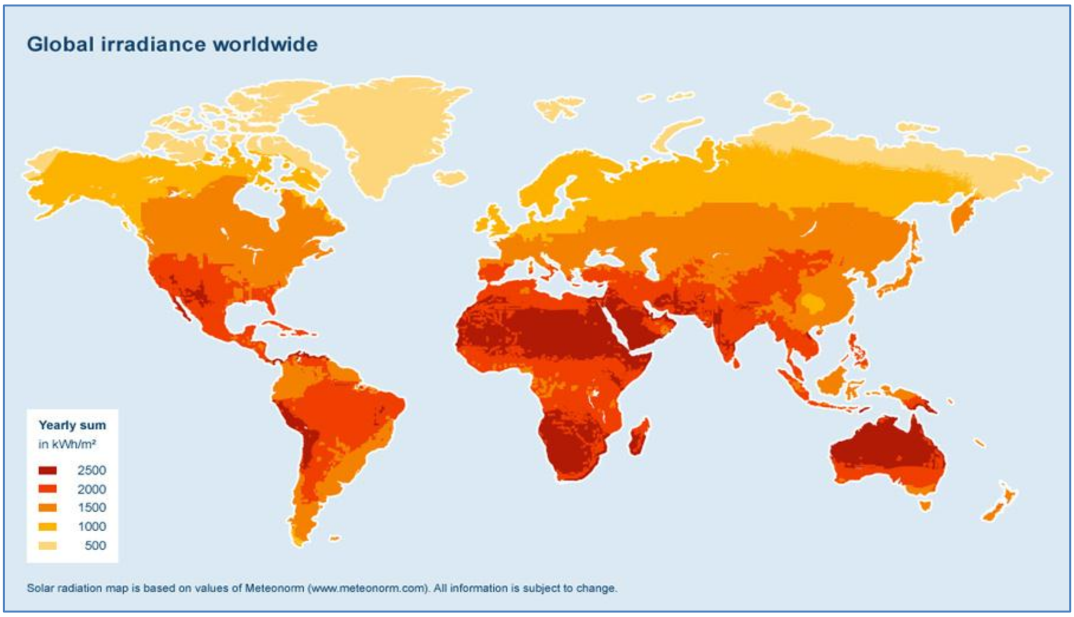

Figure III.35 : Distribution of Solar Energy among the world [3].

Solar field: The energy distribution is expressed by the annual global solar radiation on a horizontal plane (in kilowatt-hours per square meter and per year).

We can see that most parts of Africa, North Australia, Saudi Arabia and northern Middle America are probably the best regions to build solar power plants. Everywhere else, the solar irradiance is weaker. Interestingly, Germany, not exactly known for its extremely long and sunny summers produces by far the most solar energy worldwide as of 2011 due to huge subsidies that ended in 2018.

III. 2. 2. Annual solar energy in Morocco

Morocco has a great potential for the production of solar energy, and the Photovoltaic system is the preferred solution for exploiting this solar potential in Morocco, is estimated at more than 3,400 MWp, an average solar irradiation of 2500 kWh/ m²/year, Morocco has a considerable solar deposit.

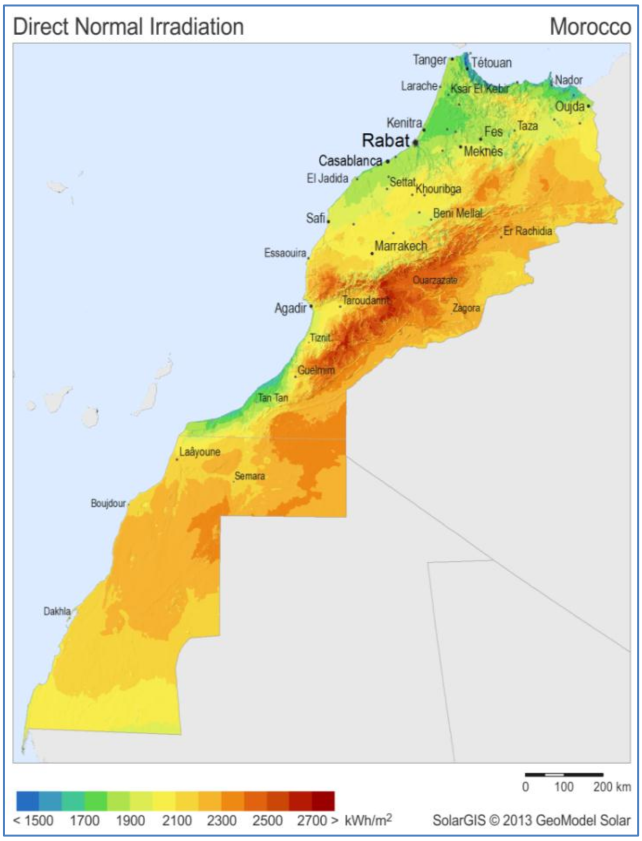

Figure III.36: Potential of solar energy in Morocco [4].

Morocco's green energy opportunity

More than a third of Morocco's electricity production capacity comes from renewable sources: Hydro, wind energy, and solar. But after counting imports, Morocco uses far more fossil fuels than renewables.

Morocco is paving the way in the Middle East and North Africa with its national adoption of a renewable energy plan. Utilizing government sponsored programs to link private renewable suppliers with the larger power grid, solar and wind power have transformed from cottage industries to the heart of the country's long-term economic plan. While Morocco has looked both outwardly and domestically to develop its energy infrastructure, the next challenge will be to fully integrate renewables in a way that promotes local involvement and sustainability. If proven successful, such a program could encourage a wider acceptance and use of renewable energy throughout the region.

Morocco's Solar Plan establishes a target to develop 2,000 MW of solar capacity by 2020, which will be comprised of both solar photovoltaics and concentrated solar power (CSP). Unlike solar photovoltaics (PV), which use solar cells to directly convert sunlight to electricity, the CSP technology in Morocco's case will focus sunlight to heat fluid that is used to propel turbines, which generate electricity.

III. 3. Exposure effect on the reception of solar radiation

The efficiency of a solar panel varies with the orientation, inclination and angle of incidence of the sun's rays. The position that you are going to give to your solar panels will therefore have an influence on production. Different geographical regions experience different weather patterns, so the site where we live is a major factor that affects the solar system design from many ways; determination of the orientation of the panels, finding the number of days of autonomy when the sun does not shine in the skies, and choosing the best tilt angle of the solar panels.

The objective of this part is to allow you to determine the optimal position for each month, each season and all year of the solar panels for a given installation.

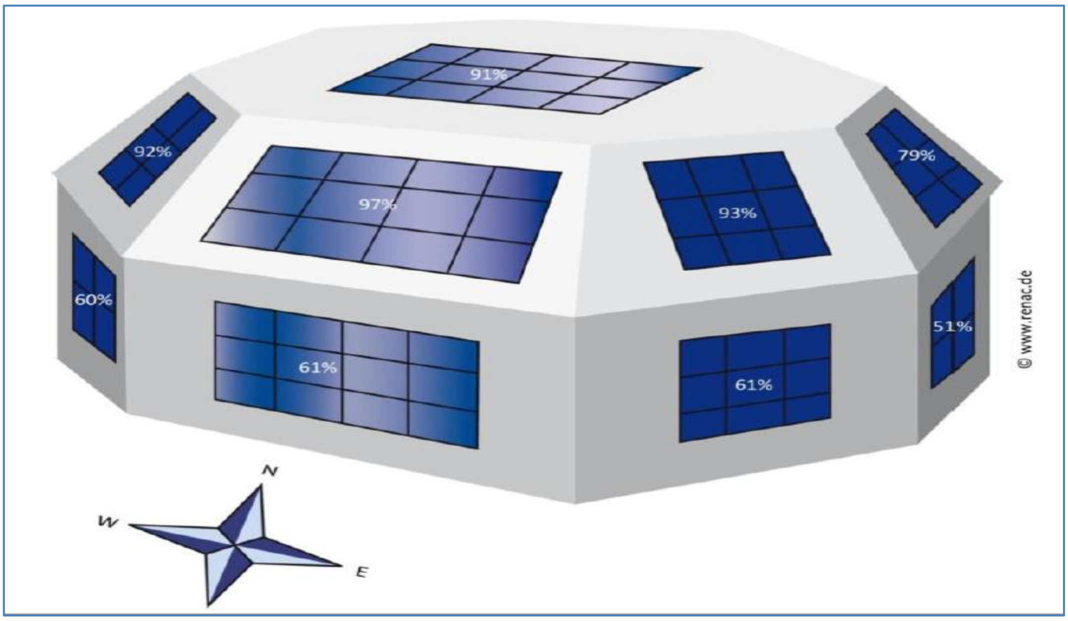

Figure III.37 : Different orientation and inclinations, and quantity of solar radiation received on each surface compared to the optimum of 30° and orientation due south [5].

The main aim of this research study is un-earth the optimum tilt angle for roof top solar system installation (fixed tilts and orientations) and the extent to which deviation from the optimum affects the output of the solar system. The study seeks obtain the best Photovoltaic module tilt angle that can reduce the installation cost of solar system installation. This study applied to the technical assessment for rooftop Solar Photovoltaic system installation in Settat city. The effects of tilt angle on the output of Solar Photovoltaic Systems would be analyzed using Matlab. The optimum tilt angle and the corresponding PV output would be estimated monthly and annually.

The position of a panel is in fact:

- Its orientation, or azimuth, that is the angle it will make with the north-south axis in the horizontal plane.
- Its inclination that is the angle it will make with the horizontal plane.

III. 3. 1. Orientation of solar panel

The atmospheric absorption is lower when the sun is at the highest point in the sky, that is, due south in the northern hemisphere and due north in the southern hemisphere. This is because the distance that radiation must travel in the atmosphere is shorter when the sun is directly above the target location.

The orientation of the panels is important to capture a maximum of sunlight and therefore produce a maximum of energy. South-facing roofs receive the most sunlight, and therefore the most solar energy during the day.

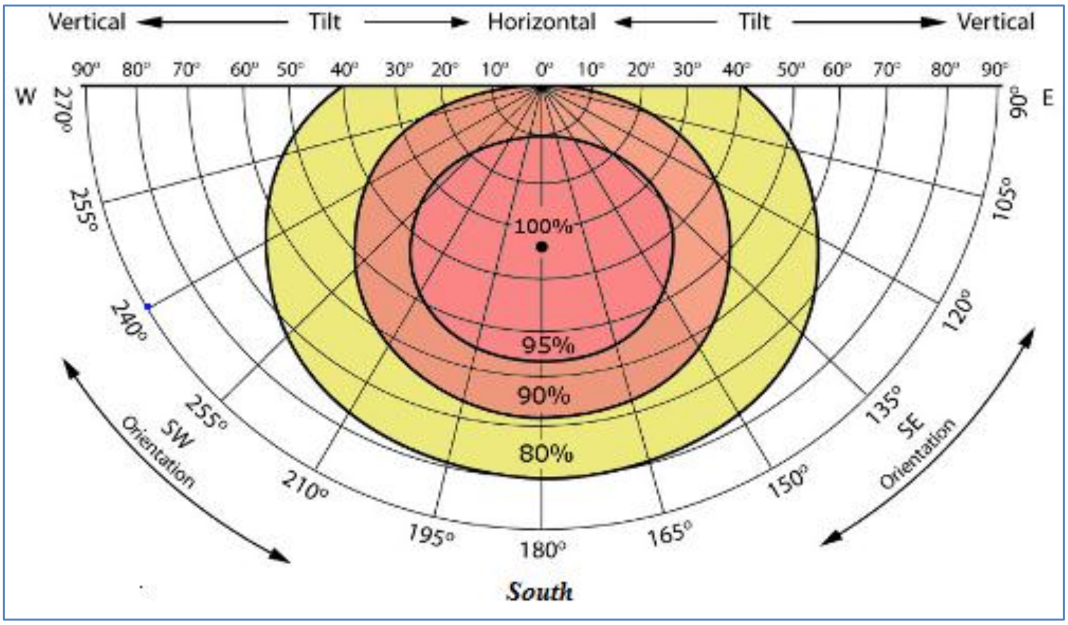

Figure III.38 : Percentage of solar gains depending on the orientation of the solar panel [6].

If you refer to the diagram above, you will see that further you are from the south, the more your production will be affected.

In the case of "self-consumption" for the solar production, it can make sense to orient the panels east/west rather than south-facing. East-facing panels will produce more energy in the morning, west-facing more energy in the late-afternoon. With respect to energy autonomy, the goal is not to produce the maximum but what is needed.

III. 3. 2. Tilt angle of solar panel

The power generated by the solar systems is associated with the solar energy radiated on modules. Thus, to estimate the energy generated by the solar modules, we must consider the architecture of solar system on a tilted surface at various azimuths so to receive the maximum solar radiation. To maximize solar power, the only flexible factor is tilt angle of panels. Particularly, for a fixed module, the collected solar energy is highly dependent on tilt and azimuth angles of solar panels.

Since only about 20% of the incident solar radiation is scattered light, fixed solar panels do not have a significant negative effect on efficiency. This is while the primary benefit of a tracking system is to collect solar energy for the longest period of the day, and with the most accurate alignment as the Sun's position shifts with the seasons. However, operating and maintenance costs of a tracking system are high and they cannot be always used. Therefore, it is a best choice in most cases to install solar panels at an optimum tilt angle.

The value of the inclination corresponds to the angle made by the module with the horizontal.

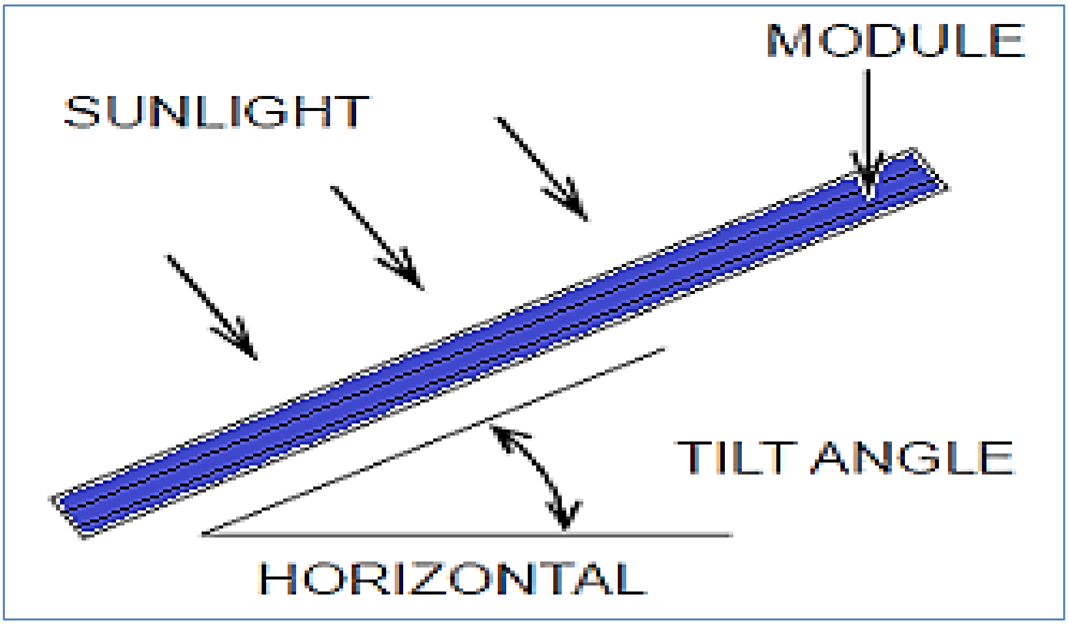

Figure III.39 : Tilt angle for the solar module.

Optimum tilt angle of solar panels is generally that which optimizes the production of solar panels during the least sunny month. Indeed, the sizing of your panels is based on this month.

III. 4. Calculation of optimal tilt angle and orientation for solar photovoltaic arrays

To get the most from position-fixed (or seasonally adjusted) photovoltaic or thermal solar panels, you need to point them in the direction that captures the most sun.

For systems with variable inclination, there is an orientation and an angle of inclination, which allows maximizing the monthly electricity production by capturing a maximum of solar radiation.

III. 4. 1. Optimal orientation

The angle given as the orientation for solar panel with respect to the south is called Azimuth. Geographic azimuth is always measured clockwise from a north, independently of the observation point [7].

Sun Path in winter

In winter (Jan, Feb, March) the sun's path is lowest for the northern hemisphere. The solar radiation received is the lowest of the year.

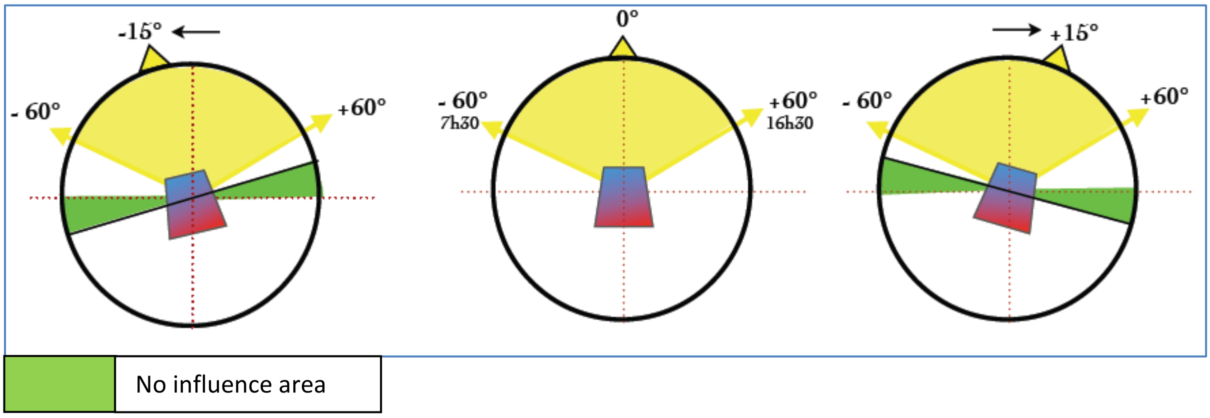

Path of the sun in autumn and spring

In autumn and spring the path of the sun is the same, for the northern hemisphere, the solar radiation received is more important and therefore the longest of the year.

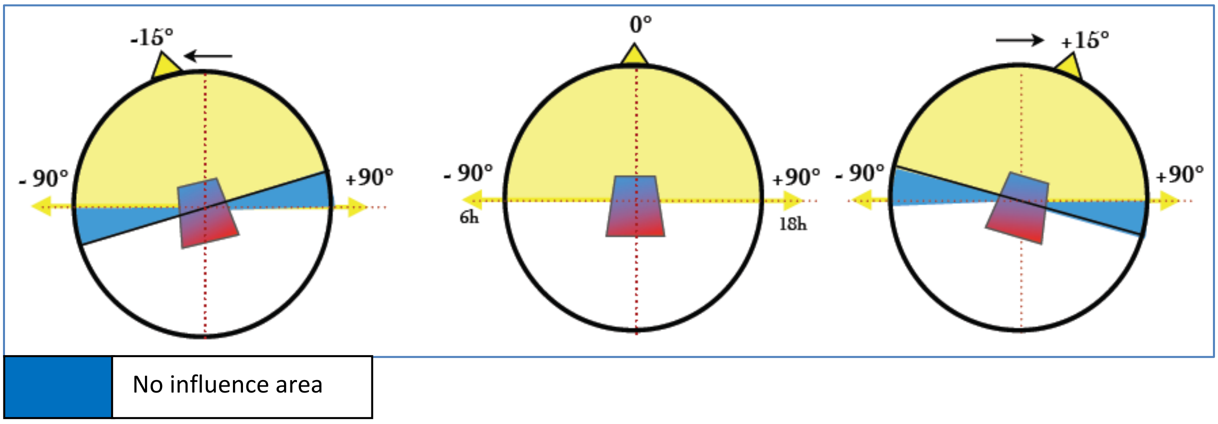

Path of the sun in summer

In summer, the sun's path is highest for the northern hemisphere. The solar radiation received is the strongest of the year.

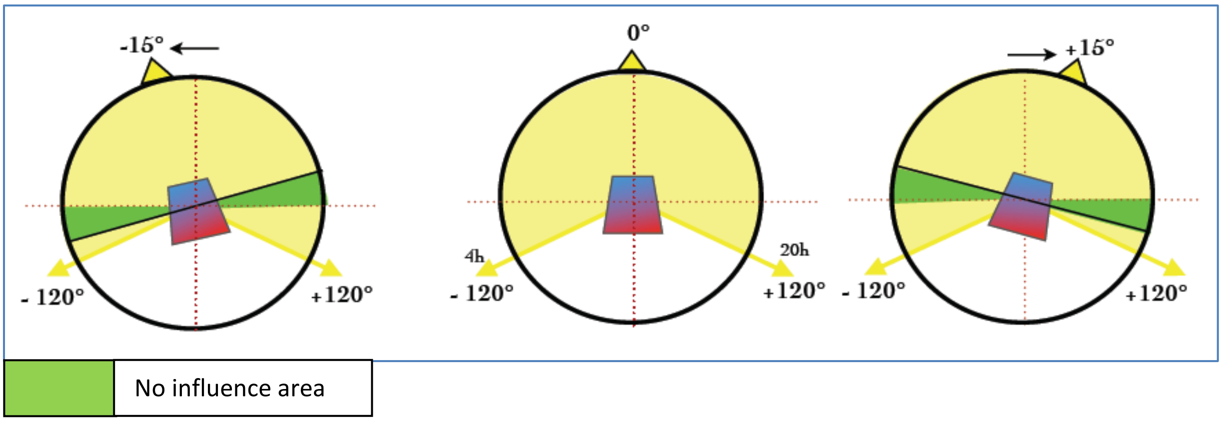

A slight change in azimuth has no influence on the insolation time.

The solar diagram

Every day, the sun describes a trajectory whose two main coordinates, φ and h, are represented on a graph. Each geographical point potentially has its own graph of the race of the sun, whose graphs depend on the longitude, latitude and altitude of the place.

The latter also makes it possible to indicate the azimuth and the height of the possible obstacles which stand in front of a determined solar installation [8].

Using a Matlab code, this plots the height of the sun in the sky as a function of azimuth during summer (August) and during the winter solstice (December).

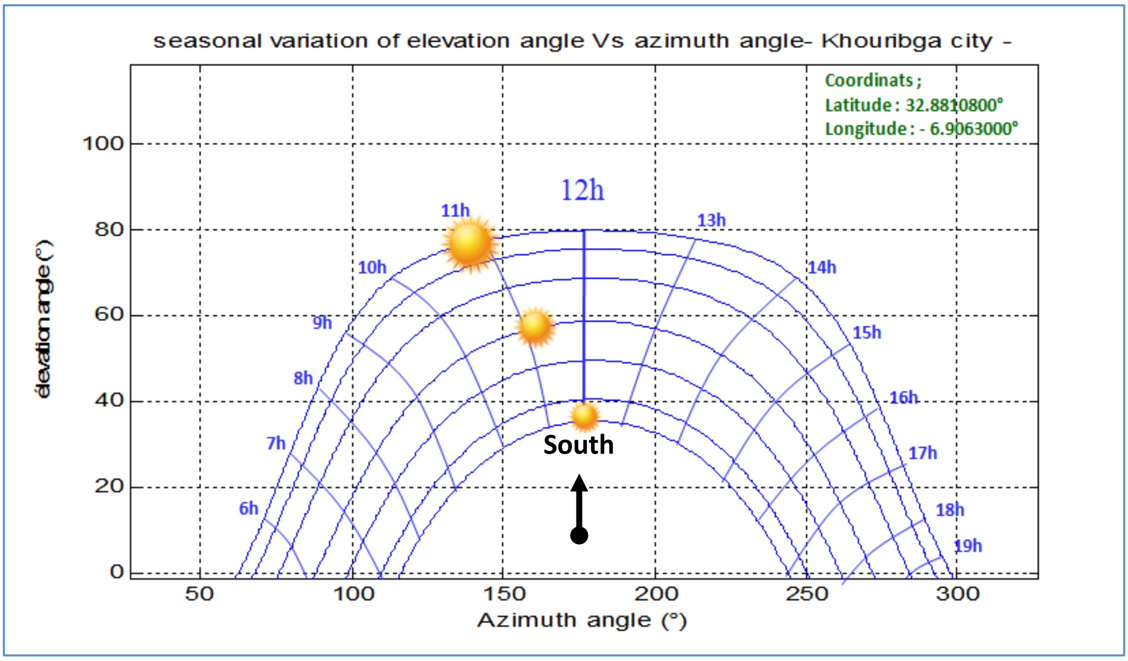

Figure II.40: Diagrams of the azimuth ϕ and elevation h with the notion of time.

This graph, consequently allows determining the periods of time and days during which the installation will not directly receive the direct solar radiation. The graph above presented the race of the sun at Khouribga city, with the hours of the day. We always have symmetry with respect to the south, so we will choose an orientation to the south or close.

III. 4. 2. Optimum Tilt Angle

Fixed solar systems

The fixed panels are installed in a fixed position throughout the year (azimuth and tilt), in integrated or superimposed mode. The optimum performance is obtained for a south orientation with an inclination corresponding to the latitude of the place. we can calculate the annual energy by a simple integral in a regular time interval from a surface of $1m^2$ with different angles of inclination from 0° to 90°, for determinate the optimal tilt angle of the solar panels to access the maximum energy received.

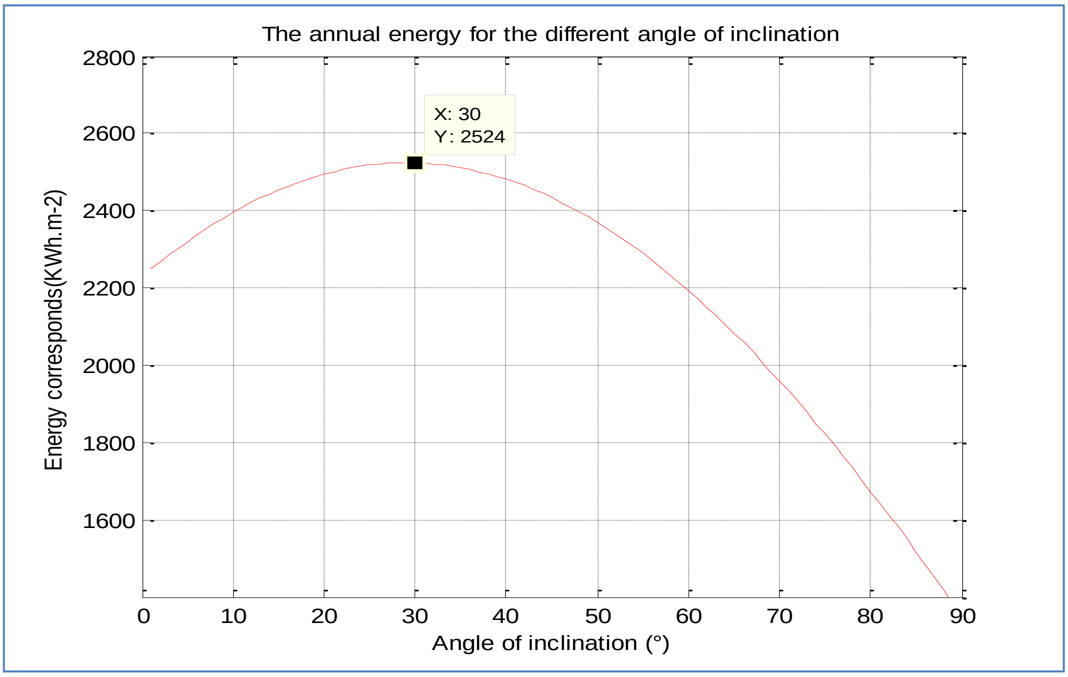

Figure III.41 : The annual solar energy for the different tilt angle.

From figures, we deduce the optimum angle of inclination (α_{opt}) for each month and for the whole year. We found that in relation to the site of Khouribga city, the optimum angle for the whole year α_{opt} = 30° and the received energy is E = 2524 kWh/m^2.

III. 5. Optimal Tilt angle and orientation in Khouribga city:

The efficiency of a PV module varies according to the angle of incidence of the solar radiation; it is possible to determine the most suitable position of the solar panels for the best energy efficiency [9, 10 and 11].

The position of the PV solar panel is determined according to two criteria:

The orientation (azimuth): This part is relatively simple. The panels should be oriented to the south in the northern hemisphere and, conversely, to the north in the southern hemisphere.

Inclination: It will then be important to determine an optimum tilt angle.

For express the value of the optimum tilt angle for PV solar panels, several proposals were studied and performed. One of these studies is presented below:

Taking into account the above formulations, the counting energy is developed in MATLAB to derive the energy received annually, seasonal and per month. This was achieved by a simple integral calculation in a regular time interval equal to 3 minutes, and applied to a surface of panel 1 m^2 choosing inclination angles varying from 0 to 90 degrees with step 1 degrees.

III. 5. 1. Monthly Tilt Angle

With adjustable panels, we can change the inclination every month. This type of structure is generally used for ground applications or on flat roofs.

A Matlab code has been developed which calculates and plots the solar energy of each month according to the inclination of a solar module.

The values of the optimum monthly angle given in the table are as follows:

Table III.7 : The optimum inclination for each month of the year.

Months	α_{opt} tilt angle	kWh/m^2.month
January	57°	209,6
February	48°	198
March	43°	229,9
April	18°	232
may	6°	250,8
June	0°	247,9
July	5°	250,7
August	13°	238,2
September	28°	218,6
October	43°	215,9
November	54°	200,1
December	59°	202,3
Annual radiation [kWh/m^2.year]		**2694**

This allows us to deduce the optimum tilt angle of the solar panel which would lead to the maximum energy production for a given month and for a year.

III. 5. 2. Seasonal Tilt Angle

The seasonal average was calculated by finding the average value of the tilt angle for each season, and the implementation of this requires that the collector tilt be changed four times in a year. In winter (December, January, and February) the tilt should be 55°, in spring (March, April, and May) 19°, in summer (June, July, and August) 5°, and in autumn (September, October, and November) 42°.

The figures showing the solar energy received for each season of the year, according to different angle of inclination and orientation of Khouribga city:

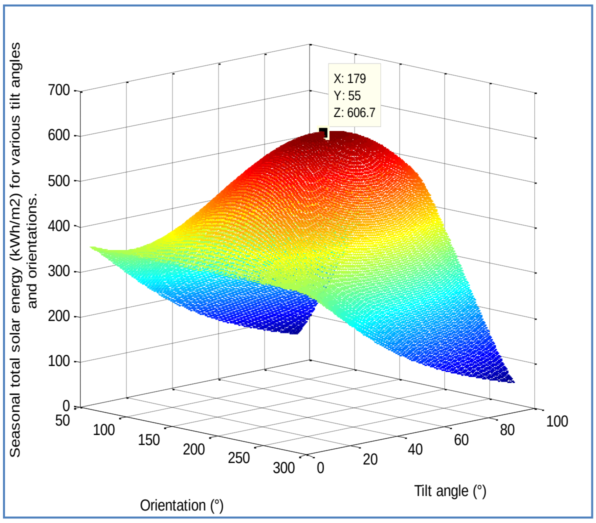

a) Winter Season

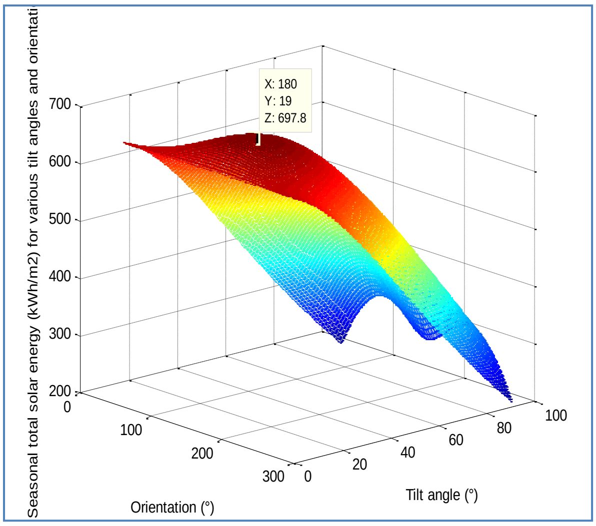

b) Spring Season

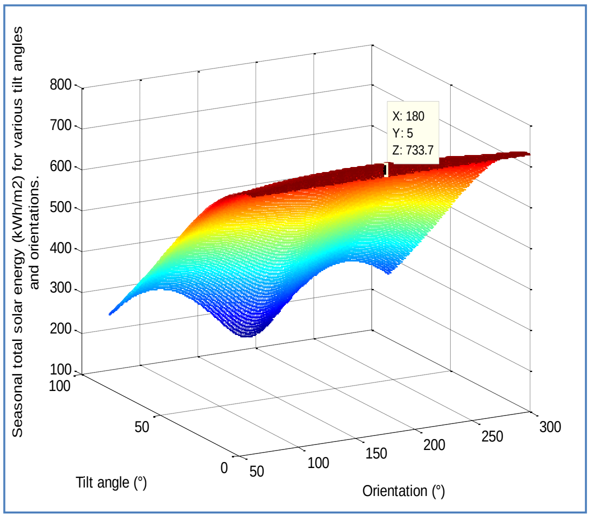

c) Summer season

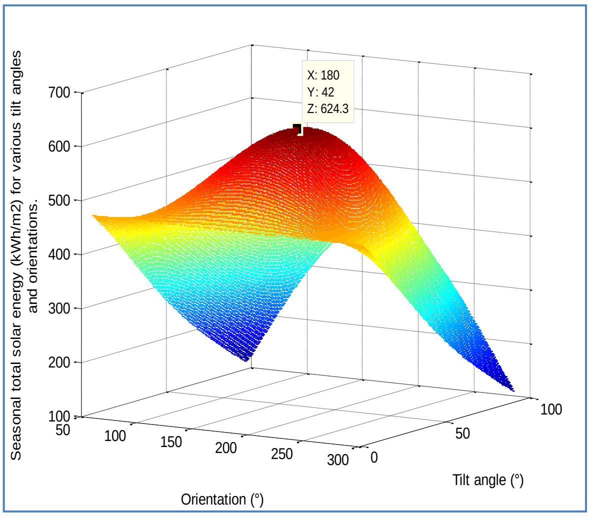

d) Autumn season

Figure III.42: Optimal tilt angle, orientation and the solar energy received for each season of the year.

The value of the seasonal tilt angle receives the maximum of seasonal solar radiations on at this tilted surface are given in Table:

Table III.8 : Seasonal and annual solar energy at Seasonal tilt angle.

Period	Months	Seasonal tilt angle	kWh/m2.Season
Winter	Dec-Jan-Feb	55°	606,6
Spring	Mar-Apr-May	19°	697,8
Summer	Jun-Jul-Aug	5°	733,7
Autumn	Sep-Oct-Nov	42°	624,2
Annual radiation [kWh/m^2.year]			**2662,5**

III. 5. 3. Annual Tilt Angle

For fixed panels are installed in a correct position throughout the year, We can calculate the annual energy by a simple integral in a regular time interval from a surface of 1m2 with angles of inclination different from 0° to 90° and the azimuth from 60° to 300° end Determine the angle of inclination and the optimal orientation of the solar panels to access the maximum energy output [12 & 13].

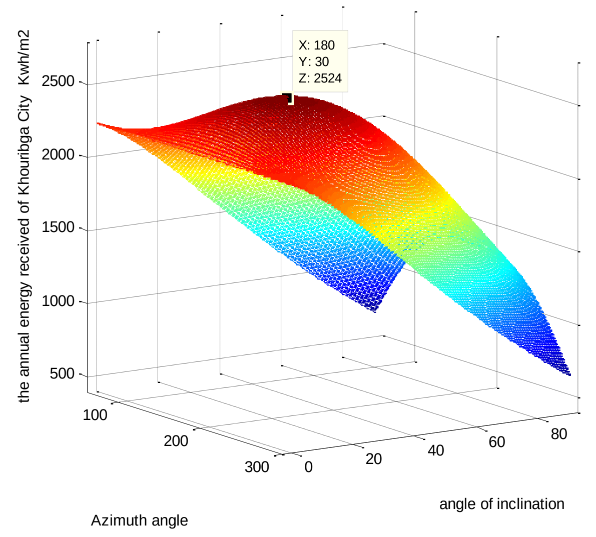

Figure III.43 : Annual solar energy yield (kWh/m2) for various tilt angles and orientations.

Accordingly, the annual solar energy yield was determined and is shown in figure 9. The peak value is 2524 kWh/m^2 which is quite good for active solar applications in khouribga city.

When the tilt angle is beyond 30◦, the annual solar yield falls slightly with increasing tilt angles. As the latitude of Khouribga city is 32°52’ north, the finding supports the argument that the optimal tilt angle for solar energy collection would be very close to the angle equivalent to the latitude of the location.

III. 6. Results and discussion

III. 6. 1. Optimal Tilt angle in Khouribga city:

We have taken a simple mathematical model (the equations) to calculate the monthly, seasonal and annual average of the incident solar irradiation on a south-facing surface with a different tilt angle relative to the horizontal, from 0° to 90° with step of 1°, and this by carrying a program executed under Matlab. See the results in the following table:

Table III.9 : Annual solar radiation at different tilt angle.

Optimum tilt angle	Monthly tilt angle	Seasonal tilt angle	Annual tilt angle	Horizontal surface
Energy received [kWh/m²/year]	**2694,0**	**2662,5**	**2524,0**	**2240,9**

From the table, it can be seen that the maximum incident energy and that received on an inclined plane by an optimum monthly tilt angle. The choice of tilt depends on the load. For example, for solar refrigeration, the best is to get the maximum energy in summer.

So to make the most of solar irradiation, the result of the table shows that it is necessary to change the solar panels inclination each month, if this is not possible, opt for the seasonal tilt angle. The improvement of the capture efficiency by the orientation and inclination of the solar panels makes it possible to obtain a rational use of the incident solar energy, thus reducing the cost of the solar system being used.

The purpose of this study was to obtain results of optimum tilt angle desired at the allotted time (monthly, seasonal and annual) to optimize the solar irradiation received by the solar panels. Khouribga in winter, the sun is low compared to the horizon, to obtain the best performance it will be necessary to favor a wide tilt angle. In spring the best tilt angle is at 19°, and in summer the optimal angle is at 5°.

We can give examples of the importance of our study:

- ***In solar thermal:*** We want to produce more heat in winter and less heat in summer. So we will try to have an optimum angle of winter, the nearest possible 55°.
- ***Air conditioners and solar refrigerators:*** We have to optimize the receive solar irradiation in summer, as a result, it is preferable to favor production in summer, and to decrease a little the one of winter,

- ***In photovoltaic and thermal solar:*** Electricity and hot water needs were constant throughout the year; the best inclination is therefore that of maximum sunshine, that is to say 30 °.

This work strategy is applied to the 20 Moroccan cities participating in the propre.ma project to calculate the optimal inclination of these cities.

III. 6. 2. Calculation of solar radiation received on the optimum tilt angle surface

We will study in this part the influence of the optimum tilt angle on the amount of solar irradiation received on a surface of 1m2, in Khouribga city we used the results of previous part, the optimal tilt angle is 30° and the direction of the azimuth 180° (south).

III. 6. 2. 1. Daily irradiation

The Matlab code that we used, allows us to calculate and plot the daily solar irradiation received on an optimal exposure surface of the typical days of each month. The results are given in the table below;

Table III.10 : Values of the daily irradiation of the typical days of each month

The energy received per days (wh/m^2)					
Month	Days typical	N°of days	Direct energy	Diffuse energy	Total energy
January	17	17	5621	401	6022
February	16	47	6288	505	6793
March	16	75	6734	675	7409
April	15	105	6736	891	7627
May	15	135	6403	1083	7486
June	11	162	6132	1194	7326
July	17	198	6119	1207	7326
August	16	228	6323	1101	7424
September	15	258	6395	916	7311
October	15	288	6094	699	6793
November	14	318	5567	512	6079
December	10	344	5286	411	5697

We have added curves giving the daily variations of the solar irradiation, indicating the maximum of direct, diffuse and global solar energy arriving at a surface of optimal exposure;

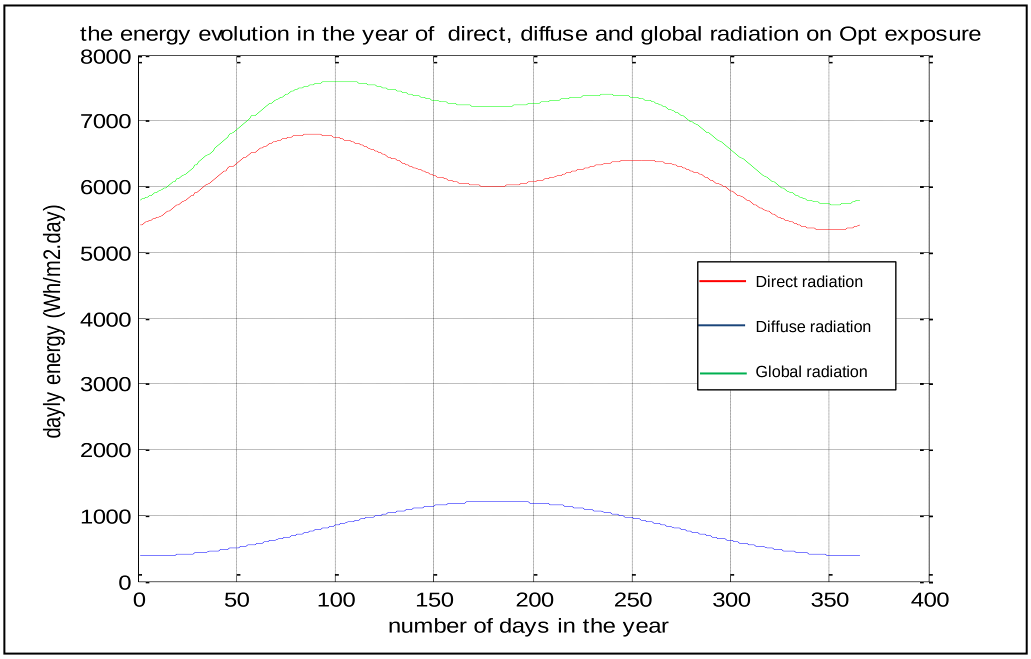

Figure III.44 : Evolution of direct, diffuse and global solar radiation in the year, on optimum exposure.

The analysis of the curves obtained above indicates that the values of direct, diffuse and global solar radiation are maximum in summer and minimum in winter in Khouribga city. The global radiation energy exceeds 7000 Wh/m^2 in the summer days, on the other hand, for the winter days extend between (5700 and 7000 Wh/m^2).

III-6-2-2 The energy that accumulates for each month

We used the same calculation method of the previous part; the cumulative energy calculation is done by integrating the power formulas between sunrise and sunset. This method estimates the monthly energy received on an inclined surface of 30° and facing south. The results are shown in the figure below:

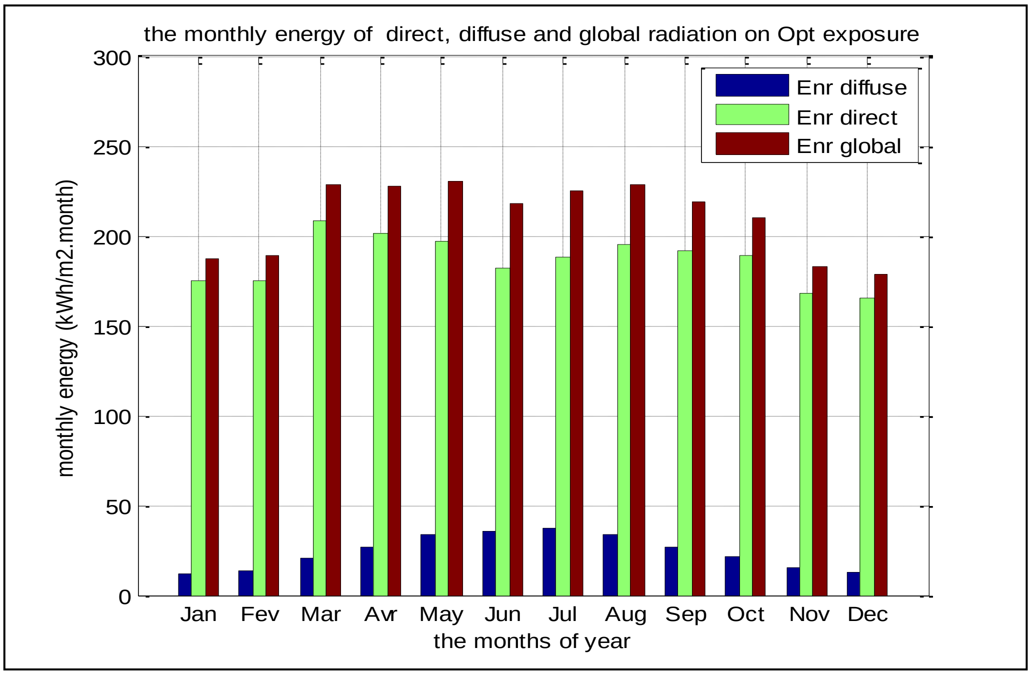

Figure III.45: The monthly direct, diffuse and global solar radiation, of optimum exposure.

We can summarize the results which are given by the histogram in the table below;

Table III.11 : The monthly cumulative energy of optimum exposure.

The energy received per month (kwh/m²)			
Month	Direct energy	Diffuse energy	Total energy
January	173.08	12.33	185.41
February	173.85	13.78	187.63
March	207.54	20.74	228.28
April	201.51	26.69	228.20
may	198.19	33.60	231.79
June	183.58	35.91	219.48
July	189.82	37.17	226.99
August	195.83	33.87	229.71
September	191.27	27.27	218.55
October	188.07	21.49	209.56
November	166.60	15.20	181.80
December	164.04	12.44	176.48
all year	**2233.4**	**290.6**	**2524**

The provides information on the distribution of solar energy for each month, the energy is superior to 200 kWh/m^2 of the 8 months; corresponding the summer and intermediate months of the year, for the winter months their energy is below 200 kWh/m^2.

In the end, we get on the global of annual energy received on a surface of the optimum tilt angle (30°) and facing south; at Khouribga city is 2524 kW/m^2.

III. 6. 3. Effect of Tilt and Orientation angles of solar panels on their production

Generally, for the installations aiming at maximum annual production, the inclination given to the solar panel corresponds to the angular value of the latitude of the place of installation, with an orientation towards Ecuador, that is to say, to South for the localities situated in the northern hemisphere, and a northerly orientation for localities located in the southern hemisphere. Indeed, when you are in the northern hemisphere, the sun is seen longer in the southern hemisphere throughout the year.

To these various general recommendations, we can add that to facilitate the flow of rainwater and the evacuation of objects and dust that could settle on the panel; there is provided a minimum inclination of 5 ° to 10 ° for photovoltaic panels. For the thermal solar panel operating by thermosiphon, at least 15 ° is required to assist the thermosiphon effect.

Methodology

We used our programming of mathematical formulas under Matlab, to construct a solar gain based on the tilt and orientation of solar panels for the city of Khouribga. The calculation of sunshine on an inclined plane in Matlab is based on the algorithm that we developed using the mathematical formulas of solar radiation.

For each site, first the annual radiation received on a surface oriented due south and inclined at latitude is simulated and taken as a reference value. The annual radiations for different orientations and inclinations were then recorded and compared to the reference. The simulations were performed in 1° steps for orientation and in 1° steps for tilt angle.

Results and discussions

The following figures represent the percentage of the annual reference radiation depending on the orientation and inclination adopted. It is shown below, on the abscissa we find the orientation, from 0 ° (North) to 360 ° (North) passing through the East (90 °), the th (180 °) and the West (270 °).

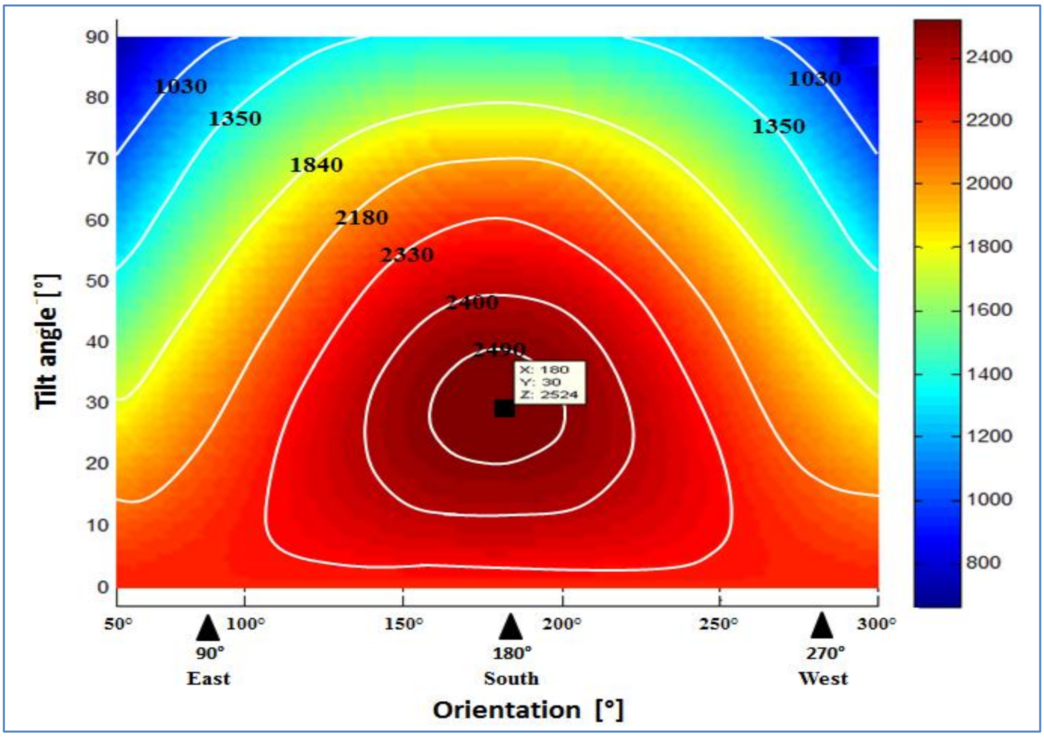

Figure III.46 : Annual solar energy yield (kWh/m2) for various tilt angles and orientations.

Accordingly, the annual solar energy yield was determined and is shown in Fig. The peak value is 2524 kWh/m^2 which is quite good for active solar applications in khouribga city. When the tilt angle is beyond 30°, the annual solar yield falls slightly with increasing tilt angles. As the latitude of Khouribga city is 32°52'North, the finding supports the argument that the optimal tilt angle for solar energy collection would be very close to the angle equivalent to the latitude of the location.

The following table shows the relative output of solar panels based on their angle and orientation. It shows the further away from being at a 30 degree roof angle and facing due south the less efficient the panel would be. Interestingly if you placed your panels on a flat roof facing towards the sky they would only perform 10 percent less than optimal.

Table III.12 : Relative distribution in percent (%), of the solar radiation received as a function of the orientation and tilt angle in Khouribga city.

Khouribga - Morocco 32°52'N **(** 2524 kWh/m^2/year)

90	29	33	38	42	45	48	51	52	53	54	54	54	54	54	54	53	53	51	50	47	44	41	36	32	27
85	31	37	41	45	49	53	55	57	59	60	60	60	60	60	60	59	58	57	54	52	48	44	40	35	30
80	34	39	45	49	53	57	60	62	64	65	66	66	66	66	66	65	63	62	59	56	53	48	44	38	33
75	38	43	48	53	57	61	64	67	69	71	72	72	72	72	71	70	68	66	64	60	56	52	47	42	36
70	41	46	52	57	61	65	69	71	74	76	77	77	77	77	76	75	73	71	68	64	60	56	51	45	40
65	44	49	55	60	65	69	73	76	78	80	81	82	82	82	81	80	78	75	72	68	64	59	54	49	43
60	47	53	59	64	68	73	76	79	82	84	86	86	87	86	85	84	82	79	76	72	68	63	58	52	46
55	51	56	62	67	72	76	80	83	86	88	89	90	90	90	89	87	85	82	79	75	71	66	61	56	50
50	55	60	65	70	75	79	82	86	89	91	92	93	94	93	92	90	88	85	82	78	74	69	64	59	54
45	58	63	68	73	77	81	85	88	91	93	95	96	96	96	95	93	91	88	85	81	77	72	67	62	57
40	62	67	71	75	80	84	87	90	93	95	97	**98**	**98**	**98**	96	95	93	90	87	83	79	75	70	66	61
35	66	70	74	78	82	86	89	92	94	96	**98**	**99**	**99**	**99**	**98**	96	94	92	89	85	82	78	73	69	65
30	69	73	77	80	84	87	90	93	95	97	**98**	**99**	**100**	**99**	**98**	97	95	93	90	87	83	80	76	72	69
25	73	76	79	82	85	88	91	93	95	97	**98**	**99**	**99**	**99**	**98**	97	95	93	91	88	85	82	79	76	72
20	76	79	82	84	87	89	91	93	95	97	97	**98**	**98**	**98**	97	96	95	93	91	89	86	84	81	79	76
15	80	82	84	86	88	89	91	93	94	95	96	97	97	97	96	95	94	93	91	89	87	85	83	81	80
10	83	84	86	87	88	89	91	92	93	93	94	94	94	94	94	93	93	92	90	89	88	87	85	84	83
5	86	86	87	88	88	89	89	90	91	91	91	91	91	91	91	91	90	90	89	89	88	87	87	86	85
0	88	88	88	88	88	88	88	88	88,2881	88	88	88	88	88	88	88	881	88	88	88	88	88	88	88	88
	60	**70**	**80**	**90**	**100**	**110**	**120**	**130**	**140**	**150**	**160**	**170**	**180**	**190**	**200**	**210**	**220**	**230**	**240**	**250**	**260**	**270**	**280**	**290**	**300**
				East									**South**									**West**			

Relative distribution, in percent, of the solar radiation received as a function to the orientation and tilt angle in Khouribga city.

Depending on whereabouts you are in the world will alter the optimal angle and orientation. These figures are only really suitable for the Khouribga city in Morocco and then there is some variation across the country. In the far north of Tanger your panels would perform better if your roof angle was 32 degrees. For the far south of Laayoun the optimal roof angle would be closer to 25 degrees.

Conclusion III

The tilt angles of solar panels should be adjusted monthly, seasonal or the yearly to extract the maximum energy from solar panels.

The construction of structures dedicated to solar installations or architectural modifications in order to comply with these recommendations are therefore generally not justified. We have drawn up a diagram and the table, allowing you to quickly determine the percentage of solar energy collected on a solar panel based on its orientation and inclination relative to conventional optimal tilt angle and orientation.

In this chapter, we studied the effects of orientation for a solar panel and the optimum tilt angles for harvesting solar energy in Khouribga city and thereafter the other 20 Moroccan cities. The results found of this study are calculated by using the mathematical models programmed under MATLAB.

References III

[1] EL-ASSEFRY Karim & M'HAMDI Kamilia, "Etude, conception et dimensionnement de la deuxième tranche du projet solaire d'OUARZAZATE : La centrale photovoltaïque 100 MW," Phd, Ecole Nationale de l'Industrie Minérale (E.N.I.M.), 2011, pp.18,

[2] Aftim Acra, Zeina Raffoul and Yester Karahagopian, "Guidelines for Household Application in Developing Countries", Solar Disinfection of Drinking Water and Oral Rehydratoin Solutions, Department of Environmental Health Faculty of Health Science American University of Beirut Beirut, P.O.Box 811721-1984

[3] E Kabir, P Kumar, S Kumar, AA Adelodun, "Solar energy: Potential and future prospects" Renewable and Sustainable Energy, vol. 12, pp. 675–698, 2018.

[4] E.Karim and M.Kamilia, "Study, design and dimensioning of the second tranche of the solar project of OUARZAZATE: The 100 MW photovoltaic plant", National School of Mineral Industry (ENIM), 2011, pp .18,

[5] Bendjellouli Zakaria, "Contribution à la modélisation d'une cellule solaire" Mémoire de Magister, Université de BECHAR – Algérie - Faculté des Sciences et Technologie, 2009, pp. 8-10,

[6] Jaques Teller, "Confort Thermique," Universite de ligé, 2013, pp.1-4.

[7] Alain Ricaud Jan, "Gisement solaire et transferts énergétiques," Master Renewable Energies University of Cergy-Pontoise , 2011,

[8] Ahmed Ennaoui, "Photovoltaic Solar Energy Conversion (PVSEC)" Helmholtz-Zentrum Berlin für Materialien und Energie- Free University of Berlin- Allemand, 2014,

[9] Klein S. A."Calculation of monthly average insolation on tilted surfaces" Solar Energy Vol. 19, 325- 329, 1977,

[10] M. Jamil Ahmad, G.N.TIWARI, "Optimization of Tilt Angle for Solar Collector to Receive Maximum Radiation" The Open Renewable Energy Journal, 2009, 2, 19-24,

[11] K. ULGEN, "Optimum Tilt Angle for Solar Collectors" Energy Sources, Part A, 28:1171–1180, 2006.

[12] Danny H.W. Li and Tony N. T. Lam, "Determining the Optimum Tilt Angle and Orientation for Solar Energy Collection Based on Measured Solar Radiance Data" International Journal of Photoenergy, Vol 2007, Article ID 85402.

[13] H. Gunerhan and A. Hepbasli, "Determination of the optimum ilt angle of solar collectors for building applications" Building and Environment, vol. 42, no. 2, pp. 779–783, 2007.

Chapter IV

MODELING OF SOLAR RADIATION ON THE GROUND

IV. 1. Introduction

The knowledge of the solar radiation has a major interest for the study and the design of the solar energy systems. Thus, a good design is possible only if the measures are available in a continuous manner in space and in time. To estimate the solar potential, it is essential to know the characteristics of the solar radiation reaching the Earth's surface at a given location. Radiation reaching the ground depends on the reflectance of the terrestrial surface and atmospheric effects. To know the energy received by a given site, it is necessary to locate this site on the earth's surface, to know the position and trajectory of the sun in the sky and the movement of the earth around the sun.

A solar system directly and instantaneously converts solar energy into electrical energy without using fuel. Indeed, PV technology exploits the photoelectric effect, whereby "doped" semiconductors generate electricity when exposed to the solar radiation.

The annual production of electrical energy in a PV installation depends on various factors. Especially:

- Incidental solar radiation at the installation site.
- Tilt and orientation of panels.
- Presence where there is no shading.
- Technical performance of system components (mainly modules and inverters).

The study or applications of solar energy at a given site are dependent on more complete and detailed data on the solar radiation of this site, the aim of this chapter is presented the method used in the calculation and describe the available data by trying to extract some useful information. We present the method used in the calculation and describe the available data by trying to extract some useful information. In our study we use programs through MATLAB to estimate the totality of the solar radiation. Moreover, we will study the theoretical solar field available in Settat city, a series of insolation and irradiation data calculate, and then we apply the same strategy of this work to the 20 Moroccan cities in different time scales (every 3min, every day, every month and all year).

In our study, we use MATLAB to estimate the totality of the solar radiation on any inclined surface. The developed program allows us to extract the right angle under which the maximum energy could be absorbed by the solar cells. Moreover, we will study in the last part the influence of exposure (orientation and inclination) on the amount of solar radiation received on a surface of $1m^2$, The example detailed hereafter relates to a photovoltaic pumping installation installed at Faculty of Science and Technology of Settat-Morocco (latitude 33.029° and longitude −7.619°) [1]. and the among objectives of this work, is to propose optimization runs, in order to minimize the harmful effects of partial shading on the systems of photovoltaic solar panels by the use of different position modes. We also approach from a global perspective, allowing us to reach reliable and real results of the productivity of a PV installation under the shading effect. The study of our installation, based on estimating the annual production and the losses due to the phenomenon of shading, a simple calculation based on the system performance ratio, allows us to release the electrical productivity of the installation completed by a practical study of the shading effect by the use of" Shadow Mask Close". This method was applied to the photovoltaic installation of the 1.5 kWc located at the Faculty of Science and Technology in Settat city and to calculate the energy output of the photovoltaic panels, before calculating the effect of shading influence on this photovoltaic installation.

IV. 2. Statistical models for calculating solar radiation

Among the essential benefice of the sun is the irradiation that is transmitted to the earth. Those irradiations are used by humans in order to create energy: either heat or electricity. The irradiations that are used are mainly the ones with a wavelength that varies from 0.25 to 3 μm. Therefore, it is important to know how the calculations are done in order to estimate the irradiations. However, using manual calculations with the equations that are presented below is a very long process it is important to have an idea about the different instruments and software that are used in order to get the solar irradiance immediately [2].

But before giving some methods of calculating these values, it is interesting to know some information concerning extra-terrestrial solar radiation. Indeed, all estimation methods are based on the calculation of its value and its spectral energy distribution, to which we will apply the attenuation characteristics of atmospheric constituents as a function of wavelength.

IV. 2. 1. Extra-terrestrial solar radiation I_0 (W/m^2)

Solar radiation incident outside the earth's atmosphere is called extra-terrestrial radiation. On average the extra-terrestrial irradiance is 1367 W/m^2 (French agency for the study and development of solar energy). This value varies by ±3% as the earth orbits the sun. The earth's closest approach to the sun occurs around January 4th and it is furthest from the sun around July 5th.

If we adopt the average value of I_0 = 1367 W/m^2 the energy of the irradiation which corresponds to it, but not all of this energy comes to earth due to presence of the atmosphere.

The variations of the extra-terrestrial solar radiation are mainly due to the activity of the sun and to the elliptical trajectory of the earth around the sun, the satellite measurements made it possible to establish an empirical formula, of acceptable precision, giving the solar constant I_0 as a function of number of day j in the year [3]:

$$I_0 = 153.(1 + 0,033.cos(0,984.j)) \quad (1)$$

If high precision is required, it is possible to consider a Fourier series expansion of the acquired data; these which resulted in [4]:

$$I_0 = 1353 + 45,32.cos(d) + 0,88018.cos(2.d) - 0,00461.cos(3.d) + 1.8037.sin(d) + 0,09746.sin(2.d) + 0,18412.sin(3.d) \quad (2)$$

With:

d = 0,984.j

The programming of these two formulas allows to have an idea quantified on I_0 for a year.

Which gives the averages on; I_{oc} and I_{op} :

With:

$I_{oc} = I_o$: according to equation 1 and $I_{op} = I_o$: according to equation 2

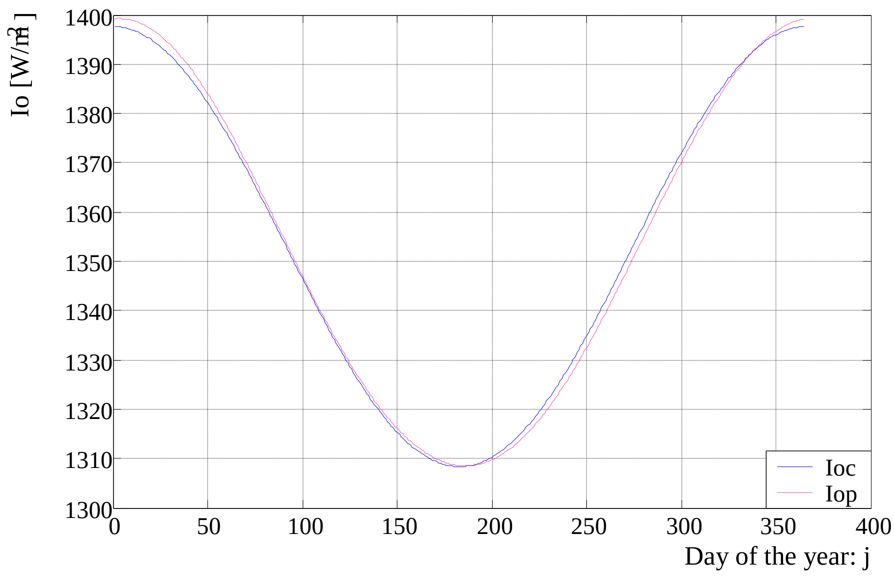

Figure IV.47 : Solar constant according to the two expressions of the equations.

From these results it comes out:

The formulas can be integrated into the calculation process with the desired precision in all serenity; which facilitates programming.

The small differences between I_{oc} and I_{op} encourage us to use the simplified formula of Io, with complete confidence, to know [3 & 4]:

$$I_0 = 1353(1 + 0.033.\cos(0{,}984.j))\ [W/m^2] \qquad (3)$$

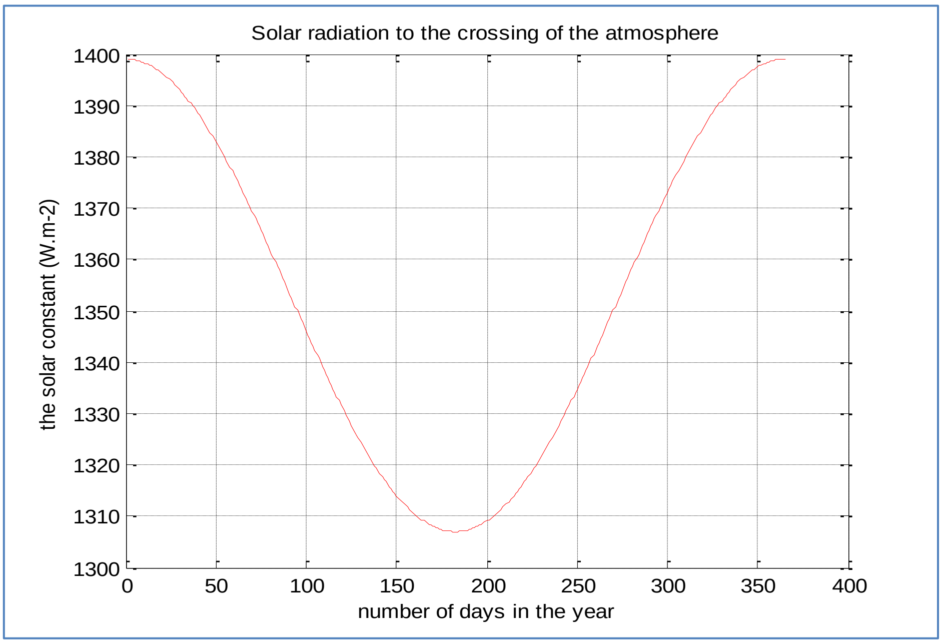

Figure IV.48 : Variation of the extra-terrestrial solar irradiance.

The programming of the extra-terrestrial solar radiation formula provides a numerical idea about I_0 for any year. And the value of I_0 received by the earth’s surface is of the order of 1367W/m^2 on average.

IV. 2. 2. Air mass effect

The intensity of absorption and scattering that the solar radiation undergoes when crossing the atmosphere is linked to the quantity of molecules encountered by this radiation. The Air Mass is the path length which light takes through the atmosphere normalized to the shortest possible path length (that is, when the sun is directly overhead). The Air Mass quantifies the reduction in the power of light as it passes through the atmosphere and is absorbed by air and dust. Under the normal temperature and the pressure conditions the Air Mass is defined by the following expression [5]:

$$AM = \frac{p}{1013}.\frac{1}{\sin(h)} exp(-\frac{y}{7{,}8}) \qquad (4)$$

Where

p: air pressure (N/m^2).

h: is the angle from the vertical (zenith angle), on the horizon (h = 90° at the zenith).

y: altitude in (km).

In the normal condition (p = 1013 N/m^2) and sea level (y = 0), expression simplified of Air Mass is:

$$AM = \frac{1}{sin(h)} \quad (5)$$

When the sun is directly overhead, the Air Mass is 1.

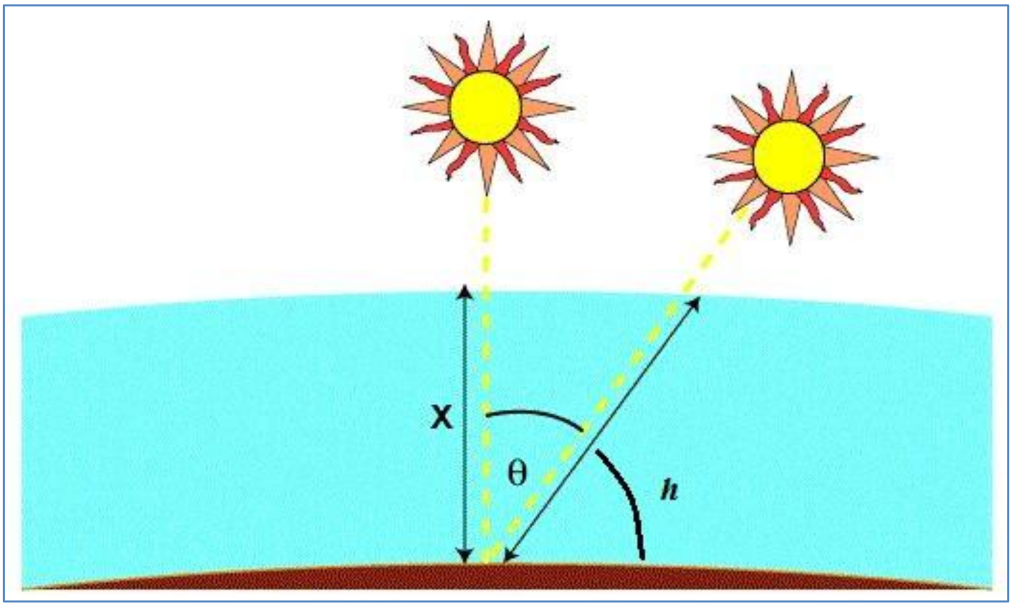

Figure IV.49 : Representation of Air mass.

So when the sun is at the zenith we have AM_1, with a sun at 30° of the horizon we will have AM_2 and for the sun at 48 ° the AM is 1.5; by convention AM_0 designates solar radiation outside atmosphere, the following table gives the solar constant (I_0) according to the number of air mass, and the values of the air mass A.M according to solar height:

Table IV.13: The solar constant (I_0) and solar height (h) as a function of the number of Air Mass.

A.M	0	1	1,5	2	3	4	5
I_0 (W/m2)	1367	931	834	755	610	530	430
The solar height (h)	90°	90°	42°	30°	20°	14,5°	11,5°

An easy method to determine the air mass is from the shadow of a vertical pole.

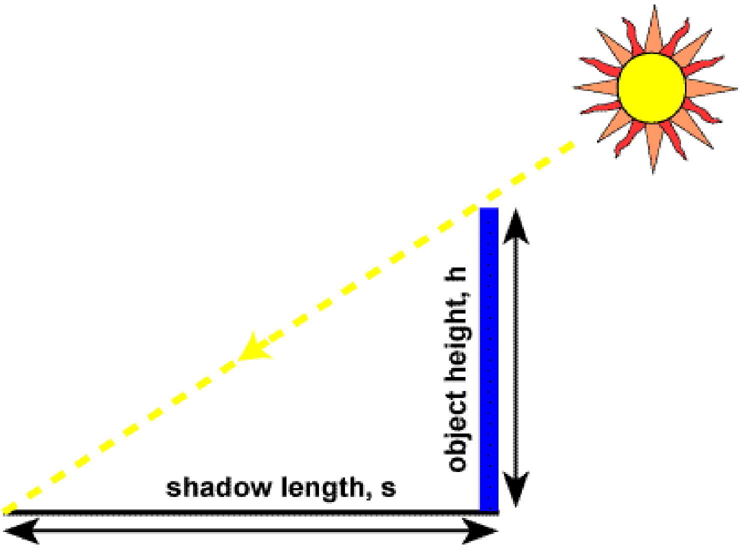

Air mass is the length of the hypotenuse divided by the object height h, and from Pythagoras's theorem we get:

$$AM = \sqrt{1 + (\frac{s}{h})^2} \quad (6)$$

The above calculation for air mass assumes that the atmosphere is a flat horizontal layer, but because of the curvature of the atmosphere, the air mass is not quite equal to the atmospheric path length when the sun is close to the horizon. At sunrise, the angle of the sun from the vertical position is 90° and the air mass is infinite, whereas the path length clearly is not. An equation which incorporates the curvature of the earth is:

$$AM = \frac{1}{\cos(\theta) + 0{,}50572(96{,}07995 - \theta)^{-1{,}6364}} \quad (7)$$

IV. 2. 3. The incidence angle

The angle of incidence of the solar radiation with any surface of inclination and orientation is the angle formed by the direction vector of the solar radiation and the normal leaving the surface. This angle of beam radiation on an arbitrarily tilted plane is a bit trickier to derive [1].

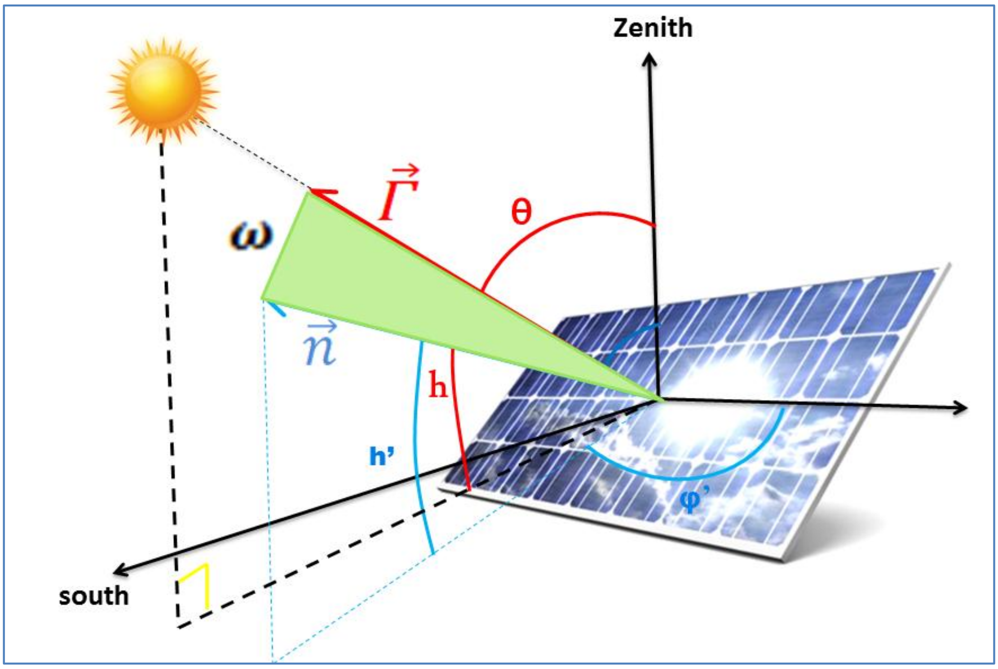

Figure IV.50 : The geometric relations between the solar horizontal coordinates and the incidence angle ω.

What we now want to find is the angle ω between the Sun vector $\vec{\Gamma}$ and the normal vector $\vec{n}$ of the tilted plane.

Where:

$\vec{\Gamma}$: The unit vector carried by the direction of the solar rays.

$\vec{n}$: The unit vector carried by the normal to the surface.

ω: The angle of incidence between ($\vec{\Gamma}$, $\vec{n}$).

$$\vec{\Gamma} = \begin{cases} \sin(\theta).\cos(\varphi) \\ \sin(\theta).\sin(\varphi) \\ \cos(\theta) \end{cases} \quad \text{and} \quad \vec{n} = \begin{cases} \cos(\theta').\cos(\varphi') \\ \cos(\theta').\sin(\varphi') \\ \cos(\theta') \end{cases}$$

We make the scalar product of two vectors, $\vec{\Gamma}$ and $\vec{n}$ for determining the angle ω ;

$$\vec{\Gamma}.\vec{n} = \|\vec{\Gamma}\|.\|\vec{n}\|.\cos(\omega) = \cos(\omega)$$

$$\vec{\Gamma}.\vec{n} = \sin(\theta)\sin(\theta')\cos(\varphi)\cos(\varphi') + \sin(\theta).\sin(\varphi).\sin(\theta').\sin(\varphi') + \sin(\theta).\sin(\theta')$$

And we have :

$$\sin(\varphi)\sin(\varphi') + \cos(\varphi)\cos(\varphi') = \cos(\varphi - \varphi')$$

As before, we can now find the cosine of the angle θ as the dot product between $\vec{\Gamma}$ and $\vec{n}$. We thus find:

$$Cos(\omega) = \cos(h).\cos(\varphi - \varphi').\sin(\theta') + \sin(h).\cos(\theta') \qquad (8)$$

IV. 2. 4. Theoretical solar irradiation on the earth

Extraterrestrial radiation is affected in various ways during passage through the atmosphere. This section reviews these mechanisms and describes the properties of the solar radiation available at Earth's surface. A short discussion on the radiation and energy balance of Earth is also included.

The previous section allowed us to accurately assess the solar radiation outside the atmosphere, arriving on a surface normal to the incident radiation; but at ground level the radiation received is dependent on multiple constraints:

- Optical: The atmospheric composition layer; humidity, pollution, suspended particles....
- Geometric: Orientation and inclination of the fixed plane collectors.
- Geographical: Latitude, climatic data, configuration, site position...

For solar applications there are several mathematical approaches; which process the solar spectrum received on the ground as a whole; more precisely the power likely to be drawn from a surface with a given orientation (from the south) and of a determined inclination (with respect to the horizontal). Let us quote those which use the various means of investigation and which allow results to be adjusted to reality with an acceptable margin of error.

IV. 2. 4. 1. Hottel's method

In a simplified manner this method read the average value of the power received on the ground, by a horizontal surface, visibility used by meteorologists and coefficients that include atmospheric conditions at the altitude of the site. Obviously, when the capture surface has a given orientation and inclination, to correct this formula by coefficients that take into account the conditions of use [6].

The power received on the ground by a horizontal surface, is given by the following relationship:

$$I_t = a_0.\sin(h).\{a_0 + a_1.\exp(-a_2/\sin(h))\} \tag{9}$$

Where the coefficients a_0, a_1 and a_2 are dependent on visibility:

$$\begin{cases} a_0 = 0{,}4237 - 0{,}008200.(6 - z)^2 \\ a_1 = 0{,}5055 + 0{,}00595.(6{,}5 - z)^2 \\ a_2 = 0{,}2711 - 0{,}01858.(2{,}5 - z)^2 \end{cases} \quad \text{For altitudes less than 2.5km}$$

$$\begin{cases} a_0 = 0{,}2538 - 0{,}0063.(6 - z)^2 \\ a_1 = 0{,}7678 + 0{,}001.(6{,}5 - z)^2 \\ a_2 = 0{,}249 - 0{,}081.(2{,}5 - z)^2 \end{cases} \quad \text{For an urban haze atmosphere}$$

It should be noted that this method allows the interpolation, for a given altitude, of the coefficients in the above-mentioned visibility range.

Some similar models consider that the atmosphere is transparent and keeps its optical properties constant through the different parameters and coefficients of the models.

Consider now the uncertain conditions of the atmospheric layer and in particular the cloud masses: Sky totally or partially covered for specified durations. A basic approach is to visually estimate the veiled proportion of the sky at regular time intervals. It therefore implies the human factor which results in dispersions, on measures, unacceptable.

This parameter designates the sunshine, if t is the fraction of the time during which the sky is clear and T the total duration of the day (from sunrise to sunset) we define sunshine by:

$$\sigma = \frac{t}{T} \quad \text{It's obvious that:} \quad 0 \leq \sigma \leq 1$$

Where t and T are expressed in the same unit of the time (usually in hours).

If we know the hour angle of the sunrise or sunset (compared to the local noon), the total duration of the day is:

$$T = 2.\omega_{ls}/15 \tag{10}$$

$$\sigma = \left(\frac{15}{2.\omega_{ls}}\right).t \tag{11}$$

With:

ω_{ls}: In degree [°].

t : In hour.

Several researchers have tried to link linear insolation and radiation with linear mathematical equations. The most used correlations are of two types; Angstrom-type σ relationships that only relate to local site conditions (Remember that σ is also) and Angstrom Black type relationships that incorporate the solar constant.

$$H_h = H_{hc}.(a_0 + a_1.\sigma) \qquad [J/(m^2.\ day)] \quad : \text{Angstrom-type}$$

With:

H_h : Global energy received by a sky whose veiling is defined by unit of horizontal surface.

H_{hc} : Energy received under the same conditions of measurements but by clear sky.

$$H_h = H_0.(b_1 + b_2.\sigma) \qquad [J/(m^2\ jour)] \quad : \text{Angstrom-Black type.}$$

H_0 : Energy received by a surface arranged horizontally, outside the atmosphere in [J/(m^2.day)].

$$H_0 = \int_{tls}^{tcs} I_0 . sin(h) . d(t) \tag{12}$$

Or :

t : Solar (or local) time.

t_{ls} : Sunrise time.

t_{cs}: Sunset time.

These regressions are all based on large series of daily measurements of sunshine which can be used directly to have daily correlations or grouped into monthly classes represented by their average, When using them specify the data used: Daily, monthly or yearly.

Table IV.14: The values of b1 and b2 obtained by linear regression for the regions of Casablanca [6].

Coeff.	Jan	Feb	Mar	Apr	may	Jun	Jul	Aug	Sept	Oct	Nov	Dec
b_1	0,23	0,29	0,25	0,32	0,30	0,31	0,40	0,37	0,38	0,21	0,22	0,17
b_2	0,49	0,45	0,53	0,44	0,47	0,45	0,34	0,36	0,32	0,52	0,48	0,52

Table IV.15: The annual average according to this table is :

Coeff.	The annual average on b_1	The annual average on b_2
Casablanca	0,288	0,448

These values and those of the table, allowed us to have the following results relating to the city of Casablanca according to Angstrom Black:

Table IV.16: Values of H_h according to Angstrom Black's relationship for the city of Casablanca.

Month	σ	Hh [Joule/m^2 j]
Jan	0,60	12454194
Feb	0,66	12608628
Mar	0,75	12685845
Apr	0,84	13071931
May	0,95	12685845
Jun	1,00	12917496
Jul	1,00	13071931
Aug	1,00	12840279
Sep	0,89	12068108
Oct	0,74	12299760
Nov	0,61	12299760
Dec	0,58	11990891
Average	0,81	12531411

For applications requiring the determination of instantaneous values of power or energy, other approaches such as the indices of clarity K_t of the type are to be considered:

$$K_t = f(I_h/I_{0,h}) \qquad \text{Whether} \qquad K_t = I_h.\sin(h)/I_0$$

Or

$$K_t = f(H_h/H_0) \quad \text{Whether} \quad K_t = H_h/H_0)$$

Or

$$K_t = f(I_{diff}/I_h) \quad \text{Whether} \quad K_t = I_{diff}/I_0$$

Or

$$K_t = f(H_{diff}/H_h) \quad \text{Soit} \quad K_t = H_{diff}/H_h$$

With:

I_h and H_h : Global values received on a horizontal plane on the ground.

H_0 : Value received on a horizontal plane, excluding the atmosphere.

I_0 : Solar constant outside atmosphere.

We note that, in general, the regressions on the mean values have a linear dependence whereas the correlations on the daily values are of the third and the fourth degree in K_t.

We quote the example of correlation on the daily values of the Maghreb countries:

$$K_t = H_{diff} / H_0 \tag{13}$$

For the Arab Maghreb: Algeria, Morocco and Tunisia:

$$\frac{H_{diff}}{H_h} = -0{,}759 + 5{,}869.k_t - 8{,}884.{k_t}^2 + 3{,}590.{k_t}^3 \tag{14}$$

For our part we justify these dispersions by the means used: Measuring instruments and the various reflectivity's due to the ground, neighborhoods and meteorological data (pollution, cloud, humidity, dust).

Correlations from instantaneous power values use the idea that flux and irradiation are uniform and remain relatively constant over time intervals of the order of one hour. Justifying this; by the low angular path of the sun during this time. The definition of the coefficient of clarity integrates the height h of the sun which confers a correction over time almost instantaneous.

The basic formulation generally used is:

$$k_t = \frac{I_{diff}}{I_h}.sin(h) \tag{15}$$

But the diffuse is determined from the direct I_{dir} and the global I_h; that is to say:

$$I_{diff} = I_h - I_{dir} \qquad (16)$$

So:

$$k_t = \frac{I_h - I_{dir}}{I_h} . sin(h) = \left(1 - \frac{I_{dir}}{I_h}\right) . sin(h) \qquad (17)$$

IV. 2. 4. 2. Davies & Hay model

Davies and Hay model determines the direct and diffuse irradiance from the sky (ground reflected irradiance is not included in this algorithm) on a tilted surface using the surface tilt angle, surface azimuth angle, The declination, The hour angle, The horizon and horizontal coordinate system, extraterrestrial irradiance, sun zenith angle, and sun azimuth angle.

Our calculated radiation is based on formulae derived from the model of Davies & Hay. In order to proceed with these we first determine the required geographical and astronomical Parameters.

Based on these parameters we can calculate the different components of the solar radiation [7]:

<u>Calculation of direct radiation:</u>

As proposed by Davies & Hay the direct radiation relationship is expressed as,

$$\mathrm{I} = \mathrm{I\_sc}\, [(1 - \alpha_0)\mathrm{T_r} - \alpha_w]\mathrm{T_a}\cos(\mathrm{T_z}) \qquad (18)$$

Where α_0 is the coefficient corresponding to the absorption of direct solar radiation by the ozone layer; given by:

$$\alpha_0 = \frac{0{,}0658U_0}{1+(103{,}6U_0)^3} + \frac{1{,}082U_0}{(1+138{,}6U_0)^{0{,}805}} + \frac{0{,}2118U_0}{0{,}042U_0 + 3{,}23*10^{-4}{U_0}^2} \qquad (19)$$

Here U_0 is the thickness of the ozone layer corrected by the optical path of the solar radiation through the layer; defined by:

$$U_0 = lm_r$$

Here m_r being the relative optical air mass given as:

$$m_r = [cos(t_z) + 0{,}15(93{,}885 - t_z)^{-1{,}253}]^{-1} \qquad (20)$$

The amount of ozone in a vertical place (thickness of the reduced ozone layer, in cm, at STP), represented by l is,

$$l = \left(\frac{1}{1000}\right)\{235 + \left[150 + 40sin(0{,}9856(n_j - 30)) + 20\, sin(3L)\right]sin^2(1{,}28\varphi)\} \qquad (21)$$

L and φ are respectively the longitude and latitude.

Transmission coefficient of molecular diffusion, T_r, is represented by Davies et al. as,

$$T_r = 0{,}972 - 0{,}08262 m_a + 0{,}00933 {m_a}^2 - 0{,}00095 {m_a}^3 + 0{,}000437 {m_a}^4 \qquad (22)$$

Where, the corrected air mass m_a is expressed by,

$$m_r = \frac{P}{P_0} m_r = \frac{exp(-0{,}0001184\, z)}{cos(t_z) + 0{,}15(93{,}885 - t_z)^{-1{,}253}} \qquad (23)$$

Here t_z is the zenith angle is the complement of h; which is the height of the sun,

$$t_z = 90° - h$$

The absorption coefficient α_w, of the direct light by the water vapor is given by the following relationship:

$$\alpha_w = \frac{2{,}9\, X_w}{(1 + 141{,}5\, X_w)^{0{,}635} + 5{,}925\, X_w} \qquad (24)$$

X_w being the thickness of condensable water corrected by the optical path of the radiation through the layer:

$$X_w = m_a U_w \qquad (25)$$

and U_w, the thickness of condensed water in the vertical (cm), given by

$$. U_w = \frac{0{,}493}{T} HR\; exp(26{,}23 - \frac{5416}{T}) \qquad (26)$$

Along with the corrected air mass m_a expressed as,

$$m_a = m_r \left(\frac{P}{1013}\right)^{0{,}75} \left(\frac{273}{T}\right)^{0{,}5} \qquad (27)$$

P is atmospheric pressure (mbar). It can be calculated from,

$$P = P_0 exp(-0{,}0001184\, Z) \qquad (28)$$

With P_0 the atmospheric pressure at sea level (P_0 = 1013 mb), z the altitude of the site (m) relative to sea level, T the temperature (K) and RH the relative humidity (in %).

Transmittance after aerosol scattering T_a , is given by Motion Mächler as,

$$T_a = (1{,}003 - 0{,}125\alpha)\, exp[-\beta m_a (1{,}089\alpha + 0{,}5123)] + (0{,}12445\alpha - 0{,}0162) \qquad (29)$$

$$\beta < 0{,}5$$

Here α and β are respectively the coefficient characterizing the view of the sky and the Angstrom disorder coefficient. Their calculation is based on two experimental determinations of the attenuation coefficients $K_{a\lambda 1}$and $K_{a\lambda 2}$ corresponding to the wavelength where the absorption by the water vapor does not take plae (λ1 = λ2 = 380 nm and 500 nm respectively).

Calculation of diffuse radiation:

Diffuse radiation on a horizontal plane is the sum of three diffuse componentsD_r, D_a and D_m:

$$D_r = T_{sc} T_0 T_a (1 - T_r) 0{,}5 \cos(t_z) \tag{30}$$

D_r represents the diffuse radiation after Rayleigh scattering, where T_0 is the transmittance after absorption by ozone.

$$T_0 = (1 - \alpha_0) \tag{31}$$

The diffuse radiation after scattering by aerosols is,

$$D_a = I_{sc} (T_0 T_r - \alpha)[F_c \omega_0 (1 - T_a)] \cos(t_z) \tag{32}$$

Here ω_0 is the albedo of dispersion in the atmosphere. For urban / industrial areas ω_0 is 0.6 and for rural / agricultural areas it is 0.9. F_c is the direct dispersion coefficient of the atmosphere. Table below presents the values of F_c according to the zenith angle.

Table IV.17: Values of Factor Fc Depending On the Zenith Distance from Robinson

$\theta_z(°)$	0	10	20	30	40	50	60	70
F_c	0,92	0,92	0,90	0,90	0,90	0,85	0,78	0,68

Expression of the diffuse radiation from the phenomenon of multi reflection is given by,

$$D_m = \frac{(I + D_a + D_r)\rho\rho'}{(1 - \rho\rho')} \tag{33}$$

Where, ρ is the ground albedo and ρ′ is the clear sky albedo for the site in question, given by the relationship;

$$\rho' = 0{,}0685 + 0{,}17 \times \omega_0 \times (1 - T'_a) \tag{34}$$

Along with T'_a indicating the transmittance of solar radiation after scattering from aerosols and should be calculated for a value of air mass equal to:

$$m_{a1} = 1{,}66(\exp(-0{,}0001184\, z)) \tag{35}$$

$$T'_a = (1{,}003 - 0{,}125\,\alpha)\exp[-\beta m_{a1}(1{,}089\,\alpha + 0{,}5123)] + (0{,}12445\,\alpha - 0{,}0162) \tag{36}$$

The 0.17 factor is (1 - F_c) for 53° and θ_z = (1 - F_c) is the backscatter coefficient.

So the illumination due to diffuse radiation is:

$$D = D_r + D_a + D_m \tag{37}$$

Calculation of global radiation

The global radiation in a horizontal plane is calculated through the equation,

$$G = I + D \tag{38}$$

Calculations of direct, diffuse and global radiation component (I, D, and G) was carried via Matlab view. The different formulae discussed above were used to get to the final equations for I, D and G given by equations of Davies and Hay model.

IV. 2. 4. 3. Complete model for tilted plane global radiation

The complete model for global radiation on a tilted plane is [8 & 9]:

$$I_g = I_{dir} + I_{dif} + I_{gref} \tag{39}$$

With the formula for each component in Equations of direct, diffuse and reflected radiation, the complete model is:

$$I_g = I_{dir}.R_b + I_{dir}\left[(1 - A_i)\left(\frac{1+cos(\alpha)}{2}\right) + A_i.R_b\right] + \left(I_{dir} + I_{dif}\right).\rho\left(\frac{1-cos(\alpha)}{2}\right) \tag{40}$$

When converting beam radiation between planes we use the geometric factor R_b , which is defined as the ratio of beam radiation on the tilted plane to beam radiation on the horizontal plane:

$$R_b = \frac{I_{dir-T}}{I_{dir}} \tag{41}$$

Following the same reasoning as in the figure below, we find that if I_{dir-n} denotes the beam radiation on a plane perpendicular to the incident radiation, Then:

$$I_{dir-T} = I_{dir-n}.\cos(\theta) \quad \text{and} \quad I_{dir} = I_{dir-n}.\cos(\theta_z)$$

$$R_b = \frac{I_{dir-n}.cos(\theta)}{I_{dir-n}.cos(\theta_z)} = \frac{cos(\theta)}{cos(\theta_z)} \tag{42}$$

We can then express I_{dir-T} the beam radiation on the tilted plane as:

$$I_{dir-T} = R_b.I_{dir} \tag{43}$$

Where the anisotropy index A_i is defined as the ratio between the incident beam radiation I_{dir} and the extraterrestrial radiation I_0 on the horizontal plane:

$$A_i = \frac{I_{dir}}{I_0} \tag{44}$$

Thus, since I_0 is the incident radiation that would be theoretically possible if there was no atmosphere, A_i is the fraction of radiation that is preserved as beam radiation after it has passed through the atmosphere [10 & 11].

Under clear conditions, I_{dir} approaches I_0, causing A_i to be close to 1, and the diffuse is treated in the same way as beam radiation:

$$I_{dir\text{-}T} \approx R_b . I_{dir}$$

When there is no beam radiation A_i is zero, and the diffuse radiation is considered purely isotropic:

$$I_{dir\text{-}T} = I_{dir}\frac{(1+cos(\alpha))}{2} \qquad (45)$$

Where I_{dir} is modified only by the view factor to the sky.

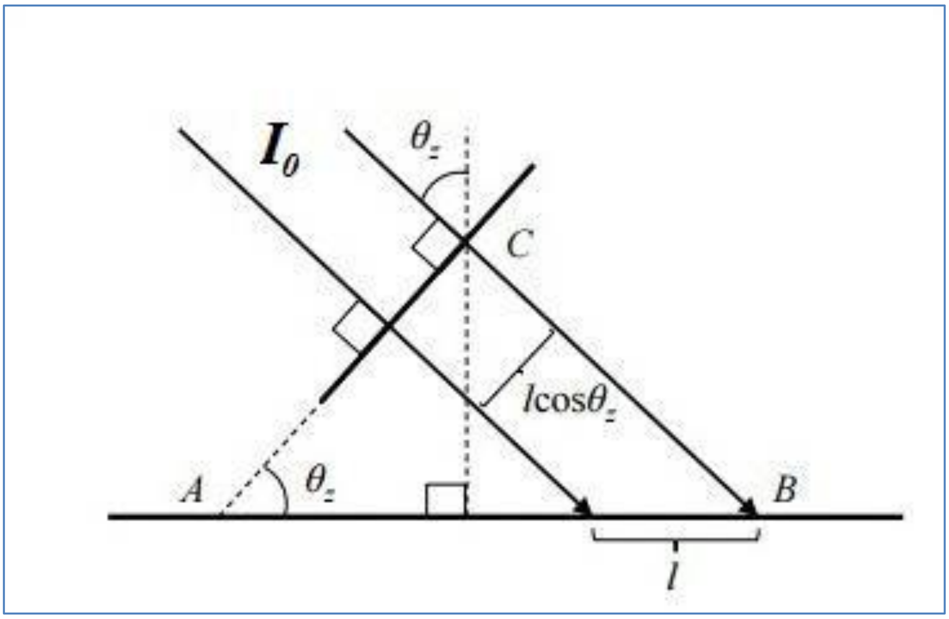

Figure IV.51 : Conversion between extra-terrestrial radiation with normal incidence and extraterrestrial radiation on the horizontal plane.

IV. 3. Study of global solar radiation and optimal tilt angle and orientation for solar photovoltaic arrays: case of Settat city, Morocco

The power or energy received by a surface is dependent on several factors according to its orientation, its inclination on the other hand it is composed of the same basic solar elements which are the direct, diffuse and reflected irradiation.

All the geographical characteristics of a site in the process of study are identified; our focus is on that of Settat city (latitude 33.029° and longitude -7.619°) which shows the direct, diffuse and global irradiation, estimated every typical day and monthly, considering the inclination and orientation of our photovoltaic installation is 32° and West-East (270 °) [1].

Figure IV.52 : Image of the photovoltaic pumping installation at FST of Settat.

IV. 3. 1. Study of solar radiation received on the surface of our installation in Settat city

In order to calculate the productivity of a fixed photovoltaic solar module at a given inclination we must first calculate the energy received by this module each day. To do this we therefore started by calculating the radiative flux taking into account both its direct and diffuse components but without albedo.

IV. 3. 1. 1. Daily distribution of solar radiation throughout the year

The distribution of daily values of solar radiation was calculated for the whole year. A more detailed analysis consists in doing this calculation month by month. We find the different components of solar radiation calculated over the whole year, it is assumed that the sky is very clear all year round.

We have developed a Matlab code that calculates the daily solar irradiation of typical days of each month for our installation in Settat city.

The results are given in the table below, which shows the estimated overall solar radiation for each typical day of each month of the year;

Table IV.18: Energy received for each typical day in (Wh/m^2).

Month	Days typical	N° of days	Direct energy	Diffuse energy	Total energy
Jan	17	17	3089,42	389,26	3478,68
Feb	14	47	3947,96	489,96	4437,92
Mar	16	75	4911,95	657,31	5569,26
Apr	15	105	5712,50	874,56	6587,07
May	15	135	6093,47	1066,95	7160,41
Jun	16	162	6151,75	1174,14	7325,89
Jul	16	198	5985,29	1184,04	7169,33
Aug	15	228	5616,49	1080,04	6696,52
Sep	15	258	4936,11	900,79	5836,89
Oct	15	288	4011,80	689,05	4700,86
Nov	14	318	3166,61	503,71	3670,31
Dec	10	344	2788,68	404,41	3193,09

The monthly maxima correspond to the days of the maximum duration of the day (the lowest values in December-January, and the highest in June-July), but also to that of the atmospheric mass ($m=\frac{1}{\sin(h)}$), direct ground radiation depends on m: in winter the highest sun height h is low, hence a solar ray path in the larger atmosphere and greater attenuation.

The monthly minima correspond to the days of the months of January and December (3200 Wh/m^2.days) and the absolute maximum in May and June (7300 Wh/m^2.days).

IV. 3. 1. 2. The cumulative energy for each month of the year

The evaluation of the cumulative monthly energy, in one month on the inclined and oriented surface, is done by integration of power. We used same classic method, which uses the power calculation expressions to calculate the solar energy received on our installation.

The results of the cumulative monthly energy for each month are shown in the table below:

Table IV.19: The monthly and annual irradiation received on our installation (kwh/m^2).

Months	Diffuse irradiation	Direct irradiation	Total irradiation
Jan	12,16	94,04	106,2
Feb	13,59	106,90	120,49
Mar	20,45	149,98	170,43
Apr	26,31	170,41	196,72
May	33,12	188,36	221,48
Jun	35,40	183,77	219,17
Jul	36,64	184,88	221,52
Aug	33,39	172,99	206,38
Sep	26,89	147,05	173,94
Oct	21,18	123,45	144,63
Nov	14,99	94,54	109,53
Dec	12,26	86,09	98,35
All year	**286,38**	**1702,5**	**1988,88**

Provides information on the cumulative energy distribution of the months, but there is a slight maximum higher than 200 kWh/m^2 Corresponding to the summer months of high sunshine days, and that below 120 kWh/m^2 For the winter months, appear a very marked seasonal effect the form of a grouping of bars of the histogram four by four:

- Those of the summer: May, June, July, August > 200 kWh/m^2
- Those of winter: November, December, January, February < 120kW/m^2
- Intermediate: March, April, September, October.

Through this representation the annual global energy received on the plan of our installation is 1988.9 kWh/m^2.

IV. 3. 1. 3. Sunshine Tables

The amount of electricity produced by a solar panel obviously depends on the amount of sunshine at the location of the installation. Knowing the sunshine you have is essential to design a photovoltaic installation.

We thus obtain two tables of solar irradiation (global and diffuse irradiation) received on 1 m^2 of our installation.

We can represent the daily average values for each month of the year according to the notion of time, in the real case without shading them from the previous shadow mask; we deduce the table of sunshine for the installation in the real case with the shadow of the ridge.

Table IV.20: The diffuse solar irradiation received on the surface of our installation

	Jan	Feb	Mar	Apr	May	Jun	July	Aug	Sep	Oct	Nov	Dec
05:00-05:30	0	0	0	0	0	0,20	1,59	0	0	0	0	0
05:30-06:00	0	0	0	0	3,15	5,31	2,37	0,03	0	0	0	0
06:00-06:30	0	0	0	3,81	13,89	17,86	12,84	5,52	0,68	1,06	0	0
06:30-07:00	0	0	1,98	14,28	26,24	29,63	26,49	18,40	8,99	2,26	0,07	0
07:00-07:30	0	0,85	9,81	24,96	33,91	37,09	35,53	30,29	22,30	11,35	2,70	0
07:30-08:00	2,61	7,01	19,53	31,26	38,73	41,96	41,32	37,53	31,25	22,20	10,78	3,57
08:00-08:30	9,58	15,68	25,52	35,08	41,95	45,31	45,22	42,15	36,54	28,53	19,14	11,18
08:30-09:00	16,49	20,85	28,93	37,58	44,21	47,71	47,97	45,28	39,92	32,26	23,80	17,35
09:00-09:30	19,68	23,72	31,07	39,30	45,84	49,47	49,96	47,48	42,21	34,65	26,53	20,70
09:30-10:00	21,72	25,49	32,49	40,53	47,04	50,77	51,44	49,06	43,81	36,25	28,29	22,69
10:00-10:30	23,01	26,64	33,48	41,41	47,91	51,74	52,52	50,22	44,94	37,35	29,45	23,96
10:30-11:00	23,85	27,42	34,17	42,04	48,55	52,44	53,32	51,05	45,74	38,102	30,21	24,79
11:00-11:30	24,40	27,95	34,64	42,47	48,99	52,94	53,88	51,64	46,27	38,59	30,71	25,33
11:30-12:00	24,76	28,29	34,95	42,74	49,26	53,25	54,25	52,01	46,60	38,87	30,98	25,65
12:00-12:30	24,97	28,48	35,11	42,87	49,39	53,41	54,44	52,20	46,74	38,96	31,08	25,79
12:30-13:00	25,08	28,54	35,17	42,94	49,46	53,48	54,52	52,28	46,83	39,05	31,16	25,87
13:00-13:30	25,12	28,60	35,21	42,94	49,48	53,49	54,55	52,30	46,79	38,96	31,08	25,86
13:30-14:00	25,03	28,54	35,13	42,81	49,29	53,34	54,42	52,15	46,59	38,70	30,83	25,69
14:00-14:30	24,73	28,35	34,92	42,55	48,99	53,04	54,12	51,83	46,20	38,24	30,38	25,35
14:30-14:00	24,34	28,02	34,57	42,14	48,52	52,56	53,65	51,32	45,59	37,55	29,69	24,80
14:00-14:30	23,74	27,52	34,05	41,54	47,86	51,88	52,96	50,58	44,72	36,54	28,68	23,98
14:30-15:00	22,87	26,83	33,32	40,72	46,96	50,96	52,03	49,56	43,51	35,11	27,23	22,80
15:00-15:30	21,62	25,76	32,29	39,59	45,75	49,72	50,77	48,17	41,84	33,09	25,14	21,08
15:30-16:00	19,81	24,29	30,85	38,04	44,12	48,08	49,09	46,28	39,51	30,20	21,83	18,35
16:00-16:30	15,58	22,21	28,83	35,90	41,91	45,87	46,83	43,70	36,21	24,44	8,32	6,33
16:30-17:00	2,48	16,67	25,90	32,88	38,85	42,89	43,75	40,09	30,65	7,27	7,20	0
17:00-17:30	0	1,63	16,23	28,01	34,45	38,70	39,44	34,63	14,46	0,03	0	0
17:30-18:00	0	0	0,32	10,75	25,78	32,27	32,73	20,90	0,67	0	0	0
18:00-18:30	0	0	0	0,03	4,13	15,82	15,27	1,83	0	0	0	0
18:30-19:00	0	0	0	0	0	0,04	0,03	0	0	0	0	0

Table IV.21 : The global solar irradiation received on the surface of our installation.

	Jan	Febr	Mar	Apr	May	Jun	Jul	Aug	Sept	Oct	Nov	Dec
05:00-05:30	0	0	0	0	0	0,20	1,59	0	0	0	0	0
05:30-06:00	0	0	0	0	3,15	5,31	2,37	0,03	0	0	0	0
06:00-06:30	0	0	0	3,82	26,24	29,64	12,84	5,53	0,69	2,27	0	0
06:30-07:00	0	0	1,98	14,28	33,91	37,09	26,49	18,41	9,00	11,36	0	0
07:00-07:30	2,60	3,86	9,82	24,96	38,73	41,97	35,54	30,29	22,31	22,21	2,70	0
07:30-08:00	9,58	7,01	19,53	31,27	41,96	45,32	41,32	37,54	31,26	28,53	10,78	3,57
08:00-08:30	16,19	15,68	25,52	35,08	70,57	81,75	45,23	42,16	36,55	32,27	19,14	11,18
08:30-09:00	19,68	20,85	28,93	39,48	119,31	128,31	68,22	47,20	39,93	36,67	23,81	17,35
09:00-09:30	21,71	23,72	32,27	77,52	169,58	176,31	114,48	90,75	63,97	81,22	26,55	20,70
09:30-10:00	36,56	25,72	66,20	130,51	219,78	224,27	162,59	140,87	115,59	132,67	39,03	22,70
10:00-10:30	85,75	62,53	120,76	184,06	268,50	270,89	211,00	191,55	167,91	183,04	86,73	47,67
10:30-11:00	134,30	115,33	175,24	236,47	314,50	315,00	258,31	241,22	219,08	230,56	135,05	94,98
11:00-11:30	180,17	167,10	227,78	286,28	356,65	355,53	303,31	288,50	267,55	273,78	181,04	141,02
11:30-12:00	221,76	215,99	276,86	332,21	393,92	391,50	344,88	332,15	311,95	311,45	223,06	183,87
12:00-12:30	257,98	260,49	321,14	373,11	426,16	422,63	381,99	371,08	351,09	343,92	259,75	221,98
12:30-13:00	288,73	299,36	359,71	408,56	452,41	448,27	414,15	404,80	384,94	369,07	291,41	255,04
13:00-13:30	312,04	332,79	392,41	437,81	471,58	467,22	441,07	432,86	412,18	386,08	315,92	281,84
13:30-14:00	327,07	358,74	417,48	459,56	483,11	478,95	461,32	453,80	431,67	394,23	332,36	300,96
14:00-14:30	333,08	376,38	434,18	473,17	486,57	483,03	474,32	467,00	442,74	392,94	339,97	311,56
14:30-14:00	329,39	385,03	441,89	478,12	481,61	479,13	479,62	471,96	444,86	381,64	338,05	312,90
14:00-14:30	315,32	384,06	440,11	474,01	467,99	467,02	476,87	468,27	437,57	359,77	325,94	304,27
14:30-15:00	290,25	372,90	428,38	460,51	445,53	446,55	465,79	455,63	420,45	326,75	302,95	284,94
15:00-15:30	253,70	351,03	406,31	437,35	414,09	417,62	446,21	433,77	393,11	281,84	268,42	254,27
15:30-16:00	185,30	317,95	373,49	404,28	373,49	380,11	417,99	402,45	355,11	210,85	218,80	208,80
16:00-16:30	27,28	273,46	329,62	361,02	323,48	333,86	380,99	361,38	305,84	56,55	75,78	67,04
16:30-17:00	0,00	188,48	273,97	307,24	263,14	278,40	335,00	310,09	238,51	0,02	0	0
17:00-17:30	0,00	16,52	154,15	238,10	176,62	210,46	279,48	245,88	101,73	0	0	0
17:30-18:00	0,00	0,00	2,65	80,19	24,52	91,42	210,68	133,57	4,20	0	0	0
18:00-18:30	0	0	0	0,03	4,13	15,82	15,27	1,83	0	0	0	0
18:30-19:00	0	0	0	0	0	0,04	0,03	0	0	0	0	0

IV. 3. 2. Influence of the tilt angle on the acceptance of the solar irradiation

The tilt angle has a major impact on the solar radiation incident on a surface. For a fixed tilt angle, the maximum power over the course of a year is obtained when the tilt angle is equal to the latitude of the location [12 & 13].

We will study in this part the influence of exposure (orientation and inclination) on the amount of solar irradiation received on a surface of $1m^2$, The example detailed hereafter relates to a PV pumping installation installed at FST of Settat which ensures the irrigation of the green areas and all plants of the establishment.

In a first step, we made a theoretical study of the solar field arriving at a surface of 1 m2 of our PV installation inclined by 32 ° and oriented towards the West (270 °).

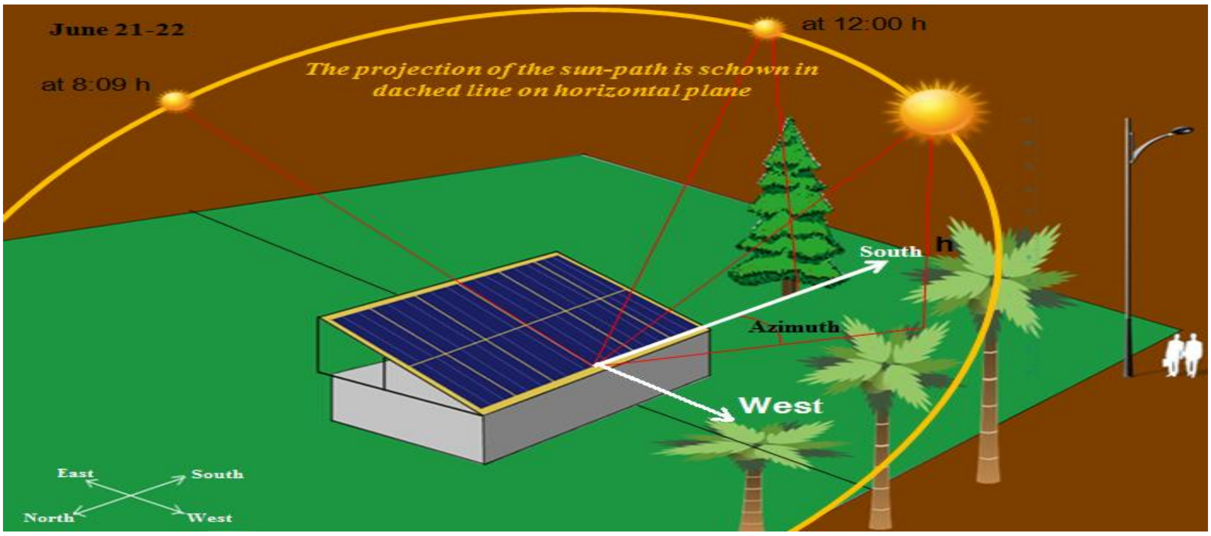

Figure IV.53 : 3D drawing of the PV installation in real exposure.

Then we compare with the case if the installation is well installed, we use the results of the previous part, the optimum tilt angle is 29 ° and the orientation towards the south (the 180 ° azimuth).

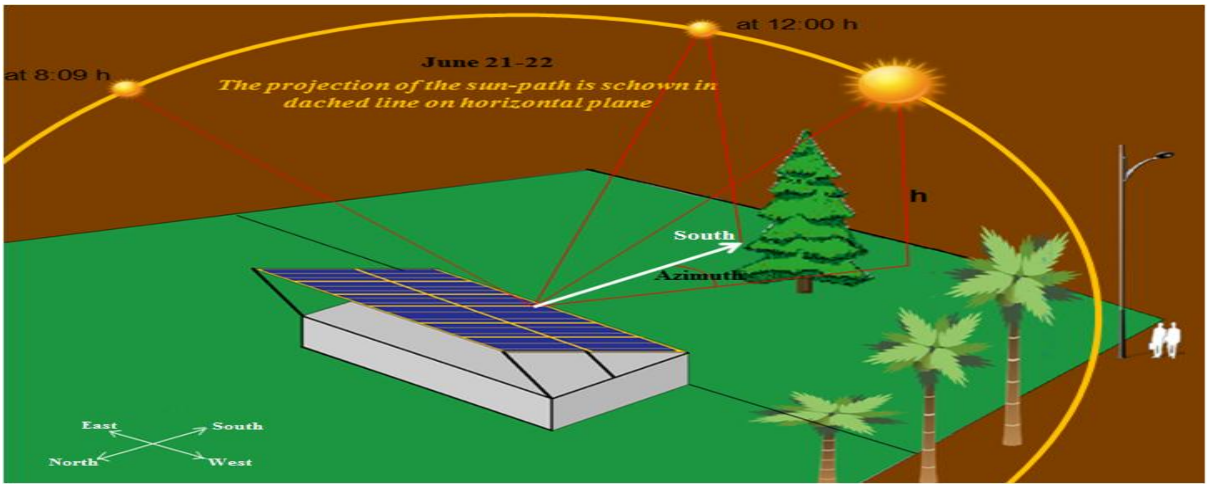

Figure IV.54 : 3D drawing if the PV installation is well exposed.

IV. 3. 2. 1. Calculation of daily irradiation

In order to calculate daily irradiation, the equations (1 to 45) are used and a Matlab code has been developed which calculates and plots the daily irradiation of the typical days of each month for our installation of Settat city.

We added in this part the winter solstice giving the daily variations of the solar radiation with the:

Optimal inclination and orientation ($\boldsymbol{\alpha}_{opt}$ =29° & $\varphi = 180°$), Actual Exposure (α =32 ° & φ =270 °).

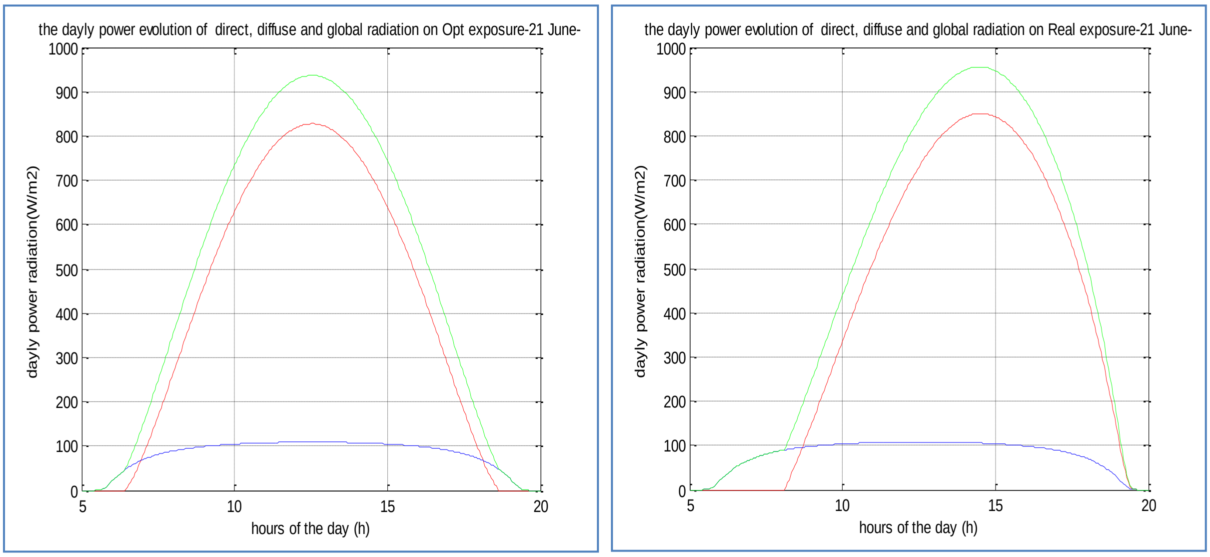

Figure IV.55 : The daily power evolution of direct, diffuse and global solar radiation, of optimum exposure (June21).

In June 21, for optimal exposur; the direct irradiation begins to reach the surface of the installation at 05: 45h and takes the maximum value at 12: 30 h. on the other hand for real exposure; the direct irradiation reach at the installation at 8:05 am of the day, and takes the maximum value at 14:27 h.

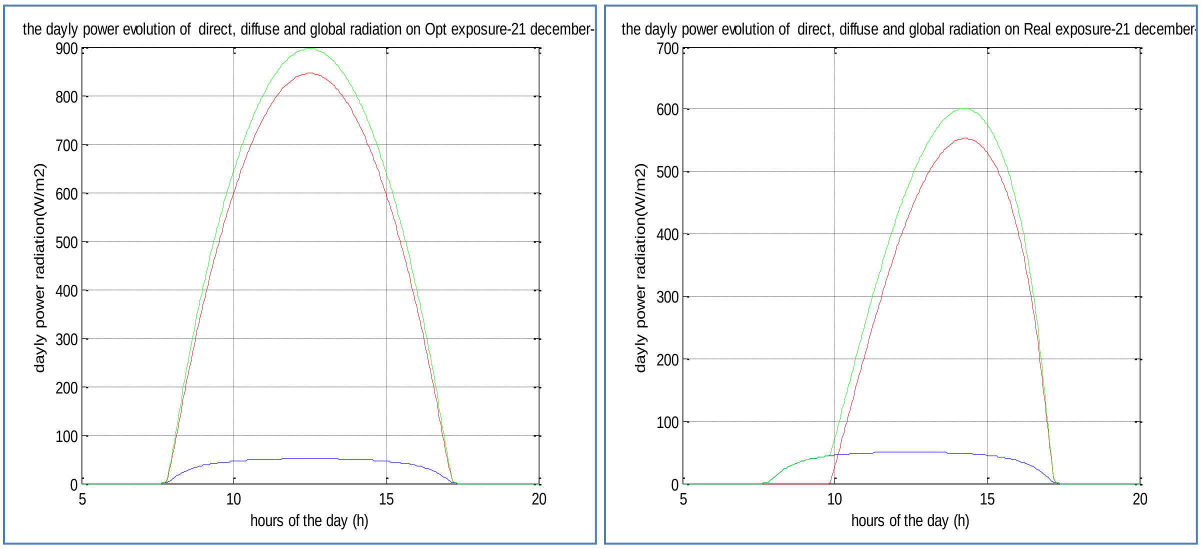

Figure IV.56 : Daily power evolution of direct, diffuse and global solar radiation, of actual exposure (december21).

It is the same things for 21 December; the direct irradiation begins to reach the surface of the installation at 07: 40 h and takes the maximum value at 12: 27 h. For optimal exposure, and for actual exposure, direct irradiation reaches the facility at 09:48 of the day, and takes the maximum value at 14:15.

And it is obviously clear that the maximum power received is very important for the optimum position of the inclination and the orientation.

IV. 3. 2. 2. Cumulative energy for each month of the year

The distribution of the daily values of solar irradiation was calculated for the whole year. A finer analysis is to do this calculates month by month. The calculations of the various components of the solar radiation, calculated over the whole year, it is assumed that the sky very clear in the days of the year.

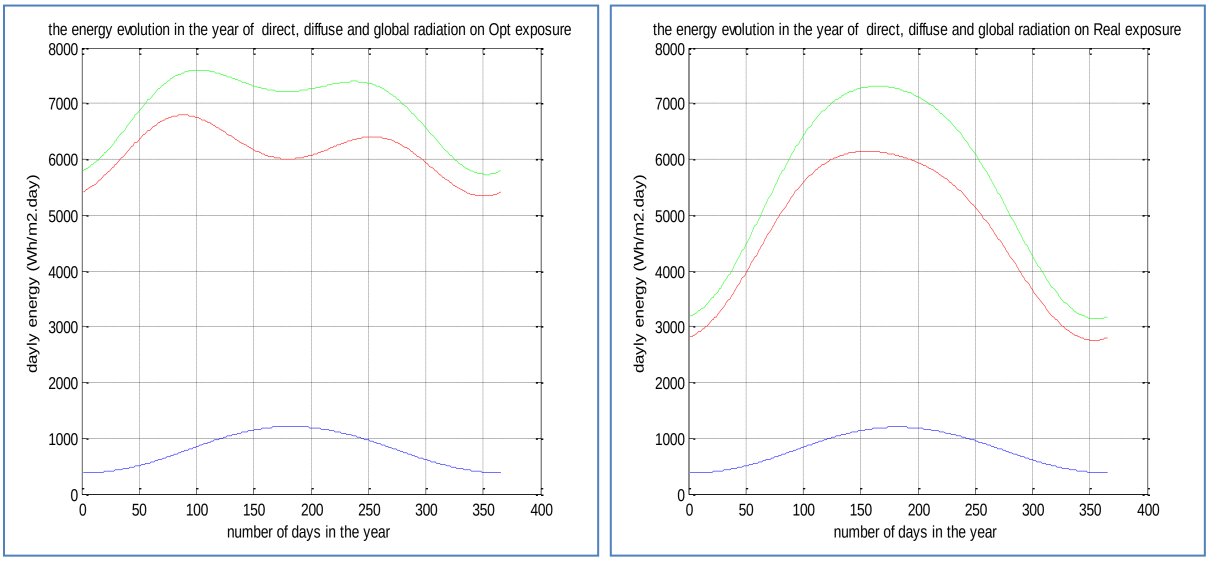

Figure IV.57 : Evolution of direct, diffuse and global solar radiation in the year, for optimum exposure and actual or real exposure.

The two figures show that the energy received is strongly influenced by the inclination and orientation of the installation. During the year, the optimum position receives the maximum of the solar irradiations. In the case of the actual installation the maximum values are in the months of (May, June and July) are expected more than 7000 Wh/m^2.day.

The results of the typical days are summarized in the table below:

Tableau IV.22: The daily solar radiation of the typical days of each month in (Wh/m^2) for the two modes of positions

The energy received per days (Wh/m²)				
Months	Days typical	N° of days	Real exposure	Opt exposure
Jan	17	17	3478.68	6022.24
Feb	14	47	4437.92	6793.05
Mar	16	75	5568.42	7409.02
Apr	15	105	6587.07	7409.88
May	15	135	7160.41	7486.34
Jun	16	162	7352.89	7325.76
Jul	16	198	7169.45	7325.52
Aug	15	228	6696.53	7424.03
Sep	15	258	5836.90	7311.10
Oct	15	288	4700.86	6793.03
Nov	14	318	3670.31	6078.59
Dec	10	344	3193.09	5696.95

For Settat city the optimum position (inclination of 29° and orientation towards the south). The daily values of the monthly solar radiation relative to this position are the most energetic (from 7300 to 7700 Wh/m^2.day) in most months of the year to October).

In the same context, the solar energy incident on the surface of the PV panels is given in the following figures, and in the same logic of interpretations (an optimal position with the position of the actual installation).

We perform a comparison for the two positions modes, the results of the cumulative monthly energy for each position is shown in the figure below:

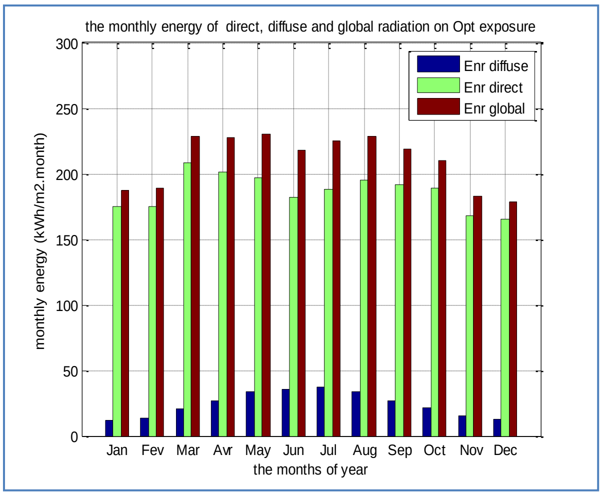

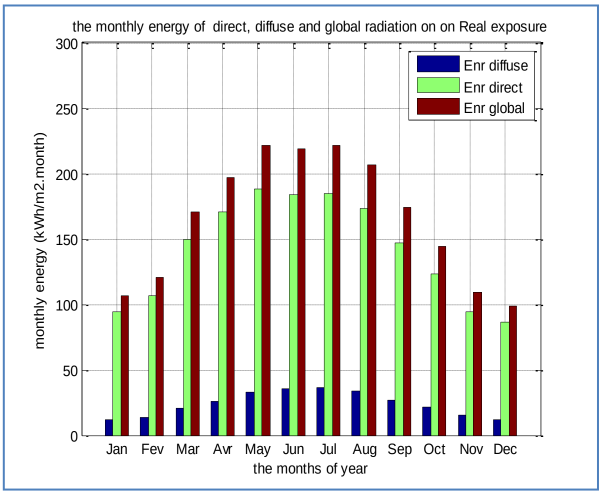

Figure IV.58 : The monthly direct, diffuse and global solar radiation, of optimum and actual exposure.

In the following table we summarize the comparison of the total monthly energy received on a surface of 1m^2, in both position modes;

Table IV.23: The monthly cumulative energy for the two modes of positions

The energy received per month (kWh/m²)		
Months	Real exposure	Opt exposure
Jan	106.20	187.00
Feb	120.49	188.69
Mar	170.43	228.61
Apr	196.72	227.46
May	221.48	230.17
Jun	219.16	217.57
Jul	221.53	225.21
Aug	206.39	228.62
Sep	173.94	218.47
Oct	144.63	210.41
Nov	109.52	183.20
Dec	98.35	178.15
all year	**1988,8**	**2523,5**

In this part we find that for the month of June, the installation in the real exposure receives the expected energy 219,164 kWh/m^2, more than if the installation is well exposed will receive a value of 217,568 kWh/m^2, and for the other months of the year, the optimum position receives the energy more than the installation in the case of real exposure.

The maximum energy can be captured by positioning the PV panels at the optimal exposure, the energy received is (2523,5 kWh/m^2) Even more than if the installation in the optimal exposure case, and that it is only of 1988,8 kWh/m^2 in a real exposure.

Percentage distribution:

On the basis of the diagram below, it is possible to determine for each zone the loss of energy by the deviation of inclination and orientation with respect to the ideal situation at Settat (south, inclination of 29 °).

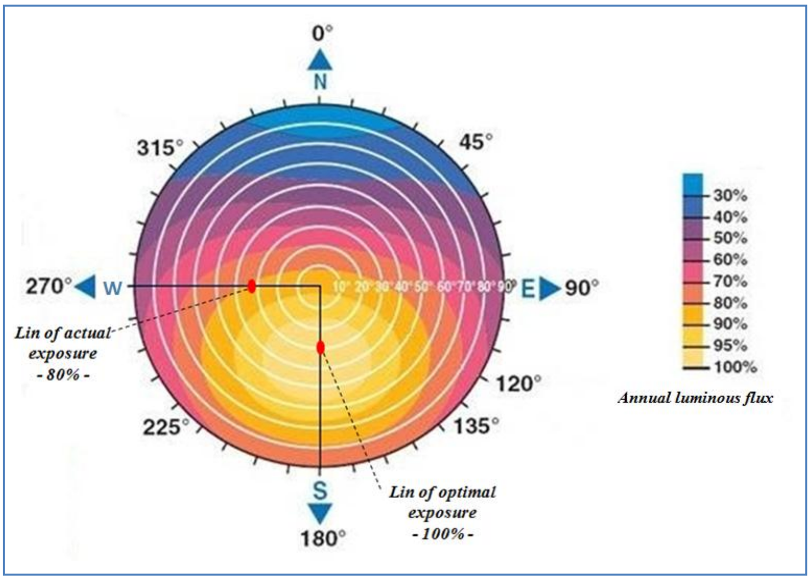

Figure IV.59 : Solar radiation (in percentage) with respect to the ideal situation as a function of inclination and orientation.

The figure shows; case of optimum exposition (tilt angle 29° and oriented south) still have from 95% to 100% of the energy received by the sun. On the other hand; case of our installation in the actual exposure (tilt angle 32° and oriented West) have 80% of the energy received by the sun [14 & 15].

Comparing the real exposure and optimum exposition, the percentage decrease in the solar energy received is 20%.

$$\left(\frac{2523{,}5-1988{,}8}{2523{,}5}\cdot 100 = 21{,}18\,\% \text{ or } 100\% - 80\% = 20\%\right)$$

IV. 4. Study of the influence of shading on the productivity of our photovoltaic installation

In the state where we found the installation, the modules are oriented West with an inclination of 32° relative to the horizontal. Photovoltaic panels are placed on a roof and influenced by a set of obstacles (trees, pole ...) which creates remarkable shading on the photovoltaic cells (see the following image) [16 & 17].

Figure IV.60 : The shading on the our installation at FST Settat.

General hypothesis:

When a shadow appears on a photovoltaic module, and due to the wiring, we consider the all modules of our installation receive only the diffuse radiation.

The objective:

Our object is to study the energy losses due to the shading phenomenon of carried on our photovoltaic installation. The modules presented in two strings, for each string the modules are wired in series, this is has the effect of reducing electricity production.

In the case of our photovoltaic installation in Settat, there are mainly proximity obstacles: five trees and a pole that are shown in the following figure:

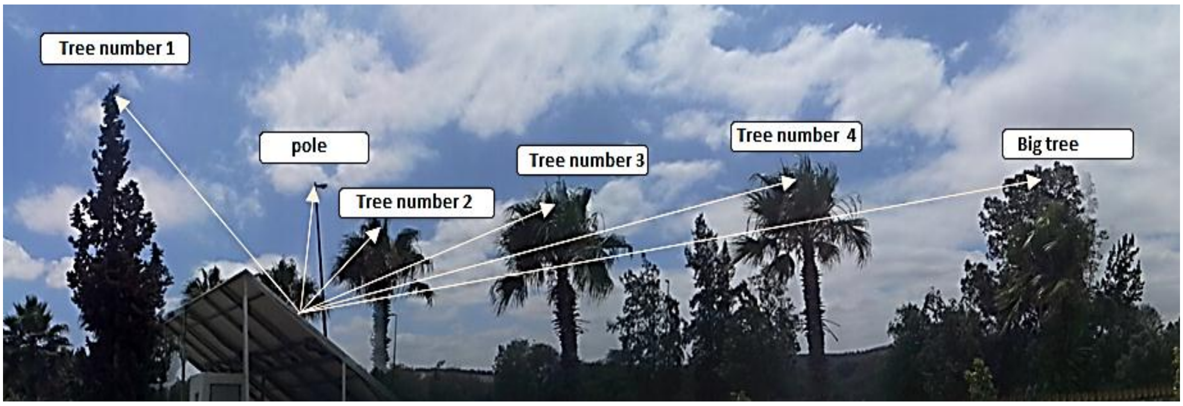

Figure IV.61 : Presence of obstacles (five trees and a pole) for the case of our PV installation.

The shading masks survey:

The mask survey (shade survey) provides the information needed to calculate these losses. It is necessary to know the expected orientation and inclination of the panels to perform this calculation.

They are simple and sufficiently precise so that the mask readings can be used in the production and sizing calculations of a photovoltaic field. One of these methods, using a compass and a clinometer [18];

Materials needed:

The tools needed to complete this step are a compass (which will make it possible to measure the azimuth of a point) and a clinometer (measuring the height of a point).

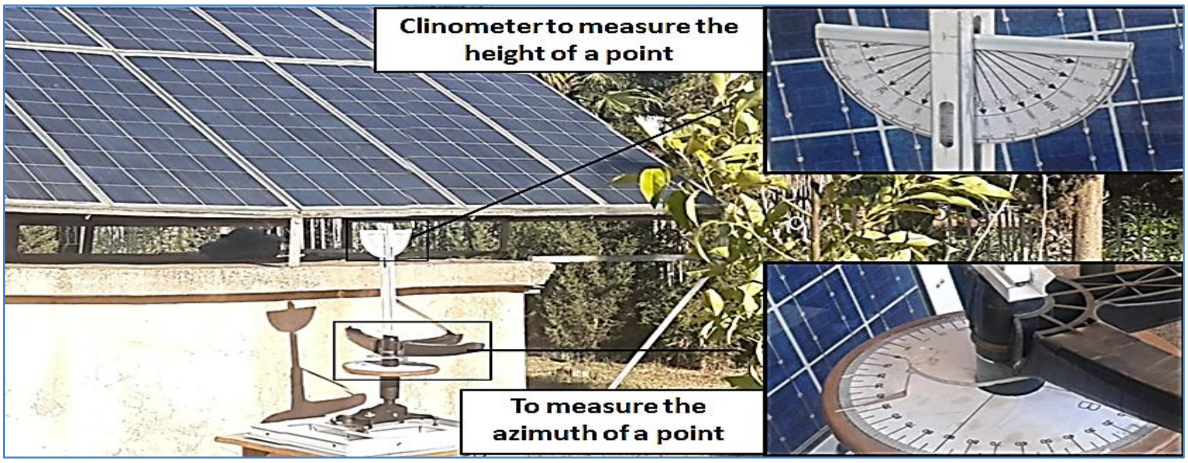

Figure IV.62 : The instrument for measuring elevation and azimuth.

IV-4-1 Identify the characteristic points of the obstacle geometry

Once the characteristic points of the geometric shape of the obstacle have been determined, the following consists in transferring these points on the graph of the solar course. For it, the azimuth and the height of each of the characteristic points defined above are measured. The azimuth is measured with the compass and the height is measured with the clinometer [19].

For example, the height of the red point is the angle noted H below:

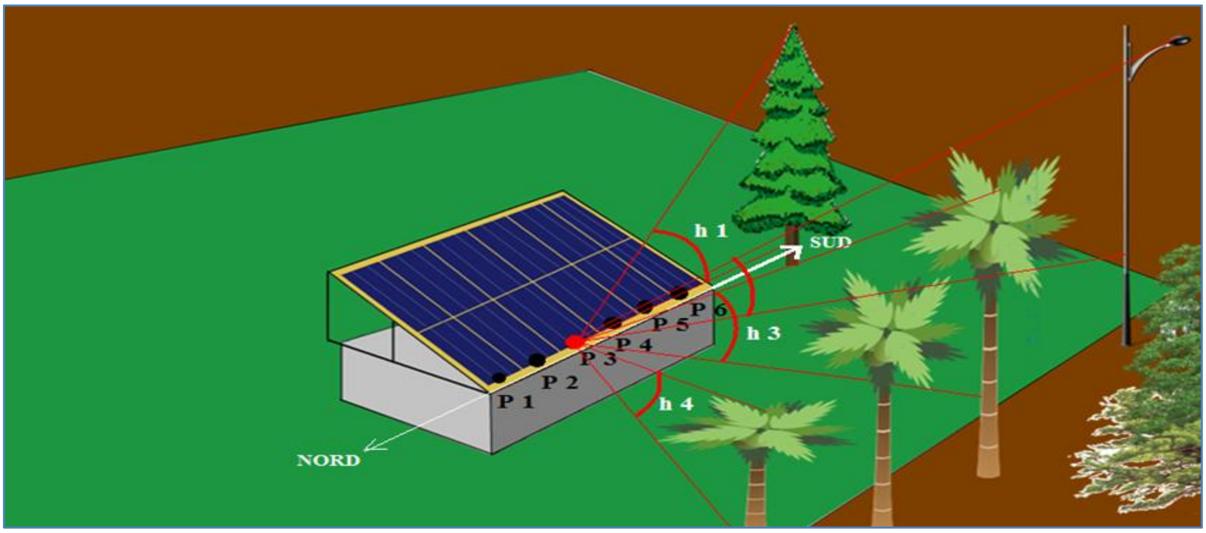

Figure IV.63 : Measure the height of each characteristic point.

The azimuth of point A is the angle noted AZ below:

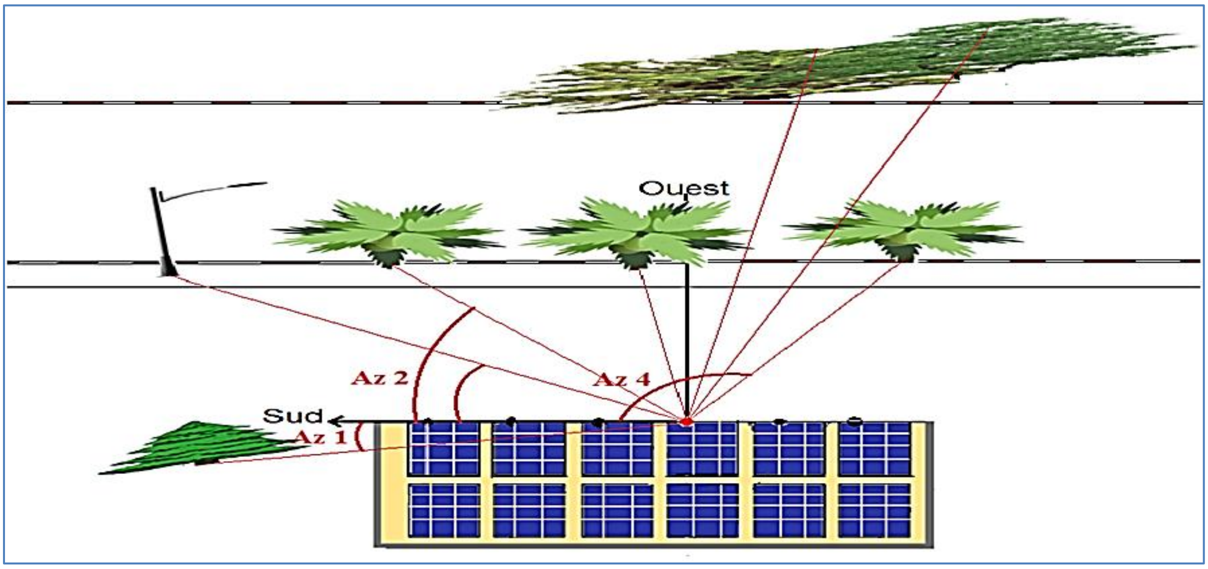

Figure IV.64 : Measure the azimuth of each of the characteristic points.

The measurements (with the compass and the clinometer) of the azimuth and the height of the modulus point P3, allowed to know the values of (AZ and H) of the characteristic points the geometry shape of the obstacles. We then report these values in the graph of the course of the sun (The diagram above).

The diagram above is what is called a P3 modulus mask reading. We can see that we find the shape of a lamppost, three palms and two trees.

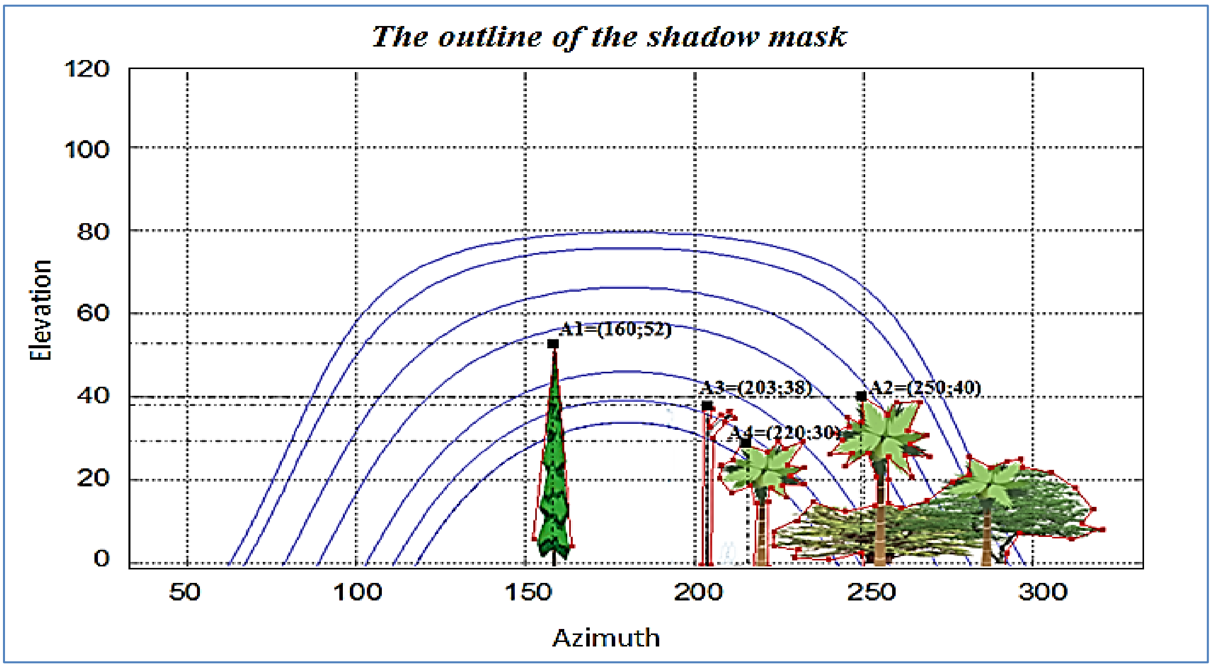

Figure IV.65 : The characteristic points on the graph of the course of the sun.

Then, simply post the points on the graph of the race of the sun, knowing that the abscissa axis of this graph represents the azimuth and the ordinate axis represents the height.

We also show overlay the shadow masks for the other PV modules. We finally obtain the shadow mask that influences the production of all modules of our photovoltaic installation.

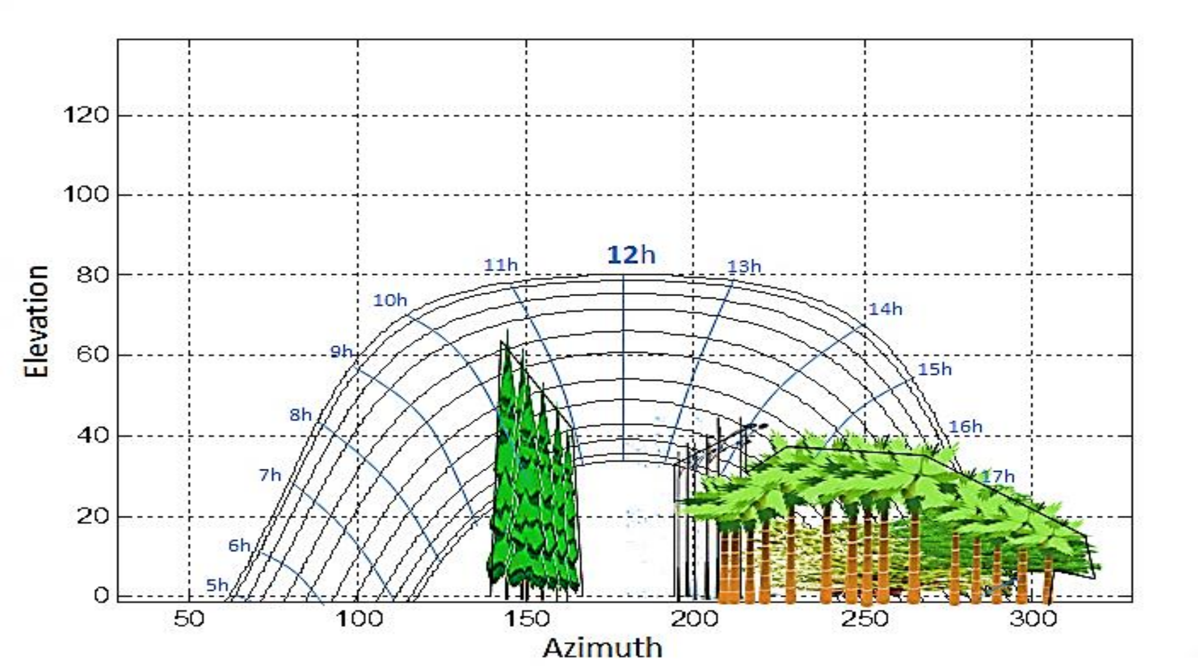

Figure IV.66 : Mask of shadow of the obstacles reported on the 1st line of the installation.

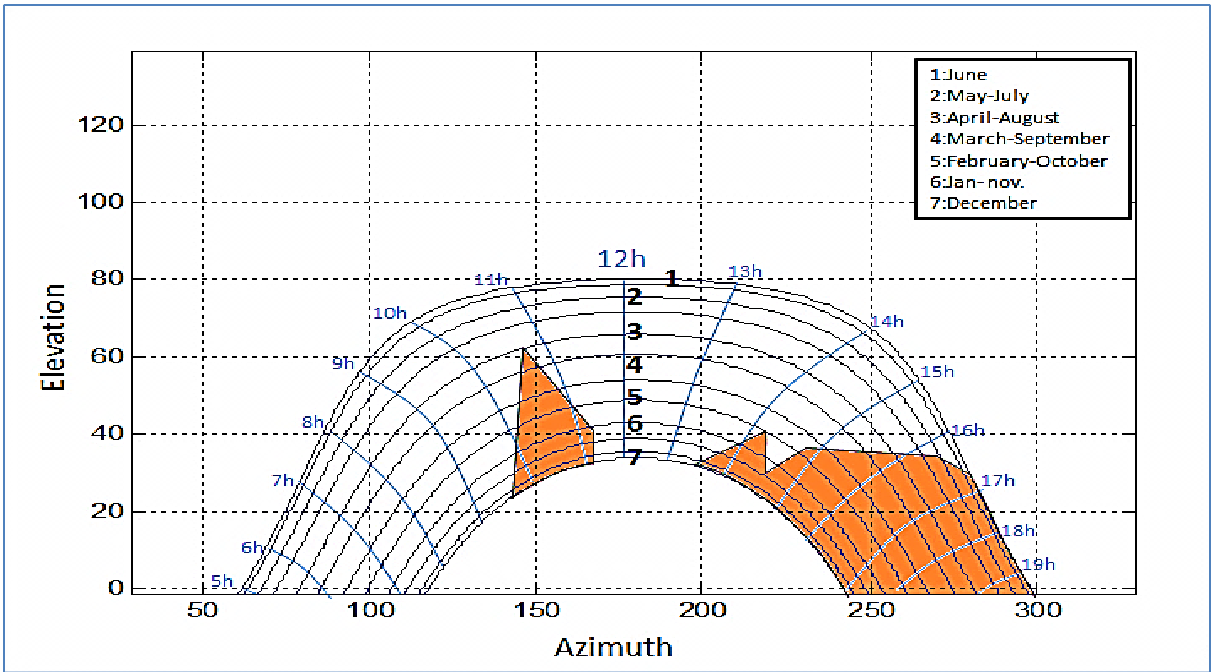

Figure IV.67 : Surface of the drop shadow on the entire installation.

The effective shadow mask is obtained by the orange surface. This makes it possible to determine the loss coefficient to be applied to the production of the photovoltaic field.

To determine the sunshine tables for each group and line of modules, we compare the shadow mask with the sun's trajectory for each hour of a typical day of each month. When the trajectory of the sun is superimposed with the shadow mask we get a shadow on the modules. In this case we replace the values of the global radiation with the values of diffuse radiation. So we get the following table:

Table IV.24: Representative table of the solar energy received on our PV installation with shading in Wh/m^2.

	Jan	Feb	Mar	Apr	May	Jun	July	Aug	Sep	Oct	Nov	Dec
05:00-05:30	0	0	0	0	3,15	5,32	0	0	0	0	0	0
05:30-06:00	0	0	0	0	13,89	17,87	2,38	0,04	0	0	0	0
06:00-06:30	0	0	0	3,82	26,24	29,64	12,84	5,53	0,69	2,27	0	0
06:30-07:00	0	0	1,98	14,28	33,91	37,09	26,49	18,41	9,00	11,36	0	0
07:00-07:30	2,60	0,86	9,82	24,96	38,73	41,97	35,54	30,29	22,31	22,21	2,70	0
07:30-08:00	9,58	7,01	19,53	31,27	41,96	45,32	41,32	37,54	31,26	28,53	10,78	3,57
08:00-08:30	16,19	15,68	25,52	35,08	70,57	81,75	45,23	42,16	36,55	32,27	19,14	11,18
08:30-09:00	19,68	20,85	28,93	39,48	119,31	128,31	68,22	47,20	39,93	36,67	23,81	17,35
09:00-09:30	21,71	23,72	32,27	77,52	169,58	176,31	114,48	90,75	63,97	81,22	26,55	20,70
09:30-10:00	36,56	25,72	66,20	130,51	219,78	224,27	162,59	140,87	115,59	132,67	39,03	21,72
10:00-10:30	23,02	26,65	120,76	184,06	268,50	270,89	211,00	191,55	167,91	37,36	29,45	23,02
10:30-11:00	23,86	27,43	34,18	236,47	314,50	315,00	258,31	241,22	45,74	38,11	30,22	23,86
11:00-11:30	24,41	167,10	227,78	286,28	356,65	355,53	303,31	288,50	267,55	273,78	30,71	24,41
11:30-12:00	221,76	215,99	276,86	332,21	393,92	391,50	344,88	332,15	311,95	311,45	223,06	183,87
12:00-12:30	257,98	260,49	321,14	373,11	426,16	422,63	381,99	371,08	351,09	343,92	259,75	221,98
12:30-13:00	288,73	299,36	359,71	408,56	452,41	448,27	414,15	404,80	384,94	369,07	291,41	255,04
13:00-13:30	312,04	332,79	392,41	437,81	471,58	467,22	441,07	432,86	412,18	386,08	315,92	281,84
13:30-14:00	25,03	358,74	417,48	459,56	483,11	478,95	461,32	453,80	431,67	394,23	30,84	25,69
14:00-14:30	24,73	376,38	434,18	473,17	486,57	483,03	474,32	467,00	442,74	392,94	30,39	25,35
14:30-14:00	24,34	28,03	441,89	478,12	481,61	479,13	479,62	471,96	444,86	37,55	29,70	24,81
14:00-14:30	23,75	27,53	440,11	474,01	467,99	467,02	476,87	468,27	437,57	36,54	28,69	23,99
14:30-15:00	22,87	26,80	428,38	460,51	445,53	446,55	465,79	455,63	420,45	35,12	27,23	22,80
15:00-15:30	21,62	25,77	406,31	437,35	414,09	417,62	446,21	433,77	393,11	33,10	25,15	21,09
15:30-16:00	19,81	24,30	30,85	404,28	373,49	380,11	417,99	402,45	39,51	30,21	21,85	18,35
16:00-16:30	15,59	22,22	28,83	35,90	41,91	333,86	46,84	43,71	36,21	24,45	8,33	6,33
16:30-17:00	2,48	16,67	25,91	32,88	38,85	42,90	43,76	40,10	30,65	7,28	0	0
17:00-17:30	0	1,64	16,24	28,02	34,45	38,71	39,44	34,63	14,46	0	0	0
17:30-18:00	0	0	0,33	10,76	25,79	32,28	32,74	20,91	0,67	0	0	0
18:00-18:30	0	0	0	0	4,14	15,82	15,27	1,84	0	0	0	0
18:30-19:00	0	0	0	0	0	0	0	0	0	0	0	0

(yellow)	***The global Solar irradiation***
(green)	***The diffuse Solar irradiation***

IV. 4. 2. Calculation of both electricity production and electrical productivity

Electricity production

The electrical production of a photovoltaic installation obviously depends on the solar irradiation. Therefore it is impossible to tell in advance how much electricity will produce a solar panel without knowing the amount of solar energy received on this panel (the production will be different depending on where you install it and even according to the position you give it).

The objective of this part is to evaluate the electrical production of our installation for the two modes of positions (with and without shading). For this, we will give a simple formula for a detailed estimate of the electrical production of our installation [20].

So we have the following relation:

$$E = G.S.\eta_{global} \tag{46}$$

E : monthly or annual electricity production [kWh]

G : monthly or annual irradiation received on the PV installation, [kWh/m²] (The two tables of sunshine for each mode of position, they are expressed in Wh /m^2)

S : available module surface [m²] (The total area of our PV installation is : S = 9,9696m^2)

$\boldsymbol{\eta_{global}}$: Overall efficiency of the installation (Efficiency of the panel is $\eta_{panneau}$=12%, and the Performance Factor Fp=0,8)

So the overall Efficiency is η_{global} = 0,8*0,12 = 0,096 $\eta_{global} = 0.096$

So : **E** = G×9,9696×0,096 (E = G×0,957)

We now calculate the monthly production from the previous tables of sunshine, of the whole of our installation:

Table IV.25: The monthly electricity production of our installation for the two modes positions.

	Position without shading in Kwh/m²	Position with shading in Kwh/m²
Jan	108,24	42,67
Feb	122,51	62,48
Mar	170,90	1 36,10
Apr	194,91	169,68
May	218,39	199,31
Jun	216,05	203,12
Jul	218,92	185,83
Aug	204,37	177,08
Sep	172,54	142,19
Oct	143,87	91,92
Nov	109,59	43,20
Dec	99,28	37,29
All year	**1979,57**	**1249,62**

Electrical productivity

We call photovoltaic productivity, the ratio of the power that a photovoltaic module provides over a period (one day, one month or one year) divided by the power produced under the STC (standard test conditions) of the module.

This indicator measures the light intensity of our region, in other words, the yield in kWh per kWp in an optimal configuration (Panels are facing South, inclination 29 °). To calculate it we use the equation below;

$$Pr = \int \frac{P.dt}{P_{stc}} \quad (47)$$

P : the power available at the terminals of the photovoltaic panel.

P_{stc} : Power of a cell, a module, a system measured in the Standard Test Conditions (Watt-peak-Wc):

- Solar irradiation = 1 000 W/m²
- T_{cell} = 25 °C
- A.M = 1,5

Again, we use a Matlab code to calculate the monthly productivity of our PV installation for both modes of exposure; finally we deduce the following productivity table:

Table IV.26: monthly productivity of our installation kW_h /kW_p.

	Position without shading in kWh/kWc	Position with shading in En kWh/kWc
Jan	70,58	29,63
Feb	80,08	43,39
Mar	113,27	94,52
Apr	130,74	117,84
May	147,20	138,42
Jun	145,23	141,07
Jul	147,43	129,06
Aug	137,17	122,98
Sep	115,60	98,75
Oct	96,12	63,84
Nov	72,79	30,00
Dec	65,36	25,90
All year	**1321,57**	**1035,42**

Results and interpretation

According to the results of our calculation of the electrical production, we notice that the production of two positions increases according to the angular height of the sun, that is, if the angle of the Solar Height is large, the more the production is increased. We see a very sharp deterioration in the electricity production of 1979,59 kWh for a position without shading to 1490,87 kWh in the case of real position if one takes account the shading (24.68% loss), this is due to a shadow of the trees and a pole on the modules of the installation.

Then we notice that ridge shading plays a big part in productivity losses. Previously we got for the whole year, only with the shade, a productivity of 1035.42 kWh / kWp. We therefore lose 286.44 kWp because of the shadow of the ridge, a 22% decrease in productivity compared to this position without shading.

We also notice, that the winter months (November, December, January and February) are the months when productivity is lower, and the losses in winter is greater compared to the other months, this is due to our shadow masks because of low angular height of the sun in winter in the region of Settat. We find that the lowest percentage loss is in the summer months (May, June, July and August).

Conclusion IV

Climate change and the geographical location have a great influence on the operation of a given solar technology. The electrical or thermal energy produced is directly related to the weather data. These are therefore a very important tool for any monitoring measure productivity of different solar technology; and decision support regarding the best technology for which output is the least vulnerable to climate change.

The first part in this chapter, an evaluation of the solar radiation potential in Settat city through a theoretical modeling of the solar radiation in clear skies. The empirical models can be used to estimate the daily, monthly and annual average solar radiation in areas where there are no appropriate measurement devices available.

In the second part, we studied the effects of orientation for a solar panel and the optimum tilt angles for harvesting solar energy in Settat city in Morocco. The optimum tilt angle plays an important role in enhancing the energy collection of solar panels. The research in the first part of this work given the daily, monthly and yearly solar radiation, as well as some fundamental notions that intervene for the calculation of the solar irradiation arriving on an inclined surface and we have also calculated the different radiations fluxes involved in the energy balance and then compared the results obtained by theoretical formulations in two positron modes, the actual position of the installation and the optimum position in Settat city. The comparative study between the values of the calculated solar irradiation showed us the importance of the inclination and then orientation of the panels on the reception of the solar energy received.

The shading effects can drastically reduce solar power productivity. It is important to have identified the elements that can shade a photovoltaic field and minimize the impacts they can have on a production. Regular monitoring (quarterly, monthly, weekly or even daily) of our production is the best way to ensure the proper functioning of our facility.

For that we studied in the final part, the influence of shading on the production of our photovoltaic installation and the difference of production for the two modes of positions (without and with shading), and the mask survey (shading survey) which provides the information needed to calculate production losses due to shading.

References IV

[1] Nfaoui, M., El-hami, K. (2018) Optimal tilt angle and orientation for solar photovoltaic arrays: case of Settat city in Morocco. (2018) International Journal of Ambient Energy, 2, 162-8246.

[2] M. Vasiliev, M. Nur-E Alam, K. Alameh, ‘Initial Field Testing Results from Building-Integrated Solar Energy Harvesting Windows Installation in Perth, Australia’ (2019) Applied Sciences DOI: 10.3390/app9194002.

[3] Ennaoui, Ahmed. 2014. “Photovoltaic Solar Energy Conversion (PVSEC).” Helmholtz-Zentrum Berlin für Materialien und Energie, Free University of Berlin, Allemand.

[4] Bouchouicha Kada. “MODELISATION MULTISPECTRALE DES IMAGES SATELLITAIRE -Application : Quantification du bilan d’énergie Sol-Atmosphère” doctoral thesis 06/2017, Mohamed-Boudiaf University of Science and Technology, Oran, Oran, Algeria.

[5] Bird, R. E and Riordan, C. J, (1986): ‘’Simple solar spectral model for direct and diffuse irradiance on horizontal and tilted planes at the earth's surface for cloudless atmospheres’’, Journal of Climate and Applied Meteorology, 25 (1):87-97, 1986.

[6] A. Islahi, S. Shakil, M. Hamed. ‘Hottel’s Clear Day Model for a typical arid city - Jeddah’(2015) International Journal of Engineering Science Invention. Vol 4 - PP.32-37.

[7] Hay, J.E., Davies, J.A., (1980): Calculations of the solar radiation incident on an inclined surface. In: Hay, J.E., Won, T.K. (Eds.), Proc. of First Canadian Solar Radiation Data Workshop, 59. Ministry of Supply and Services, Canada.

[8] Al-Mostafa ZA, Maghrabi AH, Al-Shehri SM., (2014): Sunshine-based global radiation models: a review and case study. Energy Convers Manage 2014;84:209–16.

[9] Akinoğlu, B. G. et ECEVIT, A., (1990): A further comparison and discussion of sunshine-based models to estimate global solar radiation. Energy, 1990, vol. 15, no 10, p. 865-872.

[10] Dogniaux R., (1984): ‘’De l’influence de l’Estimation du Facteur Total de Trouble Atmosphérique sur l’Evaluation du Rayonnement Solaire Direct par Ciel Clair. Application aux Données Radiométriques de l’IRM à Uccle’’, Institut Royal Météorologique de Belgique (IRM), Miscellanea, Serie C, N°20, 1984.

[11] Hay J. (1979): Calculation of monthly mean solar radiation for horizontal and tilted surfaces. Solar Energy 1979;23, 1979.

[12] Oulimar B., (2010): diagnostic sur les différents modes de collecte énergétique, rapport d’activité, URER-MS, 2010.

[13] K.R. Ajao, R.M. Ambali and M.O. Mahmoud (2013): Determination of the Optimal Tilt Angle for Solar Photovoltaic Panel in Ilorin, Nigeria, Journal of Engineering Science and Technology Review 6 (1) (2013) 87 -90.

[14] K. ULGEN,(2006) :Optimum Tilt Angle for Solar Collectors, Energy Sources, Part A, 28:1171–1180, 2006.

[15] Danny H.W. Li and Tony N. T. Lam (2007): Determining the Optimum Tilt Angle and Orientation for Solar Energy Collection Based onMeasured Solar Radiance Data, International Journal of Photoenergy Volume 2007, Article ID 85402, 9 pages doi:10.1155/2007/85402.

[16] Y. SCHIMOT, A. TREY, G. RENARD, “Conception d’un dispositif optique pour l’amelioration de la performance énergetique d’un site de production d’électricité photovoltaique,” Projet 1004,IUT,2010.

[17] Lahcen EL IYSAOUY, Mhammed LAHBABI, Abdelmajid OUMNAD. Etude et comparaison des différentes configurations de Panneaux Photovoltaïques sous l'Effet d'ombrage partiel, https://www.researchgate.net/publication/320002891 .

[18] A.Dolara, G. C. Lazaroiu, S. Leva, and G. Manzolini, "Experimental investigation of partial shading scenarios on PV (photovoltaic) modules," Energy, vol. 55, pp. 466–475, Jun. 2013.

[19] R.Ramaprabha and B. L. Mathur, "A Comprehensive Review and Analysis of Solar Photovoltaic Array Configurations under Partial Shaded Conditions," Int. J. Photoenergy, vol. 2012, pp. 1–16, 2012.

[20] Y.-J.Wang and P.-C.Hsu, "An investigation on partial shading of PV modules with different connection configurations of PV cells," Energy, vol. 36, no. 5, pp. 3069–3078, May 2011.

Chapter V

EVALUATION OF THE THERMAL BEHAVIOR OF A PHOTOVOLTAIC CELL AND ANNUAL PRODUCTION OF THE PV-TEG HYBRID SYSTEM

V. 1. Introduction

In 2018, total energy consumption reached 20.767 million tons of oil equivalents (Mtep) 42% were eventually consumed in electricity and 58% directly into fuel (Super petrol, Butane, Propane as well as Gasoil, Fuel, Coal and Natural Gas). Morocco in 2018 we see that petroleum products represented 52% of consumption, 31% for coals, 4% for natural gas and 13% for electricity produced from renewable sources [1].

Photovoltaic can be recognized as one of the most promising renewable energy sources. On the other hand, Morocco is located within the world solar belt and has more than 3000 sunny hours per year and More than 3.400 MW_p [2]. Currently, global production of PV modules of the multicrystalline silicon solar cells is constantly increasing for reasons of lower estimated costs than those of monocrystalline silicon [3]. Knowing, the 13% of incident energy on the photovoltaic solar panel is extracted in the form of electrical energy. Accordingly the greater amount of incident energy is dissipated as the heat, for that the temperature is a very important parameter in the behavior of photovoltaic solar modules.

It is known that the major problem of the photovoltaic systems in terms of performance is the elevation of its temperature. This elevation happens because of the conversion to heat of a large part of the striking solar irradiation into the PV cells. This is due to the thermalization of excited electrons containing high energy and the absorption of photons with low energy.

After having quantified the dependence between efficiency and cell temperature, to identify the issue, we will present the thermal behavior in and around the modules, as well as an equation adapted to the problem. Finally, several meteorological variables, which govern the various phenomena of heat dissipation from cells to the outside, have a significant influence on the thermal behavior of the modules. The study of this influence will make it possible to identify essential phenomena to which we will attach particular importance in this work.

Certainly, in addition to the photovoltaic systems the electrical production of the PV-TEG hybrid system is related to climatic conditions. These climatic conditions vary yearly, monthly and daily, also depend on geographic coordinates. The purpose of this chapter is to evaluate the performance of the Thermal behavior of a photovoltaic module and the electric power produced of the hybridization of PV system with TEG generator under the weather conditions of Khouribga city in Morocco. A set of factors have been considered like the radiation, the ambient temperature, the wind velocity and the geographic coordinates.

V. 2. Meteorological data of khouribga city.

The city of Khouribga is located in the north-west of the Beni Mellal-Khénifra region, it is characterized by a series of low-altitude phosphate plateaus, and alluvial depressions of small and medium-sized hills of 750 m altitude, is bounded by the province of Settat to the west, the province of Khemisset to the north, the province of Khenifra to the east and the provinces of Beni Mellal and Fquih ben Salah to the south. The province of khouribga is characterized by a semi-arid continental climate, has a warm Mediterranean climate with dry and very hot summer, and a cold winter [4 & 5].

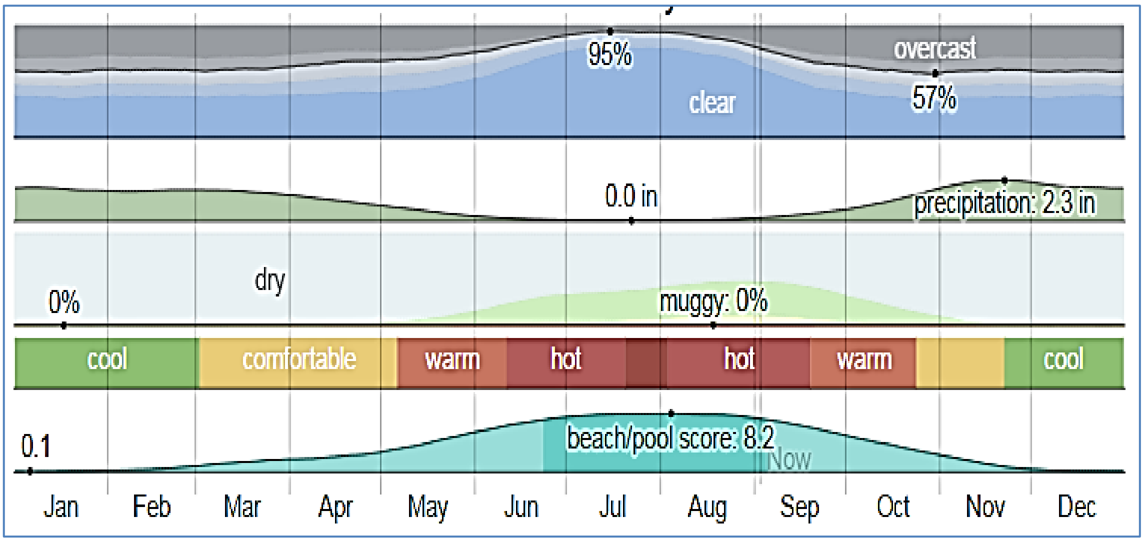

Figure V.68 : Climate summary of Khouribga [4].

In Khouribga, the summers are short, hot, arid, and clear and the winters are long, cold, and partly cloudy. Over the course of the year, the temperature typically varies from 2 °C to 35 °C and is rarely below -1 °C or above 41 °C.

V. 2. 1. Rainfall

The average annual rainfall at the Moulay Bouzekri station is 310 mm. The rainy season is characterized by a start in October and an end in May representing the wet season where almost all rainy episodes occur, ie 85% of the annual rainfall. The lowest average rainfall is recorded in July with only 2 mm. In January, rainfall is the most important of the year with an average of 50 mm [4 & 5].

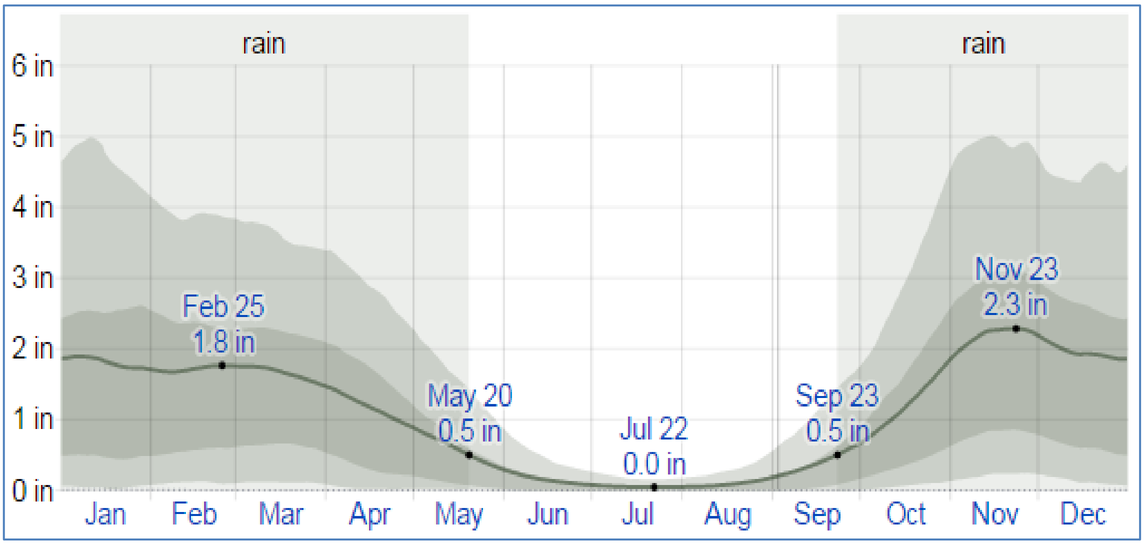

Figure V.69 : Average Monthly Rainfall [4].

The rainy period of the year lasts for 7.9 months, from September 23 to May 20, with a sliding 31-day rainfall of at least 0.5 inches. The most rain falls during the 31 days centered on November 23, with an average total accumulation of 2.3 inches.

The rainless period of the year lasts for 4.1 months, from May 20 to September 23. The least rain falls around July 22, with an average total accumulation of 0.0 inches.

V. 2. 2. Temperatures

The province of khouribga is characterized by a semi-arid climate with thermal amplitudes of around 20 °C [4]:

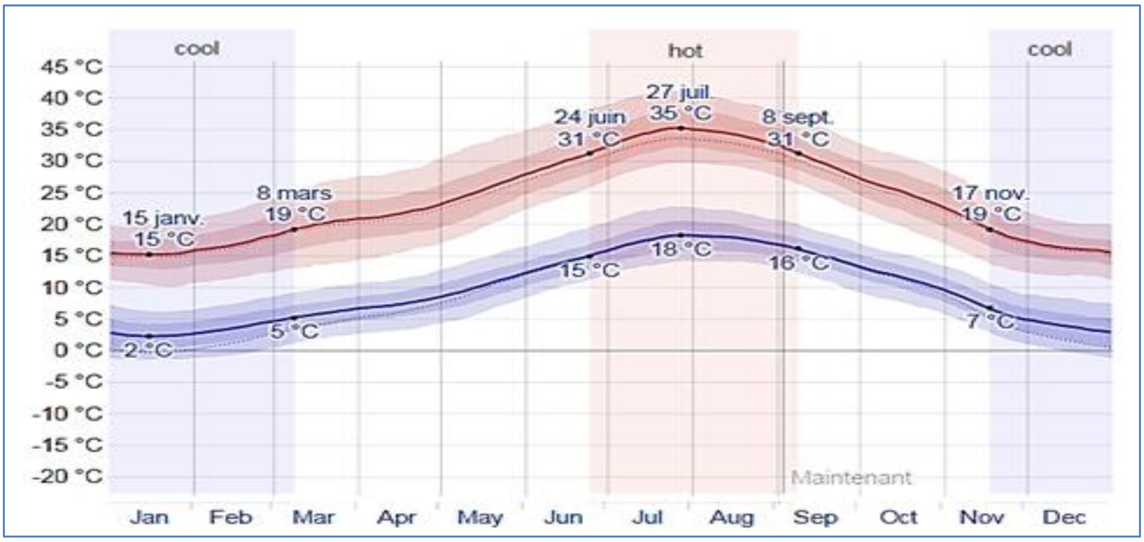

Figure V.70 : Average High and Low Temperature [4].

The hot season lasts for 2.5 months, from June 24 to September 8, with an average daily high temperature above 31 °C. The hottest day of the year is July 27, with an average high of 35 °C and low of 18 °C.

The cool season lasts for 3.7 months, from November 17 to March 8, with an average daily high temperature below 19 °C. The coldest day of the year is January 15, with an average low of 2 °C and high of 15 °C.

V. 2. 3. Wind regime

The prevailing winds in the region are those from the NNE which are weak in intensity. Examination of the series of wind speeds measured on site, at 10 m, between December 2016 and December 2017 shows that the average speed is 3.9 m/s. The speed is less than 6 m/s for 75% of the measurements and less than 9 m/s for 98% of the measurements [5].

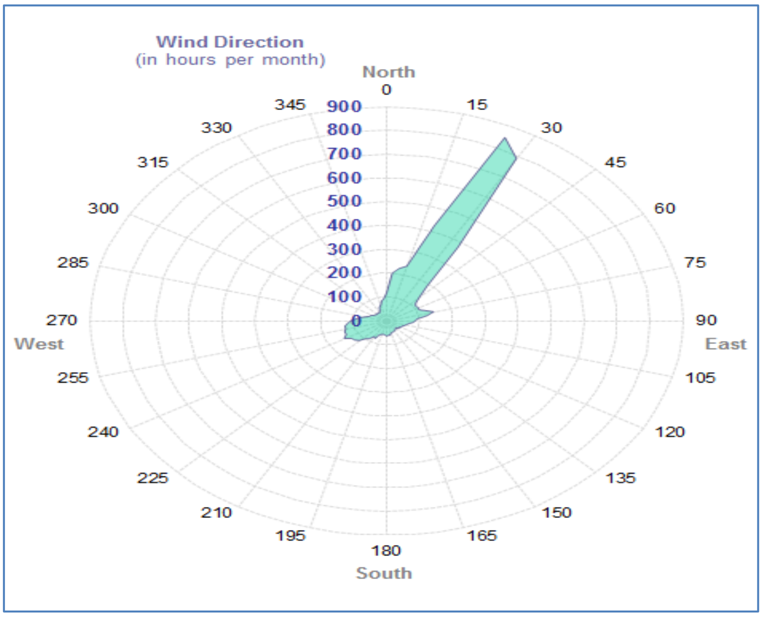

Figure V.71 : Compass wind rose [5].

This section discusses the wide-area hourly average wind vector (speed and direction) at 10 meters above the ground. The wind experienced at any given location is highly dependent on local topography and other factors, and instantaneous wind speed and direction vary more widely than hourly averages.

V. 2. 4. Solar energy

An application of this work is used to calculate the annual solar energy developed in Matlab according to the horizontal surface, in the case of Khouribga city is located under 32°52 'North as latitude and under -6°54 'West as longitude.

The theoretical results of daily and Monthly variations of solar radiation arriving on a horizontal surface are summary in the table below [3, 6 and 7];

Table V.27 : Daily, monthly and yearly energy received.

			The energy received per days (wh/m^2)			The energy Received per Month (kwh/m^2)		
Month	**Days typical**	**N° of days**	**Direct energy**	**Diffuse energy**	**Total energy**	**Direct Energy**	**Diffuse Energy**	**Total Energy**
January	**17**	**17**	3442	397	3839	106,7	13,2	119.9
February	**16**	**47**	4346	526	4872	121,7	14,7	136.4
March	**16**	**75**	5490	713	6203	170,2	22,1	192.3
April	**15**	**105**	6439	947	7386	193,2	28,4	221.6
may	**15**	**135**	6906	1153	8059	214,1	35,7	249.8
June	**11**	**162**	6982	1273	8255	209,4	38,2	247.6
July	**17**	**198**	6804	1248	8052	210,9	39,6	250.5
August	**16**	**228**	6350	1163	7513	196,9	36	232.9
September	**15**	**258**	5546	970	6516	166,4	29,1	195.5
October	**15**	**288**	4481	742	5223	138,9	23	161.9
November	**14**	**318**	3535	544	4079	106,1	16,3	122.4
December	**10**	**344**	3122	431	3553	96,8	13,4	110.2
Annual radiation [kWh/m^2.year]						***1931,1***	***309,8***	***2240,9***

The average of daily incident shortwave solar energy experiences extreme seasonal variation over the course of the year, given in the figure below.

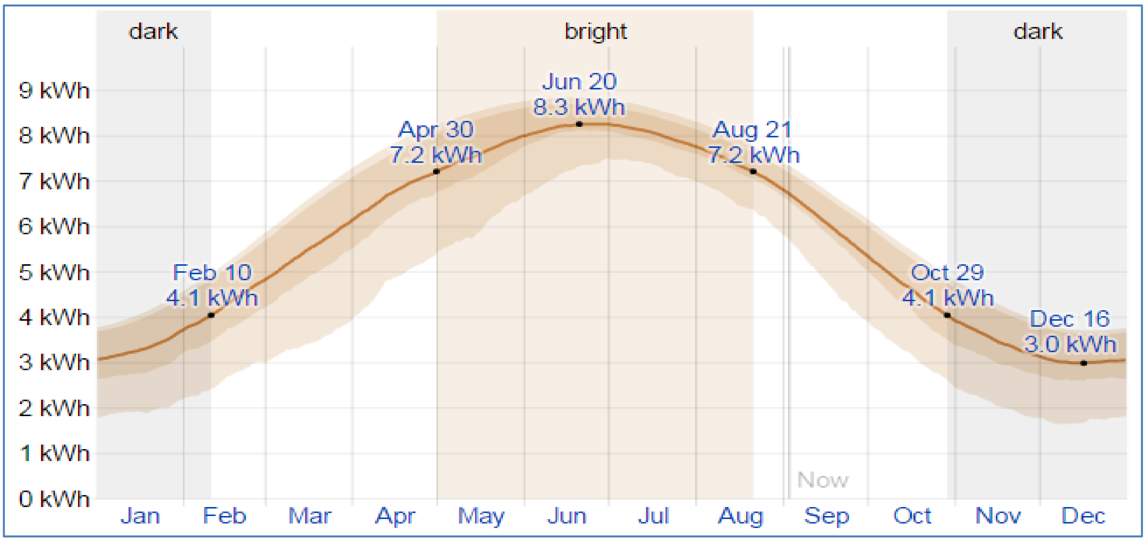

Figure V.72 : Average Daily Incident Shortwave Solar Energy [4].

The brighter period of the year lasts for 3.7 months, from April 30 to August 21, with an average daily incident shortwave energy per square meter above 7.2 kWh. The brightest day of the year is June 20, with an average of 8.3 kWh.

The darker period of the year lasts for 3.4 months, from October 29 to February 10, with an average daily incident shortwave energy per square meter below 4.1 kWh. The darkest day of the year is December 16, with an average of 3.0 kWh.

V. 2. 5. Summary table of the meteorological data

Currently, in Morocco, measurements of the ambient temperature, wind speed and solar radiation, data are performed in an instantaneous and continuous manner; this study is carried in the Khouribga city of latitude 32◦52.86′ North and longitude −6◦54.37′ west.

To study the influence of this parameter on a PV module, we take a day from July 2018 in Khouribga with a solar radiation received on optimum tilt angle of 30° and the orientation towards the south (the 180° azimuth) [6&7].

Table V.28 : The July average variation of temperature, wind speed and solar radiation.

Hour (h)	Temperature (c̊)	wind speed (m/s)	solar radiation (wh/m²)
06H	23	3	10
07h	23	3	130
08h	26	3	344
09h	31	3	555
10h	34	6,1	734
11h	37	6,1	867
12h	39	6,1	938
13h	41	6,1	944
14h	41	6,1	883
15h	40	7,2	760
16h	39	7,2	588
17h	38	7,2	379
18h	36	8,3	163
19h	34	8,6	27
20h	33	8,3	0

The table shows the meteorological forecast for Khouribga in July. We have given the local essential meteorological data of our city Khouribga: ambient temperature, wind speed and solar radiation, and we can then add the other parameters like; humidity, rainfall.... as well as weather conditions for local outdoor activities.

V. 3. Heat exchanges between the Photovoltaic module and its environment

The photovoltaic module is a plate that absorbs the solar radiation, subjected to the wind and to a radiative environment formed by the sky and the ground or a roof.

The optical behavior of the encapsulation, allows solar cells to absorb part of solar radiation. Part of the energy absorbed can be converted into electricity, with efficiency of 10% to 15% for commercial crystalline silicon modules [8]. The rest of this energy (85 to 90%) is stored (temperature rise) or evacuated from the cells to the outside of the encapsulation, by thermal conduction.

The faces of the module dissipate this thermal energy in convective or radiative form, in the infrared. Some of the heat can also be dissipated in conductive form to the module support. This flow is however neglected in most theoretical models, because the induced gradients in the plane of the module are small compared to those caused by natural or forced convection.

V. 3. 1. Description of the thermal behaviour of a Photovoltaic silicon module

Photovoltaic modules are submitted to several meteorological parameters (solar radiation, ambient temperature, sky temperature, wind) whose short-term variations are difficult to predict. The large number of input parameters of such a model is a handicap. This approach is, however adopted by a certain number of authors [8&9] when they have the necessary meteorological data.

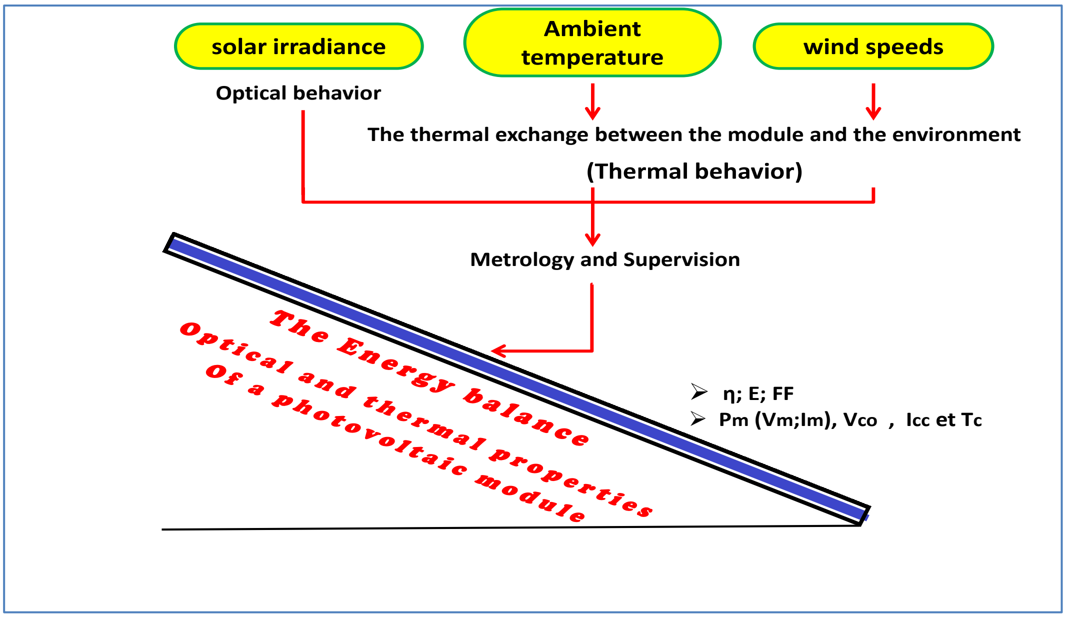

Figure V.73 : Modeling of the thermal behavior of a photovoltaic module.

The general structure of the equation, on which stand the literature models, is shown in the diagram in Figures 5 & 6. A set of meteorological data makes it possible to determine the operating temperature of a photovoltaic module: the ambient temperature gives and the solar radiation exchange with the sky,

In this context, the solar radiation is the main energy source while wind and ambient temperature govern the two main dissipation modes of thermal energy.

V. 3. 2. Theoretical approaches "mathematical models"

Different authors have developed the methods of integrating the thermal behavior of modules in their models for describing modules in real operating conditions. The objective of this section is to present the methods used to directly estimate the module temperature.

V. 3. 2. 1. Operating cells Temperature T_c.

The CEI 61215 standard provides a definition of nominal operating cell temperature (NOCT). The NOCT is measured for an open circuit photovoltaic module, well ventilated, subject to an illumination of 800 W/m², with an outside temperature of 20 °C and wind speed of 1 m/s.

Studies in the literature describe models having the same structure as the approach consisting in using NOCT, but taking into account the influence of meteorological parameters, rear side Temperature of the modules is expressed as a function of the ambient temperature, solar radiation, wind speed and some parameters determined experimentally according to the following formulas:

1-First Approach[10]

$$T_c = Ta + \left(\frac{NOCT - 20°C}{0.8}\right).S \qquad (1)$$

- T_c = Cell temperature °C.
- T_a = Ambient temperature °C.
- S = solar irradiance (1 kW/m^2).

2-Second Approach[11]

$$T_c = T_m + \frac{E}{E_0}.\Delta T \qquad (2)$$

- T_m = Measured back-surface module temperature, (°C).
- E = Measured solar irradiance on module, (W/m^2).
- E_0 = Reference solar irradiance on module, (1000 W/m^2).

$$T_m = E.\left(e^{a+b.WS}\right) + T_a \qquad (3)$$

Where:

- a = Empirically-determined coefficient establishing the upper limit for module temperature at low wind speeds and high solar irradiance.
- b = Empirically-determined coefficient establishing the rate at which module temperature drops as wind speed increases.
- WS = Wind speed measured at standard 10 m height, (m/s).

Table V.29 : Empirically determined coefficients used to predict module back surface temperature as a function of irradiance, ambient temperature, and wind speed [11].

Module Type	Mount	a	b	ΔT (°C)
Glass/cell/glass	Open rack	-3,47	-.0594	3
Glass/cell/glass	Close roof mount	-2,98	-.0471	1
Glass/cell/polymer sheet	Open rack	-3,56	-.0750	3
Glass/cell/polymer sheet	Insulated back	-2,81	-.0455	0
Polymer/thin-film/steel	Open rack	-3,58	-.113	3
22X Linear concentrator	Tracker	-3,23	-.130	13

3-The Third Approach [3 & 12]

Modelling of the convective exchanges between the photovoltaic module and its environment;

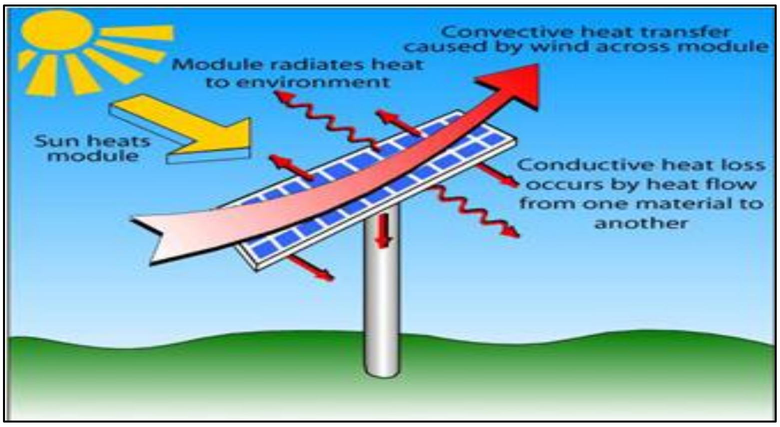

Convection phenomena have been studied by many experiments. We find in the literature a lot of empirical models, each responding to the needs of the designer,

- ***Natural convection turbulent:***

$$h_{cv} = k.(T - T_a)^{\frac{1}{3}} \quad (4)$$

- ***forced convection depending on the flow velocity h_{cv} = f (v):***

- Mc-Adams : h_{cv} = 5,7+3,8v

- Wattmuff : h_{cv} = 2,8+3,0v

➢ ***Natural convection / forced convection :***

- Churchill, 1977 :

$$h_{cv} = \sqrt[3]{h_{nae}{}^{3} + h_{forc}{}^{3}} \qquad (5)$$

Consider a maximum function: h_{cv} = max (h_{nae} ; h_{forc}) which is numerically, almost equivalent to the previous formulation. We assume the natural convection is predominant below a wind speed of (0,45 m/s).

With;

Ta is the temperature of the fluid at infinity, that is to say, in the framework of this study, the ambient temperature (depending on the implementation of the module).

K is the factor for the natural convection coefficient (S.I).

➢ ***wind influence on the Cell temperature;***

When the wind speed in the vicinity of modules increases, convective exchanges are favored, and therefore their temperature decreases [3].

$$\frac{T-T_a}{G} = f(v) \qquad (6)$$

$$(T - T_a)\frac{1000}{G} = 0{,}00712v^2 - 2{,}411v + 32{,}92 \qquad \textbf{(King)}$$

$$(T - T_a)\frac{1000}{G} = 0{,}3826v^2 - 5{,}270v + 36{,}22 \qquad \textbf{(Cadarache)}$$

V. 3. 2. 2. Modelisation of the PV-TEG Hybrid System

The PV-TEG hybrid system presented here consists of a photovoltaic panel based on crystalline silicon cells and TEG thermoelectric generators [13]. The TEG module is adjunct directly in the lower side of the photovoltaic panel. To estimate the annual performance of this hybrid system per unit area, the surface of the PV cell and the TEG generator are both assumed to be equal to 1 m^2. The most of conventional PV panels are formed of numerous layers. In our investigation, we assume the following principal layers that are sequentially in the top of photovoltaic panel the glass follow by EVA, solar cells, EVA and finally Tedlar. Each layer has a thermal resistance that can increase the temperature of the solar cell and can reduce the heat flux through the TEG module. The TEG generator is formed of semiconductor elements, thermally connected in parallel and electrically in series so as to be placed between two ceramic plates [14 & 15].

Energy balance equation:

Before solar radiation G reached the surface of the photovoltaic panel, Firstly, a part of it is absorbed by the glass G_a with α_g is glass absorption coefficient, another part G_r is reflected, while the remaining part G_t is transmitted through it and through EVA which is supposed to be transparent towards the solar cell. The heat by conduction through EVA and glass layers is denoted $Q_{EVA-glass}$, it is lost on the surface of the glass by natural convection $Q_{N,g}$, and forced convection $Q_{F,g}$.

When the transmitted radiation G_t reached the solar cell, only a small part is converted into electricity P_{pv} through photovoltaic effect, and the other part is absorbed $G\,\alpha_{PV}\,\tau_g$ by the cell material with α_{Pv} is solar cell absorption coefficient and τ_g is the transmissivity of the glass. A portion of the energy absorbed is lost in the ambient by radiation $Q_{R,PV}$ to the ground $Q_{R,PV,gro}$ and to the sky $Q_{R,PV,sky}$ and by conduction $Q_{EVA-glass}$ through EVA and glass. The remaining part passes through solar cell, EVA and Tedlar and is noted $Q_{PV-EVA-tedlar}$, it will be delivered on the top of the ceramic hot side of the TEG generator. The thermal contact between the thermoelectric module and the PV module is supposed to be perfect, so that the heat passes down the PV module will be completely delivered to the TEG generator. This heat will be passed through the ceramic hot side layer of the TEG generator Q_h . When it reaches the thermoelectric element based on telluride bismuth a part of it will be converted directly into electricity by Seebeck effect. Parallel to this effect, there exists Peltier effect and the Joule effect due to the electric current flowing through the TEG, and Fourier's heat conduction due to the temperature gradient, and finally the Thomson effect that occurs as a result of the occurrence of a temperature gradient besides a presence of an electric current. Finally, the heat that passes through the ceramic cold layer Q_c will be dissipated by forced convection $Q_{F,cr}$, natural convection $Q_{N,cer}$ and radiation $Q_{R,cr}$ to the sky $Q_{R,cr,sky}$ and to the ground $Q_{R,cr,gro}$.

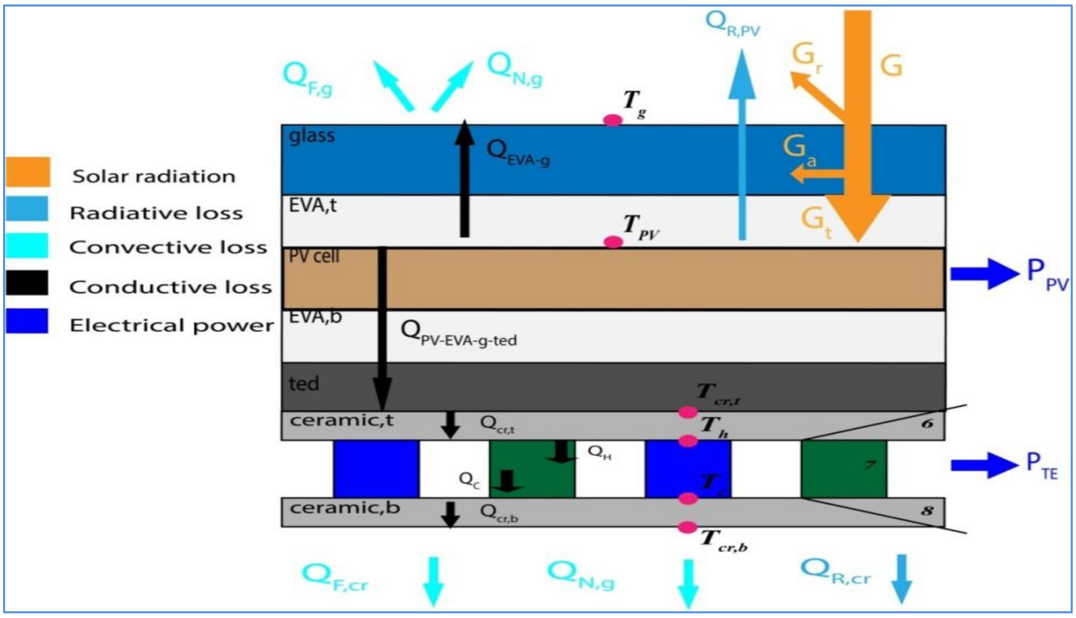

Figure V.74 : Description of the layers constituting the PV-TEG hybrid system.

From the last description and according to fig.V.74 and the previous description, six equations was obtained with six surface temperature, which are the top glass surface temperature, the top crystalline cell temperature, the top ceramic hot side surface temperature and the bottom ceramic cold side surface temperature. The calculation of these temperatures conducts to calculating the generated power of the present system. The resolution of this system with six nonlinear equations is carried out by applying the method of Newthon-Raphson. The equations associated with energy balance in this hybrid system can be formulated in the following manner [16]:

$$\begin{cases} 0 = GaA_{PV} + Q_{EVA-g} - Q_{F,g} - Q_{N,g} \\ 0 = -Q_{PV-EVA-tedlar} + G(\alpha_{PV}\tau_g)A_{PV} - Q_{EVA-g} - Q_{R,PV,gro} \\ \quad -Q_{R,PV,sky} - P_{PV} \\ 0 = Q_{PV-EVA-tedlar} - Q_h \\ 0 = Q_h - Q_{cr,t} \\ 0 = Q_c - Q_{cr,b} \\ 0 = Q_{cr,b} - Q_{R,cr,gro} - Q_{R,cr,sky} - Q_{F,cr} - Q_{N,cr} \end{cases} \quad (7)$$

Thermal Resistance:

The thermal resistances presented in the model are: that of the EVA and the glass in top of solar cells R_{EVA-g}, that of the crystalline cell R_{EVA-g}, EVA and tedlar $R_{PV-EVA-tedlar}$, and that of the hot ceramic layer R_{Cr}.

$$R_{EVA-g} = \frac{L_{EVA}}{A_{PV}k_{EVA}} + \frac{L_g}{A_{PV}k_g} \quad (8)$$

$$R_{PV-EVA-tedlar} = \frac{L_{EVA}}{A_{PV}k_{EVA}} + \frac{L_{tedlar}}{A_{PV}k_{tedlar}} + \frac{L_{PV}}{A_{PV}k_{PV}} \quad (9)$$

$$R_{cr} = \frac{L_{cr}}{A_{TE}k_{cr}} \quad (10)$$

With:

- L and k are length and conductivity of each layer.
- A_{PV} is the area of the panel.

Radiation Resistance:

We note the radiation resistances on the top of crystalline cell to the ground $R_{R,PV,gro}$ and to the sky $R_{R,PV,sky}$ are:

$$R_{R,PV,gro} = \frac{1}{\epsilon_g F_{gro} \sigma A_{PV} (T_{PV}+T_{gro})(T_{PV}^2+T_{gro}^2)} \quad (11)$$

$$R_{R,PV,sky} = \frac{1}{\epsilon_g F_{sky} \sigma A_{PV} (T_{PV}+T_{sky})(T_{PV}^2+T_{sky}^2)} \quad (12)$$

With:

T_{PV}, T_{gro} and T_{sky} are the temperature of the PV panel, the ground and the sky, $\epsilon_g$is the glass emissivity, σ is the Stefan-Boltzmann constant, F_{gro} and F_{sky} are configuration factor of the ground and the sky.

For the radiation resistance on the lower of ceramic layer: to the ground $R_{R,cr,gro}$ and to the sky $R_{R,cr,sky}$ [17]:

$$R_{R,cr,gro} = \frac{1}{\epsilon_g F_{gro} \sigma A_{PV} (T_{cr}+T_{gro})(T_{cr}^2+T_{gro}^2)} \quad (13)$$

$$R_{R,cr,sky} = \frac{1}{\epsilon_g F_{sky} \sigma A_{PV} (T_{cr}+T_{sky})(T_{cr}^2+T_{sky}^2)} \quad (14)$$

The temperature of the sky can be found according to the reference [18]:

$$T_{sky} = 0.0552\ T_a^{3/2} \quad (15)$$

The ground temperature is often taken for the calculation of the radiation exchange as the same as the ambient temperature T_{gro}= T_a [16, 17 an 18].

The configuration factors $F_{PV,gro}$ for ground and $F_{PV,sky}$ for sky:

$$F_{PV,gro} = \frac{1}{2}\left(1 - \cos(\theta)\right) \quad (16)$$

$$F_{PV,sky} = \frac{1}{2}\left(1 + \cos(\theta)\right) \quad (17)$$

With $F_{PV,gro}$ and $F_{PV,sky}$ are the configuration factors respectively for the ground and the sky:

$$F_{cr,gro} = \frac{1}{2}\left(1 - \cos(\pi - \theta)\right) \quad (18)$$

$$F_{cr,sky} = \frac{1}{2}\left(1 + \cos(\pi - \theta)\right) \quad (19)$$

Heat Transfer Coefficient for the Forced Convection:

Since the photovoltaic panel is always installed outside, the influence of wind speed must necessarily be considered. Therefore, the coefficient of heat transfer for forced convection due to wind speed can be determined using the formula proposed by [19]:

$$h_w = 5.678\left\{a + b\left[\frac{\left(\frac{294.26}{273.16+T_a}\right)V}{0.3048}\right]^n\right\} \quad (20)$$

a, b and n are constant values given by reference [20] for the texture of smooth surfaces.

Heat Transfer Coefficient for the Naturel Convection:

In the top of the glass, for an inclined plate with a heated surface facing upwards with a nearly constant heat flow, correlation obtained for the heat transfer coefficient $h_{N,g}$ is in the form [21]:

$$h_{N,g} = 0.14\left[(GrPr)^{1/3} + (Gr_{cr}Pr)^{1/3} + 0.56(Gr_{cr}Pr\cos\theta)^{1/4}\right]\frac{k_a}{L} \quad (21)$$

For $105 < GrPr\cos\theta < 1011$ and $15° < \theta < 75°$

Gr_{cr} is the Critical number;

Gr is Grashof number;

Pr is Prandtl number;

In the bottom of the hot ceramic layer, for heated surfaces inclined downwards, the natural convection heat transfer coefficient correlation recommended by Churchill and Chu (1975) was given a [21]:

$$h_{N,cr} = [0.825 + \frac{0.387Ra^{1/6}}{\left[1+(0.492/Pr)^{8/16}\right]^{8/27}}]^2\frac{k_a}{L} \quad (22)$$

R_a is Rayleigh number.

Heat Loss by Naturel Convection:

In the top of the glass layer:

$$Q_{N,g} = A_P h_{N,g}(T_g - T_a) \tag{23}$$

In the bottom of the ceramic layer:

$$Q_{N,cr} = A_{PV} h_{N,cr}(T_{cr} - T_a) \tag{24}$$

Heat Loss by Forced Convection:

In the top of the glass layer:

$$Q_{F,g} = h_w A_{PV}(T_g - T_a) \tag{25}$$

In the bottom of the ceramic layer:

$$Q_{F,cr} = h_w A_{TE}(T_{cr} - T_a) \tag{26}$$

Heat Loss by Radiation:

$$Q_{R,PV,gro} = \frac{(T_{PV} - T_{gro})}{R_{R,PV,gro}} \tag{27}$$

$$Q_{R,PV,sky} = \frac{(T_{PV} - T_{sky})}{R_{R,PV,sky}} \tag{28}$$

$$Q_{R,PV,sky} = \frac{(T_{PV} - T_{sky})}{R_{R,PV,sky}} \tag{29}$$

$$Q_{R,PV,sky} = \frac{(T_{PV} - T_{sky})}{R_{R,PV,sky}} \tag{30}$$

Heat Transferred by Conduction:

$$Q_{EVA-glass} = \frac{(T_{PV} - T_g)}{R_{EVA-g}} \tag{31}$$

$$Q_{PV-EVA-tedlarr} = \frac{(T_{PV} - T_{cr})}{R_{PV-EVA-tedlar}} \tag{32}$$

$$Q_{cr,t} = \frac{(T_{cr,t} - T_h)}{R_{cr}} \tag{33}$$

$$Q_{cr,b} = \frac{(T_C - T_{cr,b})}{R_{cr}} \tag{34}$$

The heat through the hot side of the thermoelectric elements Q_H and the heat of its cold side Q_c can be written as follows [22]:

$$Q_H = n_{TE}(s(T_H)I_{TE}T_H - \frac{I_{TE}^2 R_{TE}}{2} + \frac{(T_H - T_c)}{R_{TE}} - \frac{\mu(T_c)I_{TE}(T_H - T_c)}{2}) \tag{35}$$

$$Q_c = n_{TE}(s(T_c)I_{TE}T_c + \frac{I_{TE}^2 R_{TE}}{2} + \frac{(T_H - T_c)}{R_{TE}} + \frac{\mu(T_H)I_{TE}(T_H - T_c)}{2} \tag{36}$$

The temperature dependence properties for the bismuth telluride are given by Schwingshackl et al (2013):

I_{TE} is the electrical current passes through the TEG element [22], with R_C is the resistance of the load:

$$I_{TE} = \frac{n_{TE}[(s(T_H)T_H - s(T_c)T_c) - \mu(T_H - T_c)]}{n_{TE}\ R_{TE} + R_C} \tag{37}$$

n_{TE} : is the number of thermoelectric element its determining by obtaining a surfaces equal to that of the PV cell 1 m^2.

The heat that passes through the cold ceramic layer Q_c :

$$Q_{cr,b} = \frac{(T_c - T_{cr,b})}{R_{cr}} \tag{38}$$

The Overall Efficiency:

The overall efficiency of the PV-TEG can be defined as the ratio between the sum of the output power of the TEG generator with the PV cell and the solar radiation incident on its surface [22 & 23]:

$$\eta_T = \frac{P_T}{A_{PV}\ G} \tag{39}$$

With:

P_T : the output power of the overall system, which is the sum of the electrical power generated by the two modules defined by:

$$P_T = P_{PV} + P_{TE} \tag{40}$$

P_{PV} : the output power of the PV cell which is equal to:

$$P_{PV} = A_{PV}\ G\ \eta_{PV} \tag{41}$$

P_{TE} : the output power of the TEG generator which is equal to:

$$P_{TE} = Q_H - Q_c \tag{42}$$

The Efficiency of the PV Cell:

The efficiency of the PV cell [22]:

$$\eta_{pv} = \eta_{ref}[1 - \beta_{ref}(T_{PV} - T_{ref})] \quad (43)$$

With is the PV cell efficiency at the reference temperature T_{ref} = 25 °C, and reference solar radiation G_{ref} =1000 W/m^2, and is the temperature dependence coefficient of the cell [24].

The TEG Efficiency:

The TEG efficiency can be defined as the ratio between the electrical power generated by the TEG generator and the solar radiation incident on the hybrid system[22, 23 and 24]:

$$\eta_{TE} = \frac{P_{TE}}{Q_{cr,t}} \quad (44)$$

V. 4. Results and Discussion

The thermal models involve a set of input parameters, which are used to identify the thermal behavior of a photovoltaic solar panel. These parameters are implemented in the mathematical formulas written under MATLAB programming.

On the other hand; the photovoltaic modules are subject to meteorological variables (illumination, ambient temperature and wind speed) that are difficult to predict in the short-term. The simulation of their behavior, especially their heating, in practice, it is interesting to know the heating of the modules in a form representative of a long period.

V. 4. 1. Modeling of the Thermal Behavior of a Photovoltaic Cell under Arid and Semi-arid Sites Conditions: Case of Khouribga City in Morocco

A set of meteorological data is used to determine the operating cell temperature of a photovoltaic module: ambient temperature, wind speed and solar radiation.

In this part we will treat an experimental study at the Laboratory of solar systems (CEA/LITEN/DTS) on the Cadarache platform [8], Saint-Paul-lez-Durance, France, then we will compare it with the programming results of the theoretical mathematical models to represent the impact of this meteorological variables on the temperature of a photovoltaic module.

V. 4. 1. 1. Properties of the photovoltaic module used: (BP 585 (BP Solar)).

	BP 585	BP 580[4]
Maximum power (P_{max})[2]	85W	80W
Voltage at P_{max} (V_{mp})	18.0V	18.0V
Current at P_{max} (I_{mp})	4.72A	4.44A
Warranted minimum P_{max}	80.8W	76W
Short-circuit current (I_{sc})	5.0A	4.7A
Open-circuit voltage (V_{oc})	22.1V	22.0V
Temperature coefficient of I_{sc}	(0.065±0.015)%/°C	
Temperature coefficient of voltage	-(80±10)mV/°C	
Temperature coefficient of power	-(0.5±0.05)%/°C	
NOCT[3]	47±2°C	
Maximum system voltage	600V (U.S. NEC rating) 1000V (TÜV Rheinland rating)	
Maximum series fuse rating	20A (U, H versions) 15A (S, L versions)	

Figure V.75 : Electrical Characteristics of BP 585 (BP Solar) module.

A crystalline silicon photovoltaic module is composed of a set of cells, connected either in series or in parallel, so as to obtain the desired current and voltage levels. This solar panel has a manufacturing to advanced technology, which gives a high efficiency and excellent lifetime.

Limited Warranties:

- Power output for 25 years;
- Freedom from defects in materials and workmanship for 5 years.

A crystalline silicon photovoltaic module is composed of a set of cells, connected in series/parallel, so as to obtain the desired current and voltage levels. These cells are mechanically maintained by the encapsulation of the module, in ethyl vinyl acetate (EVA), which is a polymer that we melt to bond the cells to the tempered glass, of variable thickness. The whole cell, EVA and glass form the front of the module.

On the back side, depending on the applications, the cells are protected either by a sheet of Tedlar, either by glass, maintained by a new layer of EVA.

The thermophysical properties of these materials are referenced in various charts or works specific to the photovoltaic field. The values of their properties are presented in the following Table; the variety of materials used by different manufacturers may explain the possible differences from other sources.

Table V.30 : Thermal and physical properties of the materials of a PV module [8].

	ρ (kg/m3)	Cp (J/(kg.K))	λ (W/(m.K))
glass	2500	700	1,0
EVA	950	1200	0,35
silicon	2300	720	140
tedlar	1200	1700	0,16

We consider the emissivity of glass and tedlar in the infrared, for the operating cell temperature of the photovoltaic modules (from -20 °C to 70 °C approximately), is 0.90 and 0.80 respectively.

V. 4. 1. 2. Influence of the ambient temperature on the operating cell temperature

When subjected to solar radiation, the temperature of the photovoltaic modules increase compared to the ambient temperature: the lower limit of the module temperature value is therefore, from a certain level of lighting, the ambient temperature, which is characteristic of the local climate.

The following two figures show the linear relationship, as a first approximation, either experimental or theoretical, between the operating cells temperature and the ambient temperature.

We show in the first figure the measurements carried in the solar platform of Cadarache[8], All this experimental measurement are carried under NOCT conditions (Nominal Operating Cell Temperature). And we show the results of the calculation by use a Matlab code, that we have developed which calculates and plots the ambient temperature according to the operating cells temperature of a photovoltaic module.

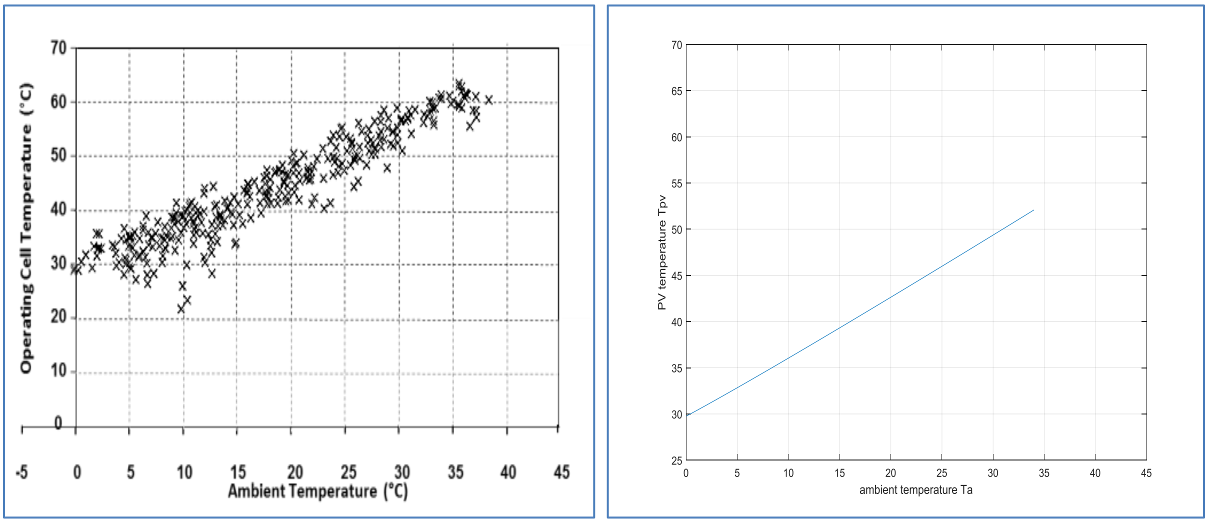

a) Measured cell temperature [8] (°C). b) Modeling cell temperature (°C).

Figure V.76 : Relationship between the operating cell temperatures and the ambient temperature, under an illumination of 800 W/m² and a wind of 1 m/s.

Fig.V.76 represents the influence of the ambient temperature on the operating cell temperature; the two figures show the relation between the temperature of an inclined module and the ambient temperature under conditions:

- Illumination of 800 W/m².
- Wind of 1 m/s.

The not strictly linear experimental relation due to the radiative exchanges between the module and the ground (or the roof), the simplicity of the relationship between the operating cell temperature and the ambient temperature thus highlighted often justifies the linearity of the two temperatures in the theoretical side.

The relationship between the two temperatures T_a and T_c is linear in the first approximation, and it shows that the operating cell temperature is an increasing function of ambient temperature of the environment where the photovoltaic panel is placed. When the ambient temperature reaches a maximum of 41 °C the operating cell temperature is around 60 °C, so the efficiency in this risky case drops.

V. 4. 1. 3. Influence of the solar radiation on the operating cell temperature

The main energy input on the modules is the incident solar radiation on the front face. The relationship between (difference temperature between the operating cell temperature and the ambient temperature) and the solar radiation, for a wind speed of 1 m/s.

The two graphs below, plotting the average value between (the ambient temperature and the operation cell temperature) depending to the illumination G, at a fixed wind speed.

The relationship between the operation cell temperature and solar radiation is linear. This linearity is however only verified for solar radiation below a certain illumination level, beyond which the module temperature decreases.

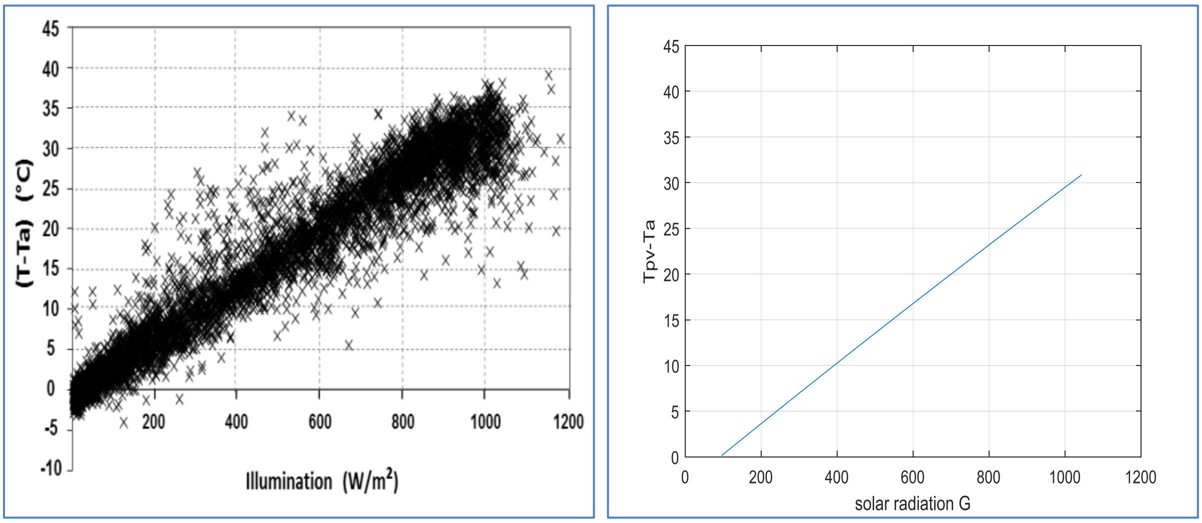

a) Experimental data of difference temperature (T - T_a) vs Illumination G [8].

b) Modeling of the difference temperature (T - T_a) Vs Illumination G.

Figure V.77 : Relation between the illumination and the difference of temperature between the module and the ambient temperature (T - T_a), for a wind speed of 1 m/s.

It also appears that the temperature difference between the ambient temperature and the operation cell temperature can be negative: the influence of the sky temperature, generally lower than the ambient temperature, is well illustrated by this phenomenon. At night, the module dissipates energy by radiative exchanges with the sky: the equilibrium temperature is therefore slightly below ambient temperature. Low lighting, in the morning or evening cannot always compensate for this radiative loss.

V. 4. 1. 4. Influence of the wind speed on the operating cell temperature

The wind speed influenced directly on the operating temperature of the module. When the wind speed near the modules increases, the convective exchanges between the Photovoltaic module and their external environments are increased, and therefore the operating cell temperature decreases.

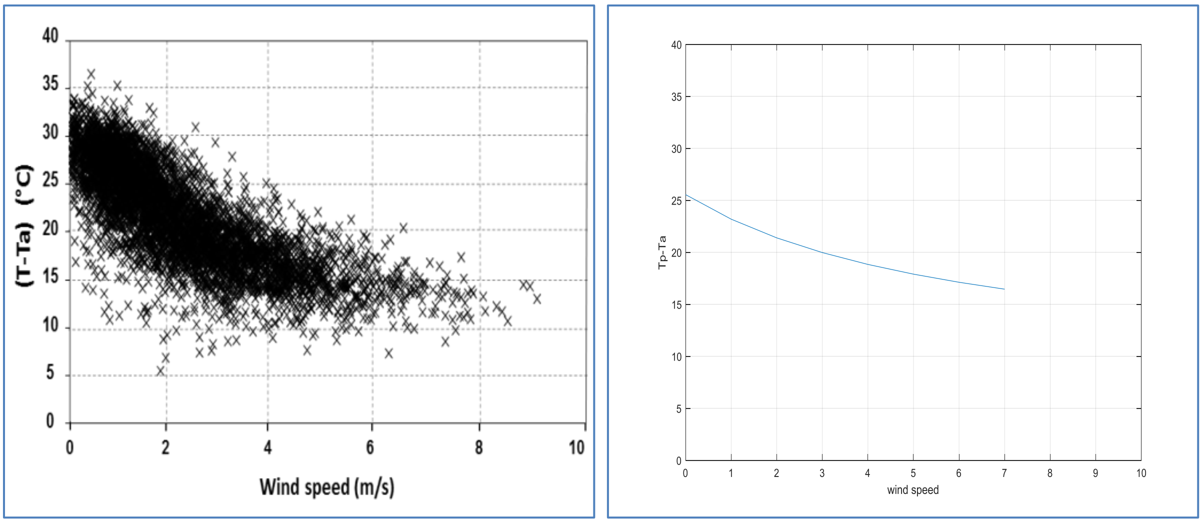

a) Measured wind speed (m/s) vs difference temperature (T - T_a) [8].

b) Modeling of the wind speed (m/s) Vs difference temperature (T - T_a).

Figure V.78 : The relationship between (T - Ta) and the wind speed, for an illumination of 800 W/m².

The slope of (T-T_a) (G) is a function of the wind speed. With fixed illumination (G = 800 W/m²), the difference of temperature T-T_a is a relatively complex function of the wind speed. The convective phenomena govern this relationship.

V. 4. 1. 5. Effect of the operating cell temperature on the efficiency of the photovoltaic module

The objective of this part is study the effects of the operating cell temperature on the electrical performance of silicon solar cells, we will present the variation of the photovoltaic efficiency as a function of the operating cell temperature, note that the effect of the latter is presented explicitly and implicitly by the energy dependence on the temperature. The results obtained are shown in the figure below:

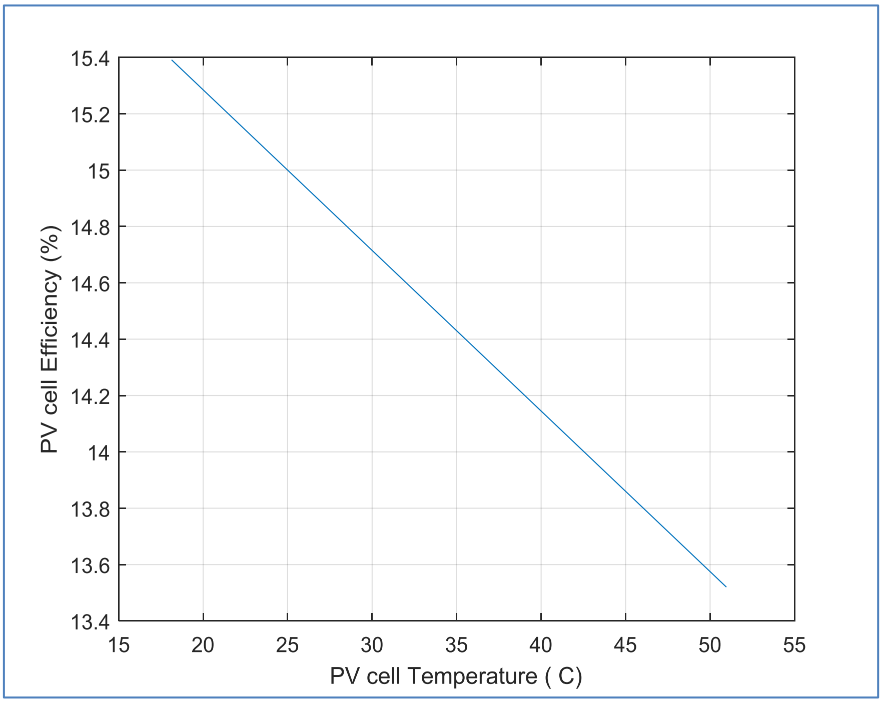

Figure V.79 : Effect of the operating cell temperature on the efficiency of the photovoltaic module.

Fig V.79 illustrates the shape of the conversion efficiency (PV η) as a function of operating cell temperature, in our temperature range 15-55 °C; the decrease in PV conversion efficiency is almost linear with the operating cell temperature, the corresponding slope (dη/dT = -0.063% /°C) is in agreement with the evaluation of Singh et al [25]; for the silicon solar cells (dη/dT = -0.042% / °C).

The efficiency is slightly sensitive to the increase in temperature: when the operating cell temperature increases by 17° C (25 °C to 42.5 °C) under an illumination of 1000 W/m^2, the efficiency decreases by 1%.

V. 4. 2. Evaluation of the Annual Production of the PV-TEG Hybrid System at Khouribga City in Morocco

Certainly, the electrical production of the PV-TEG hybrid system is related to climatic conditions, which consists of radiation, ambient temperature and wind velocity. These climatic conditions vary yearly, monthly and daily, also depend on geographic coordinates. The purpose of this research is to evaluate the performance of the hybridization of PV system with TEG generator through the electric power produced and to compare it with the PV system operating by itself under the weather conditions of Khouribga city in Morocco. A set of factors have been considered like the radiation, the ambient temperature, the wind velocity and the geographic coordinates. The different types of energy loss that we considered include energy loss by radiation, by naturel convection, by forced convection and by reflection in the top surface of the glass. We studied this system for two cases, the case with solar tracker and the case with a fixed optimal angle. Among the phenomena that occur in the hybrid system of PV-TEG, we site the follow effects (photovoltaic, Seebeck, Joule, Thomson, Peltier). All of which are included in the model. The TEG thermoelectric properties are considered dependent of temperature. The results obtained showed that the TEG generator can slightly improve the conversion of solar radiation into electricity by combining it with silicon-based monocrystalline solar cells. The contribution of TEG in the efficiency of the hybrid system increases in the months and days where solar irradiation is important.

V. 4. 2. 1. Daily power evolution of the PV and PV-TEG hybrid system

The results presented in this part shows the daily variation of the power generated by the TEG, the PV and the PV-TEG hybrid system for the day 21 July which is the longest day of the year in two cases; the first one if the system is set up on a solar tracker and in the second case if the system is installed with an optimal tilt angle and orientation.

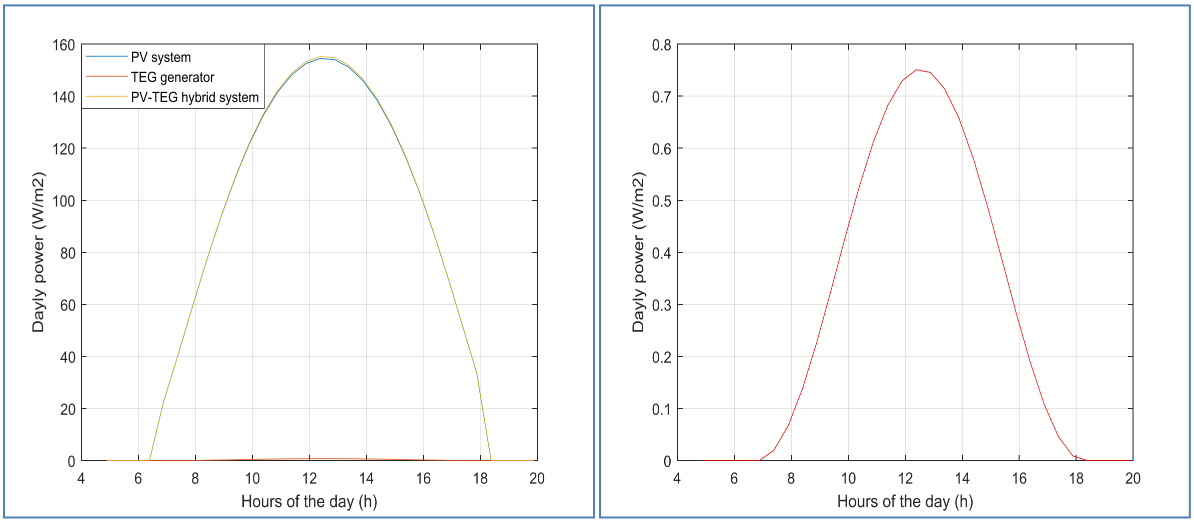

b) The daily power evolution of the PV-TEG hybrid system

a) The daily power evolution of the TEG

Figure V.80 : Daily variation of the power generated by the TEG and PV-TEG with optimal tilt angle.

According to Fig V.80 a); the hybrid system (PV-TEG) starts to generate electric power at 6 o'clock, which is the time of the sunrise, then it starts to increase until it reaches its maximum which is equal to 155 W after that it starts to decrease until sunset at 18 pm. The power generated by the latter is slightly improved with respect to the PV alone. Considering Fig V.80b); this improvement is due to the additional power generated by the TEG generator. The evolution of the power generated by the latter is similar to that of the PV-TEG hybrid system and also has a maximum power at noon which is equal to 0.75 W.

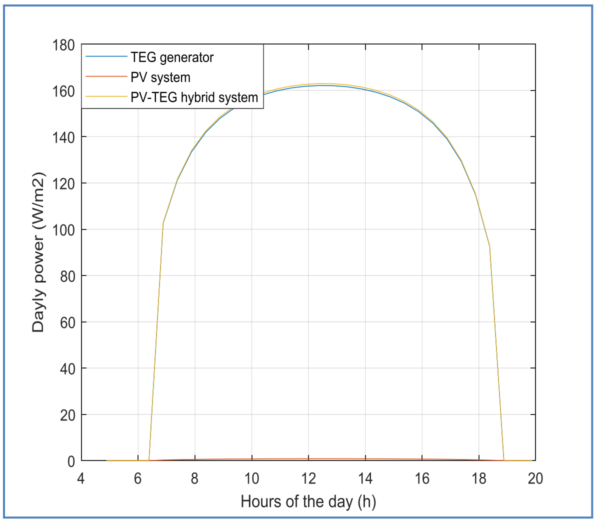

b) The daily power evolution of the PV-TEG hybrid system

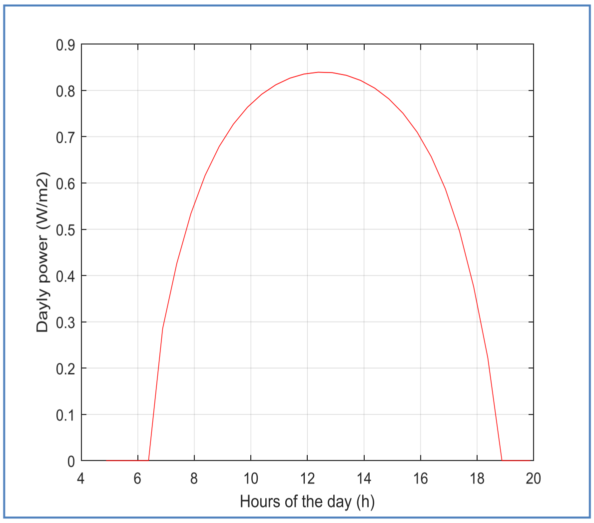

a) The daily power evolution of the TEG

Figure V.81 : Daily variation of the power generated by the TEG and PV-TEG set up on a solar tracker system.

From Fig V.81 a); it's clear that the power variation of the hybrid system is similar to that with an optimal angle, it also has a maximum at noon equal to 161 W and it's also slightly improved with respect to the PV alone. The enhancement it's also due to the TEG contribution on the overall power as shown in Fig V.81 b). The TEG power evolution has the same variation of that in the case with an optimal angle. The maximum power generated by the TEG equal to 0.85 is in the noon. The reason for this form of evolution in the power generated by all systems is mainly due to the change in solar radiation, which also changes in the same shape and reaches its maximum value at noon, since the electrical power of the all systems is related to the solar radiation. The higher the solar radiation, the higher their electrical power and when the solar radiation reaches its maximum value, the power of all systems will also reach their maximum values which are in all cases at noon.

As appears from fig V.81; in all cases the output power of the PV-TEG hybrid system is always slightly higher than that of the PV alone. On the other hand, the output power of the PV-TEG hybrid system in the case where it is associated with a solar tracker is always greater than in the case where the hybrid system is set at an optimal angle. As for the contribution of the TEG generator, it power also slightly higher in the case of a solar tracker is used.

V. 4. 2. 2. Monthly energy production of the PV and PV-TEG hybrid system

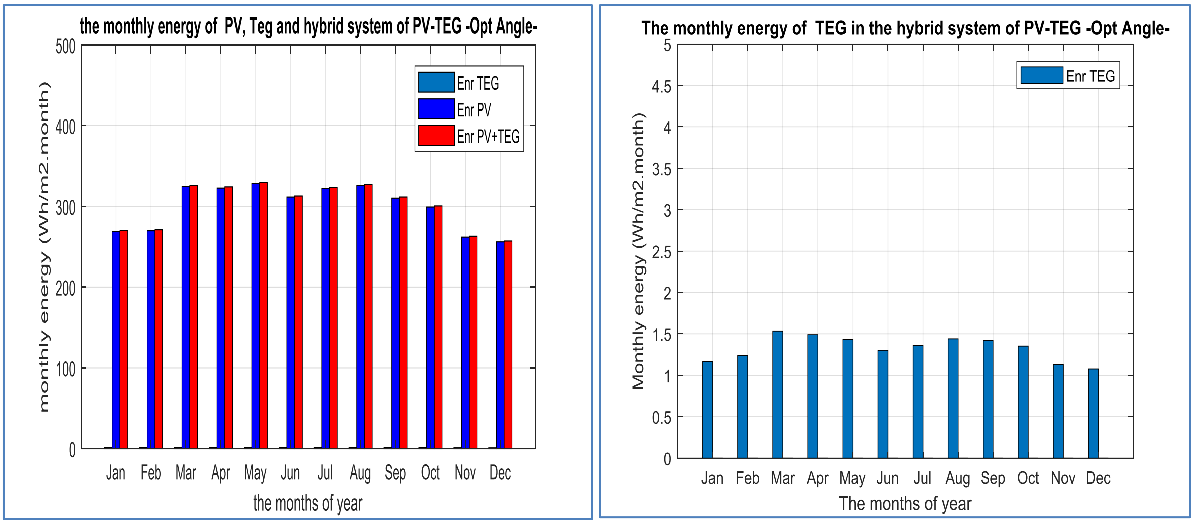

a) Monthly energy produced of the PV-TEG hybrid system

b) Monthly energy produced of the TEG

Figure V.82 : The monthly energy produced by the TEG and PV-TEG with optimal tilt angle.

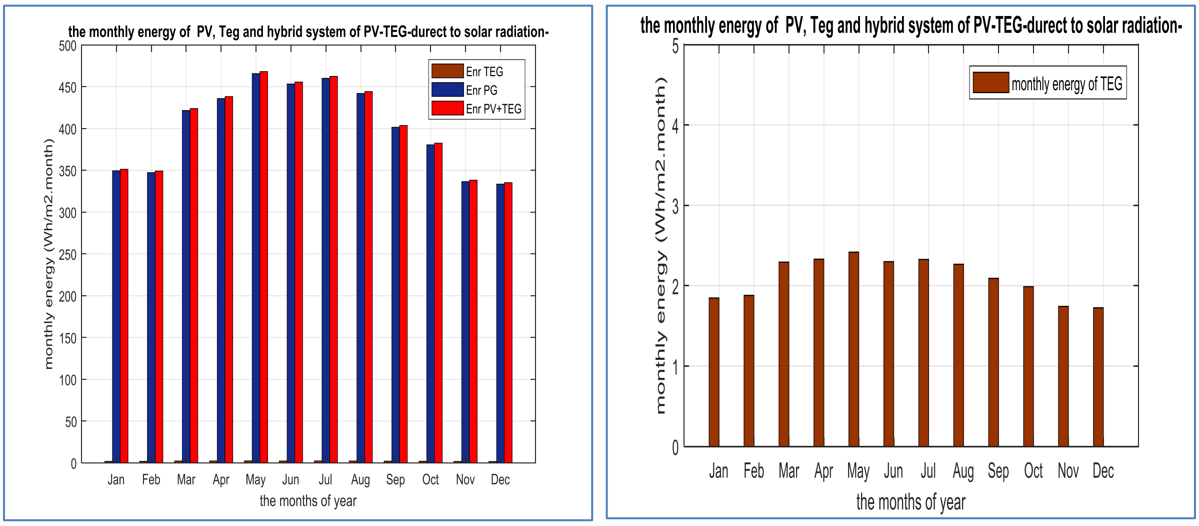

a) Monthly energy produced of the PV-TEG hybrid system

b) Monthly energy produced of TEG

Figure V.83 : Monthly energy produced by the TEG and PV-TEG set up on a solar tracker system.

In the case of a PV-TEG hybrid system with a solar tracker, the production of this system has a pyramidal shape with the peak in summer and the base in winter, as well as the generator curve TEG. The energy produced increases in May, June and July; the period of greatest production where it reaches a maximum is 55 KWh/m^2. Lower values of the winter months correspond to short days and low sunlight, and thus low production of the PV-TEG system does not exceed 40 kWh/m^2 per month in November, December and January. But for a fixed system of PV-TEG to all year long with optimal tilt angle (30° at Khouribga city and South orientation) Indeed, the distribution of electricity produced has not presented a remarkable difference between the months of the year, always stays around 300 Wh /m^2/month, it can be seen the global energy produced by PV-TEG system's exceeded 300 Wh/m^2/month from March to October and less than 300 Wh/m^2/month in the rest of the year.

As for the generator TEG, takes the same reading of the first graph. In tracking system of PV-TEG the electricity production is still better compared to the fixed system, reaches maximums in May The value of its productivity is 154 Wh/m^2, and minima in November, December and January remains lower than 120 Wh/m^2. However, for the productivity of TEG generator in a fixed system of PV-TEG is more irregular over the year, the energy produced is between 32 to 38 Wh/m^2/month in the most months of the year and exceeded 38 Wh/m^2 in March.

V. 4. 2. 3. Annual evolution of energy production of the PV and PV-TEG hybrid system

In the last part of the PV-TEG system modeling we present the evolution of the energy produced by the PV-TEG hybrid system throughout the year as well as the contribution of the TEG generator for each day of the year from 1st January to 31st December, for two cases like indicated in the previous paragraphs, the case with a solar tracker and the case with optimal tilt angle and orientation.

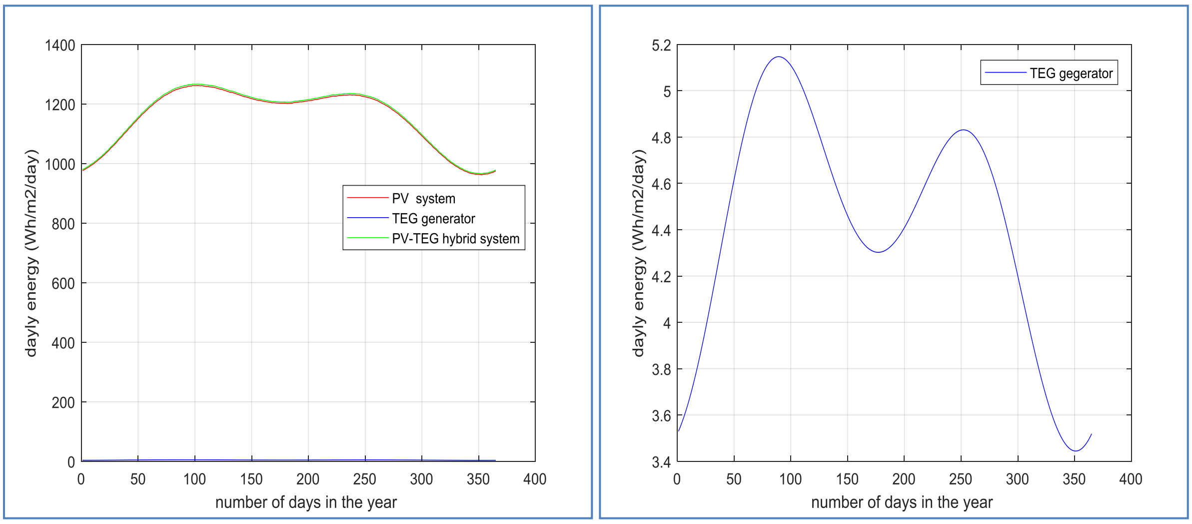

a) Evolution of Annual energy produced of the PV-TEG hybrid system

b) Evolution annual energy produced of the TEG

Figure V.84 : Daily energy produced in the year by the TEG and PV-TEG with optimal tilt angle.

From Fig V.84 a); which represents the hybrid system with an optimal angle, we note around the 110th days when the energy produced by the hybrid system is increasing, it is a period where the number of hours of sunshine increased. The energy produced reaches the maximum in April 1246 Wh /m^2. Then the energy comes down to 1213 Wh /m^2 in June, from

June to August, where the energy is semi-constant. Thereafter we can clearly see the energy reduction up to 990 Wh/m^2 at the end of the year. As we can see the energy produced by the hybrid system is slightly improved with respect to the PV alone. This is due to the additional energy produced by the TEG generator as we can see from fig V.84 b). The evolution of the energy produced by the generator TEG is low, as with the PV-TEG hybrid system, the latter also has two maximum values in April exceeds 5.8 Wh/m^2 and in August (about 0.048 Wh/m^2/day) and is lower in extremity (about 4.82 Wh/m^2/day). The form of curves could come from the fact that the inclination of panels is always fixed optimally (30° at Khouribga city) and that the position of the sun in winter is lower.

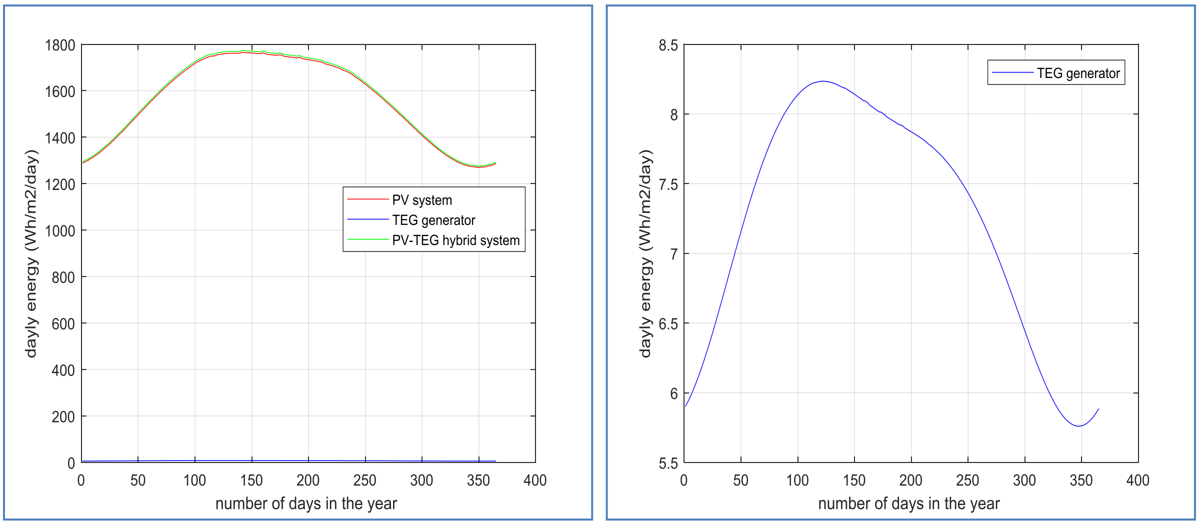

a) Evolution of Annual energy produced of the PV-TEG hybrid system

b) Evolution annual energy produced of the TEG

Figure V.85 : Daily energy produced in the year by the TEG and PV-TEG set up on a solar tracker system.

As we can see from fig. V.85 a); the evolution of the energy produced by the PV-TEG hybrid system with a solar tracker for each day of the year is not the case with an optimal angle. It starts to rise from the first day of the year until it reaches its maximum value equal to 1792.5 Wh/m^2 on the 150th day of the year and then begins to decline until it reaches its minimum value equal to 981.5 Wh/m^2 on the 350th day of the year. Then we notice that the energy started to rise slightly. As in the case of the optimal angle, the energy produced by the PV-TEG hybrid system in the second case has also improved due to the additional energy produced by the TEG generator as described in Fig V.85 b). Unlike the hybrid system, the energy produced by the TEG generator has a maximum in the 12th days of the year. As evidenced by Fig 15 the TEG generator can improve the energy produced by the hybrid PV-TEG system. This is because in all cases, either by using the solar tracker or by making the hybrid system at a fixed optimal tilt angle and orientation, the daily energy produced is always slightly larger than the energy produced by PV alone. Furthermore, the use of a solar tracker is very important in improving the daily energy produced by the hybrid system as well as the TEG generator, especially in the middle of the year. The energy produced by the hybrid system using a solar tracker is larger than that fixed on an optimal angle.

After the interpretation of the productivity of two systems; tracking and fixed systems of PV-TEG, we find that productivity of tracking system is better than a fixed system, This is due to the advantage presented by the solar tracker systems. In this system, we can track the sun throughout the months and the day. By continually track the position of the sun, and keep on cos(w) = 1 (the angle formed by the direction vector of the solar radiation and the normal leaving the surface) along the year, And this possibility is not available in the fixed system, where the value of cos(w) takes the value max at noon of solar time, and rarely reaches 1 in May and August. So the tracking system ensures maximum electricity production than fixed systems.

Conclusion V

The objective of this chapter is to help improve the prediction of the amount of energy that a photovoltaic system can be produce. The study of the thermal behavior can be therefore help to improve prediction of a photovoltaic electricity production. Ambient temperature, solar radiation and wind speed are the meteorological variables that have the most importance on the thermal exchanges of the photovoltaic module.

This work consists of two main parts; the first is the implementation of the thermal transfer equation between the photovoltaic module and its environment, according to these quantities, used to determine the operating cell temperature. Phenomenological laws governing two types of losses: convection and radiation to the sky must however be known. For this, an experimental approach is necessary: it will also make it possible to validate a simulation model of the operating cell temperature of the photovoltaic modules; the thermal behavior of the modules can finally be described from a set of input parameters of a thermal model. In the second part, we have studied the electrical energy production of the PV-TEG hybrid system in both cases of functionalizing tracking system and where the hybrid system is fixed at the optimal tilt angle and orientation.

The study is accomplished in every day and every month during the year for Khouribga city located in Morocco. Irradiation throughout the year for Khouribga city was obtained analytically and the mathematical model used for the PV-TEG Hybrid System takes into account different types of losses which are forced convection and natural convection, radiation and reflection losses. The results clearly demonstrate that the use of the solar tracker makes it possible to produce more electrical power than when the system is fixed at the optimum angle. A slight increase in electrical power was obtained using the TEG thermoelectric generator. The contribution of the TEG increases with the solar radiation intensity.

References V

[1] Bennouna, A., Energy sector at the end of 2018: Inventory and energy transition, Technical Report, Doi: 10.13140/RG.2.2.18676.40329, April 2019.

[2] Minister of Energy, Mines and Sustainable Development, Department of Energy and Mines. GIZ “Renewable energies and energy efficiency in Morocco” https://www.mem.gov.ma/en/pages/secteur.aspx?e=2 July/2020.

[3] Nfaoui, M., El-Hami, K., Numerical study and modeling of the spatial and temporal distribution of the solar field at Khouribga and the 20 Moroccan cities, American Institute of Physics. AIP Conference Proceedings, 030028 (2018); doi: 10.1063/1.5024178.

[4] Weather Spark, Ordinary weather in Khouribga https://fr.weatherspark.com 03-2018.

[5] (Masen) Moroccan agency for sustainable energy, Etude d'impact environnemental et social de la centrale solaire photovoltaique de noor bejaâd, September 2018.

[6] Nfaoui, M., El-hami, K. (2018) Optimal tilt angle and orientation for solar photovoltaic arrays: case of Settat city in Morocco. International Journal of Ambient Energy, 2, 162-8246.

[7] Nfaoui, M., El-Hami, K., Extracting the maximum energy from solar panel’, Energy Report. 4, pp. 536–545.

[8] E,A Breteque, Study of the Thermal Behavior of Photovoltaic Modules with a view to Predicting their Electrical Production on Site, Doctoral thesis, University of Provence, Institute of Industrial Thermal Systems, October 2006.

[9] Akhsassi, M,. El Fathi, A., Erraissi, N., Aarich, N., Bennouna, A., Raoufi, M.. Outzourhit A.,, Experimental investigation and modeling of the thermal behavior of a solar PV module, Solar Energy Materials and Solar Cells 180 (2018) 271–279.

[10] M. Belhadj, T. Benouaz, A. Cheknane et S.M.A Bekkouche.; Estimation de la puissance maximale produite par un générateur photovoltaïque.; Laboratoire de Physique et Dispositifs à Semi-conducteurs-Université de Béchar-Algérie- 2010.

[11] D.L. King, W.E. Boyson, J.A. Kratochvill., Photovoltaic Array Performance Model.; Sandia National Laboratories, New Mexico-United States of America-2004.

[12] K. Agroui, A. Belghachi et S. Kadri., Caractérisations Electriques et Thermiques d’un Module PV au Silicium Multicristallin en Milieu Contrôlé et sur Site Saharien., Unité de Développement la Technologie du Silicium, Centre Universitaire de Béchar-Algérie- 2003.

[13] Attivissimo, F., Nisio, A.D., Lanzolla, A.M.L., Paul, M,. Feasibility of a Photovoltaic–Thermoelectric Generator: Performance Analysis and Simulation Results’, IEEE Trans. Instrum. Meas, Vol. 64, No. 5, pp. 1158–1169- 2015.

[14] Cui, T., Xuan, Y., Yin, E., Li, Q., Li, D., Experimental investigation on potential of a concentrated photovoltaic-thermoelectric system with phase change materials,. Energy Vol.112, 122, pp. 94–102-2017.

[15] Bjørk, R., Nielsen, K.K. (2015) 'The performance of a combined solar photovoltaic (PV) and thermoelectric generator (TEG) system', Solar Energy, Vol.120, pp. 187–194- 2015.

[16] Kudish, A.I., Evseev, E.G., Walter, G., Leukefeld, T.; Simulation study of a solar collector with a selectively coated polymeric double walled absorber plate,. Energy Conversion and Management, 43, pp. 651–671-2002.

[17] Notton, G., Cristofari, C., Mattei, M., Poggi, P,. Modelling of a double-glass photovoltaic module using finite differences,. Appl. Therm. Eng. 25, pp.2854–2877- 2005.

[18] H. Nowak, The sky temperature in net radiant heat loss calculations from low – sloped roofs , Infrared Physics, vol. 29 n. 2, mai 1989, pp. 231 – 232.

[19] Palyvos, J.A;. A survey of wind convection coefficient correlations for building envelope energy systems modeling;. Appl. Therm. Eng. 28, pp.801–808 -2008.

[20] BEJAN, A., KRAUS, A.D.Heat Transfer Handbook -2003.

[21] Lamba, R., Kaushik, S.C. 'Modeling and performance analysis of a concentrated photovoltaic–thermoelectric hybrid power generation system', Energy Conversion and Management, 115, 288–298- 2016.

[22] Schwingshackl, C., Petitta, M., Wagner, J.E., Belluardo, G., Moser, D., Castelli, M., Zebisch, M., Tetzlaff, A. 'Wind Effect on PV Module Temperature: Analysis of Different Techniques for an Accurate Estimation', Energy Procedia, European Geosciences Union General Assembly, EGUDivision Energy, Resources & the Environment, ERE 40, pp.77–86- 2013.

[23] Wu, Y.-Y., Wu, S.-Y., Xiao, L;. Performance analysis of photovoltaic–thermoelectric hybrid system with and without glass cover;. Energy Convers. Manag. 93, pp.151–159- 2015.

[24] Yang, D., Yin, H. 'Energy Conversion Efficiency of a Novel Hybrid Solar System for Photovoltaic, Thermoelectric, and Heat Utilization. IEEE Trans', Energy Convers. 26, pp.662–670- 2011.

[25] P. Singh, S.N.Singh, M. Lal, M.Husain, Solar Energy Materials & Solar Cells 92 (2008) 1611–1616.

General Conclusion and Perspectives

The knowledge of the solar radiation has a major interest for the study and the design of the solar energy systems. Thus, a good design is possible only if the measures are available in a continuous manner in space and in time. To estimate the solar potential, it is essential to know the characteristics of the solar radiation reaching the Earth's surface at a given location.

The solar potential studies that have been developed in the field of solar energy in Morocco determine, the theoretical national potential of solar radiation, which is immense because of the intensity of solar radiation and the availability of large spaces of all Moroccan territory.

In this study, we suggest the theoretical calculation of the intensity solar radiation and the availability of large spaces of all Moroccan territory.

The spatial distribution of the daily values of solar irradiation was calculated for the whole year. A finer analysis is to do this calculates month by month. The computations of the various components of the solar radiation, calculated over the whole year, it is assumed that the sky is very clear all the days of the year.

Study of solar radiation according to the optimum tilt angle in 20 Moroccan cities

Solar radiation distribution is expressed as annual global solar energy received on a horizontal plane (in kilowatt hours per square meter per year). The 1st parameter influenced on the solar energy distribution is the latitude, that is to say the distance from the equator. Solar irradiation decreases as we get closer to the poles (or move away from the equator).

Morocco has a great potential for the production of solar energy, and the (photovoltaic and solar thermal) are the two technologies favored for the exploitation of this solar potential.

For the purpose of realizing a solar irradiation map at the national level, Nanosciences and Modeling laboratory of Sultan Moulay Sliman University, and in its activities, proposes a theoretical calculation method permits to construct a map of solar irradiation according to the optimum tilt angle of different 20 Moroccan cities, for the specific objectives of:

- Develop the metrology of our laboratory, with storage of the results in the database.
- Integrate the instantaneous measurements and deduce the monthly and annual productivities of the solar systems.

- Propose a method of correction and extrapolation of data to long-term.
- Propose a method to extend it to the whole of Morocco.

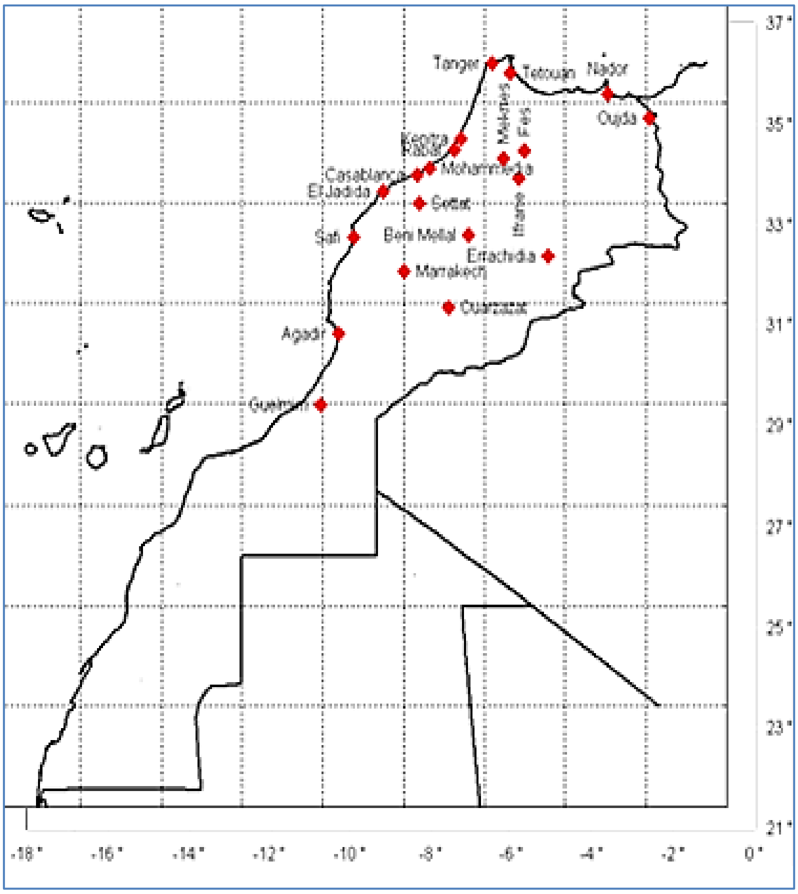

Figure VI.86 : The 20 Moroccan cities concerned by the study [1].

We show in table. 1 the results of annual solar irradiation values and the annual tilt angle for a different 20 Moroccan cities;

Table VI.31: The daily average energy of twenty Moroccan cities in (kWh/m^2.day). The maximum average daily energy is shown in brown, the minimum one is colored with yellow.

Cities	Geographical data			The average daily energy of each month											
	Latitude	Longitude	Optimal tilt angle	Jan	Feb	Mar	Apr	May	Jun	Jul	Aug	Sept	Oct	Nov	Dec
Tanger	35°45' N	-5.80000	32	5,754	6,533	7,264	7,554	7,446	7,293	7,294	7,364	7,204	6,623	5,858	5,451
Tetouan	35°34' N	-5.36667	32	5,934	6,659	7,333	7,581	7,447	7,283	7,290	7,382	7,263	6,741	6,035	5,654
Nador	35°10' N	-2.93333	31	5,737	6,506	7,249	7,561	7,465	7,314	7,312	7,375	7,209	6,632	5,870	5,452
Oujda	34°41' N	-1.91139	31	5,780	6,532	7,256	7,551	7,440	7,281	7,283	7,359	7,215	6,663	5,920	5,506
Kenitra	34°15' N	-6.57806	30	5,863	6,613	7,315	7,591	7,481	7,327	7,329	7,401	7,250	6,691	5,957	5,569
Fes	34°02' N	-5.00000	30	5,870	6,611	7,310	7,584	7,468	7,311	7,314	7,392	7,250	6,704	5,977	5,585
Rabat	34°01' N	-6.84167	30	5,898	6,639	7,328	7,590	7,470	7,313	7,317	7,396	7,257	6,710	5,987	5,604
Meknes	33°53' N	-5.55472	30	5,895	6,632	7,322	7,585	7,463	7,303	7,308	7,390	7,256	6,717	5,997	5,610
Mohammedia	33°41' N	-7.38298	30	5,947	6,676	7,346	7,588	7,455	7,293	7,300	7,390	7,266	6,737	6,028	5,655
Casablanca	33°32' N	-7.58333	30	5,968	6,692	7,353	7,587	7,448	7,284	7,292	7,387	7,270	6,749	6,046	5,677
Ifrane	33°31' N	-5.11667	30	5,935	6,658	7,332	7,580	7,445	7,281	7,287	7,380	7,263	6,743	6,038	5,656
El-jadida	33°14' N	-8.50000	29	5,964	6,692	7,361	7,610	7,487	7,329	7,334	7,415	7,281	6,745	6,037	5,672
Settat	33°00' N	-7.61667	29	5,981	6,701	7,364	7,606	7,477	7,316	7,322	7,409	7,285	6,76	6,06	5,690
Beni mellal	32°20' N	-6.36083	28	6,001	6,710	7,371	7,619	7,493	7,333	7,338	7,424	7,300	6,783	6,092	5,724
Safi	32°17' N	-9.23333	28	6,035	6,744	7,391	7,625	7,495	7,335	7,341	7,429	7,305	6,787	6,098	5,744
Errachidia	31°55' N	-4.42444	28	6,023	6,717	7,369	7,607	7,471	7,303	7,311	7,408	7,302	6,806	6,130	5,760
Marrakech	31°37' N	-8.00889	27	6,054	6,753	7,400	7,639	7,512	7,353	7,358	7,444	7,321	6,809	6,128	5,774
Ouarzazate	30°55' N	-6.89389	27	6,131	6,804	7,421	7,629	7,477	7,306	7,317	7,425	7,336	6,861	6,210	5,863
Agadir	30°25' N	-9.60000	26	6,162	6,835	7,445	7,652	7,507	7,340	7,350	7,451	7,352	6,869	6,218	5,884
Guelmim	28°59' N	-10.05738	25	6,285	6,925	7,491	7,658	7,487	7,309	7,325	7,448	7,384	6,945	6,332	6,016

E_{min}

E_{max}

The results shown in Table 1 are the annual solar irradiation values for a different 20 Moroccan cities. It is clear from the table, the annual variation of the solar irradiation obtained through the strategy applied to last parts. The spatial distribution of the daily values of solar irradiation was calculated for the whole year. A finer analysis is to do this calculates month by month. The computations of the various components of the solar radiation, calculated over the whole year, it is assumed that the sky is very clear all the days of the year. We perform a graphical comparison for a different 20 Moroccan, the results of the cumulative month energy for each city is shown in the Fig. 1.

We perform a graphical comparison for a different 20 Moroccan, the results of the cumulative month energy for each city is shown in the figure below:

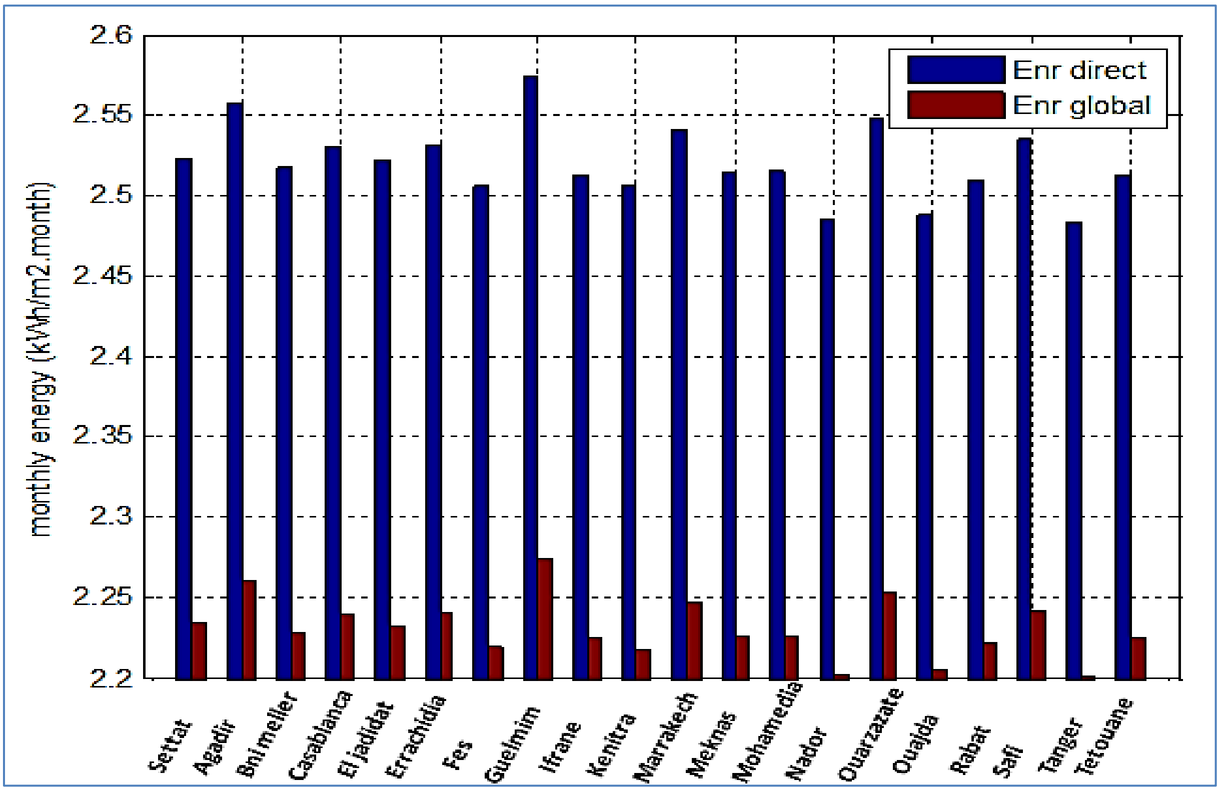

Figure VI.87 : The Annual solar energy of direct and global radiation to 20 Moroccan cities.

As shown in the map of Morocco (Figures 1 & 2) and Table 1, the latitudes of the 20 Moroccan cities studied are globally between 28°N and 36°N. To ease the discussions, we have subdivided the Moroccan territory into three regions located around the three middle latitudes:

- 28° to 31°N for the south of the country: **Guelmim**, **Agadir**, **Ouarzazate**, **Marrakech** and **Errachidia**.
- 32° to 34°N for the center of the country: **Fes**, **Rabat**, **Meknes**, **Mohammedia**, **Casablanca**, **Ifrane**, **El-jadida**, **Settat**, **Beni mellal** and **Safi**.
- 34° to 36°N for the north of the country: **Tanger**, **Tetouan**, **Nador**, **Oujda** and **Kenitra**.

In general, the energy received from the sun takes maximum values in the cities of southern Morocco, and minimum in northern Morocco cities.

It can be seen that the solar potential recoverable on the three regions of Morocco reach respectively; 2495 kWh/m²/year in the northern region, 2518 kWh/m²/year in the center and 2550 kWh/m²/year for the south of the country.

As summarized; the values of the optimum tilt angle vary decreasing from north to south, in Morocco takes the maximum value at Tangier 32° (north of Morocco of latitude 35°45' North and Longitude -5°800' West) and the minimum value at Guelmim 25° (southern Morocco of latitude 28°59' North and Longitude -10°057' West).

It is obvious that the solar irradiation decreases as we get closer to the north, and the optimum angle of inclination decreases when moving away from the equator.

Perspective the next step of our study

The climate of Khouribga province is the semi-arid and continental with hot summers and cold winters, and has a number of agricultural areas that need irrigation throughout the year, the best way to do this is to use irrigation systems of photovoltaic pumping.

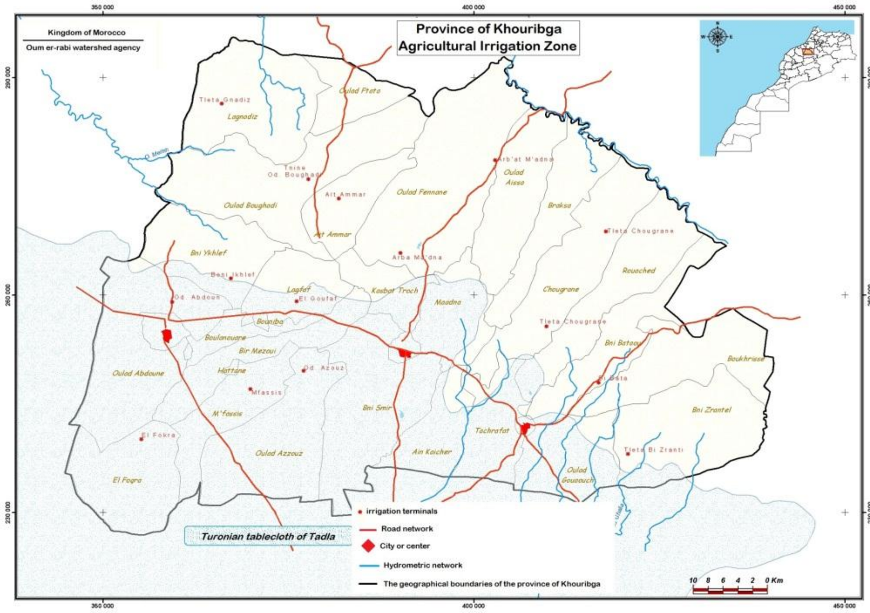

Figure VI.88 : Need monograph in Irrigation Water, province of Khouribga [2].

Our study aims to promote optimizing the use solar pumping in Khouribga province, according to the hydrological characteristics for each agricultural area in our province.

Solar pumping is characterized by a variable flow throughout the days of the year, when the photovoltaic field starts to produce electricity; the flow is produced by the pump, and it is directly related to the intensity of solar irradiation received on the photovoltaic surface.

For this reason, we have thought of maximizing the productivity of solar pump systems by integrating the seasonal tilt angle according to the borehole, the water source used and the other parameters.

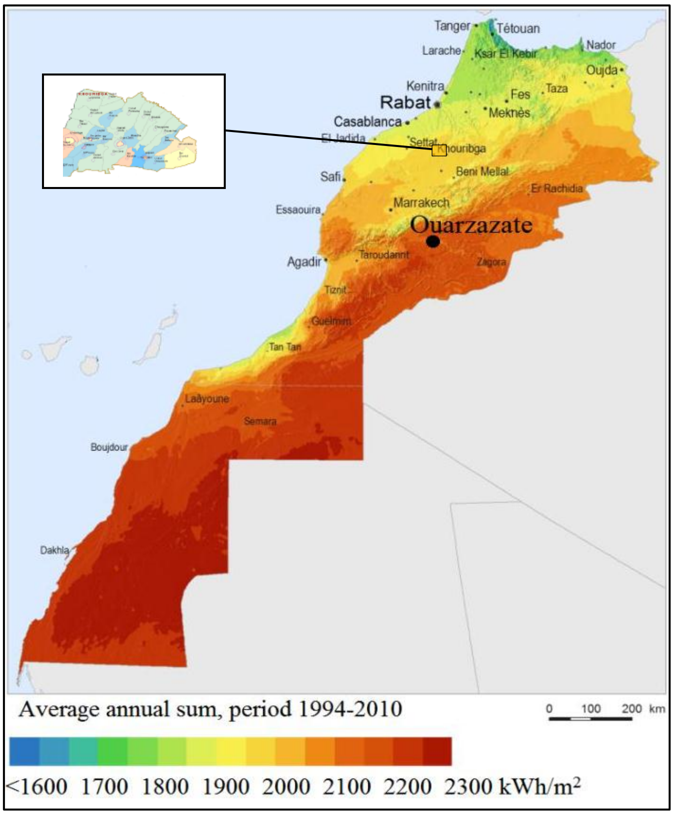

Figure VI.89 : Global Horizontal Irradiation in Morocco (kWh/m^2/year) [3].

The solar potential is estimated at more than 3,400 MW_p. With more than 3,000 hours/year of sunshine, an average solar irradiation of 2500 kWh/m^2/year, the Morocco enjoys a very significant solar potential [4].

The figure above shows that the energy received is strongly influenced by the geographical position. During the year it is the cities of the south that receive the maximum of irradiation.

The table below summarizes the optimum tilt angle and the solar energy received by this angle of the four Moroccan cities from different regions, then comparing us with that which we found in Khouribga city.

Table VI.32: Optimum tilt angle and Annual energy Received.

Cities	Optimal tilt angle	Annual energy received (kwh/m²)
Tanger	32°	2483
Oujda	31°	2488
Khouribga	30°	2524
Marrakech	27°	2541
Agadir	26°	2557

From the results of Table 1 it can be seen that the optimum tilt angle for the other four Moroccan cities takes different values, and it changes when we move north or south. The optimums tilt angle increases in the cities of the north (Tangier 32 ° and Oujda 31 °) and decreases in the cities of the south (Marrakesh 27 ° and Agadir 26 °).

As part of this study, the selection of future locations of photovoltaic systems is also an important factor as well as the choice of the different PV technologies (Monocristalline, Polycrystalline and Amorphous silicon solar cells) depending on geographic location and its environment. The orientation (azimuth and inclination) and other geographical and meteorological parameters directly influence the productivity of PV power installations.

The tilt angles of solar panels should be adjusted monthly, seasonal or the yearly to extract the maximum energy from solar panels. In this study the optimum tilt angles for Khouribga and the 20 Moroccan cities, are calculated using the mathematical models programmed under MATLAB.

The usual recommendation for the orientation to the equator, and tilt angle of latitude should not be understood as a requirement that has a very significant impact on the installation, especially in the cities studied. We call who are interested to construct the structures dedicated to solar installations or architectural modifications, to respect these recommendations. We have established a set of diagrams and tables, allowing to quickly determining the optimum tilt angle of different 20 Moroccan cities.

Finally, the yearly average optimum tilt angle in Morocco varies between 28° and 32°. This angle can be used for fixed installations or for building applications.